UNIVERSITEIT VAN PRETORIA
UNIVERSITY OF PRETORIA
YUNIBESITHI YA PRETORIA

The effects of selected therapeutic agents on cell cytotoxicity and Her-2 receptor expression using cultured breast adenocarcinoma models

by

Tracey Hurrell

A dissertation submitted in fulfilment of the requirements for the degree

Magister Scientiae

in

Pharmacology

Department of Pharmacology, School of Medicine,
Faculty of Health Sciences
University of Pretoria

Supervisor: Dr K. Outhoff
Pretoria, 2013

Declaration

University of Pretoria

Faculty of Health Sciences

Department of Pharmacology

I (full names), Tracey Hurrell

Student number: 27177476

Subject of work: The effects of selected therapeutic agents on cell cytotoxicity and Her-2 receptor expression using cultured breast adenocarcinoma models

Declaration

1. I understand what plagiarism is and am aware of the University's policy in this regard.
2. I declare that this project is my own original work. Where other people's work has been used (either from a printed source, internet or any other source), this has been properly acknowledged and referenced in accordance with departmental requirements.
3. I have not used work previously produced by another student or any other person to hand in as my own.
4. I have not allowed, and will not allow, anyone to copy my work with the intention of passing it off as his or her own work.

Signature

.....

Acknowledgements

I would like to sincerely acknowledge the following people for their contribution and support throughout the study:

- My supervisor, Dr K. Outhoff, for her guidance, understanding, support, advice and positivity throughout the course of this project
- Roche Pharmaceuticals for their kind donation of trastuzumab (Herceptin®) without which this project would not have been possible
- National Research Foundation for their generous scholarships
- The Cancer Association of South Africa (CANSA) for providing funding for this project
- Dr L. Fletcher and her team from the Department of Biostatistics of the University of Pretoria for their assistance with the statistical analysis of the data
- Dr G. Joone of the Department of Pharmacology for her continual support and patience in maintaining and culturing the cells that were used in this study
- Numerous personnel and colleagues, especially Dr A.D. Cromarty and Dr J.J. van Tonder, from the Department of Pharmacology for their support, technical assistance and encouragement
- My friends who have provided comical relief and encouragement when tasks seemed insurmountable
- My wonderful parents and sister who have done everything in their power to ensure I achieved my goals. Their love, faith and sacrifice have been indispensible in my successes thus far in life
- And most importantly, my Heavenly Father: For everything, absolutely everything, above and below, visible and invisible. Everything got started in him and finds purpose in him (Colossians 1:16)

"For any complex question there is almost certainly a simple answer that is almost always wrong"

- Henry Louis Mencken

Abstract

Introduction: Epidemiological studies suggest that at least 1 in 29 South African women will be diagnosed with breast cancer in their lifetime. Breast cancer is not a single disease. The heterogeneity of breast cancer results in four distinct molecular subtypes including aggressive human epidermal growth factor receptor-2 (Her-2) positive, where Her-2 receptors are over-expressed. Trastuzumab (Herceptin®), is a recombinant, humanized, anti-Her-2 monoclonal antibody that specifically targets subdomain IV of the extracellular domain of the Her-2 receptor and has dramatically altered the prognosis of Her-2 positive breast cancer. Trastuzumab is, however, associated with problems such as primary and acquired resistance, which has prompted investigation into improving its efficacy.

Aim: To investigate the ability of selected therapeutic agents to alter *in-vitro* cell viability, cell cycling, apoptosis and Her-2 expression in models of Her-2-positive and oestrogen receptor positive, Her-2 negative breast adenocarcinoma and bring about an alteration in the efficacy of trastuzumab.

Methods: MCF-7 cells which retain the ability to process oestrogen, and SK-Br-3 cells which over-express Her-2 gene products were used. Cells were exposed to trastuzumab, aspirin, calcipotriol, doxorubicin, epidermal growth factor (EGF-human), geldanamycin, heregulin-β1 and β-oestradiol as single agents and in combination with trastuzumab. Research methodologies included tetrazolium conversion assay for cell viability, AMC-substrate cleavage and annexin-V for apoptosis, propidium iodide staining for cell cycle analysis and anti-Her-2 affibody molecule for relative Her-2 receptor density.

Results: Cell survival of 95.39% (±2.69) for MCF-7 cells and 74.17% (±1.60) for SK-Br-3 cells was observed following trastuzumab (100 µg/ml) exposure. Trastuzumab resulted in statistically significant G1 phase accumulation in MCF-7 cells at 72 hours and in SK-Br-3 cells from 24 hours. Furthermore, trastuzumab decreased relative Her-2 receptor density in SK-Br-3 cells by approximately 35% by 24 hours but had no effect in MCF-7 cells. The anti-proliferative effects of trastuzumab were abrogated by EGF, a Her-1 ligand and heregulin-β1, a Her-3 and Her-4 ligand.

Most agents altered distribution throughout the phases of cell cycle to a certain degree, with the G1 phase accumulation observed for trastuzumab being potentiated in some combinations. Most of the agents, with the exception of doxorubicin and geldanamycin, did not promote apoptosis and appeared instead to be anti-proliferative. Geldanamycin had the greatest effect on Her-2 receptor density (approximately 80% by 24 hours) followed by EGF, heregulin and trastuzumab, with the biological molecules in combination with trastuzumab producing a further significant reduction.

Conclusion: Endogenous Her-receptor ligands (EGF and heregulin) differentially altered the viability parameters for trastuzumab which could play a role in the emergence of clinical resistance to targeted therapy. Doxorubicin with concurrent trastuzumab significantly reduced cell viability compared to each single agent in both cell lines. Furthermore, the cytostatic and cytotoxic abilities of each of the other agents either mimicked trastuzumab alone or the selected agent alone when exposed concurrently.

Table of Content

Glossary of Abbreviations, Symbols and Formulae

Ac-DEVD-AMC	Acetyl-Asp-Glu-Val-Asp-7-amido-4-methylcoumarin
ADCC	Antibody-dependent cell-mediated cytotoxicity
Akt	Protein kinase B (PKB)
ASA	Aspirin (Acetylsalicylic acid)
ATCC	American Tissue Culture Collection
B.A.D	Background aggregates and debris (also known as sub-G1)
Bax	Bcl-2-associated X protein
Bcl-2	B-cell lymphoma 2
BRCA1	Breast cancer type 1 tumour suppressor gene
cDNA	Complementary DNA
Ca^{2+}	Calcium ion
$CaCl_2$	Calcium chloride
CAM	Cellular-adhesion molecules
cAMP	Cyclic adenosine monophosphate
Caspase-3	Cysteinyl aspartic acid-protease
c-Cbl	Mammalian gene encoding CBL protein
CD44	Cluster of differentiation 44 antigen
Ckd	Cyclin-dependent kinase
CHAPS	3-[(3-Cholamidopropyl)dimethylammonio]-1-propanesulfonate
CISH	Chromogenic *in situ* hybridization
CO_2	Carbon dioxide
COX-2	Cyclooxygenase 2
CPT	Calcipotriol hydrate
CRC	Colorectal cancer cell
DBP	Vitamin D binding protein
DMEM	Dulbecco's Modified Eagle's Medium
dH_20	Distilled water
DMSO	Dimethyl sulphoxide
DOX	Doxorubicin hydrochloride
DNA	Deoxyribonucleic acid
DNase	Deoxyribonuclease
ECD	N-terminal extracellular domain
EDTA	Ethylene-diamine-tetra-acetic acid
EGF	Epidermal growth factor
EGFR	Epidermal growth factor receptor
ER	Oestrogen receptor
ERK	Extracellular signal-regulated kinases
EtOH	Ethanol

FasL	Fas ligand
FasR	Fas receptor [apoptosis antigen 1 (APO-1)]
Fab	Antigen binding region of antibody
Fc	Immune response region of antibody
FCS	Fetal Calf Serum
FDA	Food and Drug Administration
FISH	Fluorescence *in situ* hybridization
FITC	Fluorescein isothiocyanate
FL1	Fluorescence channel 1
g	Gravity
G0	Quiescent or post-mitotic state
G1 phase	First gap or growth phase
G2 phase	Second gap or growth phase
GELD (GLD)	Geldanamycin
GLOBOCAN	Global cancer control series
Grb2	Growth factor receptor-bound protein 2
HB-EGF	Heparin-binding epidermal growth factor-like growth factor
HEPES	4-(2-hydroxyethyl)-1-piperazineethanesulfonic acid
HERA	Herceptin Adjuvant trial
Her-2 (-1, -3 or -4)	Human epidermal growth factor receptor 2 (-1, -3 or -4)
HOP	HSP90/HSP70 organizing protein
HRG	Heregulin
Hrs	Hours
hsp90	Heat-shock protein 90
IAP	Inhibitor of apoptosis
IDC-NOS	Invasive ductal carcinoma not otherwise specified
IDC-NST	Invasive ductal carcinoma of no special type
IGF-IR	Insulin-like growth factor-I receptor
IHC	Immuno-histochemical
IκB	Inhibitor protein I-kappaB
IKK	IκB kinase complex
iNOS	Nitric oxide synthase
KCl	Potassium chloride
kDa	Kilo-dalton
L	Litre

M	Molar (moles per litre)
mAb	Monoclonal antibody
mAb 4D5	Murine monoclonal antibody 4D5
MAPK	Mitogen activated protein kinase
MEK	Mitogen-activated protein kinase kinase (also known as MAP2K)
mg	Milligrams
Mg^{2+}	Magnesium ion
$MgCl_2$	Magnesium chloride
ml	Millilitres
Min	Minutes
mM	Millimolar
MMP-9	Metalloproteinase-9
MMR	Mismatch repair protein
mRNA	Messenger ribonucleic acid
mTOR	Mammalian target of rapamycin
MTT	3-[4, 5-dimethylthiazol-2-yl]-2, 5-diphenyl tetrazolium bromide
MTX	Methotrexate
MUC4	Mucin-4 cell surface associated protein
m/v	mass per volume (g per 100 ml)
NaCl	Sodium chloride
$NaHCO_3$	Sodium hydrogen carbonate (sodium bicarbonate)
NDF	Neu differentiation factors
NF-κB	Nuclear factor-κB
nM	Nanomolar
nm	Nanometer
ng/ml	Nanograms per millilitre
NCCTG	North Central Cancer Treatment Group Intergroup trial
NSABP	National Surgical Adjuvant Breast and Bowel Project trial
NSAID	Non-steroidal anti-inflammatory drug
P	P-value or observed significance level
PARP	Poly(ADP-ribose) polymerase
PBS	Phosphate buffered saline
PG	Prostaglandins
pH	Percentage hydrogen
PI	Propidium iodide
PI3K	Phosphatidylinositol-3-kinase
PKC	Protein kinase C
PMSF	Phenylmethylsulfonyl fluoride
PR	Progesterone receptor
pRb	Retinoblastoma protein
p27	Cyclin dependent kinase inhibitor
p53	Tumour protein 53
p95-Her-2	Truncated form of Her-2

Raf	Proto-oncogene serine/threonine-protein kinase
RMPI 1640	Roswell Park Memorial Institute medium
RNA	Ribonucleic acid
RNase	Ribonuclease
RSA	Republic of South Africa
RXR	Retinoid X receptor
S-phase	Synthesis phase
SDS	Sodium dodecyl sulphate
SEM	Standard error of the mean
SNOM	Scanning near-field optical microscopy
Sub-G1	Cell cycle DNA fragmentation (background aggregates and debris)
T	Trastuzumab
TGF	Transforming growth factor
TKI	Tyrosine kinase inhibitors
TNF-α	Tumour necrosis factor-α
TNF-R1	Tumour necrosis factor receptor (also: Cluster of Differentiation 120)
TUNEL	Terminal deoxynucleotidyl transferase dUTP nick end labeling
UK	United Kingdom
USA	United States of America
VDR	Vitamin D receptor
VDRE	Vitamin D response elements
v/v	volume per volume (ml per 100 ml)
1,25-$(OH)_2$-D3	1,25-dihydroxyvitamin D3
17-AAG	17-allylamino-17-demethoxy-geldanamycin
α	Alpha
β	Beta
β-O	β-Oestradiol
µg/ml	Micrograms per millilitre
µl	Microlitre
µm	Micrometer
µM	Micromolar
ρg/ml	Picograms per millilitre
°C	Degrees celsius
%	Percentage

List of Figures:

Chapter 1: Literature Review

Chapter 2: Materials and Methods

Chapter 3: Results and Discussion: Trastuzumab

Chapter 4: Results and Discussion: Aspirin

Chapter 5: Results and Discussion: Calcipotriol

Chapter 6: Results and Discussion: Doxorubicin

Chapter 7: Results and Discussion: EGF

Chapter 8: Results and Discussion: Geldanamycin

Chapter 9: Results and Discussion: Heregulin-β1

Chapter 10: Results and Discussion: β-Oestradiol

List of Tables:

Chapter 2: Materials and Methods

Chapter 3: Results and Discussion: Trastuzumab

Chapter 4: Results and Discussion: Aspirin

Chapter 5: Results and Discussion: Calcipotriol

Chapter 6: Results and Discussion: Doxorubicin

Chapter 7: Results and Discussion: EGF

Chapter 8: Results and Discussion: Geldanamycin

Chapter 9: Results and Discussion: Heregulin-β1

Chapter 10: Results and Discussion: β-Oestradiol

Introduction

Theodor Seuss Geisel stated that: “You can get help from teachers, but you are going to have to learn a lot by yourself, sitting alone in a room.” This quote may also be applied to researchers: we may learn much from our predecessors, however, a novel idea may require ignoring what has been discovered and perusing the challenge without being restricted by current knowledge.

Cancer epidemiology statistics are essential in the evaluation of cancer prevalence and the efficacy of treatment regimens. In 1998, data from the GLOBOCAN series was published by the International Agency for Research on Cancer. The aim of the GLOBOCAN project was to provide contemporary estimates of the incidence and prevalence of and mortality for major type of cancers, at national levels, for 184 countries around the world. While differences in the distribution of types of cancer are evident in regions of the world, an overall estimated 12.7 million new cancer cases and 7.6 million cancer deaths occurred in 2008. (Ferlay et al., 2010)

Henry Louis Mencken (1880-1956) stated that: “For any complex question there is almost certainly a simple answer that is almost always wrong.” This is certainly true in the persistent endeavours of scientists in unravelling the delicate intricacies of carcinogenic processes. Diverse mechanisms for development of tumours result in multiple genotypes and six essential physiological modifications are thought to collectively dictate malignancy. These hallmarks of cancer are prominent targets for chemotherapeutic interventions. While much has been uncovered about the mechanics of carcinogenic processes in different tissues types, current treatment modalities possess numerous shortcomings. Many of the standard chemotherapeutic agents used for cancer therapy have little selectivity for cancer cells and target all rapidly dividing cells which may lead to severe toxicity to normal tissue.

The diversity of cancer compels treatment strategies to focus on the prominent biological features represented within the distinctive cancer classes. This requires redefining treatment principles and creating greater opportunities for the use of molecular targeted therapies. In an attempt to fill the void that exists in cancer treatment, interest in preventative measures or novel drug combinations is being revived. In this study, a Her-2 targeting monoclonal-antibody (mAb) specific for Her-2 positive breast cancer, was used in combination with commonly used chemotherapeutic agents as well as endogenous ligands and other hormones, in order to determine the potential for improvements in the efficacy of the targeted mAb.

Chapter 1: Literature Review

1.1 Cancer Pathogenesis

1.1.1 The Pathogenesis Process

The complex interlacing of carcinogenic processes suggests that cellular transformations involve synergy at multiple levels of regulation. (Lichtenstein, 2008) While carcinogenesis proceeds through discernible steps, tumours develop from intricate interactions between exogenous environmental factors and endogenous genetic and hormonal factors, leading to progressive malignant conversion. (Weinstein et al., 1988) Two major constituents of carcinogenesis integrate both mutagenesis and epigenetic changes. Mutagenesis is a rare and chaotic process that arises in individual cells and once mutagenesis has occurred within cells there is an increased likelihood of additional mutations within daughter cells. Epigenetic changes are highly ordered, heritable changes in gene expression which are independent of changes within the DNA sequence (DNA methylation, chromatin modification) and alter sub-systems of the entire genome and thus simultaneously alter multiple cells. (Lichtenstein, 2008)

The initiation of carcinogenesis usually requires only a single exposure to carcinogens, while carcinogenic progression involves multiple exposures to various carcinogenic agents which do not necessarily directly damage DNA. Promotion of carcinogenesis involves conversion of tissue into a heterogeneous malignant phenotype. Maintenance of malignant tumours requires carcinogens to propagate conformational and functional DNA changes in critical genetic targets which include proto-oncogenes, tumour suppressor genes and transcriptional regulatory sequences. Cellular and molecular events of multi-stage carcinogenesis also employ chromosome translocation, amplifications and gene transposition in malignant transformation. (Weinstein et al., 1988)

The paradigm of carcinogenesis not only involves alternative differentiation of cells which are susceptible to transformation, but also the ability of human tumours to hyper-activate signalling networks. Hyper-activation mechanisms may include constitutive activation of receptors, over production of ligands or over production of receptors. (Burstein, 2005; Lichtenstein, 2008) The common view that carcinogenesis is synonymous with transformation (differentiation) is opposed by the notion that epigenetic features may be specific to a sub-population of pre-existing cancer stem (progenitor) cells. A theory that harmoniously encompasses both points is that differentiation of pre-existing cancer stem cells results in transformation. (Lichtenstein, 2008)

1.1.2 Physiology of Normal Cells

Usually, cells existing in a quiescent state are dependent on mitogenic (chemical substance which encourages cell to commence division) growth signals. Furthermore, they respond to anti-growth signals which result in either a quiescent state (G0) or a post-mitotic state of specific differentiation. Specific differentiation results in cells which are incapable of further proliferation. The ability to induce programmed cell death (apoptosis) is latently present in all cell types; appropriate physiological stimuli result in a precisely ordered series of events, culminating in cell death.

Apoptotic signalling can be divided into sensors which monitor the intra- and extra-cellular environments, and which then regulate effector components. Death signals are conveyed via Fas ligands (FasL) and tumour necrosis factor-α (TNF-α) binding to Fas receptor (FasR) and tumour necrosis factor receptor-1 (TNF-R1) receptors respectively. To maintain order within the body, a limit to replication potential is intrinsically inherent in all cells and this appears to be independent of signals from surrounding cells or the microenvironment. This limit to replication, also known as senescence in normal cells, is determined by the progressive loss of telomeric DNA from chromosomes during replication. (Hanahan, Weinberg, & Francisco, 2000)

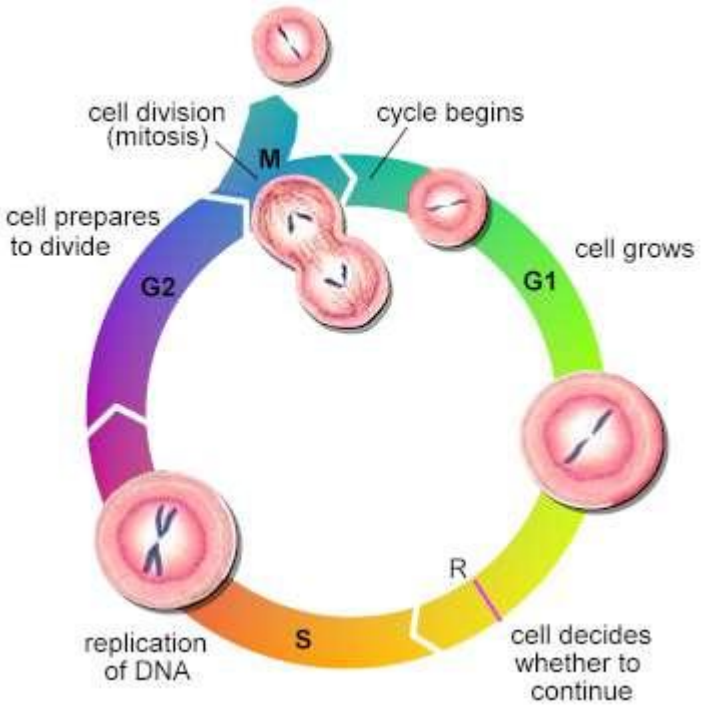

Figure 1.1: Schematic overview of the cell cycle ("Cell cycle Image")

1.1.3 Physiology of Cancer Cells

While diverse mechanisms for oncogenesis result in multiple genotypes, six essential physiological modifications are thought to collectively dictate malignancy. These distinctive hallmarks include self-sufficient growth signals, evasion of programmed cell death, insensitivity to growth inhibitory signals, limitless potential for replication, sustained angiogenesis and the ability to metastasise and invade other tissue. In stark contrast to the physiological processes occurring in normal cells, tumour cells possess a reduced dependence on exogenous growth signals, which suggests the presence of acquired growth signal autonomy and decreased dependence on the surrounding micro-environment.

Cancer cells are capable of evading terminal differentiation and disruption of anti-growth signalling which most often converges with the retinoblastoma protein (pRb) pathway and other components governing G1 cell cycle transition, resulting in unlimited proliferation. Acquired resistance to apoptosis commonly occurs by mutation of the pro-apoptotic regulator p53 tumour suppressor gene. Furthermore, anti-apoptotic survival signals transmitted via the phosphatidylinositol-3-kinase/protein kinase B (PI3-AKT) pathway may enable evasion of apoptosis in a substantial proportion of human cancers.

Telomere length maintenance in transformed cells results in unlimited replication potential and may be due to up-regulation of telomerase enzymes. The ability of cells to break free from primary tumour sites and colonize other regions of the body ultimately means that invasion and metastases are the primary cause of cancer related deaths. Alterations in cell-adhesion molecules (CAM) that anchor cells to their environment, such as E-cadherin, serve as an integral part of the acquisition of metastatic capabilities. (Hanahan et al., 2000)

These six distinct hallmarks of cancer create multiple potential targets for cancer treatment. However, they also provide many routes for cells to evade drug treatment and proceed through malignant pathways. Moreover, the implications of carcinogenic processes are not limited to cell type or location, which means that any cell in the body can become the source of malignant transformation.

1.2 Epidemiology of Breast Cancer

In 2008 an estimated 1.38 million new cases of breast cancer were diagnosed in women, which accounted for approximately 23% of all cancer diagnosed in women over this time period. Furthermore, breast cancer makes up approximately 10% of all cancers diagnosed worldwide in both sexes. These statistics make breast cancer one of the most common cancers in developed and developing regions. Breast cancer is now not only a major global health burden but is also becoming the primary cause of cancer related deaths in women. (Bray, McCarron, & Parkin, 2004; Ferlay et al., 2010)

The incidence of breast cancer varies, based on differences in reproductive, hormonal and nutritional factors between population groups as well as within geographical regions. As a result of changes in exposure to nutritional and reproductive determinants, an increase in incidence has been observed, with the lifetime risk of developing breast cancer in many Western countries now reaching as high as one-in-eight. (Bray et al., 2004)

Worldwide statistics paint a vivid image of the severity of breast cancer which are locally reflected by at least 1 in 29 South Africa women being diagnosed with this disease, with differences observed between population groups. (“CANSA - The Cancer Association of South Africa,”)

1.3 Defining Breast Cancer

Breast cancer is a heterogeneous disease comprising distinct histological and molecular subtypes that exhibit differences in both biological and clinical behaviour. (Weigelt, Geyer, & Reis-Filho, 2010; Callahan & Hurvitz, 2011) Tumour subtypes possess inherently different natural progression and thus require various primary and adjuvant treatment strategies. (Burstein, 2005)

1.3.1 Overview of Breast Cancer Subgroups

Breast cancers are divided according to histological grade and type: grade assesses the degree of differentiation while mitotic index and type refer to tumour growth patterns. The most common type of breast cancer is invasive ductal carcinoma not otherwise specified (IDC-NOS) [also referred to as of no special type (IDC-NST)] which fails to exhibit characteristics for special classification. At least 17 distinct histological types exist as special types and account for up to 25% of breast cancer diagnosed.

Terminology used to describe breast cancers, such as ductal and lobular carcinoma, define the architectural patterns and immunohistochemical profile and not the site of origin of transformation. Besides histological types, expression profiling has uncovered molecular subtypes which further contribute to the heterogeneity of breast cancer. (Weigelt et al., 2010)

1.3.2 Molecular Subtypes

Perou *et al*. (2000) put forward a molecular portrait of human breast cancer whereby a cluster analysis revealed division into oestrogen receptor (ER) positive and ER-negative, with each encompassing distinct molecular subtypes. Within this cluster analysis, the ER-positive branch was subdivided into luminal A and B whereas the ER-negative branch was subdivided into the normal breast-like, Her-2 positive and basal-like. (Perou et al., 2000; Weigelt et al., 2010)

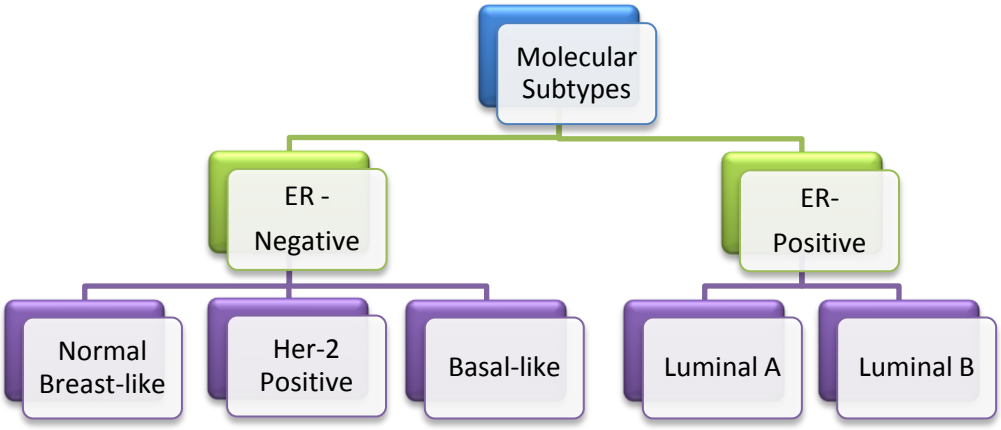

Figure 1.2: Division of Molecular Subtypes of Breast Cancer

This molecular portrait is not a definitive classification; further research may unravel subtypes that have not yet been identified. A hypothesis has been suggested that the underlying cause of breast cancer heterogeneity is dependent on the type of genetic event as well as the stage and degree of differentiation of the cell of origin. Understanding molecular features of cancer may provide treatment avenues with increased efficacy because of subtype specificity. (Weigelt et al., 2010)

1.3.3 Breast Cancer Treatment

The assumption that all cancers were localized diseases, lead to standard treatment approaches in breast cancer relying solely on surgery (radical mastectomy) for almost a hundred years. This was followed by the introduction of radiation, which makes use of high energy x-rays which produce cytocidal effects in cancerous tissue, and subsequent chemotherapy breakthroughs in the 1940's.

The combination of radiation and systemic chemotherapy has led to significant improvements in breast cancer treatment modalities. Chemotherapy may be received prior to surgery (neoadjuvant therapy) or following completion of surgery (adjuvant therapy). (Ferenc, Solár, Mikeš, Kovaľ, & Fedoročko, 2010)

Due to the diversity of breast cancer, chemotherapeutic strategies are multi-dimensional and often require potentiating or synergistic combinations. For many years, the gold standard in adjuvant therapy was anthracyclines, which include doxorubicin, epirubicin and daunorubicin. However, long term cardio-toxicity has become a limiting side effect of this approach.

Anthracycline-based regimens include combinations of non-selective anti-proliferative agents such as 5-fluorouracil, doxorubicin/epirubicin and cyclophosphamide. For ER-positive tumours, anti-oestrogens (tamoxifen) and aromatase inhibitors successfully antagonise oestrogen receptors or inhibit oestrogen synthesis. Resistance to long term oestrogen based therapy commonly arises. However, novel mechanisms to reduce aromatase inhibitor resistance may include MEK (MAP2K) inhibitors, Raf inhibitors, PI3K inhibitors, mTOR inhibitors and Akt inhibitors. (Ferenc et al., 2010)

1.4 Receptor Tyrosine Kinases

1.4.1 Her-Receptor Family

In the 1980's epidermal growth factor receptors (EGFR, also known as Her-1) and Her-2 (erbB-2/neu) receptors were strongly implicated in the aetiology of human cancer. Identification and characterization of this evolutionary ancient receptor family has played an important role in elucidating the function of monomeric receptor tyrosine kinases. (Kruser & Wheeler, 2010) The Her-family is composed of structurally related members EGFR (Her-1), Her-2, Her-3 and Her-4 which play a principal role in regulating vital cellular functions including proliferation, adhesion, motility and survival. (Hudis, 2007; Ross et al., 2009)

These monomeric tyrosine kinase receptors are large glycoproteins which consist of three structurally defined regions: two cysteine-rich regions in the N-terminal extracellular domain (ECD), a single-chain α-helix transmembrane domain and an intracellular tyrosine kinase domain. The kinase domain is flanked by a non-catalytic regulatory region and a C-terminal which are capable of intracellular signal propagation when initiated by tyrosine auto-phosphorylation sites. (Burgess et al., 2003; Zhang et al., 2005; Kruser & Wheeler, 2010)

Ligands for Her-1 (EGFR) stimulation include EGF, TGF-α, amphiregulin, betacellulin, epigen, epiregulin and heparin binding EGF-like growth factor (HB-EGF). Her-3 and Her-4 ligands include the isoforms of four structurally related heregulins (neuregulins). (Burgess et al., 2003) Her-2 receptors have no known ligands and are thus designated orphan receptors. (Ross et al., 2009)

The intricate Her-receptor network may also be functionally separated into an input layer, signal processing layer and an output layer. The input layer consists of ligands and receptor domains; high affinity Her-ligands all possess an EGF-like domain with three disulphide-bonded intra-molecular loops, which are usually part of a larger transmembrane precursor containing other structural motifs.

Specificity and potency within the signal processing layer is highly dependent on the ligand identity and receptor structural determinants. One of the main determinants is which phosphotyrosine sites are auto-phosphorylated within a dimeric complex and the resulting signalling proteins engaged. Furthermore, the extent of the kinetic signal processing depends on the Her-network switching the signal activity as well as ligand-mediated receptor endocytosis.

The output layer depends on cellular content and specific ligand-receptor dimers, which ultimately result in cell division, migration, adhesion, differentiation or apoptosis. Output is divided into mitogenic and transforming. Homo-dimeric complexes are less potent in these signalling categories than heterodimer complexes. (Yarden & Sliwkowski, 2001) Once signalling through homo- or heterodimers has occurred, receptors are internalized within endosomes and ligands are dissociated from receptors. Receptors are then either recycled back to the cell surface or undergo lysosomal degradation through c-Cbl (mammalian gene encoding E3 ubiquitin-protein ligase) mediated ubiquitinylation. (Friedländer, Barok, Szöllosi, & Vereb, 2008)

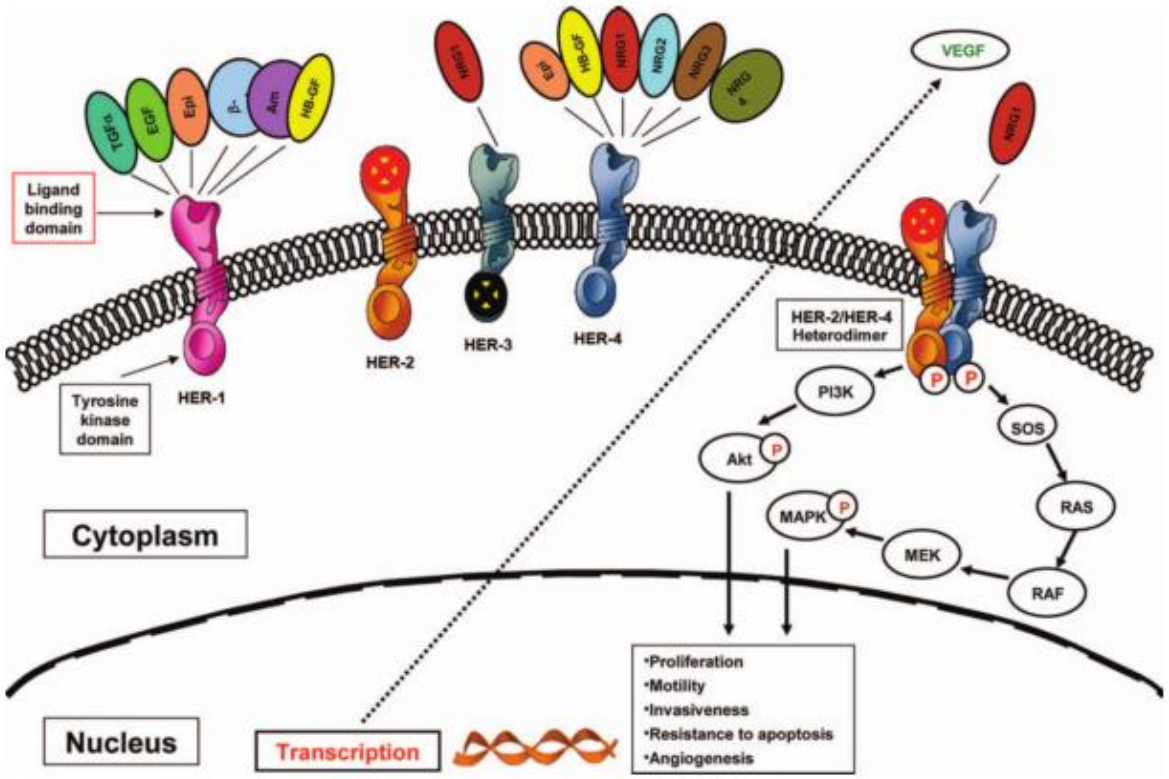

Figure 1.3: The human epidermal growth factor receptor gene family illustrating the complex crosstalk between members of the Her-family of receptor tyrosine kinases and intracellular signalling. Activated Her-receptors can function to both stimulate and inhibit downstream signalling of members of other biologic pathways. Her-2 mediated signalling is associated with cell proliferation, motility, resistance to apoptosis, invasiveness, and angiogenesis. (Ross et al., 2009)

1.4.2 Her-2 Receptors

The Her-2 receptor, a 185kDa (p^{185}) type 1 transmembrane glycoprotein, is encoded for by the human epidermal growth factor receptor (Her-2) gene and is normally expressed on the luminal surface of mammary epithelial cells. Her-2 receptors are designated orphan receptors because they reflect a similar structure to members of the Her-family but are not activated by any of the EGF family of ligands. (Schechter et al., 1984; Ross et al., 2009)

The apparent ligand independence of Her-2 receptors implies that alternate mechanisms for receptor activation are required. (Burgess et al., 2003) Activation of Her-2 receptors is therefore achieved via a process of dimerization whereby ligand activated receptors require interaction with a similar, related or identical structure in order to activate the intracellular signal cascade. (Ross et al., 2009; Yarden & Sliwkowski, 2001) The formation of these interactive dimers suggests that the signalling characteristics of the Her-family receptors are strongly interdependent. (Burgess et al., 2003)

The Her-2 receptor possesses a valine-glutamic acid substitution in the transmembrane domain which results in the ECD remaining in the open (active) conformation and consequently the dimerization arm remains constitutively exposed. This suggests that Her-2 receptors may be a preferred dimerization partner for other Her-family members. (Hutchinson & Muller, 2000; Kruser & Wheeler, 2010) The ability of the intracellular Her-2 receptor domain to auto-phosphorylate may further contribute to an increase in neoplastic transformation potential and functionality as a constitutively active kinase. (Mountzios, Sanoudou, & Syrigos, 2010)

Signalling via receptor tyrosine kinases involving homo- or heterodimer formation results in auto-phosphorylation of receptor cytoplasmic tail residues that offer docking sites for a variety of endogenous signalling molecules, adaptor proteins and enzymes, which are capable of simultaneously initiating multiple signalling cascades to promote physiological outcomes. (Hutchinson & Muller, 2000; Yarden & Sliwkowski, 2001; Kruser & Wheeler, 2010) Her-2 receptor heterodimers involving Her-3 receptors are considered the most potent signal transduction complex with the highest mitogenic potential. (Burgess et al., 2003; Tai, Mahato, & Cheng, 2010)

Patterns of dimerization ultimately influence downstream signalling pathways; different dimeric combinations are believed to mediate alternative intracellular signalling cascades which are linked to a diverse group of cellular functions. Mitogen activated protein kinase (MAPK) is an invariable target of Her-2 receptor containing dimers and leads to cell proliferation. Meanwhile, phosphatidylinositol-3-kinase (PI3K/Akt) pathways are predominantly mediated by Her-2:Her-3 heterodimers and promote cell survival. (Tai et al., 2010) Inevitably the dimers formed influence the potency and kinetics of the activated pathways. (Yarden & Sliwkowski, 2001; Friedländer et al., 2008)

Interestingly, the ability of some Her-family ligands to bind multiple primary receptors and the ability of Her-2 over-expression to bias heterodimer formation and broaden ligand specificity, may lead to possible redundancy of Her-family ligands. Her-3 receptors are incapable of intrinsic kinase activity; this indicates that under normal conditions that neither Her-2 nor Her-3 are capable of linear signalling in isolation, but are strongly dependent on horizontal networks of interaction. These horizontal networks can be adversely utilized when over expressed receptors spontaneously homo-dimerize or bias the type of dimers formed. (Yarden & Sliwkowski, 2001)

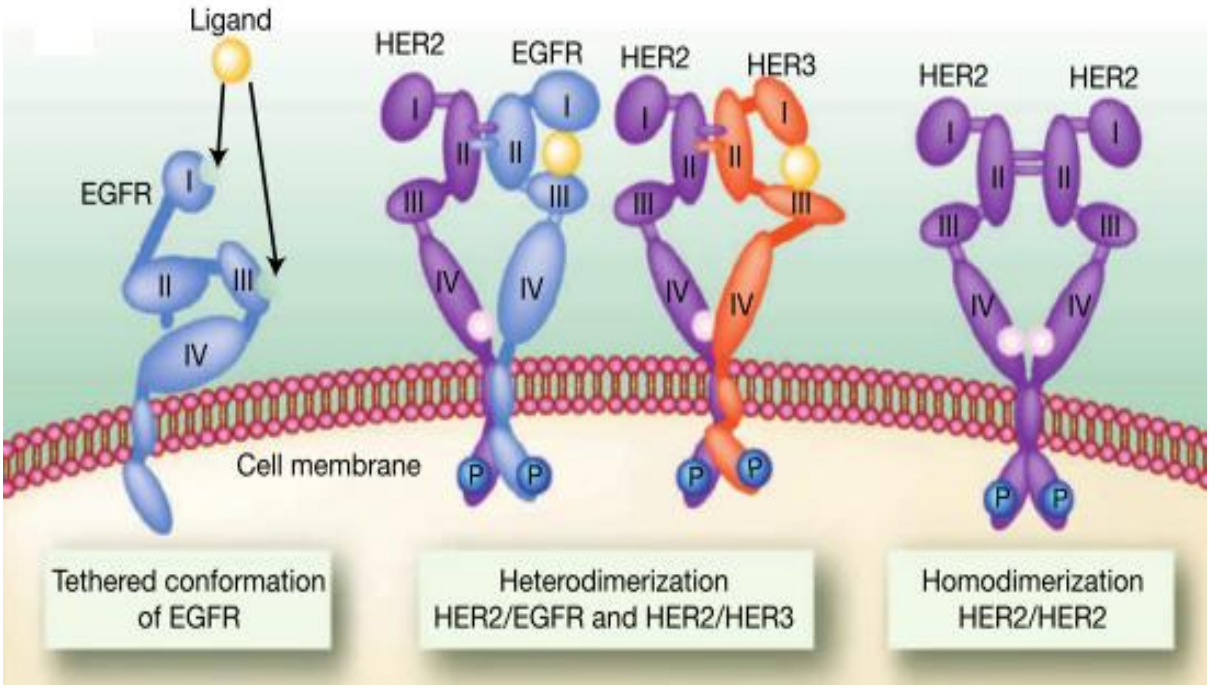

Figure 1.4: Receptor dimerization is required for Her-2 function. In the absence of a ligand, EGFR (Her-1), Her-3, and Her-4 assume a tethered conformation. In tethered receptors the dimerization site from extracellular domain II is hidden by intra-molecular interactions between domains II and IV. Growth factors alter the conformation of these receptors by binding simultaneously to two sites on extracellular domain domains: I and III. Her-2 occurs in an open position and is naturally ready for dimerization. Although no ligand has been identified for Her-2, the receptor may become activated by homodimerization or heterodimerization. (Pohlmann, Mayer, & Mernaugh, 2009)

1.4.3 Her-2 Receptor Dimers and Clusters

Characteristics such as modularity, redundancy and the opportunity for various combination interactions are an important aspect of signal diversification of the Her-signalling network. Modularity is a theory by which a continuum exists defining the degree to which system components are separate or interact. This is displayed in the Her-family by strong internal connections while maintaining weaker environmental connections. Further characterisation of the Her-family network illustrates a bow-tie structure, where the input of multiple growth factors with overlapping specificities activate dimers which promote signalling through a common signalling pathway or core process after which gene translation through multiple transcription factors leads to multiple outputs. (Citri & Yarden, 2006)

Crystallographic analysis illustrates that Her-family ligands induce a transition of Her-receptors from a closed to an open conformation which are then capable of dimerization via domain II interactions**.** That Her-receptors exist as inactive monomeric receptors which undergo ligand induced dimerization prior to activation is currently undergoing reconsideration due to new insights. Firstly, it has been suggested that inactive receptors may not be monomeric in nature and secondly, that high order clusters of receptors in both active and inactive states may exist. (Nagy, Claus, Jovin, & Arndt-Jovin, 2010)

Her-family structure suggests that the basic functional unit of Her signalling is the receptor dimer which appears to exist in a pre-dimerized state. Each receptor consists of four sub-domains; leucine-rich repeats in sub-domain I and II (also designated L1 and L2) form right-handed β-sheets capped by an α-helix responsible for ligand binding. Laminin-like, cysteine-rich sub-domains II and IV (also designated CR1 and CR2) are responsible for inhibitory interactions by sequestering the dimerization loop through direct intra-molecular interactions of cysteine groups essentially resulting in a form of auto-inhibition. (Citri & Yarden, 2006; Friedländer et al., 2008)

Pre-dimerized homo and heterodimers are partnered back-to-back with the dimerization arm in domain II of one receptor binding to the docking site at the base of domain II of the other receptor. Inhibitory interactions result in low affinity for ligands. However, simultaneous ligand binding to domains I and II alters the relative orientation of the receptor extracellular domain and relieves the inhibitory interactions between domains II and IV. High affinity ligand binding then results in the stabilized dimer undergoing a forced rotation within the membrane vicinity, and activates receptor kinase activity. (Citri & Yarden, 2006; Friedländer et al., 2008)

While biochemical, molecular and biophysical techniques have been utilized to uncover homo- and hetero-association, the detection of large scale cluster associations in addition to dimerization have not been studied as conclusively. Local accumulation of Her-family receptors may provide a focusing effect whereby an enhanced efficiency of transmembrane signalling occurs. Scanning near-field optical microscopy (SNOM) has been used to detect and characterise Her-2 cell surface clustering. For instance, Nagy *et al*. (1999) demonstrated that in addition to classic small-scale dimer associations, uneven large-scale clustering of Her-2 protein occurs on the cell surface. However, they did not determine the organization of dimers within clusters. The implication of clusters in transmembrane signalling has not yet fully been elucidated.

It was also concluded that inactive Her-1 receptors are monomeric at normal physiological levels, but density-dependent ligand-independent cluster formation occurs when over-expressed. Homoclusters of Her-2 receptors were found to possess stronger interactions than Her-1 receptors, but remained capable of being recruited into heterodimers in the presence of appropriate ligands. In the absence of ligands, pre-formed Her-2 clusters are composed of micro-clusters (5-15 receptors) associated into macro-clusters. Misinterpreting or ineffectively targeting these complex molecular mechanisms which occur in over-expressed receptor tyrosine kinases could result in failure to clinically manipulate tumour regression. (Nagy, Claus, Jovin, & Arndt-Jovin, 2010)

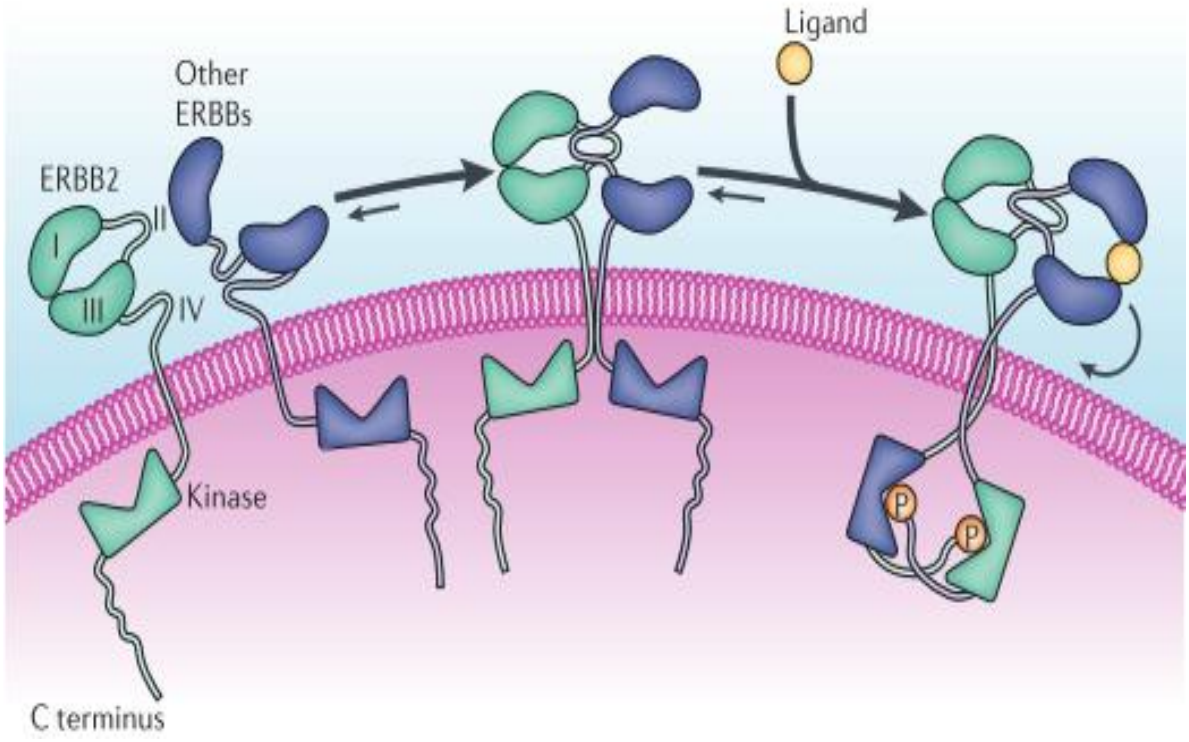

Figure 1.5: Structural basis for Her-receptor dimerization and activation. A steady-state equilibrium between receptor monomers and Her-2 (erbB2) containing heterodimers, in which dimerization is driven by ligand binding and by the constitutively active conformation of Her-2. By stabilizing a dimer and forcing a rotation in the vicinity of the membrane, Her-receptor (ERBB) ligands activate the kinase activity of the receptor. The prototypic Her in its monomeric state is autoinhibited through an interaction of domain II with domain IV. This interaction keeps subdomains I and III at a distance that does not allow the simultaneous binding of a ligand to both subdomains, and at the same time sequesters the dimerization loop. In the dimeric, ligand-bound form, domains I and III are brought together, driving a separation of the inhibitory domain II–IV interaction, which promotes the accessibility of the dimerization loop within domain II for interaction with the docking site on the dimerization partner. By contrast, the structure of Her-2 is consistent with its role as a preferred dimerization partner of the other Her-receptors: the dimerization loop of Her-2 is constitutively extended, even in the monomeric state, and a strong interaction of domains I and III closes the binding pocket, which abolishes accessibility to ligands.(P: phosphate) (Citri & Yarden, 2006)

1.5 Her-2 Positive Breast Cancer

1.5.1 Incidence of Her-2 Receptor Over-expressing Breast Cancer

Over expression of Her-2 receptors, or Her-2 gene amplification, is found in 25-30% of all primary breast tumours as well as in their metastatic sites. The mechanism of selective amplification of the Her-2 oncogene and related genetic elements is unknown, but the resulting increase of surface Her-2 receptors on tumour cells creates a unique molecular subtype of breast cancer. (Burstein, 2005)

1.5.2 Prognosis

When considering the vital functions of Her-2 receptors under normal physiological conditions, one may associate Her-2 over-expressing tumours with an increase in cellular proliferation, tumour invasiveness and motility. This makes the Her-2 receptor a clinically relevant molecular constituent of breast cancer. Over-expression is also found to correlate with lack of steroid hormone receptors, aneuploidy and a high percentage of cells in the S-phase, suggesting a proliferative advantage of these cells. (Yarden & Sliwkowski, 2001) Her-2 positive cancer is aggressive; elevated Her-2 receptor expression is observed in ductal carcinoma in-situ and invasive ductal carcinomas, but seldom in benign disorders such as hyperplasia. (Hutchinson & Muller, 2000)

A general trend of Her-2 receptor expression correlating with pathological conditions of higher histological grades of breast cancer is evident. However, gene amplification is not always seen in the natural disease progression of breast cancer. (Zhang et al., 2005) Her-2 over expressing breast cancer has been associated with a poor prognosis and a decrease in overall survival, which demonstrates clinical relevance for targeted therapy. (Borowsky, 2007; Ross et al., 2009)

Despite multiple functional abnormalities being present, tumour dependence on membrane bound Her-1 and Her-2 receptors is well established. (Kruser & Wheeler, 2010) Proliferation and survival appears to require only this single oncogenic pathway, which may be a result of Her-2 receptor resistance to internalization and high rate of recycling to the cell surface. (Pedersen et al., 2009) While homo- and heterodimer patterns have in general been characterised, it appears that when Her-2 receptors are over-expressed, the dimerization of receptors results in signalling properties that differ significantly from those normally found within this receptor family. (Burstein, 2005)

1.6 Molecular Targeted Therapy

1.6.1 General

Standard chemotherapeutic agents used for cancer therapy generally possess little selectivity for cancer cells and instead target all rapidly dividing cells. This leads to severe toxicity to normal tissue. Minimising this toxicity often requires chemotherapeutic agents to be administered at suboptimal doses, resulting in therapy failure. (Pero, Shukla, Cookson, Flemer, & Krag, 2007)

In contrast, targeted therapies are directed against accurately defined molecular targets implicated within the specific process of neoplastic transformation. The definition for molecular targeted therapies therefore does not take into account cytotoxic agents used in cancer chemotherapy such as alkylating agents and anti-metabolites or agents with a targeted approach such as topo-isomerase inhibitors and taxanes. While topo-isomerase inhibitors and taxanes are directed against a specific cellular target, the mechanisms of action of these agents are not solely associated with tumorigenesis, but are also related to normal biological processes. Meanwhile, molecular targeted therapies selectively target cancer cells, while reducing damage to cells with physiologically normal expression levels of the target. (Mountzios et al., 2010)

The biological diversity of breast cancer compels treatment strategies to focus on the prominent biological features represented within the distinctive breast cancer class. This requires redefining treatment principles. (Burstein, 2005) Her-2 receptors, localized on the cell surface, have become major targets for attempting medical interventions in a personalized molecular therapy context. The prevalence of Her-2 receptor expression is now not only used as a prognostic indicator for survival, but also as a predictor of response to targeted treatment. (Kruser & Wheeler, 2010)

1.6.2 Trastuzumab

Trastuzumab (Herceptin®; Genentech Inc, South San Francisco, CA), is a recombinant, DNA derived, humanized, anti-Her-2 monoclonal antibody, which was first licensed as a molecular targeted therapy in 1998 for use in Her-2 positive metastatic breast cancer. This targeted mAb has become an integral part of treatment regimens and has dramatically altered the natural history of this breast cancer subtype. (Perez et al., 2008; Kruser & Wheeler, 2010) Trastuzumab selectively and specifically binds to subdomain IV of the receptors' extracellular domain. (Tai et al., 2010)

Trastuzumab, which has a higher affinity than its murine predecessor, was synthesised on the foundation that the murine monoclonal antibody (mAb 4D5) was found to bind successfully to the Her-2 extracellular domains and inhibit cancer cell growth. Murine antibodies are immunogenic and therefore clinically limited. Humanising was accomplished by inserting the complementary determining region of the murine monoclonal antibody into a human IgG1 frame. (Zhang et al., 2005)

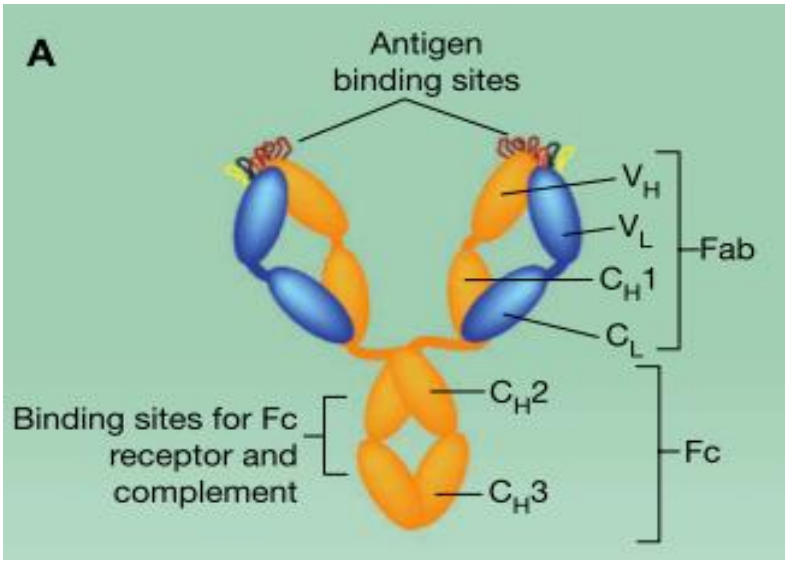

Figure 1.6: Trastuzumab schematic (IgG1 kappa). Fab (antigen binding region) and the Fc (immune responses) portions of IgG1. CH1 to CH3 indicate the heavy chain constant (domains 1 to 3) and CL indicates light chain constant domain. VH and VL denote the respective variable heavy and light chains (Pohlmann et al., 2009)

1.6.3 Trastuzumab: Mechanism of Action

Following binding to the Her-2 receptor, the multifaceted mechanism of trastuzumab action includes, but is not limited to, the induction of antibody-dependent cellular cytotoxicity by its Fc-domain and inhibition of downstream signalling, resulting in apoptosis. Furthermore, reduction of signalling through the PI3/Akt and Ras/Raf/MEK/MAPK pathways leads to alterations in cell cycle pathways, down-regulation of Her-2 protein expression and inhibition of DNA repair. (Morrow, Zambrana, & Esteva, 2009; Callahan & Hurvitz, 2011) Her-2 receptor degradation and internalisation possibly lead to a decrease in Her-2 receptor density and subsequent decrease in signalling, but not all studies illustrate an ultimate change in receptor density. (Kruser & Wheeler, 2010)

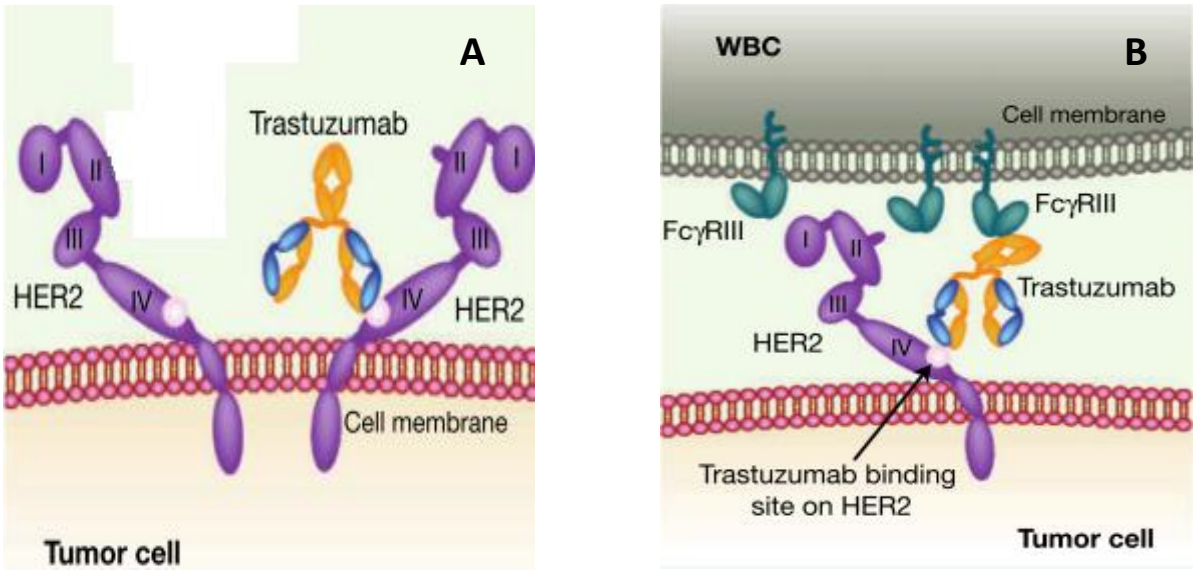

Figure 1.7: (A) Trastuzumab Fab-related function results from its binding to domain IV of Her2. (B) Trastuzumab Fc-related functions result from Fc portion binding to immune cells that express Fcγ receptor III (RIII) and trigger tumour cell death via antibody-dependent cell cytotoxicity (ADCC) (WBC :white blood cell) (Pohlmann et al., 2009)

The mechanism of action of therapeutic antibodies is not based solely on target specificity but also on the antibody structure. In addition to manipulation of multiple signalling pathways, antibodies are complex and immunologically active, which may result in complement-dependent cellular cytotoxicity. (Friedländer et al., 2008)

1.6.4 Patient Eligibility for Her-2 Directed Treatment

Optimal clinical use of trastuzumab is dependent on clearly defining the molecular mechanisms of cellular response. A defined threshold of Her-2 receptors that guarantees response to trastuzumab has not been determined. However, patients may only receive trastuzumab if Her-2 positive receptor expression has been confirmed using Food and Drug Administration (FDA) approved methods such as immunohistochemical (IHC) grading systems, fluorescence *in situ* hybridization (FISH) and chromogenic *in situ* hybridization (CISH). (Rhodes et al., 2002; Emlet et al., 2006)

FISH analysis is thought to have a greater predictive value for response to targeted therapy because it is not a subjective technique that relies on experience and opinion like IHC. (Callahan & Hurvitz, 2011) FISH possesses a decreased susceptibility to variation in tissue fixation as DNA is more resistant to formalin fixative induced damage. (Gong, Booser, & Sneige, 2005)

The IHC grading technique uses a standard method which simply describes the level of Her-2 membrane staining of the cells. A grade between 0 (no stain) and 3+ (strong complete membrane stain) is attached to the intensity of the stain. This then correlates to the level of receptor expression. (Rhodes et al., 2002) In order for the level of Her-2 receptor expression to be meaningful, a relationship between the intensity of the immunostain and the actual number of receptors was established. Correlations have been determined to approximate the following: a 0 immunostain showing no membrane staining indicating less than 20, 000 receptors per cell, 1+ immunostain showing partial membrane staining indicating 100, 000 receptors per cell, 2+ immunostain showing moderate to complete staining indicating 500, 000 receptors per cell and a score of 3+ immunostain showing complete membrane staining indicating greater than 2 million receptors per cell. For trastuzumab treatment eligibility, a score of 3+ is required. (Ross et al., 2009)

1.6.5 Alterations in Receptor Density

Gong *et al.* (2005) performed a retrospective study using FISH to compare Her-2 status in primary and (loco-regional or distant) metastatic tumour tissue and further assessed the effect of chemotherapy on Her-2 receptor status. Paraffin-embedded tissue or fine needle aspiration specimens illustrated no substantial intra-tumoural heterogeneity and concordances of 97% between primary and metastatic tissue were found. It was concluded that while Her-2 genes may be involved in initiation of carcinogenesis, this does not necessitate Her-2 requirement in tumour progression. However, in this study 40 of the 60 tumours assessed were Her-2 negative and the only discordances observed were in Her-2 positive tumours. (Gong et al., 2005) Studies like this lead to the notion that once Her-2 gene or receptor amplification had occurred within the tissue, the alterations were maintained throughout the entire progression of the cancer. This would suggest that primary and metastatic sites would essentially be identical. Even though initial studies suggested that Her-2 receptor status remained stable over time in Her-2 positive tumours, discordances between primary and metastatic sites are now being reported to reach up to 30%. (Lower, Glass, Blau, & Harman, 2009)

The concept of receptor stability lead to trastuzumab eligibility being based solely on the analysis of primary tumours. With the evidence of discordances coming to the fore, implementation of primary and metastatic site analysis may become common clinical practice in order to maintain efficacy of targeted treatments and stratify patients into appropriate therapeutic categories. (Lower et al., 2009) Whether or not chemotherapy is the primary cause of modifications in Her-2 targets or whether clonal selection during tumour progression results in differential characterisation of cell populations, is not fully understood.

1.6.6 Response to Trastuzumab Treatment Regimens

In 2005, results from three pivotal trials (National Surgical Adjuvant Breast and Bowel Project [NSABP] trial B-31, the North Central Cancer Treatment Group [NCCTG] Intergroup trial N9831 and the Herceptin Adjuvant [HERA] trial) assessing trastuzumab in an adjuvant setting were presented at the 41st Annual Meeting of the American Society of Clinical Oncology. These results showed a significant decrease in the risk of Her-2 positive breast cancer relapse when trastuzumab was administered in combination with chemotherapy, leading to the rapid adoption of targeted agents within the clinical setting. (Telli, Hunt, Carlson, & Guardino, 2007)

Trastuzumab in combination with chemotherapy or as a single agent has become the backbone of systemic treatment for Her-2 positive breast cancer within the metastatic, neoadjuvant and adjuvant settings. (Callahan & Hurvitz, 2011) Traditionally, cancer therapy is based on the introduction of new agents to already accepted or implemented regimens, but determination of optimal molecular interactions remains of great importance. (Pegram et al., 2004) Optimizing the clinical role of trastuzumab has been attempted by administration in combination with chemotherapy, such as sequential administration of doxorubicin (anthracycline antibiotic) and cyclophosphamide (alkylating agent) followed by paclitaxel (mitotic inhibitor) combined with trastuzumab or preceding trastuzumab, occurring in weekly cycles. (Perez et al., 2008)

1.6.7 Trastuzumab and Cardiotoxicity

Her-2 receptors are believed to play a critical role in the development of the embryonic heart and are hypothesised to modify stress responses in adult counterparts. A proposed model of trastuzumab-induced cardiotoxicity suggests that a loss of Her-2 signalling after trastuzumab use leads to failure of the stress responses; subsequent stress then results in an increase in cardiotoxicity susceptibility especially when co-administered with other cardiotoxic agents such as anthracyclines. (Telli et al., 2007)

Therefore, while treatment regimens including anthracyclines confer benefit in cancer regression, cardiac dysfunction including cardiac arrhythmia, heart failure and altered left ventricular function have been reported. (Dang et al., 2008) While differences exist in the definition of cardiotoxicity across clinical trials, and inclusion-exclusion criteria may differ, some observations are apparent. The emergence of asymptomatic cardiac dysfunction cannot be solely attributed to the chemotherapy or targeted agent, yet up to 4% of patients enrolled in adjuvant trastuzumab trials require trastuzumab discontinuation due to the emergence of cardiac issues. (Telli et al., 2007)

Thus, a cautious approach is required and the clinical benefit needs to be outweighed with the risk of cardiotoxicity. The ability to reverse cardiac dysfunction and restore Her-2 receptor signalling subsequent to discontinuation of trastuzumab still remains uncertain. (Telli et al., 2007) Heart failure is a progressive disease which evolves over time. The implications of trastuzumab involvement may go far beyond current clinical objectives.

1.6.8 Trastuzumab Resistance

Despite trastuzumab having enhanced selectivity for tissue containing over expressed targets, the efficacy of these treatment regimens is still hampered by inter-individual variation in response. Some studies have implied that only 30-40% of patients derive substantial clinical benefit and that long term disease remission is not achieved in 80-85% of patients. (Mountzios et al., 2010) While the most simple cause of resistance is the disruption of trastuzumab:Her-2 receptor interactions, other causes of primary and secondary resistance have prompted exploration into more effective regimens for clinical use. It has been suggested that de-novo resistance occurs in up to as many as 50% of patients, with acquired resistance often appearing early after initial response. (Callahan & Hurvitz, 2011)

Trastuzumab resistance may be a result of masking Her-2 by over-expression of components such as Mucin-4 cell surface associated protein (MUC4), CD44 (cell-surface glycoprotein) and Insulin-like Growth Factor-I Receptor (IGF-IR). MUC4 is a membrane associated, highly glycosylated protein which may sterically influence trastuzumab binding. CD44 is a hyaluronan receptor which is integral in lymphocyte homing capabilities and is capable of increasing trastuzumab cell surface clearance. Down-regulation of both MUC4 and CD44 result in an increased sensitivity to trastuzumab and may restore immune cell recruitment. IGF-IR diminishes trastuzumab responsiveness by interacting with PI3K/Akt and MAPK pathway processes as well as physical receptor interactions resulting in Her-2 phosphorylation. (Friedländer et al., 2008)

Mechanisms of primary resistance also include the expression of a truncated form of Her-2 (p95-Her-2) which lacks the trastuzumab binding regions within the extracellular domain, upregulation of alternative signalling pathways, and autophagy, which enables recycling and repackaging of proteins integral to cell survival. (Guarneri, Barbieri, Dieci, Piacentini, & Conte, 2010; Callahan & Hurvitz, 2011)

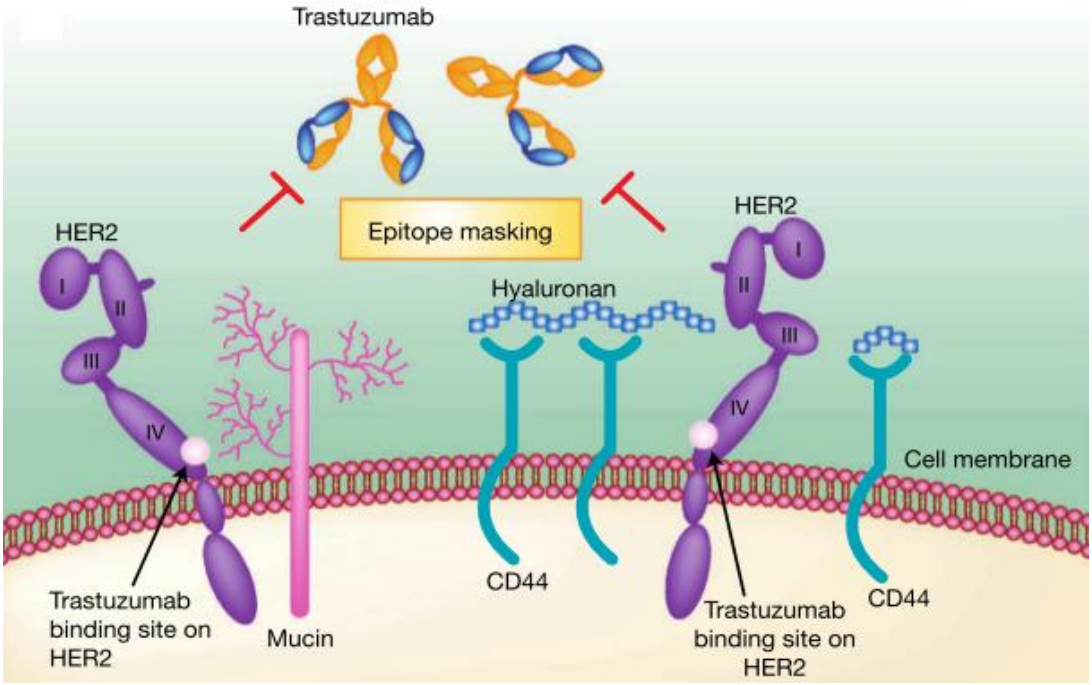

Figure 1.8: Trastuzumab resistance: Masking of trastuzumab binding epitope. Masking of trastuzumab binding epitopes by MUC4 or CD44/polymeric hyaluronan complex interfering with trastuzumab binding activity. MUC4 is a large membrane-associated mucin which contains multiple repeat regions. Glycosylation of these repeats forces them into a highly extended, rigid, hydrophilic conformation. MUC is produces by epithelial cells and is found to be over-expressed in several carcinomas and close association with Her-2 and may mask trastuzumab cognate (of same or similar nature) epitopes. CD44/hyaluronan polymer complex activates RAS and PI3K pathways, however, it is unclear whether these effects depend on Her-2 receptors. Inhibition of hyaluronan synthesis in vitro reduces hyaluronan polymer binding to CD44, and increases trastuzumab binding to Her-2 receptors. (Pohlmann et al., 2009)

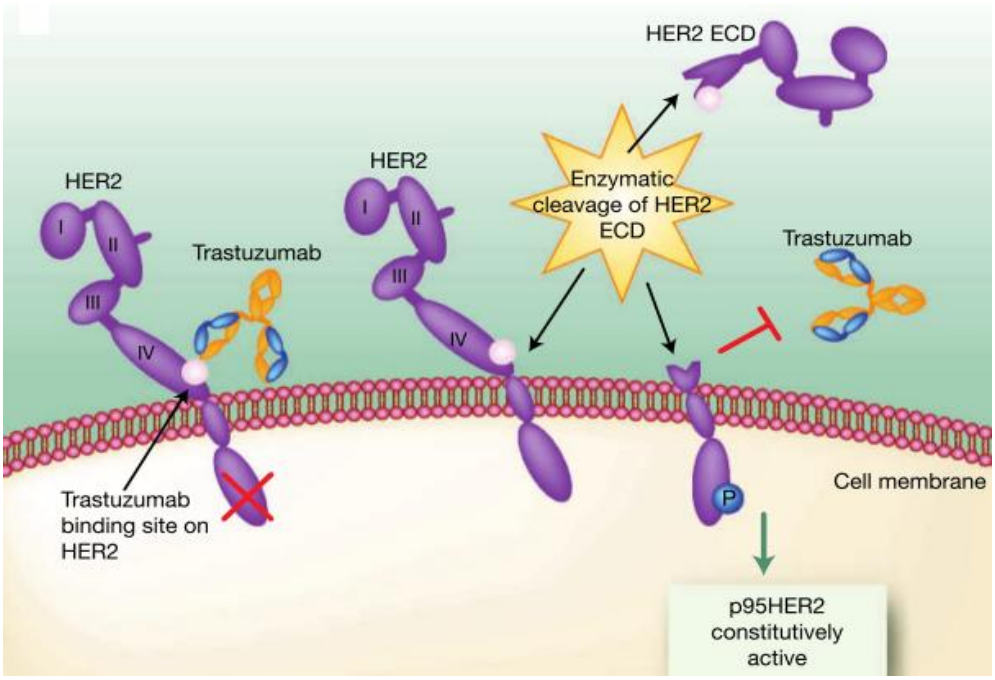

Figure 1.9: Trastuzumab resistance: A constitutively active truncated form of Her-2 receptors that has kinase activity but lacks the extracellular domain and the binding site of trastuzumab is originated from metalloprotease- dependent cleavage of the full-length Her-2 receptor (p185). Trastuzumab does not bind to p95HER2 and is therefore unable to elicit an effect against it. (Pohlmann et al., 2009)

1.6.9 Strategies to Increase Trastuzumab Efficacy

Pertuzumab inhibits Her-2 dimerization via extracellular binding near the junction of domain I-III, thereby inhibiting homo- and hetero-dimerization and mediation of ADCC along with inhibition of Akt pathway. Treatment naïve cells have shown synergistic effects of pertuzumab and concurrent trastuzumab. However, trastuzumab resistant cells possess decreased responses to pertuzumab, which suggests the presence of an intracellular signalling component of cross-resistance to Her-2 receptor targets. (Friedländer et al., 2008)

Further studies have evaluated the potential synergy of multiple Her-2 directed therapies such as combining trastuzumab with lapatinib, a small molecule tyrosine kinase inhibitor of both Her-2 and Her-1 receptors. (Callahan & Hurvitz, 2011) Newer Her-family targeting agents have now expanded to encompass antibodies, small molecule tyrosine kinase inhibitors (TKI), PI3K inhibitors, hsp90 inhibitors and mammalian target of rapamycin (mTOR) inhibitors. (Ferenc et al., 2010)

It is theoretically feasible that existing endogenous or exogenous compounds, not typically used as a part of chemotherapeutic regimens, may influence Her-2 receptor expression and/or clinical outcomes thereby directly or indirectly influencing the efficacy of trastuzumab. Compounds with potential to influence targeted therapy come from a variety of sources such as cyostatic or cytotoxic drugs, hormones and endogenous ligands which may potentiate or hinder efficacy because of lateral cross-talk between signalling pathways and the biological complexity of tumour micro-environments. This has lead to the identification of several agents that could potentially alter trastuzumab effects; these are discussed in more detail below.

1.7 Justification for Agents

1.7.1 Aspirin

Acetylsalicylic acid, better known as aspirin, is a non-steroidal anti-inflammatory drug (NSAID) known to have anti-neoplastic properties. A widely accepted mechanism of action for NSAIDs is the reduction of prostaglandin synthesis by inhibition of the inducible cyclooxygenase-2 (COX-2) pathway. It has been suggested that a coordinated relationship may exist between COX-2 and Her-2 signalling pathways. (Half, Tang, & Gwyn, 2002) Nam *et al*. (2005) found that COX-2 expression was significantly higher in Her-2 receptor over-expressing tumours compared to Her-2 receptor negative tumours, which suggests that selective inhibition of COX and Her-2 pathways may provide an added advantage in breast cancer management. This intriguing relationship made aspirin an interesting agent in the efficacy assessment of Her-2 targeting therapy.

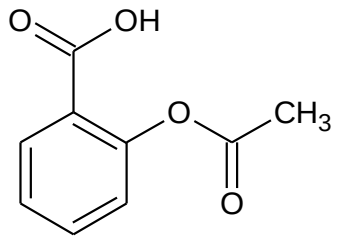

Figure 1.10: Structure of aspirin (acetylsalicylic acid)

(ACD/ChemSketch Freeware Version 11.1)

1.7.2 Calcipotriol hydrate

Calcipotriol (1,24-dihydroxy-22-ene-24-cyclopropyl-vitamin D3) is an active, low toxic synthetic derivative of vitamin D that retains similar anti-proliferative and differentiation effects to vitamin D. The vitamin D3 receptor (VDR) is a ligand dependent transcription factor implicated in the regulation of cell cycle, differentiation and apoptosis. (Zinser & Welsh, 2004) VDR are present in 80-90% of breast cancer cells which suggests that vitamin D analogues may be used for anti-proliferative effects in combination therapy for both oestrogen-dependent and independent tumours. (Buras et al., 1994; Nagpal, Lu, & Boehm, 2001)

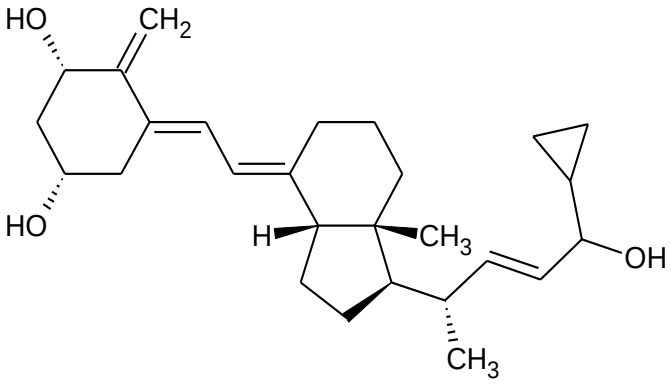

Figure 1.11: Structure of calcipotriol hydrate

(ACD/ChemSketch Freeware Version 11.1)

1.7.3 Doxorubicin hydrochloride

Doxorubicin, an anthracycline antibiotic, is one of the most effective anti-neoplastic agents used for the treatment of breast cancer. While determining the type of cancer with the greatest sensitivity to anthracycline antibiotics remains to a large degree inconclusive, multiple biochemical targets have been proposed. The most studied mechanism of doxorubicin action is to target topoisomerase II-α by maintaining the homodimeric enzyme on the 5' end of the DNA strand. (Campiglio et al., 2003) This inhibition of the topoisomerase II enzyme prevents the relaxing of super-coiled DNA. There remains strong evidence for effective anthracycline-trastuzumab regimens remain despite the reported incidence of cardiotoxicity. (Rayson et al., 2008)

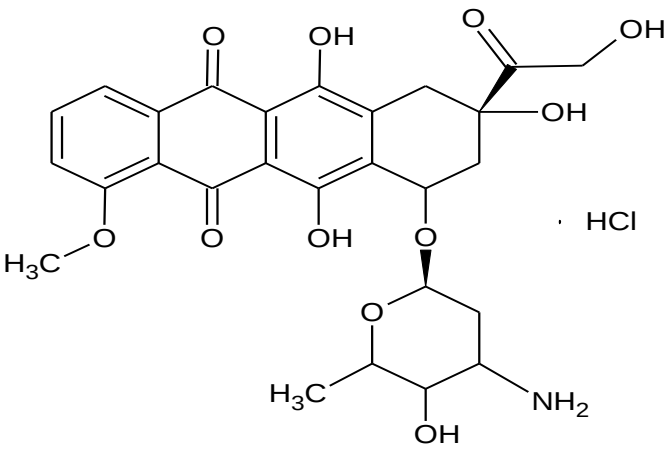

Figure 1.12: Structure of doxorubicin hydrochloride (ACD/ChemSketch Freeware Version 11.1)

1.7.4 Epidermal Growth Factor (EGF)

EGF is a polypeptide growth factor for Her-1 (EGFR) comprising 53 amino acids. Following binding, Her-1 receptors form homo- or heterodimers with Her-family members which then undergo rapid internalisation as a single entity. (Hendriks, Wiley, & Lauffenburger, 2003) Binding of receptor-specific ligands results in the formation of strongly interdependent interactive dimers with other Her-family members. (Burgess et al., 2003)

Cell membrane located Her-family receptor members, found in normal epithelium, are spatially and chronologically defined and are responsible for growth and differentiation of these cells. (Srinivasan, Poulsom, Hurst, & Gullick, 1998) Her-1 is expressed in approximately 45% of breast adenocarcinomas, most commonly associated with ER and PR negativity, which may result in synergistic effects within cellular transformation when coupled with Her-2 over-expression. (Koutras & Evans, 2008)

1 * ^ 15
NH_2 – Asn – Ser – Tyr – Pro – Gly – Cys – Pro – Ser – Ser – Tyr – Asp – Gly – Tyr – Cys – Leu -

16 * 30
Asn – Gly – Gly – Val – Cys – Met – His – Ile – Glu – Ser – Leu – Asp – Ser – Tyr –Thr -
^
31 # # 45
Cys – Asn – Cys – Val – Ile – Gly – Tyr – Ser – Gly – Asp –Arg – Cys – Gly – Thr – Arg -

46 53
Asp – Leu – Arg – Trp – Trp – Glu – Leu – Arg - COOH

Figure 1.13: Primary amino acid sequence of EGF (Richard, 1972)

Indicates that pair are involved in a disulphide bond (*)(^)(#)

1.7.5 Geldanamycin

Geldanamycin, a benzoquinone ansamycin, is capable of binding heat shock protein 90 (hsp90) which is a crucial "house-keeping" chaperone for a variety of cell signalling proteins. Ubiquitous hsp90 protein is constitutively expressed at higher levels in tumour cells than in normal counterparts. Antagonizing these multi-molecular chaperone complexes with geldanamycin results in client protein destabilization and degradation. (Bisht et al., 2003)

Under normal circumstances, hsp90 has a wide variety of client proteins which includes a diverse group of transcription factors as well as a variety of protein kinases involved in proliferation and cell cycle regulation. (Toft, 1998; Neckers, Schulte, & Mimnaugh, 1999) Furthermore, Her-2 receptors are thought to be client proteins of hsp90 and are consistently found to undergo geldanamycin induced polyubiquitination and proteosomal degradation. (Mimnaugh, Chavany, & Neckers, 1996; Bisht et al., 2003)

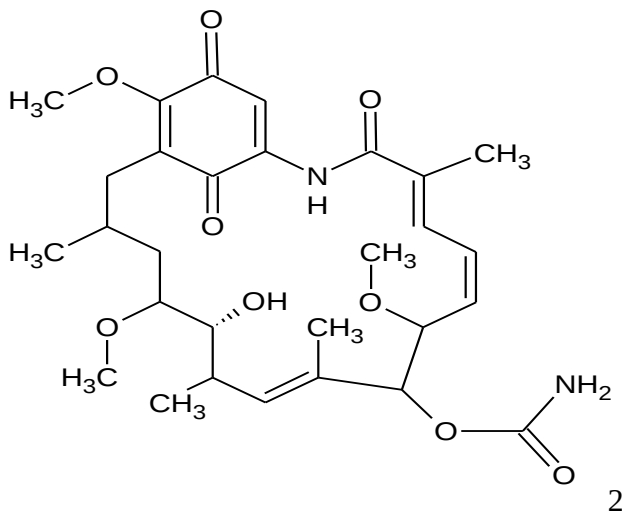

Figure 1.14: Structure of geldanamycin

(ACD/ChemSketch Freeware Version 11.1)

1.7.6 Heregulin-β1 (HRG- β1)

Heregulin-β1 (HRG-β1) and its isoform, heregulin-α (HRG-α) are polypeptide growth factors for both Her-3 and Her-4 receptors. Her-3 receptors are incapable of forming homodimers due to the absence of an active kinase domain. Therefore, signalling via Her-3 receptors in strongly dependent on lateral signalling requiring signalling competent heterodimers. It has been demonstrated that Her-2:Her-3 heterodimers are the most potent mitogenic Her-family pair and that co-operated signalling results in synergism in transformation. (Koutras & Evans, 2008; Pedersen et al., 2009)

177 * ^
NH_2– Ser - His - Leu - Val - Lys - Cys - Ala - Lys - Glu - Lys - Thr - Phe - Cys -

*
Val - Asn - Gly - Gly - Glu - Cys - Phe - Met - Val - Lys - Asp - Leu - Ser -

^ #
Met - Pro - Ser - Arg - Tyr - Leu - Cys - Lys - Cys - Pro - Asn - Glu - Phe -

226
Thr - Gly - Asp - Arg - Cys - Gln - Asn - Tyr - Val - Met - COOH

Figure 1.15: Primary amino acid sequence of heregulin-β1 (177-226)
(Barbacci, Guarino, Stroh, Singleton, Rosnck, Moyer & Andrews, 1995)

Indicates that pair are involved in a disulphide bond (*)(^)(#)

1.7.7 β-Oestradiol

Effects of oestrogen are primarily mediated via binding to oestrogen receptors (ER), a nuclear superfamily of ligand-regulated transcription factors. Oestradiol is capable of passive diffusion through the cell membrane and upon binding, conformational changes leading to homodimerization of ER result in interaction with oestrogen response elements and transcriptional regulation, bringing about genomic effects. (Stoica et al., 2003) Hormonal regulation of Her-2 receptor expression and function cannot be overlooked since research has noted an inverse correlation between Her-2 receptor expression and ER status. Postulated mechanisms include the ability of oestrogens to inhibit Her-2 receptors at mRNA level and repress transcriptional activity. (Antoniotti et al., 1994)

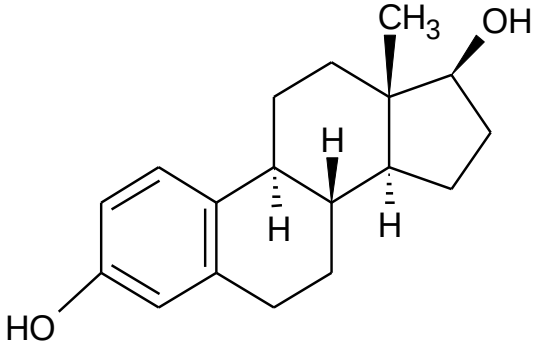

Figure 1.16: Structure of β-oestradiol

(ACD/ChemSketch Freeware Version 11.1)

1.8 Synopsis, Aims and Objectives

1.8.1 Synopsis

Her-2 positive breast cancer is found to be more aggressive, highly metastatic and carry an increased risk of recurrence and therefore a worse prognosis compared to other types of breast cancer. Current research is aimed at identifying accurate methods for diagnosing Her-2 positive breast cancer and identification of treatment strategies that will be more efficacious and decrease the prevalence of resistance. Understanding the links between alterations in Her-2 receptor expression and positive clinical outcomes remains critical.

While *in vitro* assays are essential for the determination of cellular components that may be present or absent within physiological processes, the absence of all cell-environment interactions may lead to inaccurate conclusions. However, *in vitro* models need to be completed to provide justification for the adoption of a mammary tumour model using these chemotherapeutic, ligand and hormonal combinations.

1.9 Research Aim

Trastuzumab is prescribed under strict inclusion criteria and is found to have a greater efficacy because it is reliant on binding specific targets (the Her-2 receptor) to bring about an effect. The aim of this study was to investigate the ability of chemical and biological molecules to alter or manipulate the *in vitro* cell viability, cell cycling, programmed cell death and Her-2 receptor expression in models of Her-2 receptor over-expressing and Her-2 receptor-normal adenocarcinomas and bring about alterations in the efficacy of trastuzumab.

1.9.1 Objectives

1. To determine the effects of selected agents on cell viability using the MTT cell viability assay
2. To determine the effects of selected agents on cell cycling using flow cytometric DNA quantification
3. To determine the effects of selected agents on programmed cell death via the detection of active executioner caspases and alterations in cell membrane symmetry by assessing annexin-V
4. To determine whether any of the selected agents affected surface Her-2 receptor density using flow cytometric assessment of whole cells
5. To ascertain whether any of the selected agents demonstrated additive or potentiation of effects when combined with trastuzumab

Chapter 2: Materials and Methods

2.1 Cell Culture

Adherent breast adenocarcinoma cell lines MCF-7 (ATCC Number: HTB-22™) and SK-Br-3 (ATCC Number: HTB-30™) were originally obtained from the American Type Culture Collection (ATCC; Manassas, USA) after which the cells were maintained and passaged within the Department of Pharmacology. All experiments conducted on human tissue were conducted under the certification and in accordance with the South African Human Tissue Act (No. 65 of 1983). Ethics approval for the use of commercially available human adenocarcinoma tissue was obtained from the Faculty of Health Science Student Research Ethics Committee of the University of Pretoria (Ethics number: S195/2012; see appendix).

2.1.1 Description of Breast Adenocarcinoma Cell Lines

MCF-7 and SK-Br-3 cells are epithelial cell lines derived from pleural effusions of breast adenocarcinoma and were both first isolated in the 1970's. MCF-7 cells are oestrogen receptor positive and retain the ability to process oestradiol via cytoplasmic oestrogen receptors, suggesting that this cell line still maintains characteristics of differentiated mammary epithelium. MCF-7 cells express physiologically normal levels of Her-receptors. ("ATCC: Catalog Search MCF-7,") SK-Br-3 cells are considered Her-2 receptor positive because Her-2 gene products are over-expressed whilst expressing physiologically normal levels of most other receptors and a notable absence of oestrogen receptors. ("ATCC: Catalog Search SK-Br-3,")

2.1.2 Culture Media and Conditions

MCF-7 and SK-Br-3 cells were maintained in Dulbecco's Modified Eagle's Medium (DMEM) and Roswell Park Memorial Institute Medium (RMPI 1640) respectively, supplemented with 10% heat-inactivated fetal calf serum (FCS) and 1% penicillin-streptomycin solution. Cells were incubated in a humidified atmosphere containing 5% CO_2 at a temperature of 37°C.

2.1.3 Preparation of Cells for Experiments

Cell culture work was conducted in a laminar flow cabinet and aseptic techniques and procedures were employed to maintain the integrity of sterile cultures. Adherent cells were rinsed with FCS free medium and then treated with a Trypsin/Versene (EDTA) solution facilitating release from the culture flask surface by protein hydrolysis. Cells were decanted into a centrifuge tube with FCS positive medium, to cease the serine protease action of trypsin, and centrifuged (200 *g*, 5 min). After discarding the supernatant, the cell pellet was aspirated with 1 ml of medium.

2.1.4 Cell Counting

Cells were counted using trypan blue exclusion in order to assess membrane integrity and determine the percentage of viable cells; 50 µl of the cell suspension was added to 450 µl of the counting fluid [0.2% (m/v) trypan blue solution]. The solution was loaded onto a haemocytometer and the cells counted using a Reichart Jung MicroStar 110 microscope. Counted cells were diluted to the appropriate concentrations for each experiment.

2.1.5 Cell Concentrations

Experiments conducted in 96 well plates (200 µl total volume), cells were seeded at a density of $1x10^4$ cells per well. For experiments conducted in 25 cm^2 flasks (3 ml total volume), cells were seeded at a density of $1.5x10^5$ cells per flask. Subsequently, cells were left overnight to adhere prior to being exposed to agents. Cells, medium and agents were seeded in a ratio of 5:4:1 for single compound assays and in a ratio of 5:3:1:1 for assays with concurrent trastuzumab.

2.1.6 Cell Culture Reagents

I. Bovine Fetal Calf Serum (FCS)

Fetal calf serum, which was heat inactivated at 56°C, was purchased from PAA Laboratories (Pasching; Austria). FCS was added to cell culture media to a final concentration of 10%.

II. Cell Counting Fluid

Counting fluid was made up to 0.2% (m/v) by weighing out 20 mg of trypan blue powder (Sigma-Aldrich; St Louis, USA) in 10 ml PBS (PBS: 9.23 g/L dH_2O).

III. Dulbecco's Modified Eagles Medium (DMEM)

DMEM powder (Sigma-Aldrich; St Louis, USA) was dissolved in sterile water (13.47 g/L). The pH was adjusted to 7.4 using $NaHCO_3$ (approximately 18.5 g) and medium was filter sterilised twice using a 0.22 µm cellulose acetate filter. Medium was supplemented with 1% penicillin-streptomycin solution (10 ml/L) and 10% fetal calf serum (FCS) which was subsequently stored at 4°C.

IV. Penicillin-Streptomycin Solution

Penicillin-streptomycin solution containing 10 000 units of streptomycin and 10 000 µg streptomycin/ml was added to culture media to a final concentration of 1% (v/v). (BioWhittaker; Walkersville, USA).

V. Phosphate Buffered Saline

FTA hemagglutination buffer (phosphate buffered saline: PBS)(BD Bioscience; Sparks, USA) was made using 9.23 g powder per litre dH_20 and stored at 4°C. Filter sterilisation using a 0.22 µm filter and pH adjustment were done when required.

VI. Roswell Park Memorial Institute medium (RPMI 1640)

RPMI 1640 powder (Sigma-Aldrich; St Louis, USA) was dissolved in sterile water (10.4 g/L). The pH was adjusted to 7.4 using $NaHCO_3$ (approximately 10 g) and medium was filter sterilised twice using a 0.22 µm cellulose acetate filter. Medium was supplemented with 1% penicillin-streptomycin solution (10 ml/L) and 10% fetal calf serum (FCS) which was subsequently stored at 4°C.

VII. Trypsin/Versene Solution

Trypsin/Versene solution (Highveld Biological; Johannesburg, RSA) containing 0.25% tryspin and 0.1% EDTA in Ca^{2+} and Mg^{2+} free phosphate buffered saline was used undiluted to detach adherent cells.

2.2 Test Agents

It has been suggested that some molecules may have the ability to further manipulate targets that already naturally fluctuate within certain limits in human cancer cells. The agents that were selected for this study have previously been implicated in up- or down-regulating Her-2 receptor expression.

Table 2.1: Chemical and biological molecules used to assess cell cytotoxicity and the ability to alter Her-2 receptor expression

Agents	Class	Concentration
Aspirin	NSAID	**1 mg/ml [5.5 mM]**
Calcipotriol hydrate	Vitamin D3 analogue	**1 µg/ml [2.4 µM]**
Doxorubicin hydrochloride	Anthracycline	**0.1 µg/ml [0.17 µM]**
Epidermal Growth Factor (EGF-human)	Growth factor	**0.4 µg/ml [66 nM]**
Geldanamycin	Heat Shock Protein 90 inhibitor	**20 ng/ml [0.35 µM]**
Heregulin-β1 (HRG- β1)	Growth factor	**0.2 µg/ml [28 nM]**
β-Oestradiol	Steroid hormone	**0.1 µg/ml [0.36 µM]**
Trastuzumab	Humanised mAb	**1 µg/ml - 200 µg/ml**

2.2.1 Test Compound Stock Solutions

I. Aspirin

Stock solution was made using 40 mg of aspirin powder (Sigma-Aldrich; St Louis, USA) in 1 ml dimethyl sulfoxide (DMSO)(Merck Chemicals; Darmstadt, Germany). Aliquots of 20 µl were made in sterile eppendorf tubes and stored at -80°C until reconstitution with appropriate supplemented medium.

II. Calcipotriol hydrate

Stock solution was made using 1 mg of calcipotriol hydrate powder (Sigma-Aldrich; St Louis, USA) in 1 ml DMSO (Merck Chemicals; Darmstadt, Germany). Aliquots of 20 µl were made in sterile eppendorf tubes and stored at -80°C until reconstitution with appropriate supplemented medium.

III. Doxorubicin hydrochloride

Stock solution was made using 1 mg of doxorubicin hydrochloride powder (Sigma-Aldrich; St Louis, USA) in 1 ml DMSO (Merck Chemicals; Darmstadt, Germany). Aliquots of 20 µl were made in sterile eppendorf tubes and stored at -80°C until reconstitution with appropriate supplemented medium

IV. EGF

Stock solution was made using 0.2 mg of lyophilized EGF powder (Sigma-Aldrich; St Louis, USA) in 1 ml sterile dH_20. Aliquots of 20 µl were made in sterile eppendorf tubes and stored at -80°C until reconstitution with appropriate supplemented medium.

V. Geldanamycin

Stock solution was made using 1 mg of geldanamycin powder (Tocris Bioscience; Ellisville, USA) in 1 ml DMSO (Merck Chemicals; Darmstadt, Germany). Aliquots of 20 µl were made in sterile eppendorf tubes and stored at -80°C until reconstitution with appropriate supplemented medium.

VI. Heregulin-β1 (HRG-β1)

Stock solution was made using 50 µg of lyophilized heregulin powder (Sigma-Aldrich; St Louis, USA) in 1 ml sterile dH_20. Aliquots of 20 µl were made in sterile eppendorf tubes and stored at -80°C until reconstitution with appropriate supplemented medium.

VII. β-Oestradiol

Stock solution was made using 1 mg of β-oestradiol powder (Sigma-Aldrich; St Louis, USA) in 1 ml DMSO (Merck Chemicals; Darmstadt, Germany). Aliquots of 20 µl were made in sterile eppendorf tubes and stored at -80°C until reconstitution with appropriate supplemented medium

VIII. Trastuzumab

Nominal content of each Herceptin® (Genentech Inc, South San Francisco, CA) vial is 440 mg trastuzumab powder which was reconstituted with 20 mL bacteriostatic water containing 1.1% benzyl alcohol, resulting in 21 mg/mL trastuzumab (pH approximately 6). Solution was stored at 4°C in sterile eppendorf tubes in 1 ml aliquots.

IX. Vehicle-Containing Medium

A stock solution of 5% (v/v) DMSO (Merck Chemicals; Darmstadt, Germany) containing medium was made by placing 500 µl DMSO in 9.5 ml medium. A final concentration of 0.5% DMSO was used as the vehicle treated control.

2.3 Experimental Procedures

2.3.1 Cell Viability

Cell viability was determined, after 96 hours of exposure to agents, using a quantitative-colorimetric tetrazolium conversion assay (Mossmann 1983). The assay is based on the ability of metabolically active cells to reduce the tetrazolium component of MTT (3-[4, 5-dimethylthiazol-2-yl]-2, 5-diphenyl tetrazolium bromide) into a water insoluble formazan product by the mitochondria. (MTT: Sigma Product Information)

Following exposure to test agents, cells were incubated with 20 µl of MTT for 3 to 4 hours in a humidified atmosphere containing 5% CO_2 at a temperature of 37°C. Plates were centrifuged (500 *g*, 10 min) after which the supernatant was carefully aspirated and the pellet washed with 150 µl PBS followed by a second centrifugation (500 *g*, 10 min). Plates were left overnight for the remnants of aqueous solution to evaporate, which was followed by the addition of 100 µl DMSO. Plates were mechanically agitated on a shaker until the formazan product was completely solubilised. Plates were read spectrophotometrically using an ELx800uv universal microplate reader (Bio-TEK Instruments, INC) at a dual wavelength of 570 nm and 630 nm. The intensity of the absorbance values of each well was used to quantify the cell viability relative to the untreated control.

2.3.1.1 Cell Viability Statistics

A minimum of three independent inter-day repeats and intra-day repeats were conducted. Cell viability was calculated as a percentage of the untreated control (standardised to 100% viability) and expressed as a mean (± standard error of the mean). Kruskal-Wallis was conducted to compare the mean cell viability of trastuzumab versus each agent alone versus the combination. Dunn's multiple comparison test was used for post-hoc analysis with significance set at p-value < 0.05. Statistical analysis was conducted using GraphPad Prism version 5.0 for Windows (GraphPad Software; San Diego, California, USA) [* $p < 0.05$; ** $p < 0.01$; *** $p < 0.001$]

2.3.1.2 Cell Viability Reagents

I. MTT

MTT solution (5 mg/ml) was made by dissolving 50 mg of 3-[4, 5-dimethylthiazol-2-yl]-2, 5-diphenyl tetrazolium bromide (Sigma-Aldrich; St Louis, USA) powder in 10 ml PBS. The yellow solution was filter sterilized using a 0.22 µm filter and stored at 4°C under strict exclusion of light.

2.3.2 Cell Cycle Analysis

Univariant analysis of cellular DNA content enabled subdivision of cells into specific categories, namely: pre-DNA synthetic interphase or postmitotic gap (G1), DNA synthesis phase (S), postsynaptic interphase or premitotic gap (G2) and mitosis (M). Cell cycle analysis was essential for determining primary effects of compounds and furthermore enabled the determination of apoptotic debris by assessing the sub-G1 phase. Cell cycle kinetics were assessed using flow cytometric applications after exposure for 24, 48 and 72 hours. Propidium iodide (PI) an interchelating, fluorescent, cell impermeable dye has a high affinity for both DNA and RNA making it ideal for the detection of DNA distribution throughout the cell cycle. (Darzynkiewicz, Crissman, & Jacobberger, 2004)

Cells were synchronized using FCS free medium for approximately three times the doubling time of the cell. Cell cycle controls, exposed for 24 hours only, included an untreated control (medium with 10% FCS), a G1 phase control (FCS free medium), S phase control (methotrexate; 10 µM) and a G2 control (curcumin; 20 µM). After exposure the medium from the flask was decanted and collected in 15 ml centrifuge tubes. Cells were washed with PBS, flasks were trypsinized, rinsed with FCS positive medium and the entire content decanted with collected medium. Cells were then centrifuged (200 *g*; 5 min) and the pellet re-suspended in 1 ml ice cold wash buffer (PBS with 1% FCS). Cells were centrifuged (200 *g*; 5 min) and the pellet re-suspended in 200 µl of wash buffer before adding 3 ml of ice cold 70% ethanol in a drop wise manner while agitating constantly using a vortex mixer.

Fixed samples were stored overnight at 4°C. Samples were centrifuged (200 g; 5 min) and pellet re-suspended in 1 ml PI staining solution and incubated at 37°C for 40 minutes. Samples were analysed using a Cytomics FC500 (Beckman Coulter) which provides an excitation of 488 nm with an argon-ion laser and detected the resulting red emission spectrum.

2.3.2.1 Cell Cycle Statistics

A minimum of three independent inter-day repeats were conducted. Histograms were analysed using deconvolution software which is based on the principle that the underlying distribution can be uncovered by fitting G1 and G2 peaks as Gaussian curves and the S-phase as a broadened Gaussian peak allowing subdivision into G1, S, G2 and sub-G1 [background aggregates and debris (BAD)]. Each cell cycle phase was expressed as a mean (± standard error of the mean). Kruskal-Wallis was conducted to compare the mean cell distribution of trastuzumab versus each agent alone versus the combination within each cell cycle phase (G1, S and G2) at each time point. Dunn's multiple comparison test was used for post-hoc analysis with significance set at p-value < 0.05. Statistical analysis was conducted using GraphPad Prism version 5.0 for Windows (GraphPad Software; San Diego, California, USA).

2.3.2.2 Cell Cycle Reagents

I. Curcumin

Stock solutions (4 mM) were made by dissolving 1.47 mg curcumin powder (Sigma-Aldrich; St Louis, USA) in 1 ml DMSO. Aliquots of 100 µl were made in sterile eppendorf tubes and stored at -80°C until reconstitution with appropriate supplemented medium.

II. Methotrexate

Stock solutions (2 mM) were made by dissolving 0.91 mg methotrexate powder (Sigma-Aldrich; St Louis, USA) in 1 ml DMSO. Aliquots of 100 µl were made in sterile eppendorf tubes and stored at -80°C until reconstitution with appropriate supplemented medium.

III. Propidium Iodide Staining Solution

The staining solution was made by dissolving 6 mg propidium iodide (40 µg/ml PI) and 150 µl Triton X-100 (0.1% v/v) (Sigma-Aldrich; St Louis, USA) in PBS and stored at 4°C. Approximately 30 minutes prior to use 100 µg/ml of DNase free RNase (Sigma-Aldrich; St Louis, USA) was added to the solution.

IV. 70% Ethanol (EtOH)

Absolute ethanol (99.9%) (Illovo Sugar Limited; Durban, RSA) was diluted to 70% EtOH by measuring out 70 ml of EtOH in a volumetric flask and filling the flask to 100 ml with dH_2O and was stored at -20°C until use.

2.3.3 Induction of Apoptosis

Induction of apoptosis was assessed using a fluorimetric caspase-3 and -7 assay. Caspase-3 and -7, are effector caspases which play a key role in cellular events during initiation of the apoptotic process. Caspase 3 and caspase 7 possess significant overlap in substrate specificity which can result in the detection of both executioner caspases. Ac-DEVD-AMC substrates (Acetyl-Asp-Glu-Val-Asp-7-amido-4-methylcoumarin) were hydrolysed by activated caspases, releasing a fluorescent product (AMC) and enabling relative quantification of apoptosis. (Caspase 3: Sigma Product Information)

Cells were exposed to agents at 8 different time points between 4 and 30 hours while exposure to the caspase positive control (staurosporine; 10.7 µM) was for 4 hours. Following exposure, plates were placed on ice for 30 minutes before aspirating the medium. Lysis buffer (25 µl) was added to each well and plates gently agitated on a mechanical shaker for 40 minutes. Assay buffer (125 µl) was added to each well and plates were incubated overnight at 37°C to allow complete Ac-DEVD-AMC cleavage. Opaque plates were read using a FLUOstar OPTIMA (BMG LABTECH) with excitation-emission wavelengths of 350 nm and 450 nm respectively and a gain of 900. The fluorescence intensity was standardised to that of the untreated control and expressed as a percentage.

2.3.3.1 Caspase Assay Statistics

A minimum of three independent inter-day and three intra-day repeats were conducted. Caspase activity was calculated as a percentage of the untreated control (standardised to 100%) and expressed as a mean (± standard error of the mean). Kruskal-Wallis was conducted to compare the mean fluorescence intensity of trastuzumab versus each agent alone versus the combination. Dunn's multiple comparison test was used for post-hoc analysis with significance set at p-value < 0.05. Statistical analysis was conducted using GraphPad Prism version 5.0 for Windows (GraphPad Software; San Diego, California, USA). [* $p < 0.05$; ** $p < 0.01$; *** $p < 0.001$]

2.3.3.2 Caspase Assay Reagents

I. Assay Buffer

Assay buffer was prepared by dissolving 2.383 g HEPES (20 mM)(Merck Chemicals; Darmstadt, Germany) and 58 mg EDTA (2 mM)(Labchem; Johannesburg, RSA) in 500 ml dH_20. Approximately 30 minutes prior to use, 20 µl of Ac-DEVD-AMC substrate (5 µM) and 16 µl of β-mercaptoethanol (5 mM) (Labchem; Johannesburg, RSA) were added to 40 ml of the incomplete assay buffer solution.

II. Caspase Substrate

Stock solutions (10 mM) of the Ac-DEVD-AMC substrate (Sigma-Aldrich; St Louis, USA) were made by dissolving 2.5 mg of Acetyl-Asp-Glu-Val-Asp-7-amido-4-methylcoumarin in 370 µl of DMSO. Aliquots of 5 µl were stored at -80°C until adding to assay buffer.

III. Lysis Buffer

Lysis buffer was prepared by dissolving 238.3 mg HEPES (10 mM), 307 mg CHAPS (5 mM)(Merck Chemicals; Darmstadt, Germany) and 58 mg EDTA (2 mM)(Labchem; Johannesburg, RSA) in 100 ml dH_20. Approximately 30 minutes prior to use 100 µl PMSF (1 mM) and 4 µl of β-mercaptoethanol (5 mM)(Labchem; Johannesburg, RSA) were added to 10 ml of lysis buffer.

IV. Phenylmethylsulfonyl fluoride

Stock solutions (100 mM) of phenylmethylsulfonyl fluoride (PMSF)(Sigma-Aldrich; St Louis, USA) were made up using 17.4 mg of powder in 1 ml DMSO. Aliquots of 50 µl were made in sterile eppendorf tubes and stored at -80°C until addition to 5 ml of lysis buffer.

V. Staurosporine

Stock solutions (2.14 mM) of staurosporine (Sigma-Aldrich; St Louis, USA) were made up using 1 mg powder in 1 ml DMSO. Aliquots of 50 µl were made in sterile eppendorf tubes and stored at -80°C until reconstitution with appropriate supplemented medium.

2.3.4 Apoptosis/Necrosis

Apoptosis was further assessed using a fluorochrome conjugated annexin V assay. Annexins are a group of homologous proteins that bind to phosphatidylserine in the presence of calcium. Phosphatidylserine is normally found on the inner phospholipid membrane but undergoes a loss of symmetry during apoptosis and is then found on the outer cellular membrane. (Annexin-V: Sigma Product Information,) Propidium iodide was used as a counterstain to assess membrane integrity.

Cells were exposed for 48 and 72 hours and included an untreated control, apoptosis control (staurosporine, 10.7 µM; 12 hours) and necrosis control (SDS, 0.2%; 5 minutes). Cells were trypsinized and centrifuged (200 *g*; 5 min), re-suspended in 3 ml wash buffer (1% FCS in PBS) with subsequent centrifugation (200 *g*; 5 min). Cells were re-suspended in 100 µl binding buffer and double stained with 2.5 µl of annexin V-FITC (Sigma-Aldrich; St Louis, USA) and 3 µl of propidium iodide solution. Samples were incubated in the dark for 10 minutes before conducting flow cytometry protocols using a Cytomics FC500 (Beckman Coulter).

2.3.4.1 Apoptosis-Necrosis Statistics

A minimum of three independent inter-day repeats were conducted. Quadrants analysis of scatter plots divided cells into normal cells, early apoptotic (annexin-V positive), late apoptotic or necrotic cells (annexin-V and PI positive) were analysed and converted into corresponding stacked columns. Each quadrant subdivision was expressed as a mean (± standard error of the mean). Kruskal-Wallis was conducted to compare the mean fluorescence for each quadrant of trastuzumab versus each agent alone versus the combination within quadrant group at a specific time point. Dunn's multiple comparison test was used for post-hoc analysis with significance set at p-value < 0.05. Statistical analysis was conducted using GraphPad Prism version 5.0 for Windows (GraphPad Software; San Diego, California, USA).

2.3.4.2 Apoptosis-Necrosis Reagents

I. Annexin V Binding Buffer

Binding buffer was prepared by adding 1.192 g HEPES (10 mM), 4.383 g NaCl (150 mM), 0.186 g KCL (5 mM), 99.85 mg $CaCl_2$ (1.8 mM) and 47.6 mg $MgCl_2$ (1 mM)(Merck Chemicals; Darmstadt, Germany) to 500 ml dH_20 and the pH was adjusted to 7.4.

II. PI Solution

Stock solution (3 mM) of propidium iodide (Sigma-Aldrich; St Louis, USA) was made by dissolving 10.025 mg propidium iodide powder in 5 ml dH_2O and stored at 4°C until use.

III. Sodium Dodecyl Sulfate

Stock solution [0.2% (m/v)] of sodium dodecyl sulphate (SDS)(Merck Chemicals; Darmstadt, Germany) was made by dissolving 10 mg SDS powder in 5 ml dH_2O. Stock solution was stored at 4°C until use.

2.3.5 Relative Her-2 Receptor Density

Relative Her-2 receptor density was determined using a FITC-conjugated anti-Her-2 affibody molecule, which labels the extracellular domain of the receptor. Cells were exposed to test agents for 12, 24 or 48 hours after which cells were brought into suspension by cell scraping or trypsinization (methods were compared to determine influence of sample preparation on surface receptors) and centrifuged (200 *g;* 5 min). Cell pellet was re-suspended in 3 ml wash buffer (1% FCS in PBS) and centrifuged (200 *g;* 5 min).

Cells were re-suspended in 100 µl wash buffer and 10 µl of FITC-labelled affibody molecule (final concentration ±3.7 µg/ml) was added to each sample which was incubated on ice for 30 minutes. Samples were washed with 3 ml wash buffer and centrifuged (200 *g;* 5 min) and the pellet re-suspended in 500 µl of wash buffer before conducting flow cytometry protocols using a Cytomics FC500 (Beckman Coulter).

2.3.5.1 Her-2 Receptor Density Statistics

A minimum of three independent inter-day repeats were conducted. The fluorescent intensity of the x-mean of each histogram was calculated as a percentage of the untreated control (standardised to 100%) and the percentage of triplicate repeats was expressed as a mean (± standard error of the mean). Kruskal-Wallis was conducted to compare the mean fluorescence of trastuzumab versus each agent alone versus the combination at a specific time point. Dunn's multiple comparison test was used for post-hoc analysis with significance set at p-value < 0.05. Statistical analysis was conducted using GraphPad Prism version 5.0 for Windows (GraphPad Software; San Diego, California, USA).

2.3.5.2 Her-2 Receptor Density Reagents

I. Imaging Molecule

FITC-conjugated anti-Her-2 affibody molecule (0.37 mg/ml)(Abcam; Cambridge, UK) was diluted to 37 µg/ml using PBS prior to addition to each sample, where it was further diluted one-in-ten.

2.4 Summary of Methods and Prelude to Results and Discussion

The aim was to investigate alterations in the efficacy of trastuzumab, a Her-2 mAb, by biological ligands, hormones and cytotoxic agents in models of Her-2 normal, ER positive (MCF-7) and Her-2-positive (SK-Br-3) breast adenocarcinoma cells. Cell viability using an MTT assay was assessed to determine the ultimate end-point effects of single agents as well as combinations. Furthermore, cell cycle kinetics using PI staining, apoptosis via caspase-3 and -7 assay and annexin-V/PI staining were assessed to determine the mechanism of altered cell viability. Because Her-2 receptors play an integral component in the efficacy of trastuzumab, relative surface Her-2 expression was assessed flow cytometrically.

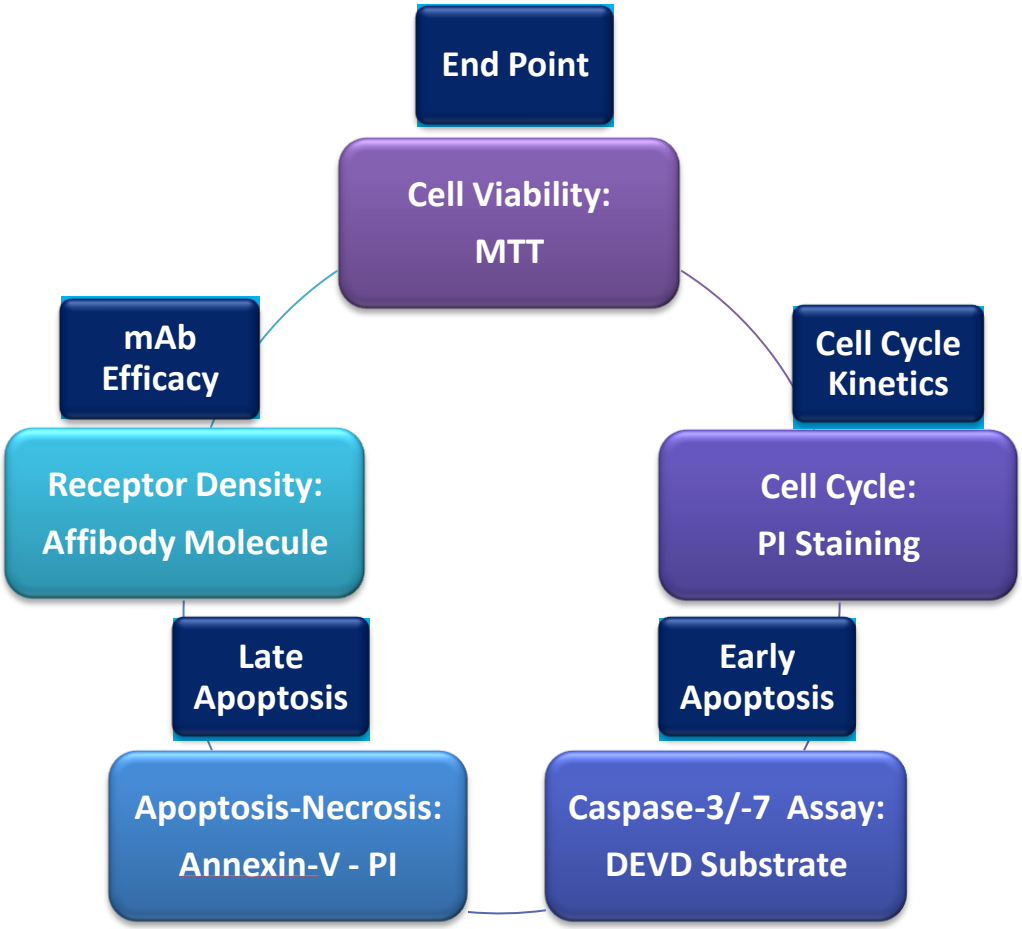

Figure 2.1: Summary of methods employed

The assays generated extensive data for each of the commercially available test agents and combinations. The following eight chapters describe the results for each, and include a discussion to facilitate ease of reading and integration. In order to compile the data in a way that is accessible to readers, chapter 3, using either controls or trastuzumab, describes how raw data was transformed, tabulated and represented in appropriate graphs.

Chapter 3: Results and Discussion: Trastuzumab

3.1 Cell Viability

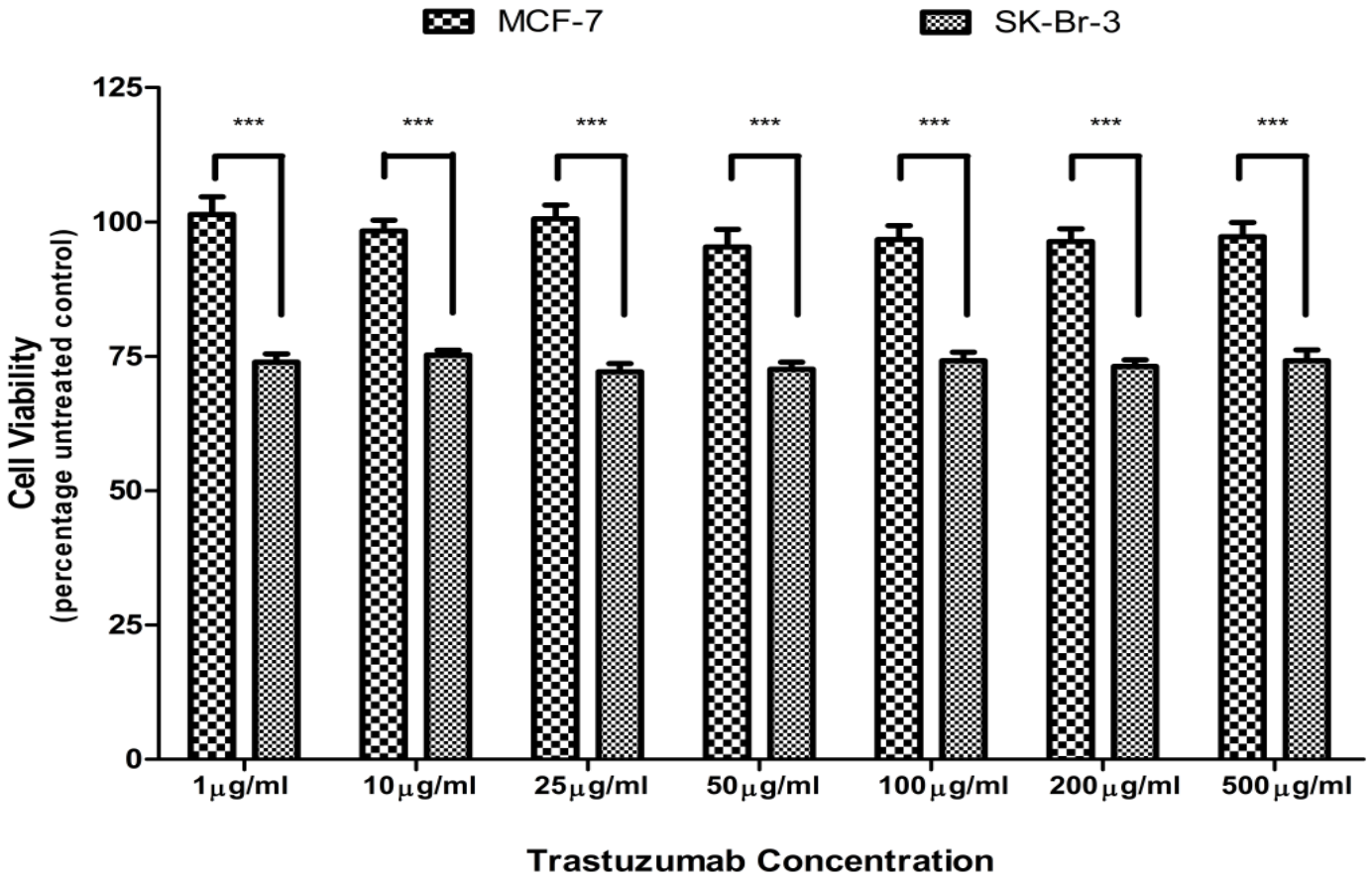

Figure 3.1: Cell viability in MCF-7 and SK-Br-3 expressed as a percentage of untreated controls. Statistically significant differences were present between MCF-7 and SK-Br-3 cells from 1 µg/ml to 500 µg/ml trastuzumab. (P < 0.001) No significant differences were found between any concentrations within a single cell line.

Table 3.1 : Cell viability results for trastuzumab

Trastuzumab Concentration	MCF-7	SK-Br-3
	Mean ± SEM	Mean ± SEM
1 µg/ml	101.39 ± 3.26	73.92 ± 1.50
10 µg/ml	98.29 ± 2.07	75.22 ± 0.91
25 µg/ml	100.59 ± 1.75	72.13 ± 1.55
50 µg/ml	95.35 ± 2.27	72.58 ± 1.31
100 µg/ml	95.39 ± 2.69	74.17 ± 1.60
200 µg/ml	96.34 ± 2.43	73.10 ± 1.26
500 µg/ml	97.27 ± 2.62	74.20 ± 1.98

Table 3.2: Cell viability results in SK-Br-3 cells for the extended trastuzumab concentration range

Trastuzumab Concentration	Mean ± SEM	Significance (P<0.001)	
		10 ρg/ml - 10 ng/ml	100 ng/ml - 500 µg/ml
10 ρg/ml	101.67 ± 3.59		
100 ρg/ml	95.92 ± 3.02		**
1 ng/ml	95.26 ± 3.52		
10 ng/ml	89.88 ± 3.64		
100 ng/ml	75.08 ± 1.81		
1 µg/ml	74.16 ± 1.45		
10 µg/ml	74.71 ± 1.39	**	
100 µg/ml	75.84 ± 1.85		
200 µg/ml	74.73 ± 1.19		
500 µg/ml	74.46 ± 2.22		

3.2 Cell Cycle Analysis: MCF-7 Controls

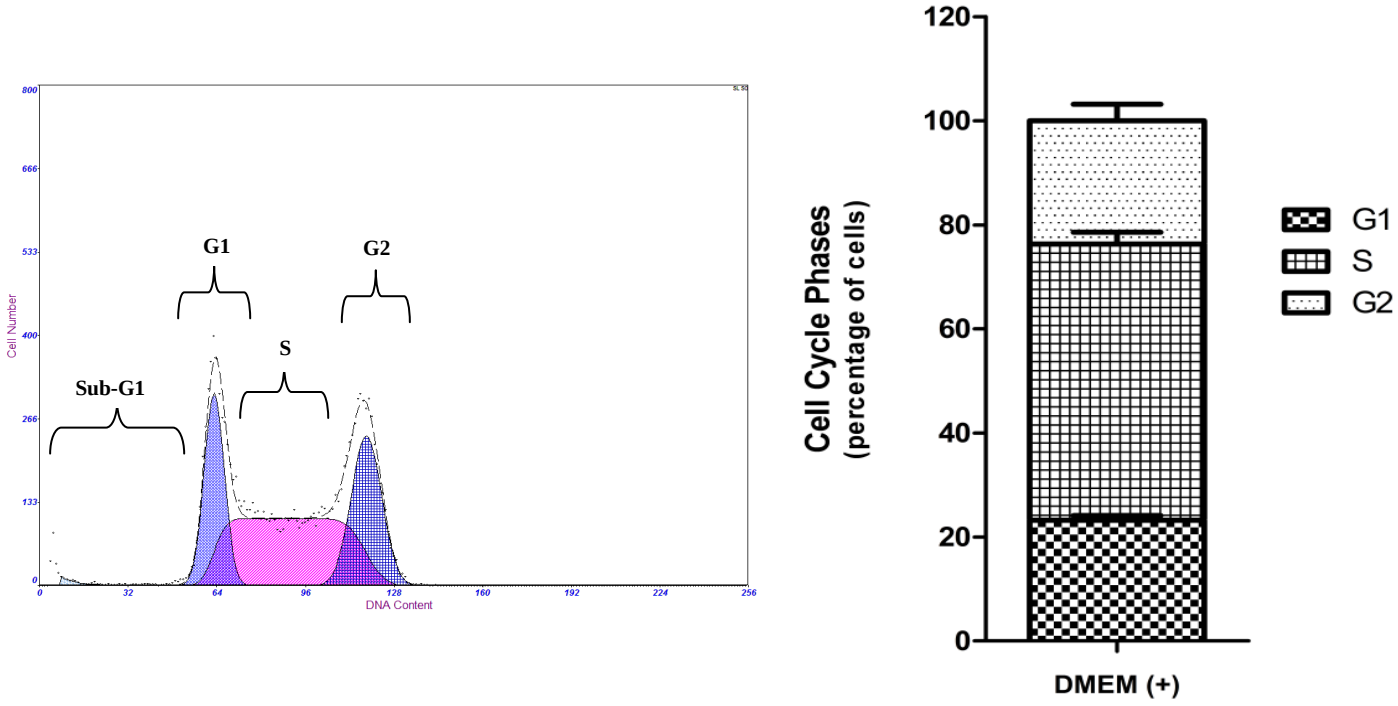

Figure 3.2: Growth Control: DMEM +

Flow cytometry histogram analysed with deconvolution software divided histogram into G1 phase (left), S phase (centre) and G2 phase (right)

Percentages from deconvolution converted into corresponding stacked column graph: G1 phase (bottom), G2 phase (middle), S phase (top)

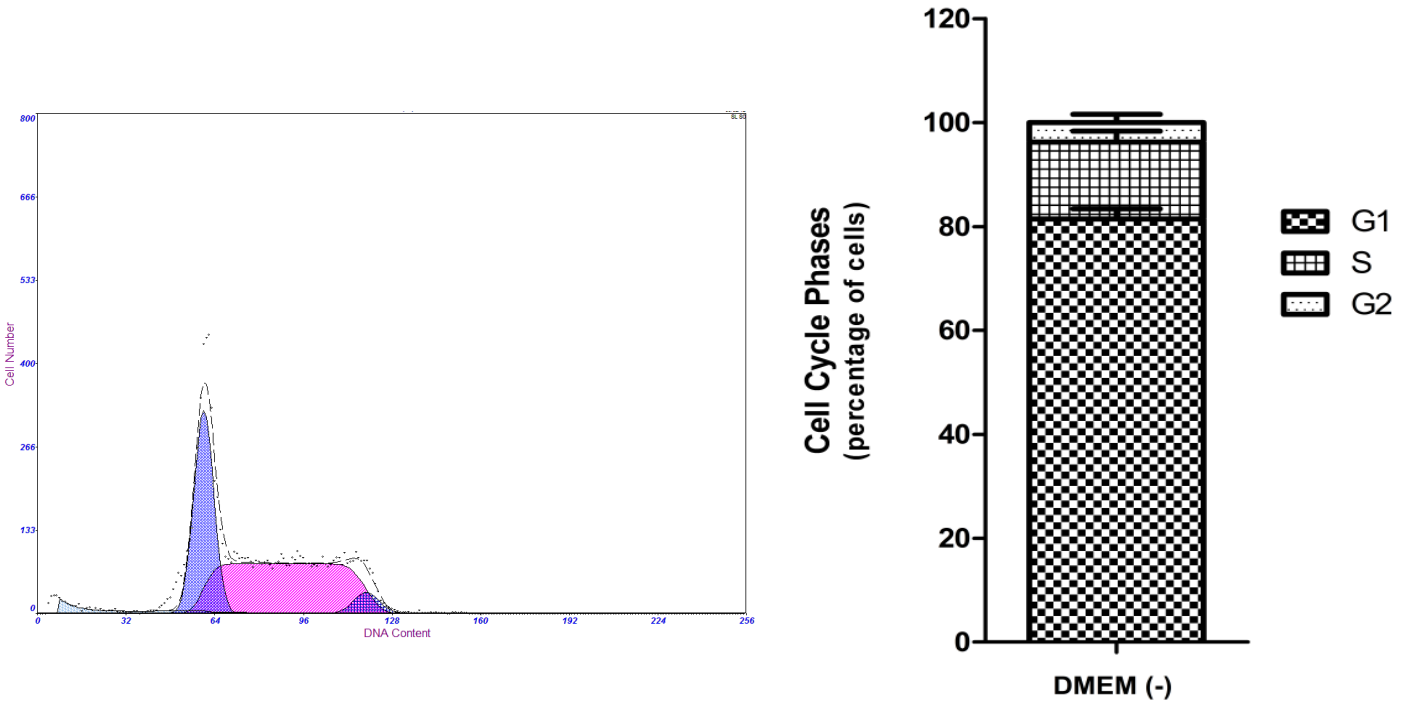

Figure 3.3: G1 Phase Control: DMEM -

Flow cytometry histogram analysed with deconvolution software divided histogram into G1 phase (left), S phase (centre) and G2 phase (right)

Percentages from deconvolution converted into corresponding stacked column graph

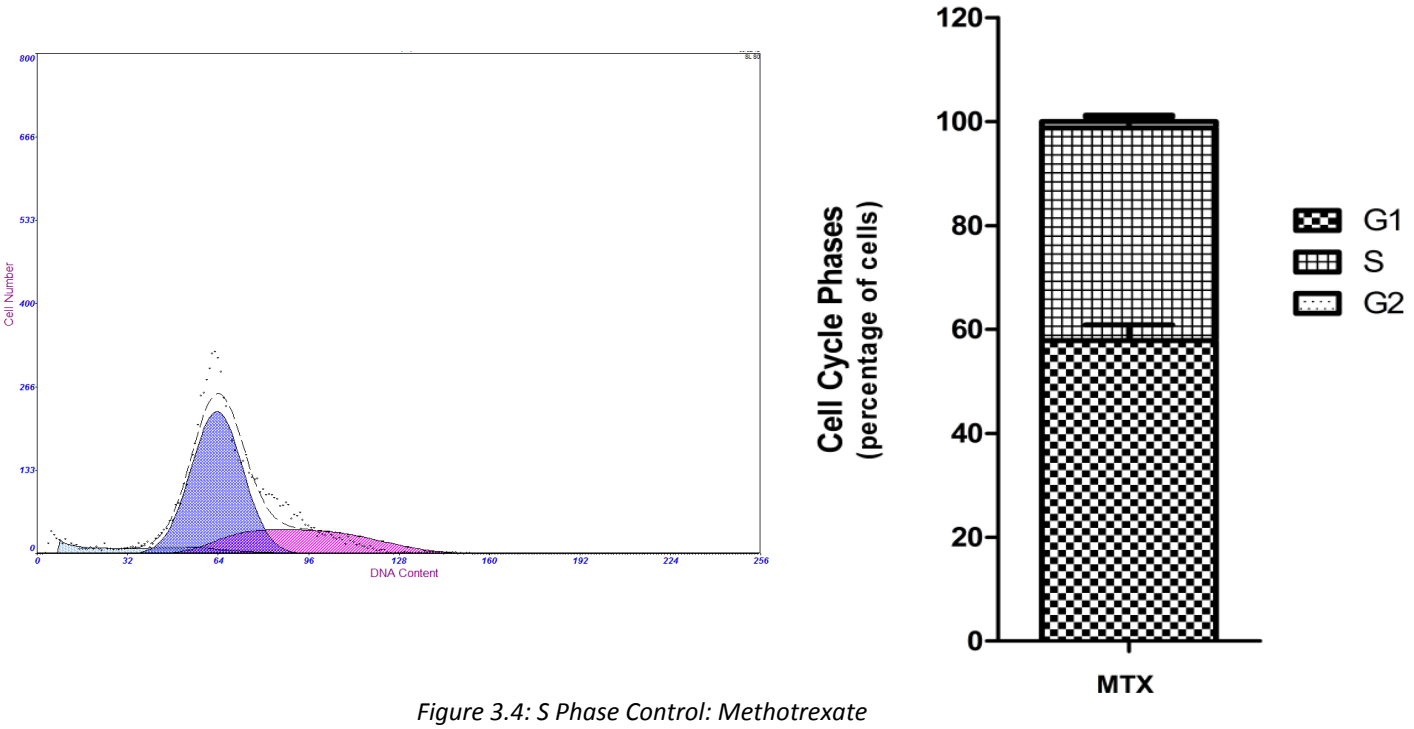

Figure 3.4: S Phase Control: Methotrexate

Flow cytometry histogram analysed with deconvolution software divided histogram into G1 phase (left), S phase (centre) and G2 phase (right)

Percentages from deconvolution converted into corresponding stacked column graph

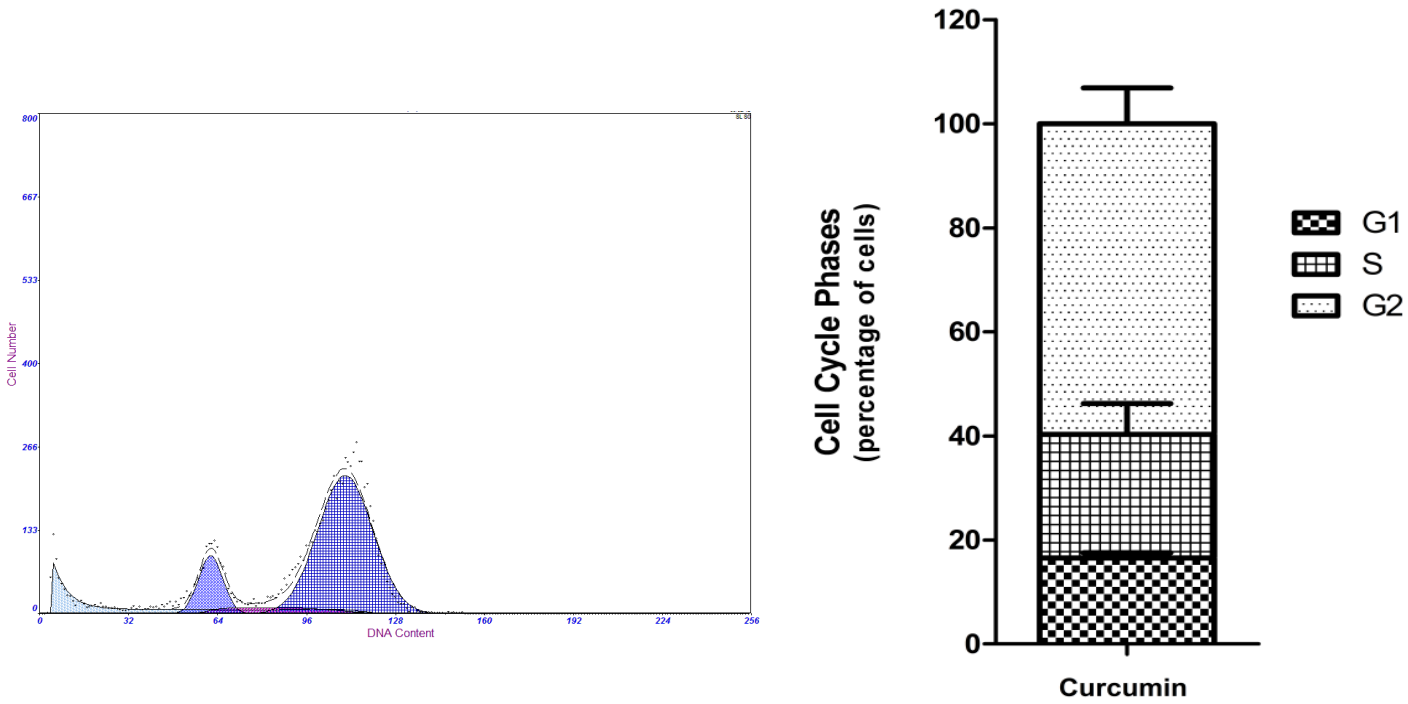

Figure 3.5: G2 *Phase Control: Curcumin*

Flow cytometry histogram analysed with deconvolution software divided histogram into G1 phase (left), S phase (centre) and G2 phase (right)

Percentages from deconvolution converted into corresponding stacked column graph

Table 3.3: MCF-7 and SK-Br-3 Controls: Percentages from deconvolution

MCF-7	**Mean ± SEM**		
24 Hours	**G1**	**S**	**G2**
DMEM +	23.25 ± 0.86	52.99 ± 2.33	23.76 ± 3.17
DMEM -	81.44 ± 1.95	14.80 ± 2.11	3.76 ± 1.58
Methotrexate	57.87 ± 2.99	40.94 ± 2.05	1.19 ± 1.19
Curcumin	16.54 ± 1.03	23.77 ± 5.91	59.69 ± 6.87
SK-Br-3	**Mean ± SEM**		
24 Hours	**G1**	**S**	**G2**
RPMI +	45.19 ± 0.65	35.68 ± 0.81	19.16 ± 0.31
RMPI -	62.49 ± 3.37	22.40 ± 1.73	15.13 ± 1.66
Methotrexate	58.70 ± 2.16	40.10 ± 1.11	1.20 ± 1.20
Curcumin	41.32 ± 1.46	21.30 ± 1.67	37.39 ± 2.48

3.2.1 Cell Cycle Analysis: Trastuzumab

Table 3.4: Cell cycle results for MCF-7 cells exposed to trastuzumab (T: Trastuzumab)

MCF-7	Mean ± SEM				Significance			
	G1	S	G2	Sub G1	C	T: 24	T: 48	T: 72
Control (C)	23.25 ± 0.86	52.99 ± 2.33	23.76 ± 3.17		-			***
T: 24 Hours	23.46 ± 1.21	53.03 ± 2.62	23.51 ± 1.63	1.87 ± 0.10		-		
T: 48 Hours	32.40 ± 2.34	50.86 ± 4.87	16.74 ± 3.22	1.89 ± 0.02			-	
T: 72 Hours	56.37 ± 4.48	33.34 ± 3.23	10.29 ± 1.72	1.89 ± 0.02	***			-

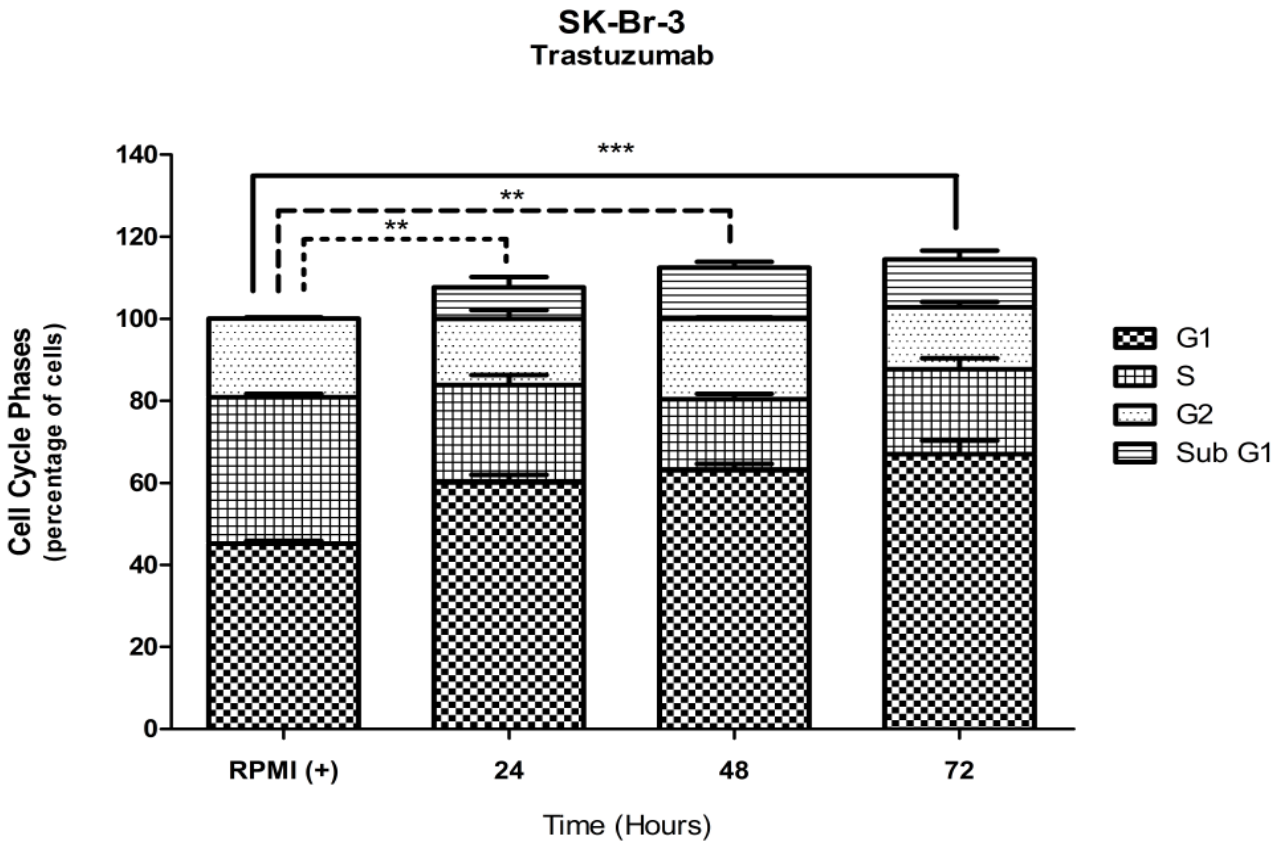

Figure 3.6: Cell cycle analysis in SK-Br-3 cells exposed to trastuzumab at 24, 48 and 72 hours expressed as a percentage in a stacked column graph after deconvolution. Statistically significant differences in the G1 phase of the cell cycle were observed between untreated control (RPMI+) and trastuzumab from 24 hours. Trastuzumab: 100 µg/ml.

Table 3.5: Cell cycle results for SK-Br-3 cells exposed to trastuzumab (T: Trastuzumab)

SK-Br-3	Mean ± SEM				Significance			
	G1	S	G2	Sub G1	C	T: 24	T: 48	T: 72
Control (C)	45.19 ± 0.65	35.68 ± 0.81	19.16 ± 0.31		-	**	**	***
T: 24 Hours	60.15 ± 1.81	23.72 ± 2.38	16.13 ± 2.07	7.68 ± 2.48	**	-		
T: 48 Hours	64.15 ± 1.41	20.84 ± 3.55	15.02 ± 4.56	11.48 ± 1.28	**		-	
T: 72 Hours	66.93 ± 3.41	20.78 ± 2.60	15.02 ± 1.38	11.69 ± 2.20	***			-

3.3 Apoptosis-Necrosis: MCF-7 Controls

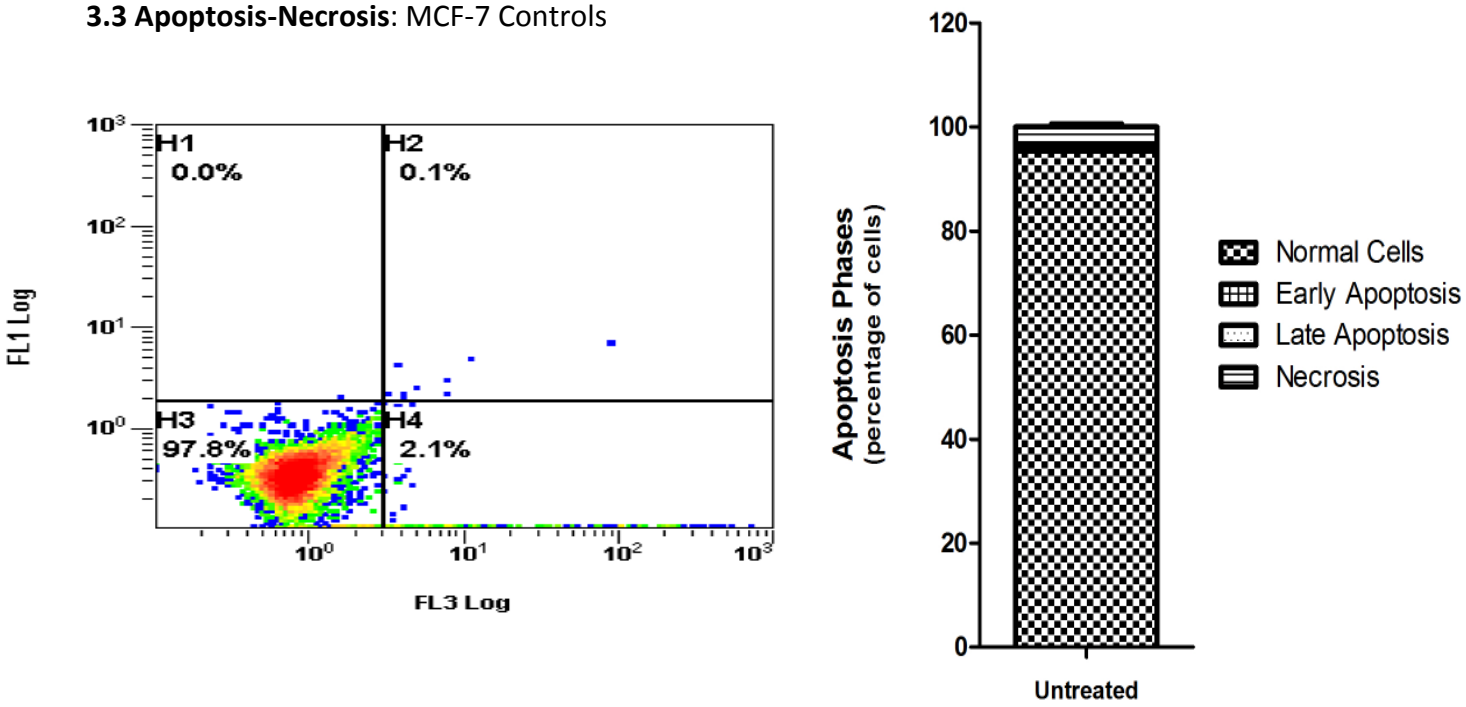

Figure 3.7: Untreated control

FL1 Log: Annexin V-FITC; FL3 Log: Propidium Iodide (PI)
H1: Early Apoptosis; H2: Late Apoptosis; H3 Normal Cells; H4 Necrosis

Histogram and corresponding stacked column graph from bottom to top:
Normal cells, early apoptosis, late apoptosis, necrosis

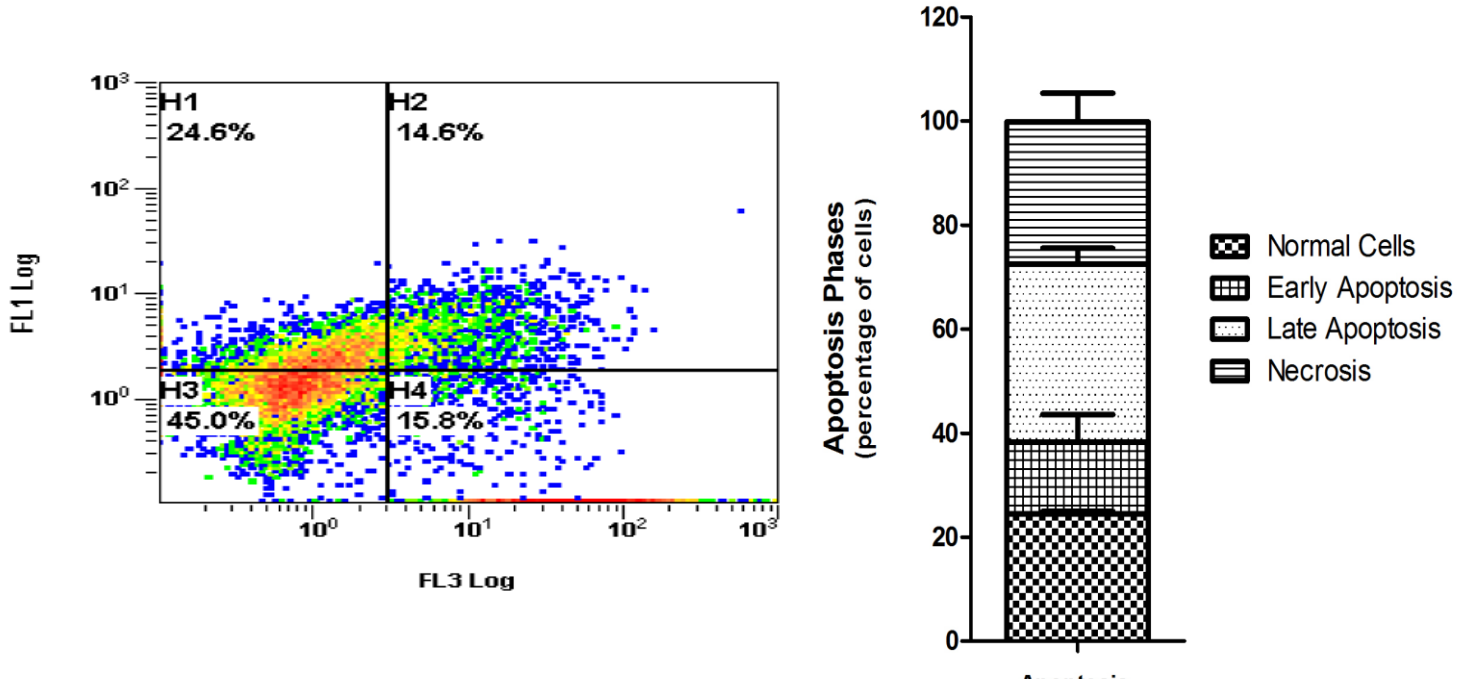

Figure 3.8: Apoptosis Control: Staurosporine

FL1 Log: Annexin V-FITC; FL3 Log: Propidium Iodide (PI)
H1: Early Apoptosis; H2: Late Apoptosis; H3 Normal Cells; H4 Necrosis

Histogram and corresponding stacked column graph

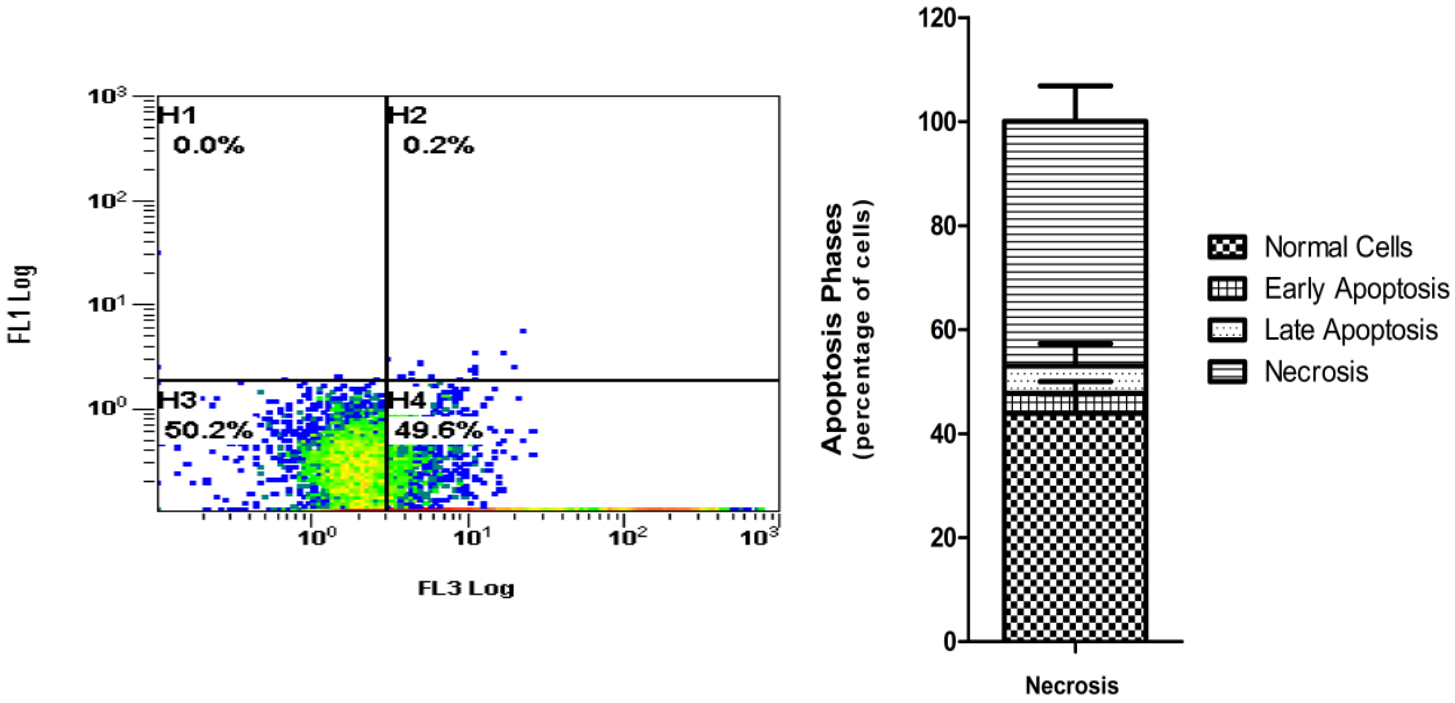

Figure 3.9: Necrosis Control: 2% SDS

FL1 Log: Annexin V-FITC; FL3 Log: Propidium Iodide (PI)
H1: Early Apoptosis; H2: Late Apoptosis; H3 Normal Cells; H4 Necrosis

Histogram and corresponding stacked column graph

Table 3.6: MCF-7 and SK-Br-3 Apoptosis-Necrosis controls: Percentage of cells in each phase

MCF-7	**Mean ± SEM**			
	Normal Cells	**Early Apoptosis**	**Late Apoptosis**	**Necrosis**
Unstained	97.03 ± 0.43	0.80 ± 0.49	0.20 ± 0.06	1.30 ± 0.66
Untreated	95.37 ± 1.07	0.80 ± 0.49	0.20 ± 0.06	3.63 ± 0.56
Apoptosis	24.43 ± 0.52	13.83 ± 5.37	34.17 ± 3.10	27.40 ± 5.47
Necrosis	43.90 ± 3.79	3.87 ± 2.25	5.30 ± 4.28	46.97 ± 6.85
SK-Br-3	**Mean ± SEM**			
	Normal Cells	**Early Apoptosis**	**Late Apoptosis**	**Necrosis**
Unstained	98.00 ± 0.45	0.36 ± 0.26	0.22 ± 0.12	1.40 ± 0.53
Untreated	91.25 ± 1.13	1.80 ± 0.47	0.50 ± 0.23	6.48 ± 1.36
Apoptosis	35.43 ± 2.78	35.50 ± 3.87	1.73 ± 0.15	27.37 ± 1.13
Necrosis	53.80 ± 2.71	2.73 ± 1.86	0.87 ± 0.57	42.60 ± 3.51

3.3.1 Apoptosis-Necrosis: Trastuzumab

Table 3.7: Apoptosis-Necrosis in MCF-7 cells and SK-Br-3 cells exposed to trastuzumab after 48 and 72 hours.

Percentage of cells in each phase (E: Early, L:Late)

MCF-7	Mean ± SEM				Significance		
	Normal	E Apoptosis	L Apoptosis	Necrosis	U	T: 48	T: 72
Untreated (U)	95.37 ± 1.07	0.80 ± 0.49	0.20 ± 0.06	3.63 ± 0.56	-		
T: 48 Hours	95.17 ± 0.89	2.43 ± 0.14	0.47 ± 0.27	1.97 ± 0.82		-	
T: 72 Hours	94.57 ± 0.54	1.03 ± 0.18	0.47 ± 0.03	3.97 ± 0.42			-
SK-Br-3	**Mean ± SEM**				**Significance**		
	Normal	**E Apoptosis**	**L Apoptosis**	**Necrosis**	**U**	**T: 48**	**T: 72**
Untreated (U)	91.25 ± 1.13	1.80 ±0.47	0.50 ± 0.23	6.48 ± 1.36	-		
T: 48 Hours	89.23 ± 0.87	2.17 ± 0.35	0.87 ± 0.06	7.76 ± 0.61		-	
T: 72 Hours	89.90 ± 0.15	1.40 ± 0.31	0.37 ± 0.12	8.33 ± 0.37			-

3.4 Relative Her-2 Receptor Density: SK-Br-3 Controls

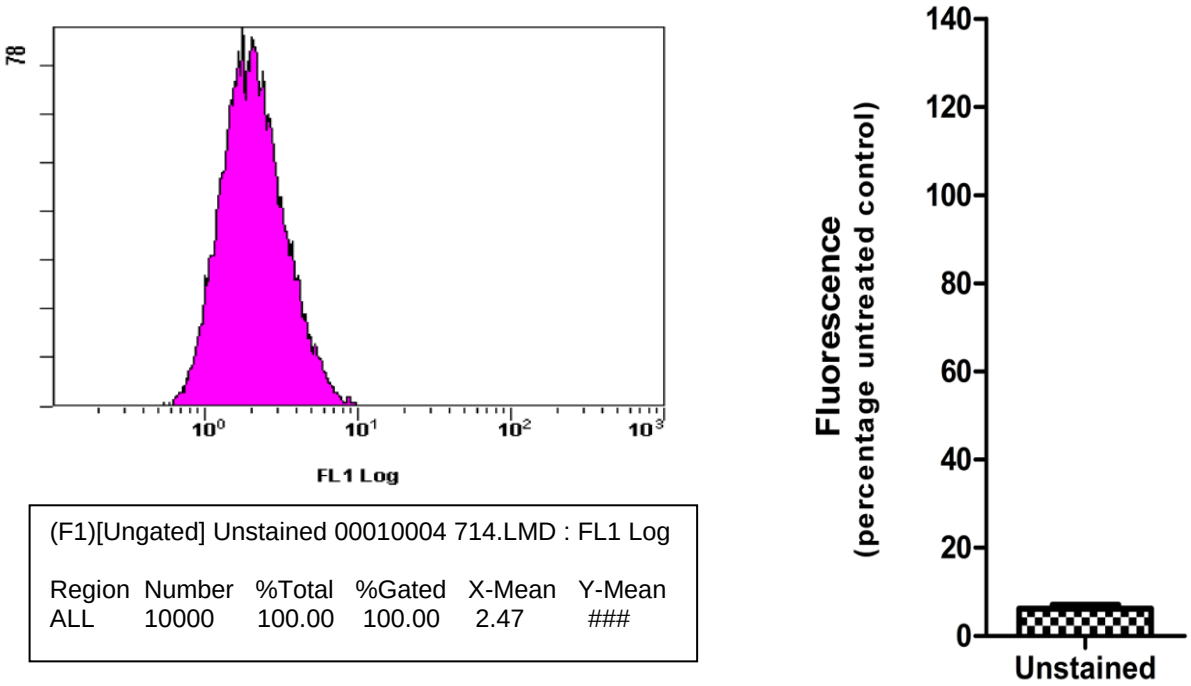

(F1)[Ungated] Unstained 00010004 714.LMD : FL1 Log

Region	Number	%Total	%Gated	X-Mean	Y-Mean
ALL	10000	100.00	100.00	2.47	###

Figure 3.10: Unstained Control

Fluorescence (x-mean) of channel 1 (FL1) expressed as a percentage of untreated controls (standardised to 100%)
FL1 Log: Anti-Her-2 Affibody Molecule

Histogram with statistics and corresponding column graph

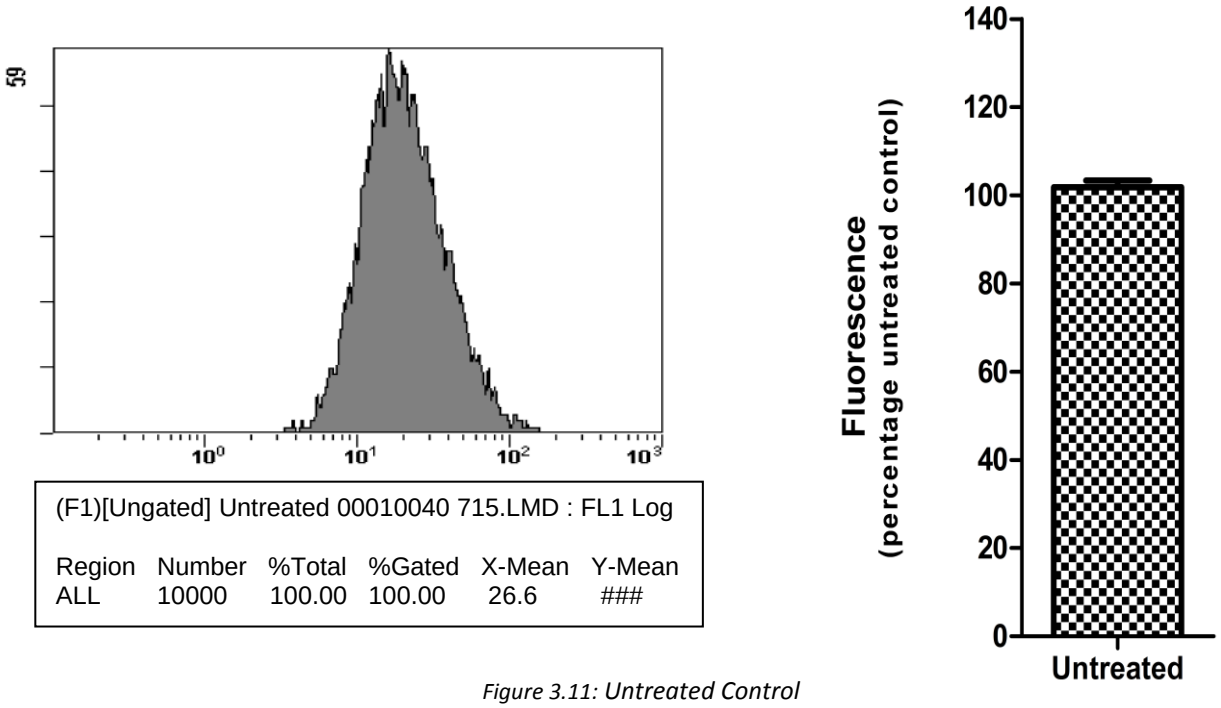

(F1)[Ungated] Untreated 00010040 715.LMD : FL1 Log

Region	Number	%Total	%Gated	X-Mean	Y-Mean
ALL	10000	100.00	100.00	26.6	###

Figure 3.11: Untreated Control

Fluorescence (x-mean) of channel 1 (FL1) expressed as a percentage of untreated controls (standardised to 100%)
FL1 Log: Anti-Her-2 Affibody Molecule

Histogram with statistics and corresponding column graph

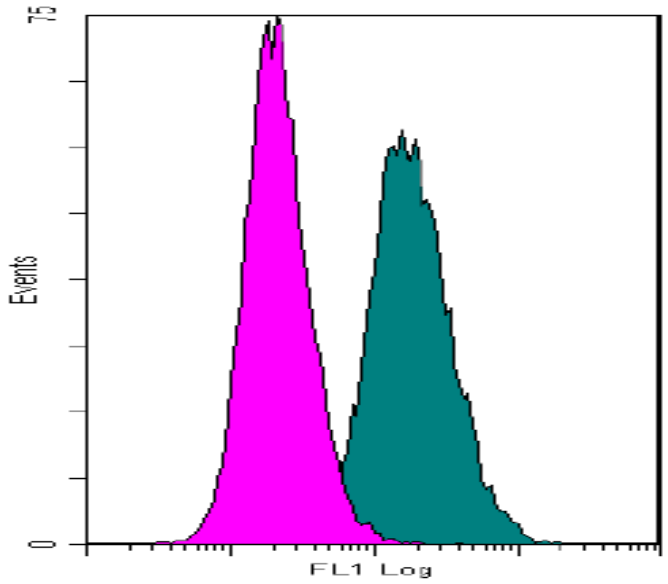

SK-Br-3	Mean ± SEM
Unstained	6.18 ± 0.91
Untreated	100.70 ± 1.42

Figure 3.12: Overlay plot of unstained (left) and untreated (right) controls of SK-Br-3 cells with the fluorescent intensity (histogram x-mean) of unstained and untreated controls expressed as a mean (± SEM)

3.4.1 Relative Her-2 Receptor Density: Trastuzumab

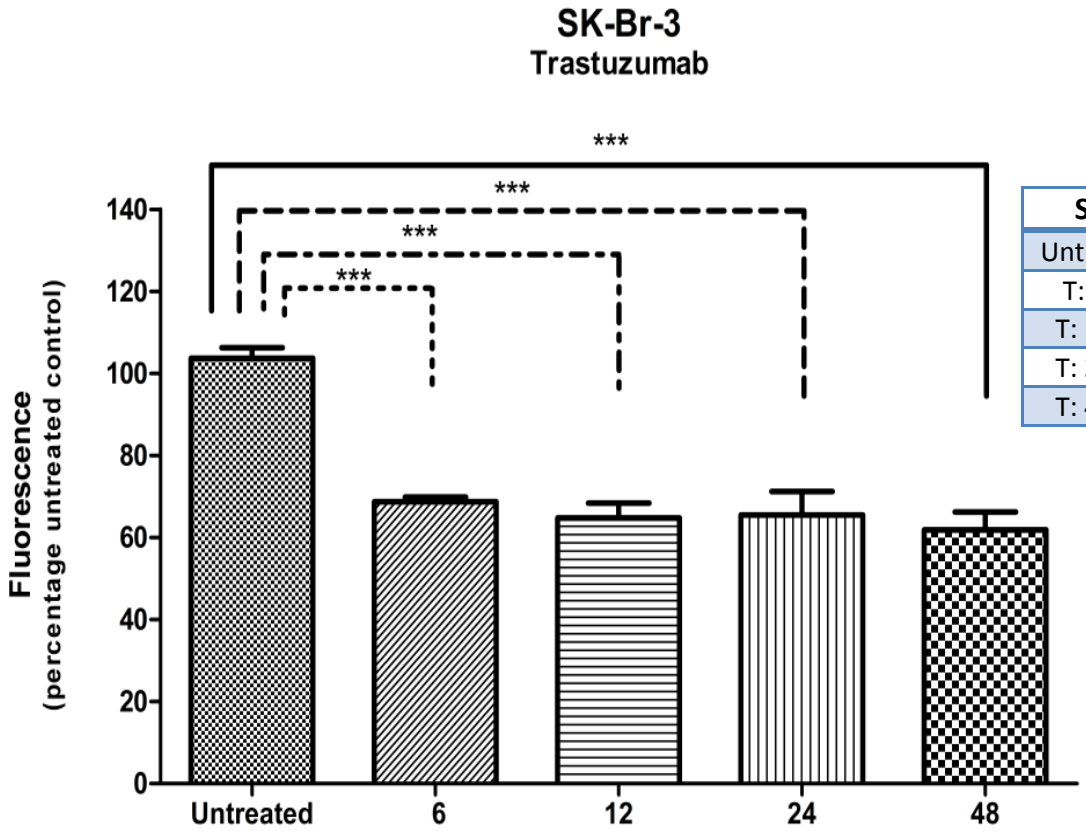

SK-Br-3	Mean ± SEM
Untreated (U)	100.70 ± 1.42
T: 6 Hours	68.69 ± 1.14
T: 12 Hours	64.77 ± 3.60
T: 24 Hours	65.47 ± 4.76
T: 48 Hours	61.83 ± 4.42

Figure 3.13: Relative Her-2 receptor density analysis in SK-Br-3 cell exposed to trastuzumab at 6, 12, 24 and 48 hours and expressed as a percentage of the fluorescence of untreated controls (standardised to 100%) along with the fluorescent intensity (histogram x-mean) expressed as a mean (± SEM). Trastuzumab: 100 µg/ml.

Trastuzumab, the recombinant DNA-derived humanized monoclonal antibody, selectively binds with high affinity to subdomain IV of the extracellular domain of over-expressed Her-2 receptors. (Murphy & Modi, 2009; Tai et al., 2010) The mechanism by which trastuzumab inhibits tumour growth remains controversial. However, postulated mechanisms include: disruption of downstream proliferative signalling pathways, antibody-dependent cell-mediated cytotoxicity, inhibition of cell cycle progression, endocytosis and degradation of Her-2 receptors and anti-angiogenic effects. (Murphy & Modi, 2009)

Not surprisingly, the results obtained in this study showed that trastuzumab was unable to elicit effects on cell viability in oestrogen-dependent MCF-7 cells expressing physiologically normal levels of Her-2 receptors. In stark contrast, trastuzumab showed significant and substantial anti-proliferative effects in Her-2 over-expressing SK-Br-3 cells after exposure to concentrations ranging from of 1 µg/ml to 500 µg/ml (Figure 3.1; Table 3.1). Thus, a certain threshold of Her-2 receptor density is required for trastuzumab to exert effects *in vitro*. Of note is that cell viability for SK-Br-3 cells was approximately 75%, for each concentration assessed and appeared completely dose-independent. In support of these experiments, Zhu *et al*. (2010) noted cell viability of approximately 60% in response to 50 µg/ml trastuzumab in SK-Br-3 cells after which the viability was slightly increased at higher concentrations. Further results indicated that trastuzumab could not inhibit MCF-7 cell growth.

A panel of breast cancer cells exposed to mAb 4D5 demonstrated no significant effect on the growth of Her-2 normal MCF-7, MDA-MB-157 or MDA-MB-231 cells. While 4D5 inhibited the growth of several breast tumour cell lines, it was suggested that the greater the dependence of cells on Her-2 mediated signalling for growth and transformation, the greater the anti-proliferative effect of 4D5. (Hudziak et al., 1989)

In an attempt to generate a dose-response curve, SK-Br-3 cells were exposed to trastuzumab at concentrations ranging from 1 ρg/ml to 500 µg/ml (Table 3.2). A decrease in cell viability from 100+% to approximately 90% occurred over the range of 1 ρg/ml to 10 ng/ml. A decrease to approximately 75% was observed in a range of 100 ng/ml to 500 µg/ml which suggests that the experiment could be saturated. This decrease was statistically significantly different compared to each concentration from 1 ρg/ml to 10 ng/ml. This led to the speculation that either the binding domains were occupied or that Her-2 receptors were internalised and degraded or unable to recycle back to the surface for further trastuzumab binding.

Assessing the same concentration over a period of seven days did not yield any apparent dose-dependence. The maintenance of cell viability at approximately 75% could have been due to the doubling time for the SK-Br-3 cells being somewhat slower than normally characterised. It was also speculated that in the presence of a certain concentration of trastuzumab the majority of cells were present in a non-dividing cell cycle state; only if a large portion of cells were still actively dividing, would a dose-dependent response be evident. The data suggested that mechanisms involved may be biased towards inhibition of cell growth rather than programmed cell death.

In order to test this premise, induction of programmed cell death was assessed by the detection of active executioner caspases. Observations over a period of 4 to 30 hours in MCF-7 and SK-Br-3 cells indicated no apoptosis in either cell line (data not shown). This suggested that both caspases-3 and -7 were only detectable at a later time point, or that the primary mechanism of trastuzumab action *in vitro* is anti-proliferative. To further test for apoptosis, an annexin-V assay was conducted. This flow cytometric assay showed no difference in fluorescent staining between untreated controls and cells exposed to trastuzumab in either cell line (Table 3.7), which further supported the concept that trastuzumab is anti-proliferative *in vitro*.

Hudziak *et al.* (1989) also found that the murine anti-Her-2 monclonal antibody (4D5) inhibited the proliferation of SK-Br-3 human breast cancer cells over-expressing Her-2. Furthermore, upon removal of the antibody after 11 days exposure, the cells were capable of resuming normal growth characteristics. This suggested that 4D5 was cytostatic as opposed to cytotoxic. However, trastuzumab has been found to inhibit cell proliferation by inducing G1 cell cycle arrest *in vitro,* which contrasts with the analyses of primary tumour tissue where apoptosis is observed. (Mohsin et al., 2005) This highlights that the ability of trastuzumab to elicit immunological responses may override other mechanistic features seen *in vitro*.

Many researchers have attempted to determine the role of inhibitor of apoptosis proteins in trastuzumab's mechanism of action. However, various methodologies and non-standardisation of apoptosis quantification assays have resulted in numerous discrepancies. Nonetheless, upregulation of phosphatidylinositol 3-kinase (PI3K/Akt) pathways have been implicated in the decreased response to trastuzumab. Survivin, a member of the inhibitors of apoptosis proteins (IAP), is a product of the PI3K/Akt pathway and plays a critical role in the inhibition of executioner caspases 3 and 7. Transfection with exogenous survivin allows cells to partially overcome trastuzumab induced reduction of cell viability. (Zhu et al., 2010; Dogan, Cumaoglu, Aricioglu, & Ekmekci, 2011)

Asanuma *et al.* (2005) found that trastuzumab is capable of reducing survivin levels in Her-2 positive breast cancer cells, and concluded that survivin levels may be somewhat regulated by intracellular signals from Her-2 via the PI3K/Akt pathway. Furthermore, survivin expression is under the regulation of transcription factor NF-κB. Therefore others have suggested that targeting the PI3K/Akt or NF-κB pathway may reduce survivin and leave cells more susceptible to apoptosis. (Dogan et al., 2011) While an increase in susceptibility was observed, additional apoptotic stimuli were required for the initiation of apoptosis. While these observation are of great importance *in vivo* where induction of ADCC is possible, if trastuzumab does not induce apoptosis *in vitro* it creates a gap in further clarification of trastuzumab's mechanism of action.

To further elucidate trastuzumab's mechanism of action, cell cycle analysis was conducted to determine the distribution of cells throughout the cell cycle after exposure to trastuzumab. In MCF-7 cells after 72 hours exposure a statistically significant G1 accumulation [$G1_{72}$: 56.37% (±4.48)] was observed (Table 3.4). In contrast, SK-Br-3 cells showed a sustained and statistically significant G1 accumulation as early as 24 hours through to 72 hours [$G1_{72}$: 66.93% (±3.41)] (Figure 3.6; Table 3.5) compared to untreated controls [G1: 45.19% (±0.65)]. While G1 accumulation began from 24 hours in SK-Br-3 cells there was no significant difference between each of the three time points.

Cyclin D-dependent kinases (cdks) and cyclin E/cdk2 are sequentially activated complexes involved in phosphorylation and inactivation of growth-suppressor protein retinoblastoma pRb; upon hyper-phosphorylation, pRb results in the release of transcription factor (E2F) initiating transcription genes for DNA replication and cell cycle progression. (Sahin et al., 2009) Consistent with the cell cycle data found in our study, Mohsin *et al*. (2005) observed that trastuzumab inhibits cell proliferation by up-regulation of cell cycle inhibitors p27 and inducing G1 cell cycle arrest.

Also using mAb 4D5, Lane *et al*. (2000) assessed its mechanisms of action in Her-2 over-expressing BT-474 ductal carcinoma cells. Cell growth was found to be significantly reduced following 4D5 exposure which correlated with a 10-fold reduction in the S-phase cell cycle fraction, and no evidence of apoptosis. Rather, exposure to 4D5 induced a dramatic G1-S phase block via modulation of cyclins and cyclin-dependent kinases complexes with a correlating accumulation of protein kinase inhibitor $p27^{Kip1}$, inactivation of cdk2 and reduction in $p27^{Kip}$ sequestration proteins. It was further demonstrated that on removal of 4D5, cells were able to re-enter the cell cycle. A dramatic increase in $p27^{Kip1}$ was observed over and above the release of sequestered $p27^{Kip1}$ which associated into complexes with cdk2 resulting in cdk2 inactivation.

It was concluded that 4D5 exposure interferes with Her-2 receptor signalling, down-regulates p27 sequestration (which allows p27 to inhibit cyclin E/cdk2 complexes) and consequently inhibits G1-S phase transition and cell cycle progression. The experiments were repeated in SK-Br-3 cells and a similar ability to form $p27^{Kip1}$-cdk2 complexes was observed, although, an increase in $p27^{Kip1}$ was not. Lane *et al*. (2000) suggested that the extent of cdk2 inactivation following reduction in receptor phosphorylation is cell type specific. Furthermore, responses may be graded, based on the level of dependence on Her-2 receptor level for mitogenic signalling. (Lane et al., 2000; Lane, Motoyama, Beuvink, & Hynes, 2001) Sahin *et al*. (2009) quantified phosphorylation and inactivation of pRb as a marker of transition between G1 and S phases. They noted that phosphorylation levels of pRb were low in cells undergoing growth arrest. By binding to upstream Her-2 receptors, trastuzumab may interfere with the phosphorylation of these growth suppressor proteins, thereby altering G1-S phase transitions.

Whether relative Her-2 receptor density is changed by trastuzumab remained an important issue. Increasing or decreasing availability of targets for trastuzumab could have far-reaching consequences for targeted therapy. Therefore, relative Her-2 receptor density was assessed with the use of a fluorescent affibody molecule that binds to a different site than trastuzumab. MCF-7 cells showed minimal difference in the overlay plot of unstained and untreated samples and trastuzumab treated samples were indistinguishable from untreated samples at any time point.

In contrast, Her-2 rich SK-Br-3 cells illustrated only a slight overlap in the tail region of the overlay plot of unstained and untreated cells. A statistically significant decrease in Her-2 receptors was observed in cells exposed to trastuzumab [$trastuzumab_{24}$: 68.69% (±1.14)] compared to the untreated control [untreated: 100.7% (±1.42)] from 6 hours (Figure 3.13). Similar decreases were obtained at 12, 24 and 48 hours. No significant differences in Her-2 receptors were apparent between time points. This significant decrease in Her-2 receptors could have been due to trastuzumab-induced internalisation of Her-2 receptors. It was not apparent whether Her-2 receptors were degraded or if recycling to the cell surface occurred beyond 48 hours, as this was beyond the experiment scope.

There are many discrepanices in the literature with regard to the ability of trastuzumab to bring about alterations in Her-2 receptor density. (Daly et al., 1997; Gong et al., 2005) Most analyses of receptor density used lysed cells, which may detect internalised receptors that had not yet been degraded. This may skew data in favour of a high receptor density. However, Hudziak *et al.* (1989) demonstrated enhanced degradation of Her-2 receptors in response to 4D5.

Assessment of Her-2 receptors performed in our experiments used flow cytometry of whole cells because trastuzumab is only effective if the receptors are available on the cell surface for binding. The concept of existing receptor reservoirs which shuttle receptors to the surface or the reliance on *de novo* synthesis in response to stimuli, is poorly understood. While the overall number of receptors within a cell may not change in response to trastuzumab and the ability of receptor numbers to be restored upon removal of trastuzumab is inconclusive, the level of surface expression remains essential for trastuzumab to exert its effects. Therefore, understanding and monitoring the molecular subtypes of cancer and divergence of predominant signalling pathways in response to therapeutic strategies is required to ensure therapeutic benefit.

In summary, our results showed that in SK-Br-3 cells, trastuzumab was anti-proliferative, altered cell cycle kinetics resulting in G1 phase accumulation and did not induce apoptosis when used alone. Furthermore, trastuzumab induced a substantial decrease in surface Her-2 receptor density. It is of importance to note that while targeted therapies have achieved great commendation because of their selectivity and specificity, efficacy remains dependent on the continual and persistent presence of targets. Analysis of total Her-2 receptor protein may not provide sufficient correlation with the efficacy of trastuzumab which could be reduced if the number of cell surface Her-2 receptors is not maintained above a certain threshold. In addition, agents that result in the recycling of Her-2 receptors may render trastuzumab clinically ineffective while agents which maintain surface Her-2 receptors may provide positive augmentation of the effects of trastuzumab.

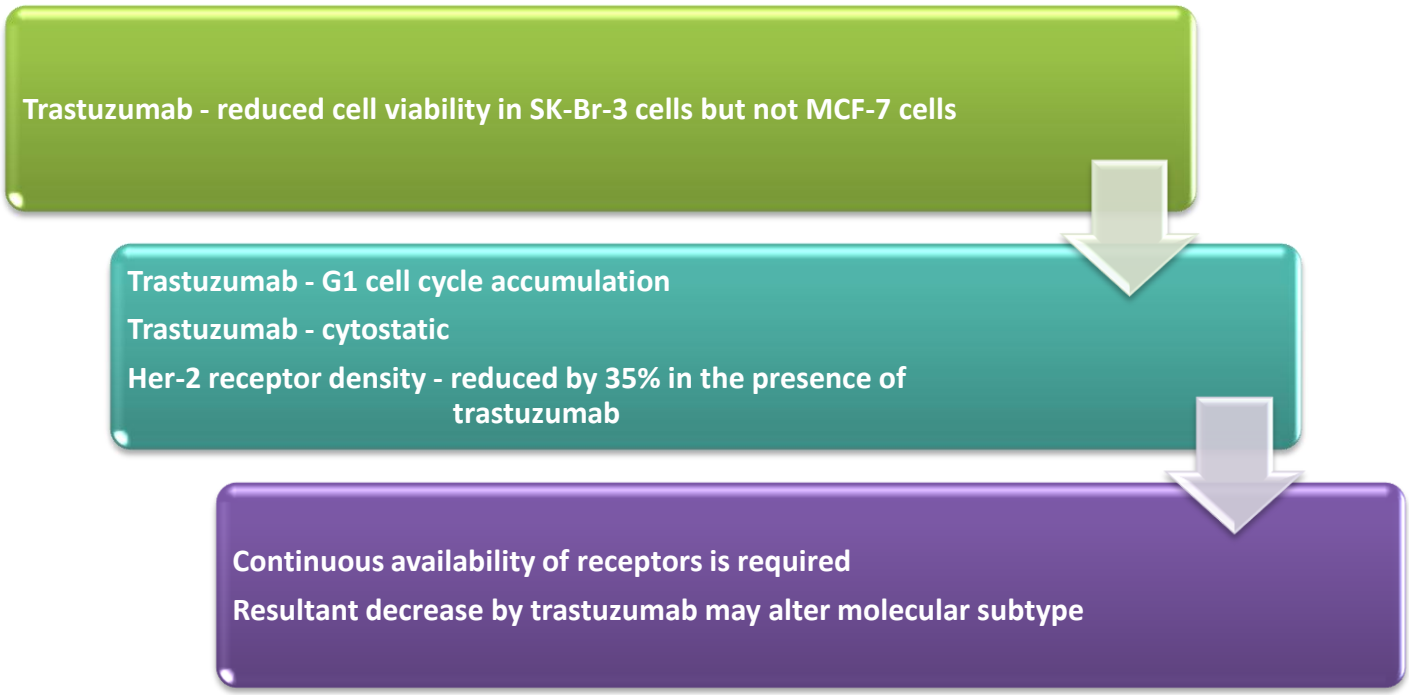

Chapter 4: Results and Discussion: Aspirin

4.1 Cell Viability

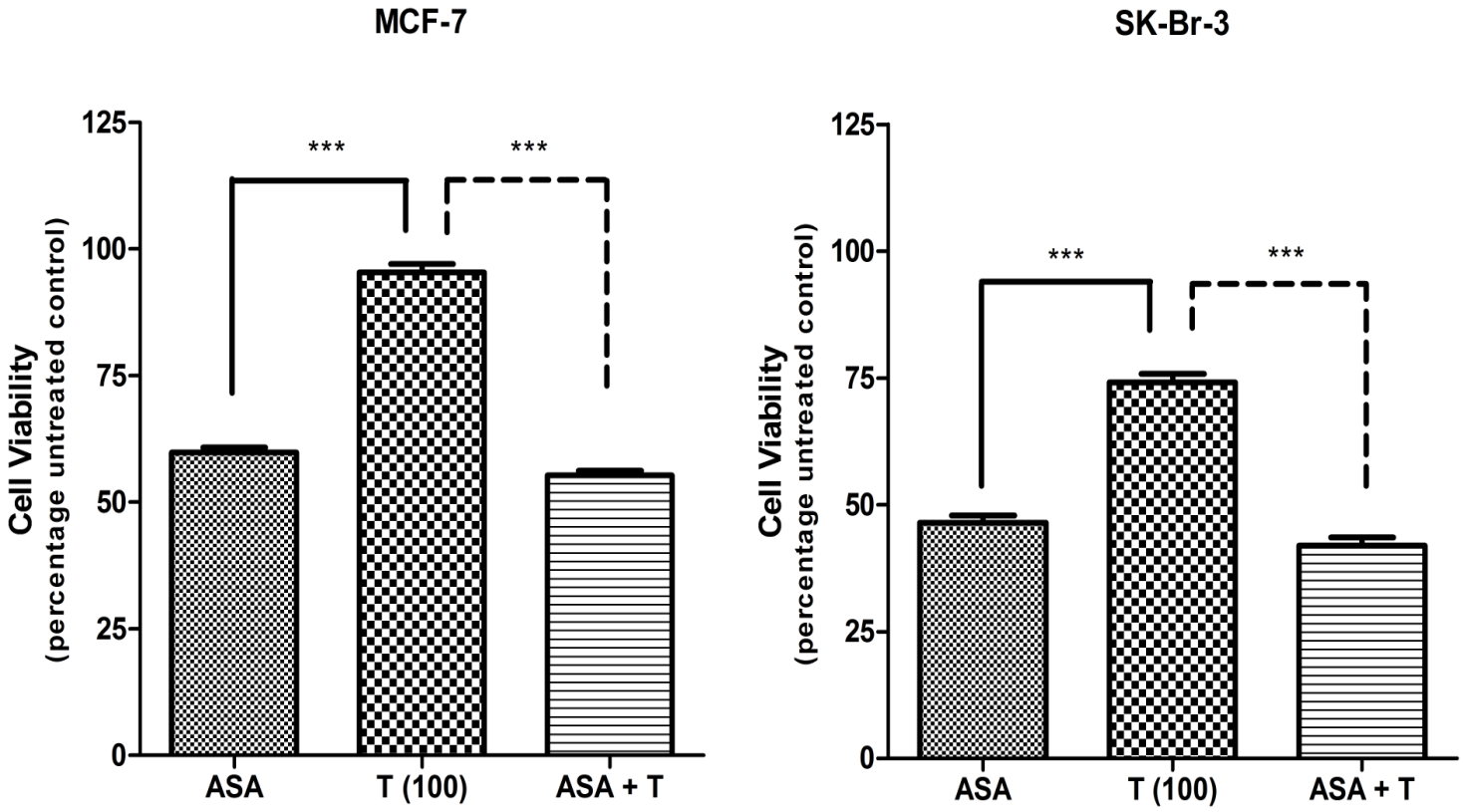

Figure 4.1: Cell viability in MCF-7 and SK-Br-3 cells expressed as a percentage of the untreated controls. Statistically significant differences were found between trastuzumab alone versus aspirin alone and the aspirin-trastuzumab combination. Further statistically significant differences (P < 0.001) were found when comparing the average cell viability of aspirin alone between MCF-7 and SK-Br-3 cells. ASA: aspirin (5.5 mM), T (100): trastuzumab 100 µg/ml. (Statistical significance followed the same trend for combinations at 25 µg/ml, 50 µg/ml, 200 µg/ml in both cell lines.)

Table 4.1: Cell viability results for aspirin and the aspirin-trastuzumab combination

	MCF-7	SK-Br-3
	Mean ± SEM	**Mean ± SEM**
Aspirin (ASA) (5.5 mM)	59.83 ± 1.05	46.50 ± 1.44
ASA + Trastuzumab (25 µg/ml)	62.23 ± 1.94	40.59 ± 2.27
ASA + Trastuzumab (50 µg/ml)	62.06 ± 1.21	42.29 ± 2.21
ASA + Trastuzumab (100 µg/ml)	55.34 ± 0.85	41.91 ± 1.62
ASA + Trastuzumab (200 µg/ml)	56.67 ± 1.36	43.62 ± 1.76

4.2 Cell Cycle Analysis

Table 4.2: Cell cycle results for aspirin, trastuzumab and the aspirin-trastuzumab combination in MCF-7 cells

MCF-7	Mean ± SEM				Significance			
72 Hours	**G1**	**S**	**G2**	**Sub G1**	**C**	**ASA**	**ASA + T**	**T**
Control (C)	23.25 ± 0.86	52.99 ± 2.33	23.76 ± 3.17		-	*	*	*
ASA	53.75 ± 6.93	27.34 ± 7.05	18.90 ± 0.22	4.17 ± 1.03	*	-		
ASA + T	57.95 ± 6.58	26.14 ± 4.14	15.91 ± 5.08	12.36 ± 4.69	*		-	
T	56.37 ± 4.48	33.34 ± 3.23	10.29 ± 1.72	1.89 ± 0.02	*			-

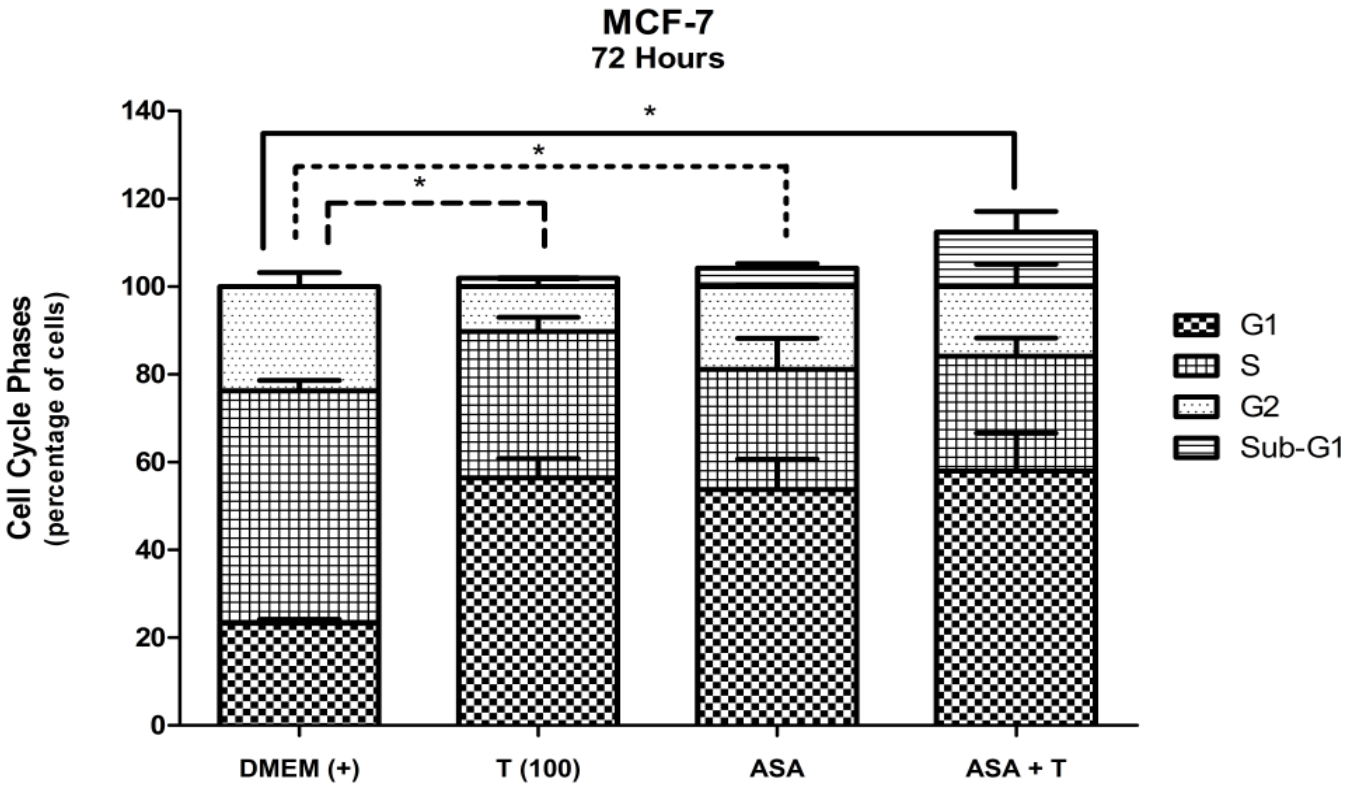

Figure 4.2: Cell cycle analysis in MCF-7 cells expressed as a percentage after deconvolution. Statistically significant differences in the G1 phase of the cell cycle were observed between untreated control (DMEM+) versus trastuzumab, aspirin and the aspirin-trastuzumab combination after 72 hours. ASA: aspirin (5.5 mM), T (100): trastuzumab 100 µg/ml [Significance followed similar trends for SK-Br-3 cells]

Table 4.3: Cell cycle results for aspirin, trastuzumab and the aspirin-trastuzumab combination in SK-Br-3 cells

SK-Br-3	Mean ± SEM				Significance			
48 Hours	**G1**	**S**	**G2**	**Sub G1**	**C**	**ASA**	**ASA + T**	**T**
Control (C)	45.19 ± 0.65	35.68 ± 0.81	19.16 ± 0.31		-	**	*	**
ASA	62.53 ± 4.41	24.79 ± 2.69	12.62 ± 2.64	10.89 ± 1.82	**	-		
ASA + T	60.52 ± 2.04	17.58 ± 2.26	21.90 ± 0.31	10.45 ± 0.82	*		-	
T	64.15 ± 1.41	20.84 ± 3.55	15.02 ± 4.56	11.48 ± 1.28	**			-
72 Hours	**G1**	**S**	**G2**	**Sub G1**	**C**	**ASA**	**ASA + T**	**T**
Control (C)	45.19 ± 0.65	35.68 ± 0.81	19.16 ± 0.31		-	**	**	***
ASA	60.95 ± 1.46	28.02 ± 3.29	11.03 ± 3.99	16.75 ± 1.52	**	-		
ASA + T	63.97 ± 2.43	17.46 ± 3.17	18.57 ± 1.31	12.56 ± 0.75	**		-	
T	66.93 ± 3.41	20.78 ± 2.60	15.02 ± 1.38	11.69 ± 2.20	***			-

4.3 Relative Her-2 Receptor Density

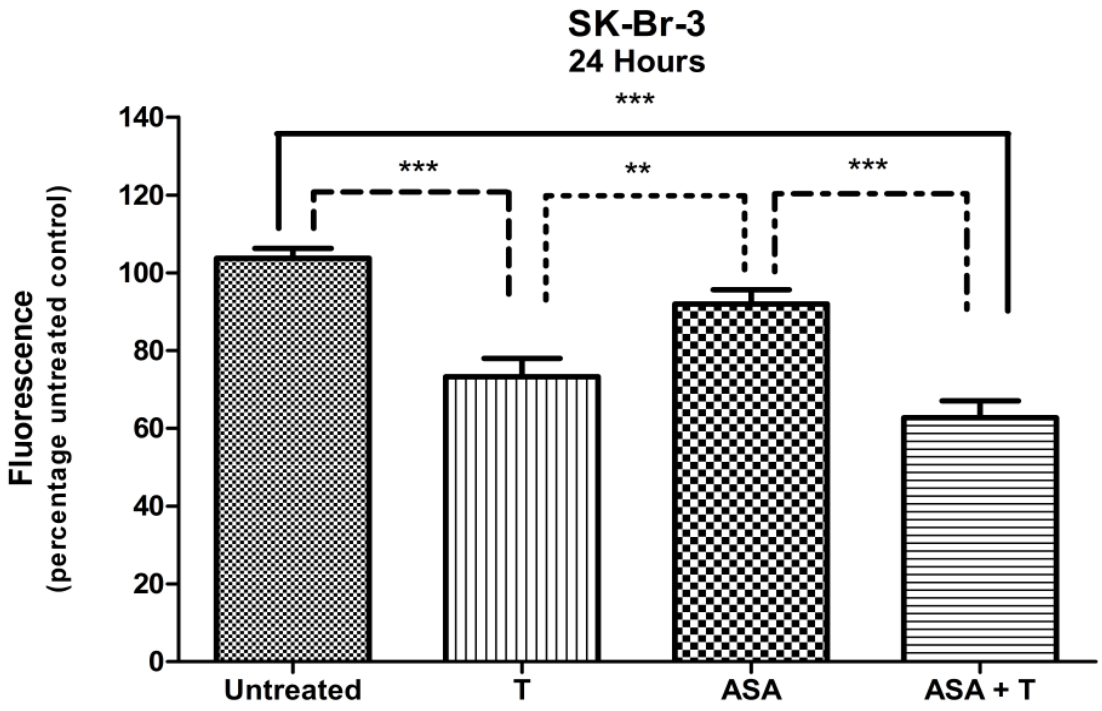

Figure 4.3: Relative Her-2 receptor density analysis at 24 hours in SK-Br-3 cells expressed as a percentage of the fluorescence of untreated controls (standardised to 100%). Statistical significance followed the same trend at 12, 24 and 48 hours. ASA: aspirin (5.5 mM), T (100): trastuzumab 100 µg/ml.

Table 4.4: Fluorescent intensity (histogram x-mean) of SK-Br-3 cells exposed to aspirin, trastuzumab and the aspirin-trastuzumab combination

SK-Br-3	Mean ± SEM	Significance			
12 Hours		**U**	**ASA**	**ASA + T**	**T**
Untreated (U)	99.49 ± 2.52	-		***	***
ASA	93.44 ± 4.12		-	***	**
ASA + T	65.40 ± 3.55	***	***	-	
T	64.77 ± 3.60	***	**		-
24 Hours		**U**	**ASA**	**ASA + T**	**T**
Untreated (U)	103.70 ± 2.61	-		***	***
ASA	91.98 ± 3.69		-	***	**
ASA + T	62.73 ± 4.32	***	***	-	
T	65.47 ± 4.76	***	**		-
48 Hours		**U**	**ASA**	**ASA + T**	**T**
Untreated (U)	100.00 ± 1.95	-		***	***
ASA	91.63 ± 1.46		-	***	***
ASA + T	64.60 ± 4.13	***	***	-	
T	61.83 ± 4.42	***	***		-

Acetylsalicylic acid, better known as aspirin, is a non-steroidal anti-inflammatory drug (NSAID) well documented for its anti-neoplastic properties which have been studied predominantly in human colon cancer. A widely accepted mechanism of action for NSAIDs is the reduction of prostaglandin synthesis by inhibition of the cyclooxygenase (COX) pathway. Cyclooxygenase-2 (COX-2) is a rate-limiting, inducible enzyme responsible for the production of prostaglandins from arachidonic acid which plays a role in the inflammatory process. Elevation of COX-2 and prostaglandins has been detected in multiple cancer subtypes; researchers such as Liu *et al*. (1996) have observed differential expression and regulation of COX enzymes in breast cancer cell lines.

Hanif *et al*. (1996) examined the effects of NSAIDs on cell proliferation, cell cycle distribution and apoptosis using two colon cancer cell lines, one possessing the ability to produce prostaglandins (PG) and one unable to produce PGs. The same effects occurred in both cell lines irrespective of PG production suggesting that NSAIDs inhibited proliferation by mechanisms independent of their ability to inhibit PG synthesis. Furthermore, exogenous PGs did not reverse NSAID effects.

Frequency and localization of COX expression has been studied in MCF-7 cells. These cells were found to lack COX-2 proteins. However, MCF-7/Her-2 transfectants expressed COX-2 proteins. While no definitive relationship associating Her-2 receptors and COX-2 could be established, it was concluded that a co-ordinated relationship may exist between these pathways due to the inducible nature of COX-2 in the presence of Her-2 receptors. (Half et al., 2002)

While COX dependent pathways have been identified, further determination of COX independent biochemical pathways are now being emphasized. Intracellular processes such as binding to inhibitor of nuclear factor κB (NF-κB) kinase β, activation of p38 kinase, uncoupling of oxidative phosphorylation, activation of nuclear receptor peroxisome proliferator-activated receptor γ affecting transcription and regulation of DNA mismatch repair (MMR) protein system may be involved in the COX- independent pathways. (Goel et al., 2003)

Alterations in the expression or functioning of the inhibitor protein I-kappaB (IκB), as well as continuous activation of essential NF-κB factors are emerging as a hallmark for various types of solid tumours where oncogenesis has been directly correlated with activation of IκB kinases that result in IκB degradation. (Rayet & Gelinas, 1999) Under normal physiological conditions NF-κB is ubiquitously expressed as a polypeptide heterotrimer (p50 [RelA], p65 and IκB-α) required for immune function and may become inappropriately activated in tumorigenesis.

NF-κB remains in a latent, inactive state in the cytoplasm by being bound to the inhibitor protein I-kappaB (IκB). Following appropriate stimulation, IκB-α is phosphorylated by the cytoplasmc IKK (IκB kinase) complex. Subsequent to phosphorylation IκB-α is ubiquitinated and targeted for proteosomal degradation which allows the remaining NF-κB heterodimer to translocate to the nucleus. Transcription of target genes that include cell growth, inflammation and apoptosis are regulated via binding to DNA sites collectively known as κB sites. (Pahl, 1999; Din, Dunlop, & Stark, 2004; Stark et al., 2007)

While carcinogens activate NF-κB, paradoxically, so do agents that are used to induce apoptosis. Furthermore the dual capability of NF-κB to activate or inactivate needs to be carefully examined in order to establish benefit in neoplastic transformation. (Aggarwal, 2004)

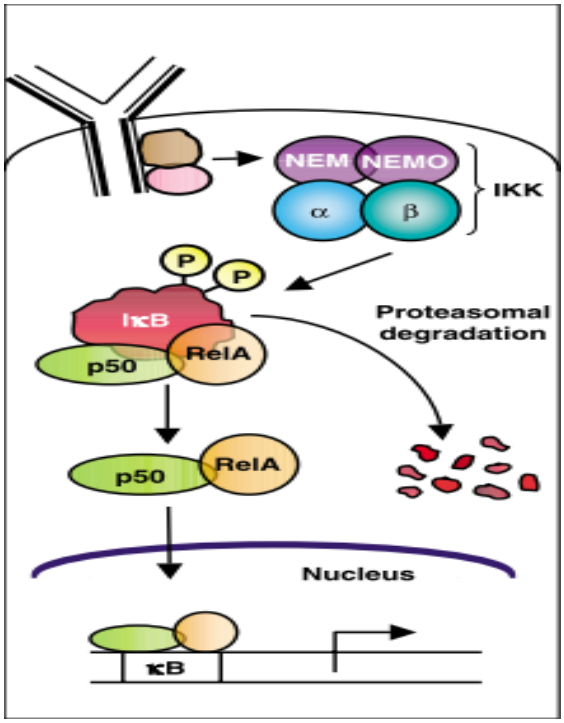

Figure 4.4: NF-kB signal transduction pathways. In the canonical (or classical) NF-kB pathway, NF-κB dimers such as p50/RelA are maintained in the cytoplasm by interaction with an independent IκB molecule (often IκB-α). In many cases, the binding of a ligand to a cell surface receptor (e.g., tumour necrosis factor-receptor) recruits adaptors to the cytoplasmic domain of the receptor. These adaptors often recruit an IKK complex (containing the α and β catalytic subunits and two molecules of the regulatory scaffold NEMO) directly onto the cytoplasmic adaptors. This clustering of molecules at the receptor activates the IKK complex. IKK then phosphorylates IκB at two serine residues, which leads to its K48 ubiquitination and degradation by the proteasome. NF-κB then enters the nucleus to turn on target genes (Gilmore, 2006)

NF-κB plays a central role in mediating immune responses but may be more accurately defined as a regulator of stress responses which allows activation of inducible responses including nitric oxide synthase (iNOS) and cyclooxygenase-2 (COX-2). Yamamoto *et al.* (1995) observed that various concentrations of TNF-α induced cyclooxygenase-2 in a time and dose-dependent fashion. It was further elucidated that in mutants of NF-κB there was a significant decrease in COX-2 which suggested that NF-κB was a transcriptional factor involved in induction of COX-2.

These results suggested that pathways involving NF-κB are not COX-independent mechanisms but more likely precursors in the COX-implicated processes. While NF-κB is involved in the transcription of over 150 target genes, specificity and selectivity of transcription may reside in the targeted cell type because not all cell types will respond equally to specific stimuli. (Pahl, 1999)

Multiple researchers have demonstrated that aspirin (1-10 mM) induced time and dose dependent phosphorylation and proteosomal degradation of IκB-α with increased nuclear translocation of NF-κB. Nuclear translocation of NF-κB was found to be cell type and environmentally specific and could be assessed by nuclear accumulation of p65, the transcriptionally active subunit of NF-κB. (Din et al., 2004; Stark et al., 2007)

A comparison of 6 colorectal cancer cell (CRC) lines with multiple non-colorectal cell lines, including MCF-7 breast adenocarcinoma cells, illustrated a concentration dependent decrease in cell viability and IκB-degradation within the CRC lines. Din *et al.* (2004) suggested that no demonstrable effect in non-CRC was present even at aspirin concentrations of 10 mM. These results were observed even though relative levels of IκB-α and p65 expression were similar in CRC and non-CRC. This study emphasized the possibility of cell-type specific molecular targets but suggests that effects of aspirin are selective to colorectal cancer cells as opposed to tissue types of other origins.

In vivid contrast to results obtained by Din *et al.* (2004) which concluded that aspirin induces no demonstrable effect in non-colorectal cell lines, in our study significant alterations in cell viability were observed. Aspirin (5.5 mM) exposure resulted in cell viability of 59.83% (±1.05) in MCF-7 cells and concurrent trastuzumab (100 µg/ml) exposure further decreased cell viability to 55.34% (±0.85). The effects were even greater in SK-Br-3 cells where aspirin-exposure caused a cell viability of 46.5% (±1.44). Once again concurrent aspirin and trastuzumab exposure resulted in an additional decline in cell viability to 41.91% (±1.62), although this was found to be statistically insignificant (Figure 4.1; Table 4.1).

Further contrasting the results by Din *et al.* (2004), research by Dejardin *et al.* (1999) illustrated that constitutive activation of NF-κB is present in some breast cancer cells. However, basal levels have been reported as considerably varied between cell lines. NF-κB activity is regulated by a family of inhibitors which include IκB-α, IκB-β, IκB-ε, Bcl-3, p100 and p105 which have also been shown to express distinctly different basal levels between cell lines. Cell-type specific molecular targets are suggested and unfortunately, this work has not been conducted on MCF-7 or SK-Br-3 cells.

In our experiment, a statistically significant difference was evident between the cell lines when exposed to aspirin. A difference in basal levels of cytosolic NF-κB could be the underlying reason for this difference in anti-neoplastic response between MCF-7 and SK-Br-3 cells. Furthermore, if one of the NF-κB family of inhibitors is the preferential target of aspirin and the level of that inhibitor is altered between the cell lines, this could also create an opportunity for differences in response.

It has also been suggested that protein-protein interactions between oestrogen receptors (ER) and transcriptionally active NF-κB (p65) may lead to inhibition of the NF-κB pathway. If ER functions as nuclear inhibitors of p65 transactivation, this would suggest that cells possessing oestrogen receptors are less likely to benefit from the ability of aspirin to target the IκB family because of the protective effect elicited by ER. (Rays, 1994; Dejardin et al., 1999) This was corroborated in our experiments where the anti-proliferative effect of aspirin in oestrogen receptor positive MCF-7 cells was lower than in SK-Br-3 cells.

No caspase-3 and -7 activation was observed in either cell line (data not shown) suggesting that executioner caspases may only be detectable at a time point beyond 30 hours or that aspirin primarily induces anti-proliferative effects. Furthermore, the annexin-V assay showed no difference in fluorescent staining between untreated controls and cells exposed to aspirin or with concurrent trastuzumab supporting the notion of aspirin being cytostatic.

Researchers have noted that aspirin (5 mM) reduced levels of survivin, a member of the inhibitor of apoptosis (IAP) family which promotes resistance to apoptotic stimuli. The reduction of survivin appears to sensitise some cancer cells to pro-apoptotic cytokines and is regulated by post-transcriptional mechanisms. (Lu et al., 2008) While researchers have observed aspirin-induced reduction in survivin levels sensitising cells to apoptotic stimuli, no evidence was found here of aspirin promoting apoptosis when used in the absence of other pro-apoptotic factors.

In MCF-7 cells it was evident that a gradual G1 phase accumulation occurred between 24 hours [$G1_{24}$: 22.71% (±1.33)] and 48 hours [$G1_{48}$: 36.23% (±1.76)] when aspirin was compared to the untreated control [G1: 23.25% (±0.86)]. At 72 hours, statistically significant G1 accumulation [$G1_{72}$: 53.75% (±6.93)] was observed in these cells. A similar trend was observed in the aspirin-trastuzumab combination reflecting significant G1 accumulation at 72 hours [$G1_{72}$: 57.95% (±6.85)] (Figure 4.2; Table 4.2).

Aspirin-exposed SK-Br-3 cells showed a statistically significant G1 accumulation from 48 hours through to 72 hours [$G1_{72}$: 60.95% (±1.45)] when compared to untreated controls [G1: 45.19% (±0.65)]. Similarly G1 accumulation was observed in the aspirin-trastuzumab combination from 24 to 72 hours [$G1_{72}$: 63.97% (±2.43)]. There were no significant differences when comparing aspirin, trastuzumab [$G1_{72}$: 66.93% (±3.41)] or the combination at 48 and 72 hours in these cells (Table 4.3).

In their assessment of survivin depletion in response to exposure to aspirin (5 mM), Lu *et al*. (2008) also observed robust G1 arrest in MDA-MB-435 (melanoma cells) after 48 hours. (Lu et al., 2008) Elder *et al*. (1996) observed considerable variation in the sensitivity of cell lines to aspirin's growth inhibitory effects with adenoma cell lines being less sensitive than carcinoma cell lines. The anti-proliferative mechanism proposed was due to G0-G1 accumulation and decreasing S-phase entry compared to controls. While G1 accumulation was observed in all cell lines, the extent of cell cycle arrest was not necessarily correlated to the sensitivity of growth inhibitory properties.

In terms of Her-2 receptor density, Her-2 deficient MCF-7 cells showed minimal difference in the overlay plot of unstained and untreated samples. Aspirin, trastuzumab and the aspirin-trastuzumab combination treated samples were indistinguishable from untreated samples at any time point. Contrastingly, in Her-2 over-expressing SK-Br-3 cells, a minor decrease in Her-2 receptors was observed in cells treated with aspirin alone [ASA_{12}: 93.44% (±4.12)] at 12, 24 and 48 hours compared to untreated controls [$untreated_{12}$: 99.49% (±2.52)], but this was found to be statistically insignificant (Figure 4.3; Table 4.4).

However, a statistically significant decrease was apparent between untreated controls [$untreated_{12}$: 99.49% (±2.52)] versus trastuzumab [T_{12}: 64.77% (±3.60)] and aspirin-trastuzumab combinations [ASA+T: 65.40% (±3.55)] at 12, 24 and 48 hours, suggesting that as a single agent aspirin has no influence on the density of Her-2 receptors on the cell surface. It cannot be concluded whether aspirin influences signal transduction downstream of the Her-2 receptor. There were insignificant differences when comparing trastuzumab alone versus the aspirin-trastuzumab combination providing evidence that in combination, trastuzumab functions to decrease Her-2 receptors in a similar or identical fashion to when it is used alone.

While pathways may intersect downstream, aspirin and trastuzumab do not appear to function harmoniously in combination. Aspirin does not appear to potentiate or augment the effect of trastuzumab *in vitro* and while Her-2 receptors were decreased in combination, this did not ultimately alter cell viability significantly compared to aspirin alone over the observed period.

Aspirin differentially and significantly altered cell viability in MCF-7 and SK-Br-3 cells. It remains important to note that trastuzumab reduced SK-Br-3 cell viability, while in combination, cell viability was drastically reduced by more than double which closely mimicked that of aspirin alone. However, the use of aspirin and trastuzumab in combination did not provide any potential prospects. Moreover, the concentrations of aspirin used, while directly comparable to those used in other studies, are too high for clinical relevance.

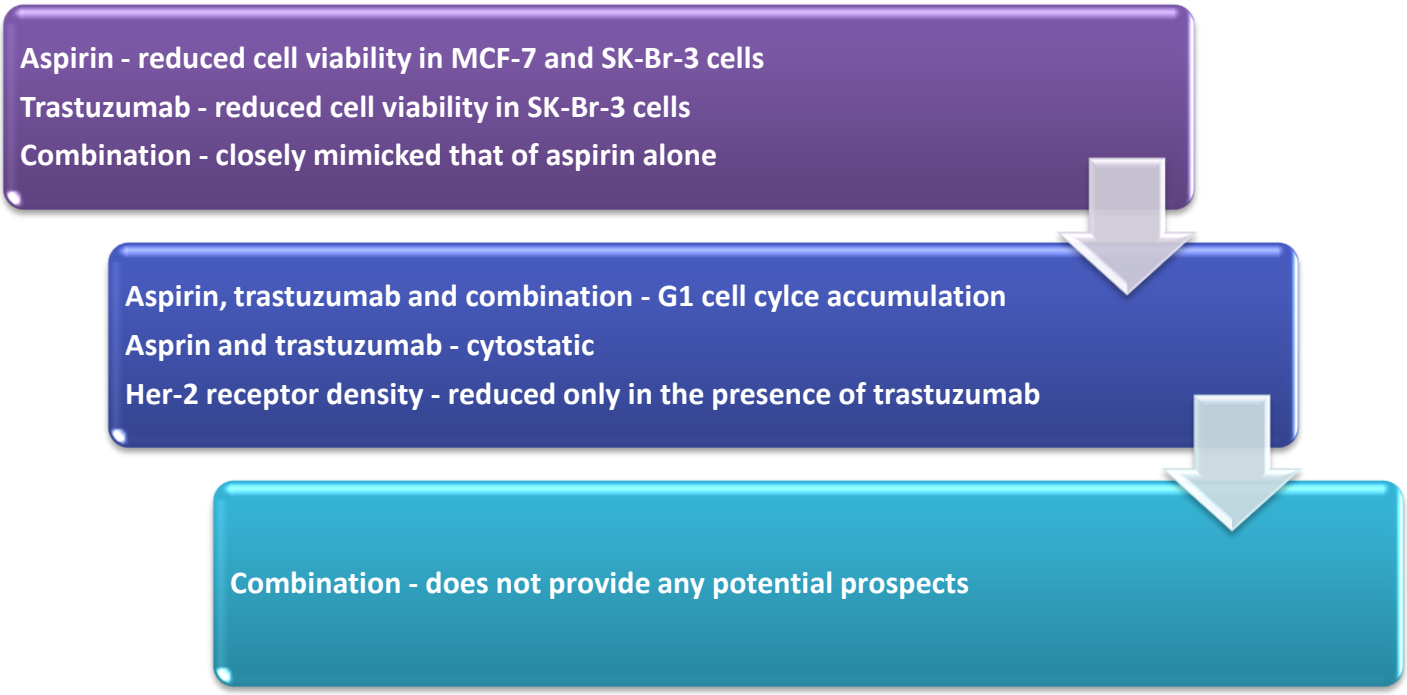

Chapter 5: Results and Discussion: Calcipotriol

5.1 Cell Viability

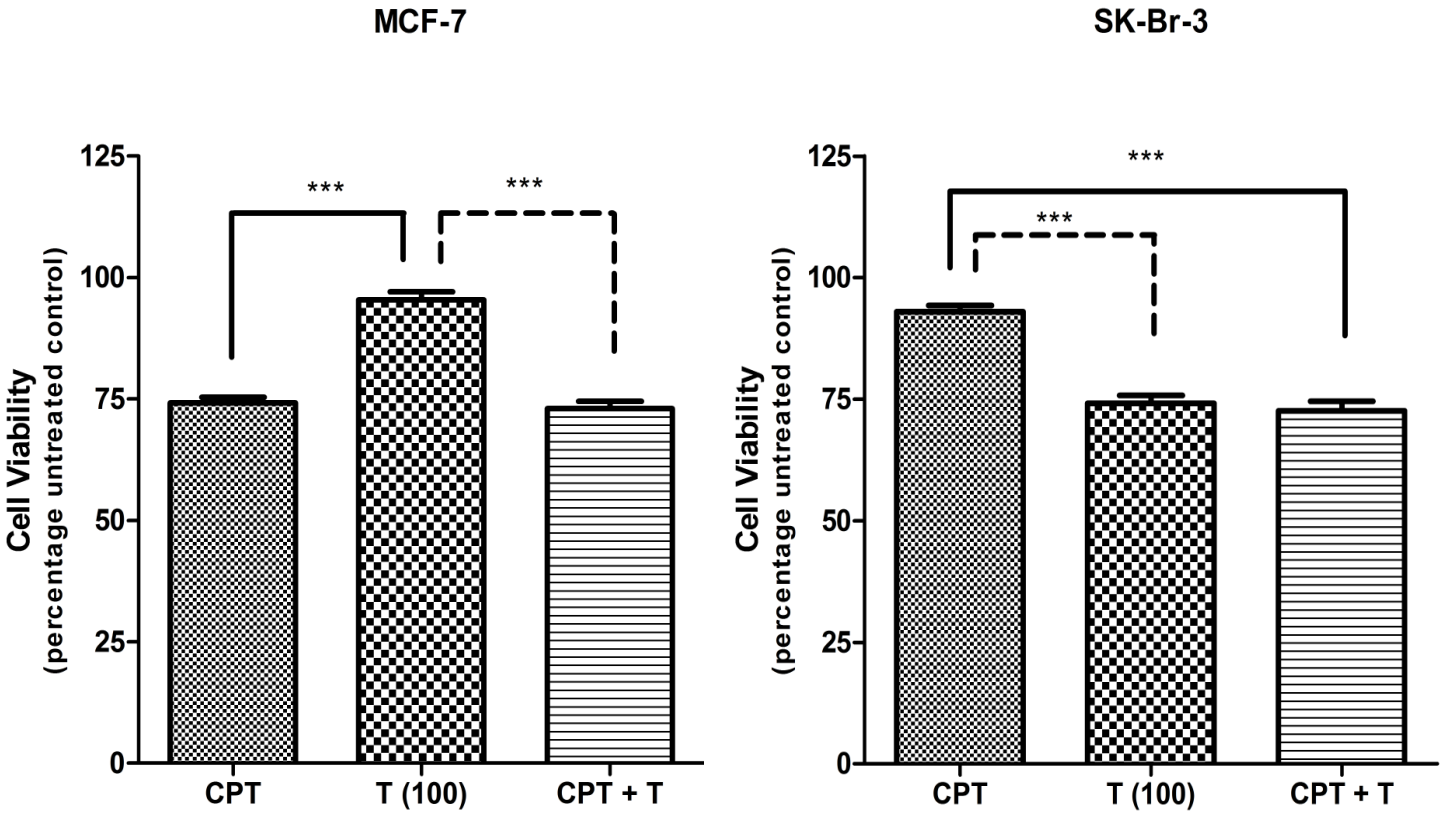

Figure 5.1: Cell viability in MCF-7 and SK-Br-3 cells expressed as a percentage of the untreated controls. Statistically significant differences were found between trastuzumab alone versus calcipotriol alone and the calcipotriol-trastuzumab combination in MCF-7 cells. Significance between calcipotriol alone versus trastuzumab alone and the combination was observed in SK-Br-3 cells. Further statistically significant differences (P < 0.001) were found when comparing average cell viability of calcipotriol alone between MCF-7 and SK-Br-3 cells. CPT: calcipotriol (2.4 µM), T (100): trastuzumab 100 µg/ml. (Statistical significance followed the same trend for combinations at 25 µg/ml, 50 µg/ml, 200 µg/ml in both cell lines.)

Table 5.1: Cell viability results for calcipotriol and the calcipotriol-trastuzumab combination

	MCF-7	SK-Br-3
	Mean ± SEM	Mean ± SEM
Calcipotriol (CPT) (2.4 µM)	74.13 ± 1.22	92.97 ± 1.29
CPT + Trastuzumab (25 µg/ml)	80.38 ± 2.30	74.52 ± 2.46
CPT + Trastuzumab (50 µg/ml)	77.88 ± 1.93	77.89 ± 2.89
CPT + Trastuzumab (100 µg/ml)	73.01 ± 1.51	72.59 ± 1.96
CPT + Trastuzumab (200 µg/ml)	71.61 ± 2.63	71.42 ± 2.04

5.2 Cell Cycle Analysis

Table 5.2: Cell cycle results for calcipotriol, trastuzumab and the calcipotriol-trastuzumab in MCF-7 cells

MCF-7	Mean ± SEM				Significance			
72 Hours	**G1**	**S**	**G2**	**Sub G1**	**C**	**CPT**	**CPT + T**	**T**
Control (C)	23.25 ± 0.86	52.99 ± 2.33	23.76 ± 3.17		-	*	*	**
CPT	44.96 ± 3.63	37.39 ± 0.56	17.62 ± 3.13	4.09 ± 1.61	*	-		
CPT + T	46.45 ± 4.91	38.14 ± 3.62	15.28 ± 2.35	6.49 ± 0.58	*		-	
T	56.37 ± 4.48	33.34 ± 3.23	10.29 ± 1.72	1.89 ± 0.02	**			-

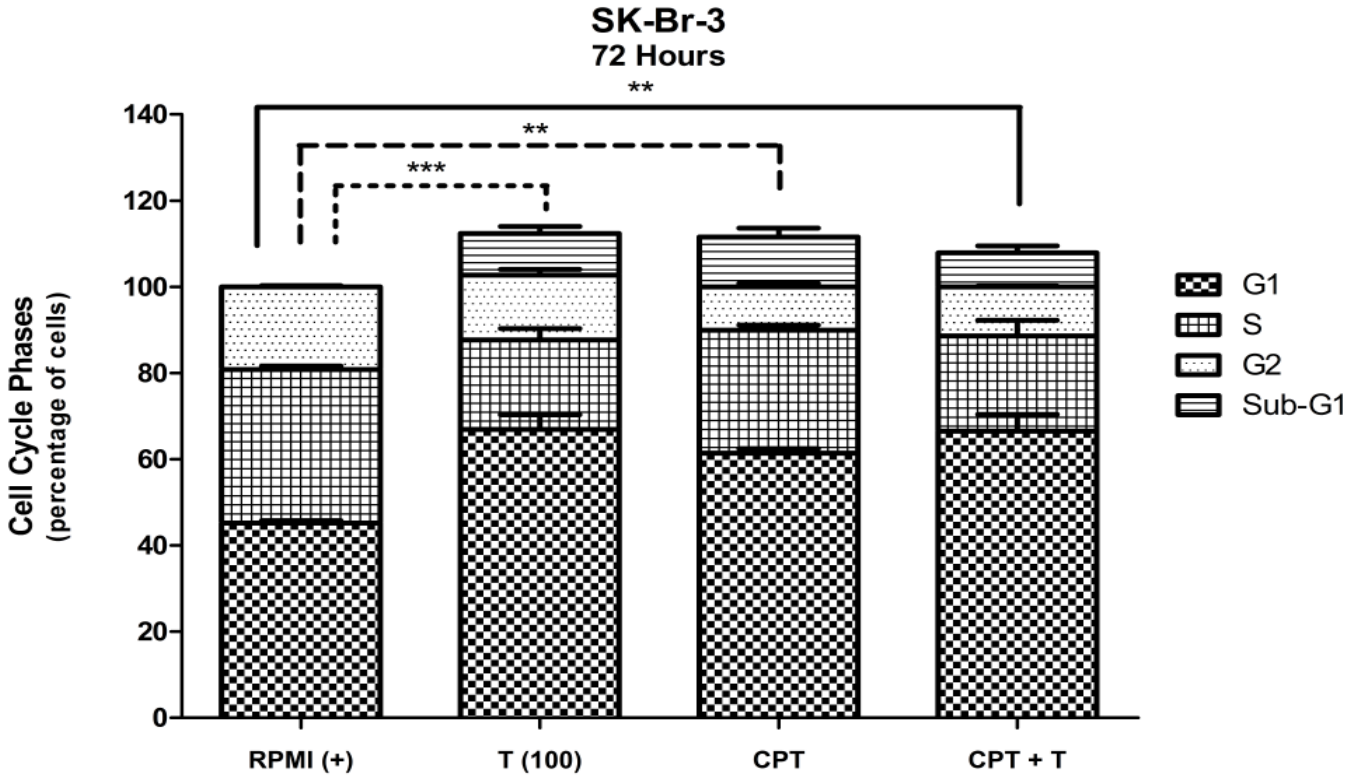

Figure 5.2: Cell cycle analysis in SK-Br-3 cells expressed as a percentage after deconvolution. Statistically significant differences in the G1 phase of the cell cycle were observed between untreated control (RPMI+) versus trastuzumab, calcipotriol and the calcipotriol-trastuzumab combination after 72 hours. CPT: calcipotriol (2.4 µM), T (100): trastuzumab 100 µg/ml [Significance followed similar trends for MCF-7 cells]

Table 5.3: Cell cycle results for calcipotriol, trastuzumab and the calcipotriol-trastuzumab in SK-Br-3 cells

SK-Br-3	Mean ± SEM				Significance			
48 Hours	**G1**	**S**	**G2**	**Sub G1**	**C**	**CPT**	**CPT + T**	**T**
Control (C)	45.19 ± 0.65	35.68 ± 0.81	19.16 ± 0.31		-	**	**	**
CPT	64.59 ± 3.86	22.99 ± 4.40	12.76 ± 0.76	9.14 ± 0.11	**	-		
CPT + T	66.88 ± 3.70	14.71 ± 1.46	18.41 ± 2.27	6.36 ± 2.47	**		-	
T	64.15 ± 1.41	20.84 ± 3.55	15.02 ± 4.56	11.48 ± 1.28	**			-
72 Hours	**G1**	**S**	**G2**	**Sub G1**	**C**	**CPT**	**CPT + T**	**T**
Control (C)	45.19 ± 0.65	35.68 ± 0.81	19.16 ± 0.31		-	**	**	***
CPT	61.42 ± 1.05	28.56 ± 1.16	10.02 ± 0.88	11.62 ± 2.04	**	-		
CPT + T	66.58 ± 3.90	22.05 ± 3.67	11.37 ± 0.26	7.92 ± 1.63	**		-	
T	66.93 ± 3.41	20.78 ± 2.60	15.02 ± 1.38	11.69 ± 2.20	***			-

5.2 Relative Her-2 Receptor Density

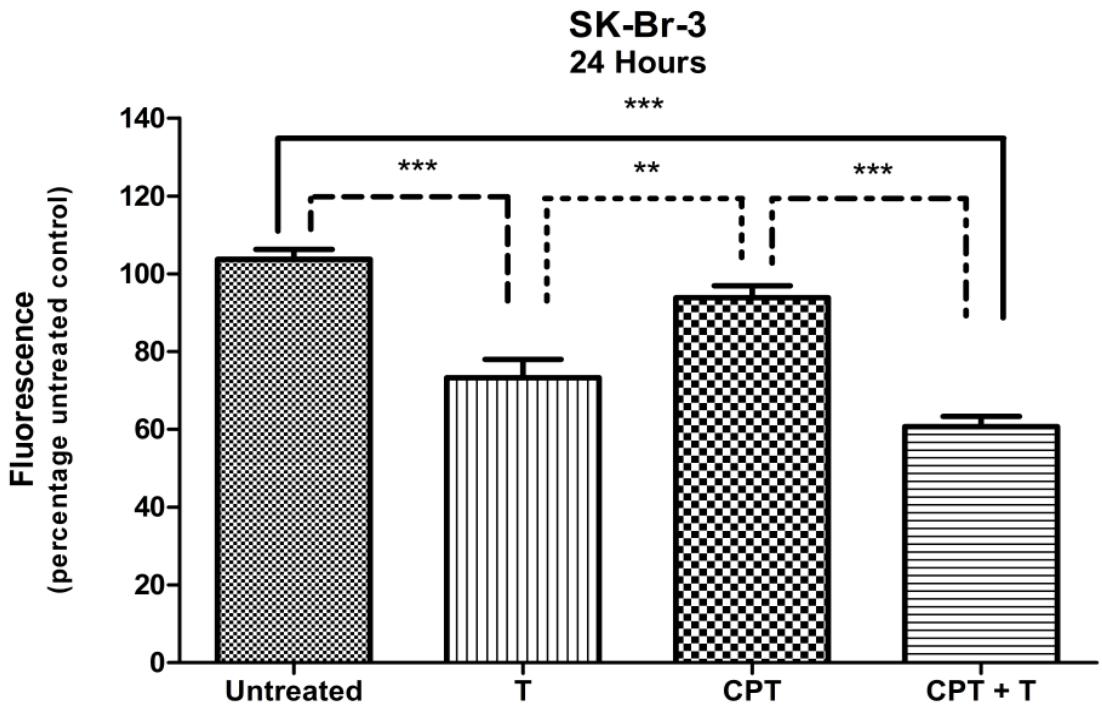

Figure 5.3: Relative Her-2 receptor density analysis at 24 hours in SK-Br-3 cell expressed as a percentage of the fluorescence of untreated controls (standardised to 100%). Statistical significance followed the same trend at 12, 24 and 48 hours. CPT: calcipotriol (2.4 µM), T (100): trastuzumab 100 µg/ml.

Table 5.4: Fluorescent intensity (histogram x-mean) of SK-Br-3 cells exposed to calcipotriol, trastuzumab and the calcipotriol-trastuzumab combination

SK-Br-3	Mean ± SEM	Significance			
12 Hours		**U**	**CPT**	**CPT + T**	**T**
Untreated (U)	99.49 ± 2.52	-		***	***
CPT	88.43 ± 4.83		-	*	*
CPT + T	62.50 ± 3.13	***	*	-	
T	64.77 ± 3.60	***	*		-
24 Hours		**U**	**CPT**	**CPT + T**	**T**
Untreated (U)	103.70 ± 2.61	-		***	***
CPT	93.88 ± 3.01		-	***	**
CPT + T	60.76 ± 2.58	***	***	-	
T	65.47 ± 4.76	***	**		-
48 Hours		**U**	**CPT**	**CPT + T**	**T**
Untreated (U)	100.00 ± 1.95	-		***	***
CPT	103.60 ± 3.92		-	***	***
CPT + T	71.09 ± 2.03	***	***	-	
T	61.83 ± 4.42	***	***		-

Fat soluble vitamin D is a biologically inert secosteroid hormone and a member of the steroid hormone receptor superfamily. Vitamin D3 (cholecalciferol) is converted to hormonally active 1α,25-dihydroxyvitamin D3 (calcitriol) by successive hydroxylation to 25-hydroxyvitamin D3 (hydroxyl-cholecalciferol via 25-hydroxylase) and then to 1α,25-dihydroxyvitamin D3 (calcitriol via 1α-hydroxylase). 1α,25-dihydroxyvitamin D3 interacts with intracellular vitamin D receptors (VDR) which undergo covalent modification via serine phosphorylation and promotes genomic and non-genomic actions. (Buras et al., 1994; Lee, Jeon, Yi, Jin, & Son, 2001)

Regulation of gene expression is accomplished by either VDR homodimers or retinoid X receptor (RXR)-VDR heterodimers which bind to promoter regions of vitamin D response elements (VDREs) and positively or negatively regulate gene transcription. VDRs are hypothesized to regulate cellular processes including immune function, apoptosis, cell cycle, cell proliferation and differentiation by these regulatory mechanisms. (Nagpal et al., 2001)(Issa, Leong, & Eisman, 2010) Non-genomic actions of vitamin D include activation of Ca^{2+}, activation of G-protein coupled receptors and alterations in protein kinase C (PKC) and mitogen-activated protein kinase (MAPK) pathways. (Bouillon R, Okamura WH, 1995; Issa et al., 2010)

VDR are thought to be expressed, with varying frequency, in 80-90% of all breast cancer cells, often reflecting the degree of cell differentiation. The extent to which VDR are present in breast tumours suggests that vitamin D analogues may be used for anti-proliferative effects in combination therapy for both oestrogen dependent and independent tumours. (Buras et al., 1994; Nagpal et al., 2001)

Calcipotriol (1,24-dihydroxy-22-ene-24-cyclopropyl-vitamin D3) is an active, low toxic synthetic derivative of vitamin D that retains similar anti-proliferative and differentiation effects to vitamin D.

Buras *et al*. (1994) studied vitamin D analogues in a panel of breast cancer cells and suggested that loss of VDR expression resulted in loss of anti-proliferative effects. In general, high levels of VDRs were found in oestrogen dependent cell lines. However, MCF-7 cells appeared to be an exception to this trend despite dose-dependent growth inhibition being observed. While the degree of VDRs present may correlate to the anti-proliferative effects of vitamin D analogues, mutations in DNA-binding domains or variation in regulatory mechanisms which control receptor targets may account for discrepancies in their anti-proliferative effects.

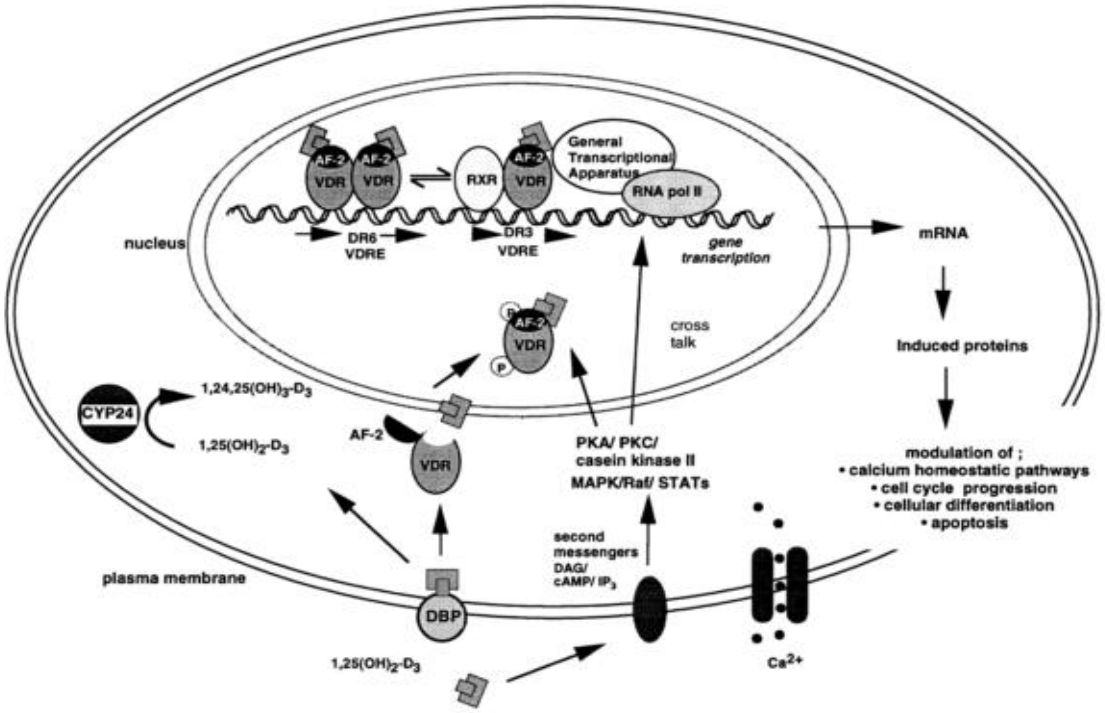

Figure 5.4: Model for the integrated cellular pathways for calcitriol action through the VDR. Calcitriol enters the cell bound to the vitamin D binding protein (DBP). The rapid non-genomic actions of calcitriol include opening of Ca^{2+} channels and activation of second messenger pathways which engage in cross talk with the nucleus. Ligand activation results in VDR phosphorylation and nuclear transport. The VDR homodimerises or heterodimerises with RXR to interact with vitamin D response elements (VDREs) in gene promoters. Interaction with the general transcription machinery is essential to initiate gene transcription. The net result is regulation of expression of proteins involved in calcium homeostasis and cell growth regulatory pathways. Also shown is the calcitriol metabolic pathway through 24-hydroxylase (CYP24)(Issa et al., 2010)

While calcipotriol and other vitamin D3 analogues primarily exert genomic effects via intracellular VDR, non-genomic signalling pathways that are independent of VDR are being implicated because discrepancies between anti-proliferative efficiency and VDR abundance have been noted. (Zhuang, Schwartz, Cameron, & Burnstein, 1997)

In our experiment, calcipotriol (2.4 µM) exposure in MCF-7 cells resulted in a significantly reduced cell viability of 74.13% (±1.22). Addition of trastuzumab (100 µg/ml) showed negligible differences in cell viability [73.01% (±1.51)] in these cells, compared to viability demonstrated by calcipotriol alone. Calcipotriol had minimal effects on SK-Br-3 cell viability [92.97% (±1.29)]. Meanwhile concurrent trastuzumab exposure resulted in a cell viability of 72.59% (±1.96) which mimicked that of trastuzumab alone and suggested that trastuzumab ultimately influenced cell viability in SK-Br-3 cells independently of calcipotriol (Figure 5.1; Table 5.1).

Cumulative data suggests that VDRs are required for synthetic analogues to elicit an effect. However, differences in constitutive receptor number and non-receptor factors modulate cell specific responses. Bursa *et al*. (1994) also noted that SK-Br-3 cells have a relative VDR expression which was more than four times higher than MCF-7 cells, suggesting that the anti-proliferative effects of calcipotriol should be greater in SK-Br-3 cells. However, the anti-proliferative effects observed in our study do not correlate with the above mentioned VDR expression, further suggesting that non-genomic effects mediated independently of nuclear VDRs are of importance.

Furthermore, Zhuang *et al.* (1997) also noted that alterations in VDR transcription activity could not account for the discrepancies in anti-proliferative effect, and that VDR levels and transcriptional activity are inaccurate indices for assessing response to vitamin D3 analogues. (Zhuang et al., 1997) Mechanisms of target gene down regulation include antagonizing the action of transcription factors. Calcitriol and a variety of its metabolites repress TNF-α induced interleukin-8 expression which is mediated via NF-κB binding sites. (Harant H, Andrew PJ, Reddy GS, Foglar E, 1997) Furthermore, VDR ligands have also been shown to inhibit components responsible for hyper-proliferation processes such as c-myc, Her-1, IL-2, IL-6 and IL-8. (Nagpal et al., 2001)

No caspase-3 and -7 activation was observed in either cell line (data not shown) suggesting that executioner caspases may only be detectable beyond 30 hours or that calcipotriol primarily induces anti-proliferative effects. Furthermore, the annexin-V assay showed no difference in fluorescent staining between untreated controls and calcipotriol alone or with concurrent trastuzumab supporting the concept of calcipotriol being anti-proliferative.

Lee *et al*. (2001) investigated the ability of calcipotriol to disturb signalling components involved in proliferation after they noted that calcipotriol inhibited proliferation without the induction of apoptosis in human squamous carcinoma cells (SCC13).

Cells exposed to calcipotriol demonstrated dephosphorylation of 170 and 66kDa polypeptides which were identified as Her-1 and Shc (transforming protein) polypeptides. Substantial levels of polypeptides were detected post-calcipotriol exposure even though phosphorylation was lacking, suggesting that polypeptide degradation had not occurred. Lee *et al*. (2001) concluded that calcipotriol may mediate anti-proliferative effects via inhibition of autocrine activation of polypeptides as opposed to inducing apoptosis. This is in line with the results obtained in this study which points to non-genomic events influencing cell viability that are independent of the number of VDRs.

In calcipotriol-exposed MCF-7 cells, G1 phase accumulation became apparent from 48 hours [$G1_{48}$: 37.81% (±3.48)] compared to the untreated control [G1: 23.25% (±0.86)]. After 72 hours statistically significant G1 accumulation [$G1_{72}$: 44.96% (±3.63)] was observed in these cells. A similar trend was observed in cells exposed to the calcipotriol-trastuzumab combination [$G1_{72}$: 46.45% (±4.91)]. However, this accumulation was not as extensive as when trastuzumab was used alone at 72 hours [$G1_{72}$: 56.37% (±4.48)] (Table 5.2). A comparison of calcipotriol and concurrent trastuzumab yielded no significant difference at any time point. The cell cycle distribution and cell viability data suggested that trastuzumab had a negligible effect when used in combination with calcipotriol because the results mimicked one another so closely.

Calcipotriol exposed SK-Br-3 cells showed a statistically significant G1 accumulation from 24 hours through to 72 hours [$G1_{72}$: 61.42% (±1.05)] compared to untreated controls [G1: 45.19% (±0.65)]. At 24 hours there was a statistically significant difference between calcipotriol [$G1_{24}$: 59.77% (±1.61)] or trastuzumab [$G1_{24}$: 60.15% (±1.81)] used alone compared to the combination [G1: 68.72% (±1.01)]. However, this trend was not evident at 48 or 72 hours. In fact, by 72 hours the difference between trastuzumab and the combination was barely distinguishable (Figure 5.2; Table 5.3). This could suggest that trastuzumab activity overwhelmed that of calcipotriol which was also reflected in the cell viability results.

Wietrzyk *et al*. (2007) studied the effects of vitamin D analogues in a wide variety of cancer types and found that calcipotriol reliably induced cell cycle arrest in the G1 phase. This is consistent with the results found in this study where calcipotriol was capable of inducing a G1 accumulation in both MCF-7 and SK-Br-3 cells.

While reviewing the molecular mechanisms of vitamin D receptor action, Issa *et al*. (2010) noted that vitamin D analogues altered proteins involved in apoptosis only once changes in cell cycle distribution had occurred in MCF-7 cells. Once the cell cycle was altered, cells proceeded to differentiate or undergo apoptosis, dependent on the regulatory proteins influenced. The changes in cell cycle distribution were primarily G1 cell cycle arrest. However, at low concentrations, vitamin D analogues like calcipotriol have also been shown to stimulate proliferation.

Thus, dose responses to vitamin D3 can produce hormetic effects resembling those of oestrogen where low concentrations stimulate cell growth while high concentrations inhibit cell growth.

Assessing cell cycle kinetics in human ductal breast epithelial tumour cells (T47D) illustrated that all concentrations which inhibited cell growth produced an increase in both G2-M phase and G1 phase transit times. Furthermore, maximal inhibitory concentrations, primarily delayed progression out of G1 phase. (Eisman, Koga, Sutherland, Barkla, & Tutton, 1989) The concentration used in our study was in the upper range of those tested by Eisman *et al*. (1989) which could explain why no G2-M phase inhibition was observed. Another difference is that Eisman *et al*. (1989) prolonged their hormone treatment by exposing cells at intervals across the assessment period.

Finally, it has also been suggested that vitamin D analogues may induce expression of cdk inhibitor proteins which include p16, $p27^{Kip1}$ and $p21^{WAF1/CIP1}$ and in doing so exert anti-proliferative effects and G1 phase inhibition by inactivating cyclin-cdk complexes. (Issa et al., 2010)

Her-2 receptor density studies revealed that MCF-7 cells showed minimal difference in the overlay plot between unstained, untreated, calcipotriol or combination treated samples at any time point. In SK-Br-3 cells, a small observable decrease in Her-2 receptors was noted when comparing untreated controls [$untreated_{12}$: 99.49% (±2.52)] to cells treated with calcipotriol alone [CPT_{12}: 88.43% (±4.83)] at 12, 24 and 48 hours, but these were found to be statistically insignificant.

In contrast, a statistically significant decrease in relative Her-2 receptor density was observed between untreated controls [$untreated_{12}$: 99.49% (±2.52)] and trastuzumab [T_{12}: 64.77% (±3.60)] as well as the calcipotriol-trastuzumab combination [$CPT+T_{12}$: 62.50% (±3.13)] at 12, 24 and 48 hours (Figure 5.3; Table 5.4) These results suggest that as a single agent, calcipotriol had minimal influence on the density of Her-2 receptors on the cell surface.

There were insignificant differences between trastuzumab alone versus the combination with calcipotriol, suggesting that in combination, trastuzumab functioned to decrease Her-2 receptors in a similar or identical fashion to when it was used alone. This result further supports the notion that the mechanism of action of trastuzumab may override calcipotriol in SK-Br-3 cells as seen throughout the results.

It has been suggested that steroid receptors such as vitamin D and Her-1 receptors are intimately related and capable of cross-talk. Whether such a relevant relationship exists between Her-2 receptors is unknown. Nonetheless, Koga *et al*. (1988) observed decreased EGF binding in cells exposed to vitamin D3 and speculated that vitamin D3 is therefore capable of reducing Her-1 receptors.

However, it was unclear whether this reduction was due to cell differentiation. (Koga, Eisman, & Sutherland, 1988) In our experiments, however, calcipotriol did not significantly reduce Her-2 receptor levels compared to untreated controls. Biphasic responses to vitamin-D3 continue to make the assessments of growth responses and Her-family receptor determination unpredictable.

While hormone and Her-family signalling pathways potentially intersect, MCF-7 cells and SK-Br-3 cells produced differential responses when exposed to the calcipotriol-trastuzumab combination. Calcipotriol results in G1 accumulation and lack of cytotoxic effect were observed in both cell lines. However, MCF-7 cells exposed to the combination resulted in a cell viability which reflected that of calcipotriol, while SK-Br-3 cell viability reflected that of trastuzumab.

However, the use of agents which produce hormetic or biphasic effects remain somewhat unpredictable and therefore cannot be accurately monitored in clinical settings. The molecular implications of using agents like calcipotriol could possibly result in vast inter-individual variation which could either promote differentiation and growth or inhibition and cell death. The use of calcipotriol and trastuzumab in combination also failed to provide any positive prospects for Her-2 positive cancer cells. The differential responses of oestrogen-dependent and Her-2 receptor over-expressing cells suggest that VDR status may not be sufficient to justify adding calcipotriol to trastuzumab targeted therapy in Her-2 positive breast cancer.

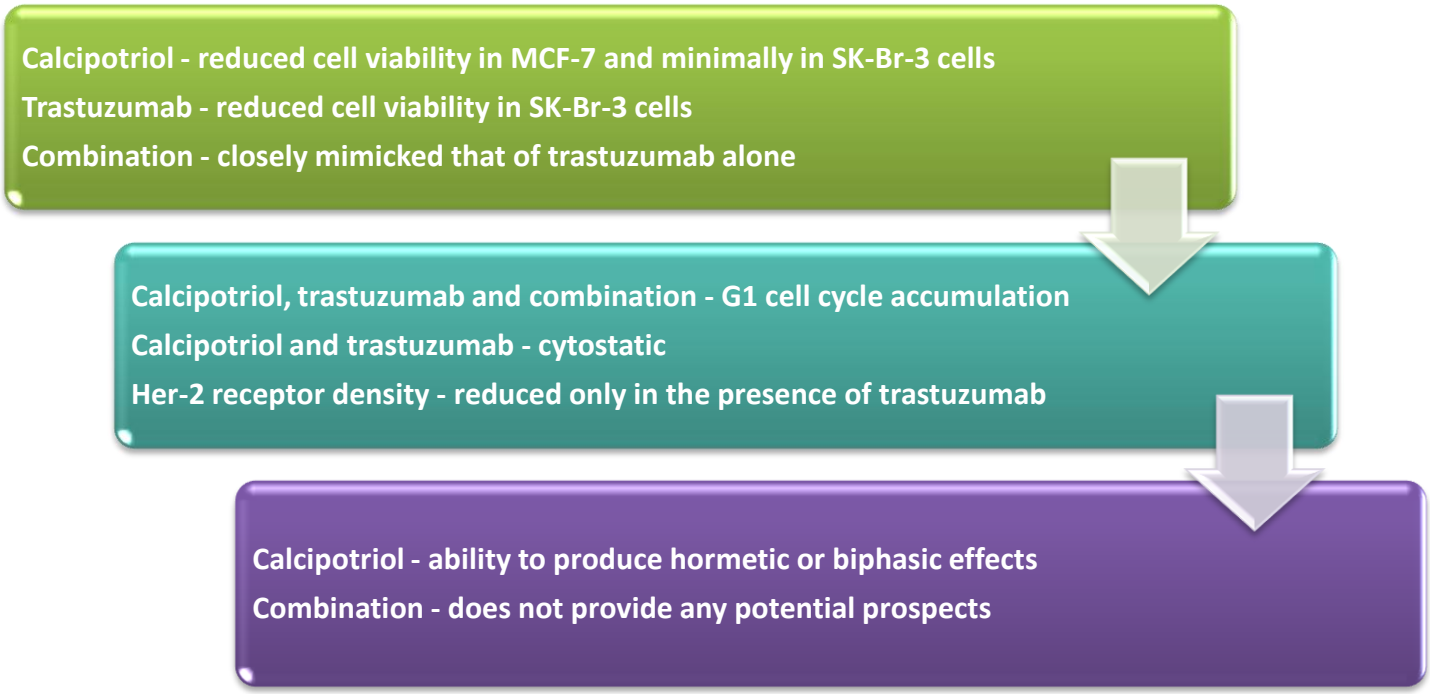

Chapter 6: Results and Discussion: Doxorubicin

6.1 Cell Viability

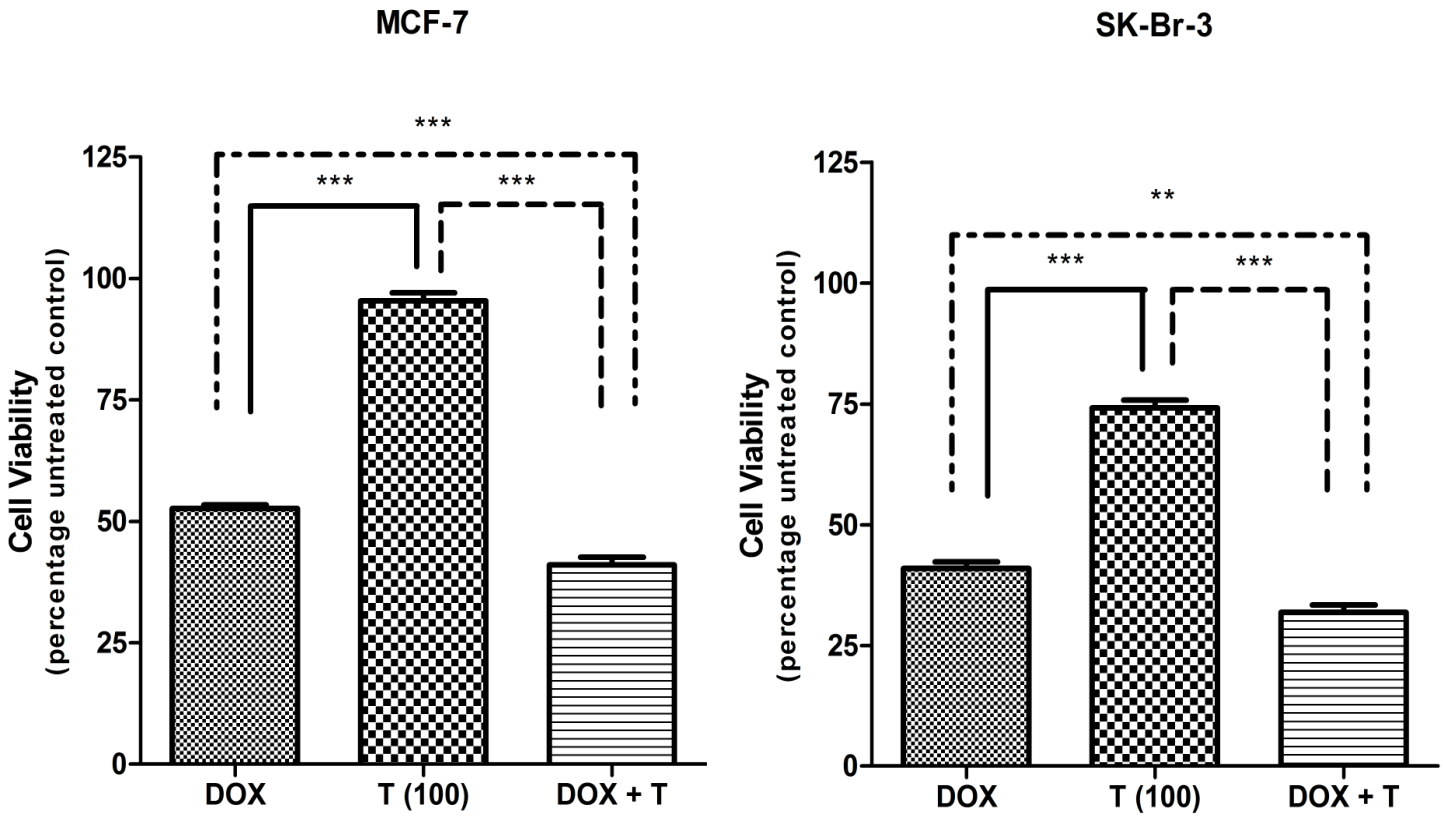

Figure 6.1: Cell viability in MCF-7 and SK-Br-3 cells expressed as a percentage of the untreated controls. Statistically significant differences were found between trastuzumab alone versus doxorubicin alone and the doxorubicin-trastuzumab combination. The combination was found to decrease cell viability more than either agent used alone in both cell lines. Further statistically significant differences ($P < 0.001$) were found when comparing the average cell viability of doxorubicin alone between MCF-7 and SK-Br-3 cells. DOX: doxorubicin (0.17 µM), T (100): trastuzumab 100 µg/ml. (Statistical significance followed the same trend for combinations at 25 µg/ml, 50 µg/ml, 200 µg/ml in both cell lines. Exception: no significance between doxorubicin alone compared to doxorubicin-trastuzumab combination at 25 µg/ml in MCF-7 cells.)

Table 6.1: Cell viability results for doxorubicin and the doxorubicin-trastuzumab combination

	MCF-7	SK-Br-3
	Mean ± SEM	**Mean ± SEM**
Doxorubicin (DOX) (0.17 µM)	52.91 ± 0.93	40.93 ± 1.39
DOX + Trastuzumab (25 µg/ml)	51.82 ± 1.69	32.00 ± 1.66
DOX + Trastuzumab (50 µg/ml)	45.17 ± 1.13	32.47 ± 1.59
DOX + Trastuzumab (100 µg/ml)	41.11 ± 1.55	31.85 ± 1.53
DOX + Trastuzumab (200 µg/ml)	43.97 ± 1.42	33.52 ± 1.48

6.2 Cell Cycle Analysis

Table 6.2: Cell cycle results for DOX, trastuzumab and the DOX-trastuzumab combination in MCF-7 cells

MCF-7	Mean ± SEM				Significance			
72 Hours	G1	S	G2	Sub G1	C	DOX	DOX + T	T
Control (C)	23.25 ± 0.86	52.99 ± 2.33	23.76 ± 3.17		-	*	*	**
DOX	22.13 ± 3.91	67.88 ± 1.85	9.99 ± 3.72	15.71 ± 3.19	*	-	**	***
DOX + T	47.86 ± 1.11	45.35 ± 1.06	6.79 ± 2.05	32.48 ± 3.79	*	**	-	*
T	56.37 ± 4.48	33.34 ± 3.23	10.29 ± 1.72	1.89 ± 0.02	**	***	*	-

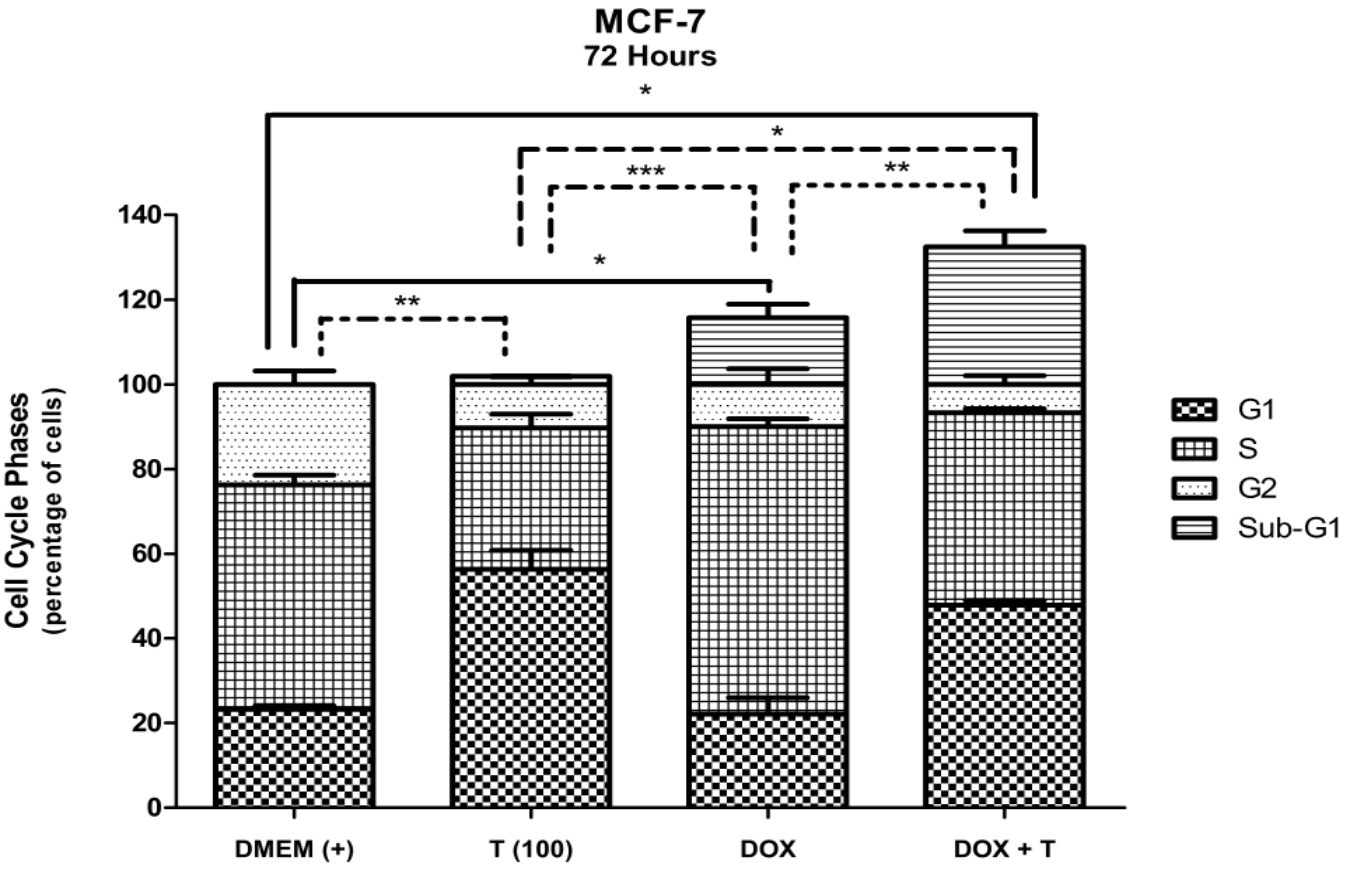

Figure 6.2: Cell cycle analysis in MCF-7 cells expressed as a percentage after deconvolution. Statistically significant differences in the G1, S and sub-G1 phases of the cell cycle were observed between untreated control (DMEM+) versus trastuzumab, doxorubicin and the doxorubicin-trastuzumab combination after 72 hours. DOX: doxorubicin (0.17 µM), T (100): trastuzumab 100 µg/ml. [Significance followed similar trends for SK-Br-3 cells]

Table 6.3: Cell cycle results for DOX, trastuzumab and the DOX-trastuzumab combination in SK-Br-3 cells

SK-Br-3	Mean ± SEM				Significance			
72 Hours	G1	S	G2	Sub G1	C	DOX	DOX + T	T
Control (C)	45.19 ± 0.65	35.68 ± 0.81	19.16 ± 0.31		-	**	**	***
DOX	48.73 ± 2.78	39.13 ± 4.96	5.47 ± 2.93	24.38 ± 1.89	**	-	*	*
DOX + T	63.95 ± 2.19	32.90 ± 3.79	3.15 ± 1.74	33.50 ± 2.21	**	*	-	*
T	66.93 ± 3.41	20.78 ± 2.60	15.02 ± 1.38	11.69 ± 2.20	***	*	*	-

6.3 Caspase 3 Assay

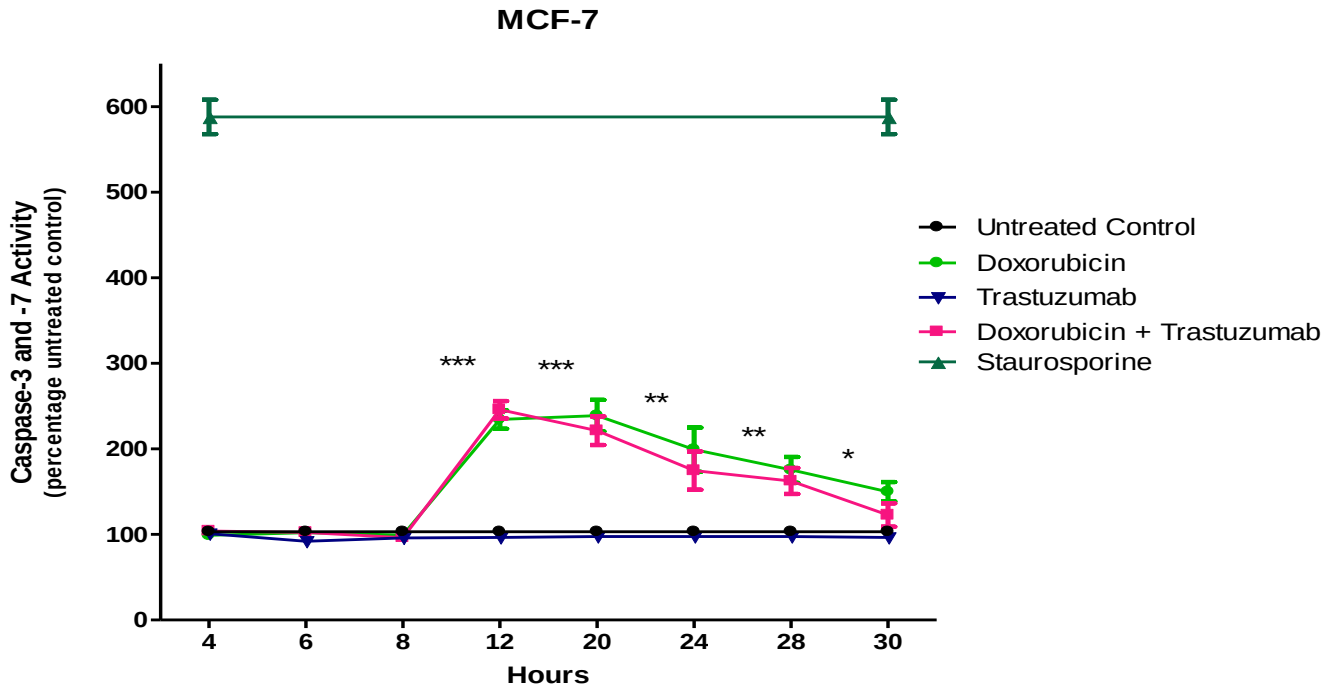

Figure 6.3: Caspase 3 assay in MCF-7 cells expressed as a percentage of untreated control (standardized to 100% caspase 3 activity). Statistically significant differences found between untreated control and both doxorubicin and the doxorubicin-trastuzumab combination at 12, 20, 24, 28 and 30 hours. Staurosporine (10.7 µM) was used as the positive control.

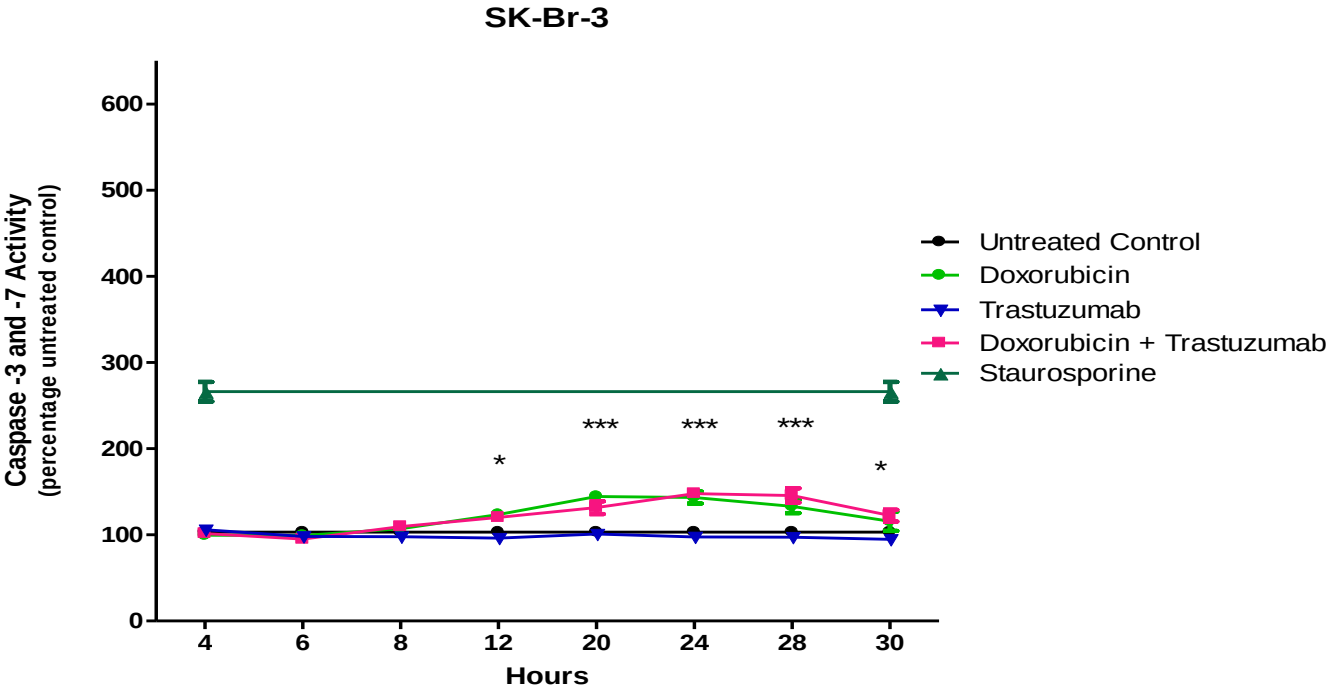

Figure 6.4: Caspase 3 assay in SK-Br-3 cells expressed as a percentage of untreated control (standardized to 100% caspase 3 activity). Statistically significant differences found between untreated control and both doxorubicin and the doxorubicin-trastuzumab combination at 12, 20, 24, 28 and 30 hours. Staurosporine (10.7 µM) was used as the positive control.

6.4 Apoptosis-Necrosis

Table 6.4: Apoptosis-Necrosis in MCF-7 cells after 72 hours

Statistical significance expressed with differences in two or more phases (E: Early, L: Late)

MCF-7	Mean ± SEM				Significance			
72 Hours	Living	E Apoptosis	L Apoptosis	Necrosis	U	DOX	DOX + T	T
Untreated (U)	95.37 ± 1.07	0.80 ± 0.49	0.20 ± 0.06	3.63 ± 0.56	-	**	**	
DOX	50.63 ± 2.38	8.73 ± 1.14	16.20 ± 2.25	24.47 ± 1.22	**	-		**
DOX + T	53.07 ± 2.81	4.90 ± 1.49	18.87 ± 3.87	25.43 ± 1.96	**		-	**
T	94.57 ± 0.54	1.03 ± 0.18	0.47 ± 0.03	3.97 ± 0.42		**	**	-

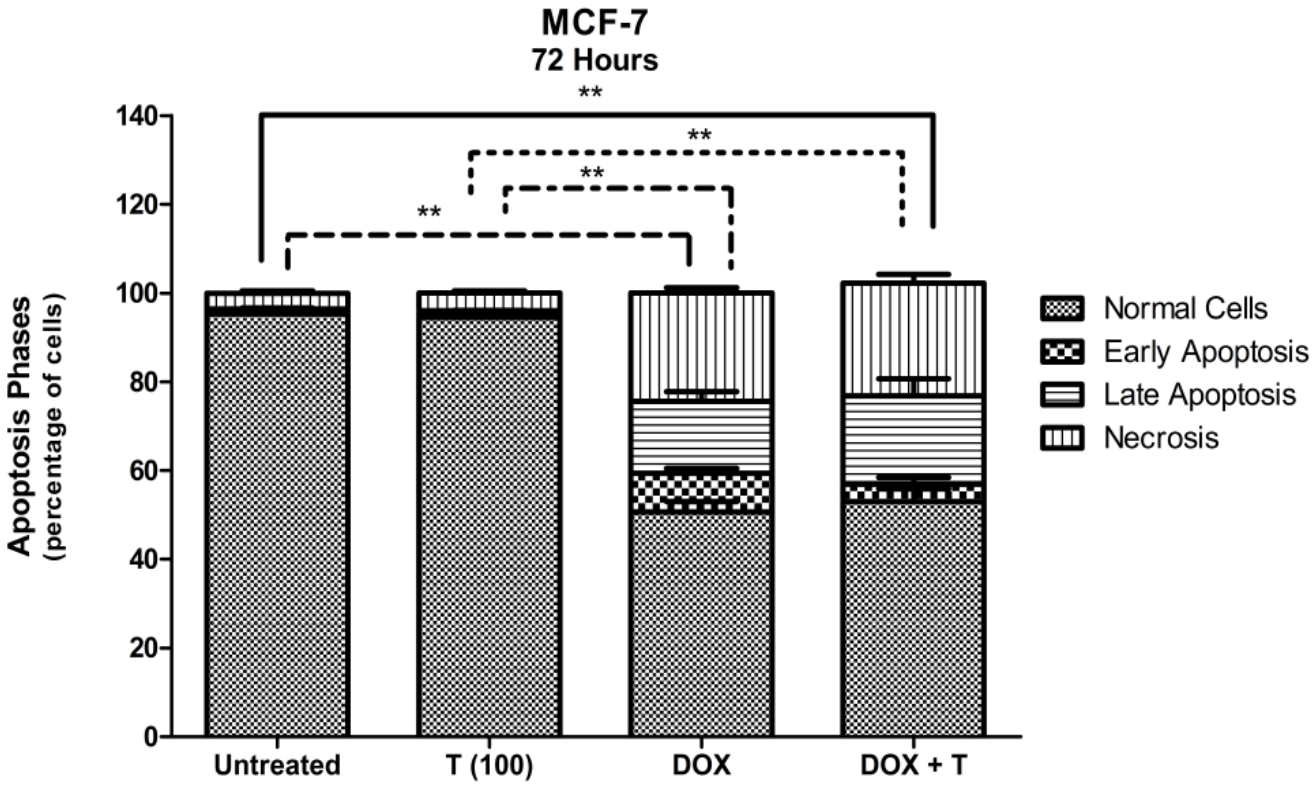

Figure 6.5: Annexin-V assay in MCF-7 cells expressed as a percentage of normal cells, early apoptosis, late apoptosis and necrosis. Statistically significant differences observed between untreated control and doxorubicin or the combination after 72 hours. DOX: doxorubicin (0.17µM), T (100): trastuzumab 100 µg/ml. [Significance followed similar trends for SK-Br-3 cells]

Table 6.5: Apoptosis-Necrosis in SK-Br-3 cells after 72 hours.

Statistical significance expressed with differences in two or more phases (E: Early, L: Late)

SK-Br-3	Mean ± SEM				Significance			
72 Hours	Living	E Apoptosis	L Apoptosis	Necrosis	U	DOX	DOX + T	T
Untreated (U)	91.25 ± 1.13	1.80 ± 0.47	0.50 ± 0.23	6.48 ± 1.36	-	***	***	
DOX	46.63 ± 1.91	7.80 ± 0.50	5.67 ± 0.60	39.90 ± 1.23	***	-		***
DOX + T	48.73 ± 1.87	8.13 ± 0.56	4.03 ± 0.32	39.17 ± 2.24	***		-	***
T	89.90 ± 0.15	1.40 ± 0.31	0.37 ± 0.12	8.33 ± 0.37		***	***	-

6.5 Relative Her-2 Receptor Density

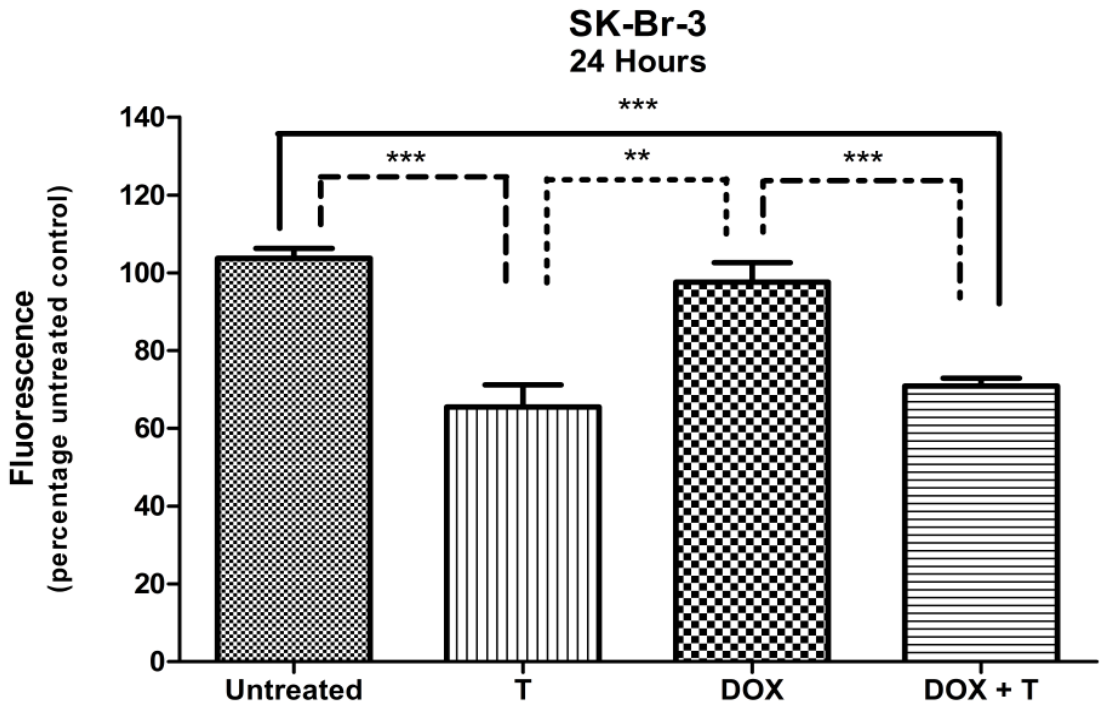

Figure 6.6: Relative Her-2 receptor density analysis at 24 hours in SK-Br-3 cell expressed as a percentage of the fluorescence of untreated controls (standardised to 100%). Statistical significance followed the same trend at 12, 24 and 48 hours. DOX: doxorubicin (0.17 µM), T (100): trastuzumab 100 µg/ml.

Table 6.6: Fluorescent intensity (histogram x-mean) of SK-Br-3 cells exposed to doxorubicin, trastuzumab and the doxorubicin-trastuzumab combination

SK-Br-3	Mean ± SEM	Significance			
12 Hours		**U**	**DOX**	**DOX + T**	**T**
Untreated (U)	99.49 ± 2.52	-		***	***
DOX	90.15 ± 2.79		-	***	**
DOX + T	62.75 ± 1.76	***	***	-	
T	64.77 ± 3.60	***	**		-
24 Hours		**U**	**DOX**	**DOX + T**	**T**
Untreated (U)	103.70 ± 2.61	-		***	***
DOX	97.58 ± 5.01		-	***	**
DOX + T	70.91 ± 1.96	***	***	-	
T	65.47 ± 4.76	***	**		-
48 Hours		**U**	**DOX**	**DOX + T**	**T**
Untreated (U)	100.00 ± 1.95	-		***	***
DOX	97.69 ± 3.74		-	***	***
DOX + T	71.39 ± 3.01	***	***	-	
T	61.83 ± 4.42	***	***		-

Doxorubicin, an anthracycline antibiotic, is one of the most effective anti-neoplastic agents used in the treatment of breast cancer. While doxorubicin possesses a high anti-tumour efficacy in a variety of cancers, its use is somewhat limited by undesirable cumulative dose-dependent cardiotoxicity. Arola *et al.* (2000) assessed acute doxorubicin-induced cardiotoxicity in winstar rats and observed that cardio-myocyte apoptosis after consecutive injections was a cumulative, multi-factorial yet modifiable form of myocardial tissue loss.

Considerable controversy surrounds the biochemical mechanisms of action and side effects of anthracycline antibiotics. Contradictory findings surrounding molecular subtype-specific sensitivity to doxorubicin remains inconclusive and hinders unifying conclusions. The most researched mechanism of action for doxorubicin is its ability to target topoisomerase II-α, an enzyme involved in cutting both strands of the DNA helices to facilitate the intertwining and super-coiling of DNA during replication. (Campiglio et al., 2003) Gewirtz *et al*. (1999) concluded that DNA-topoisomerase II complex interactions are likely the primary triggering event for both growth arrest and apoptotic event signalling.

Alternate mechanisms of action for doxorubicin include: DNA intercalation which inhibit macromolecules resulting in cytostatic or transient effects; free radical-mediated toxicity (doxorubicin in excess of 2 µM) due to the quinine structure which is capable of being an electron acceptor in oxidative-reductive reactions and resulting in DNA injury or lipid peroxidation; DNA adducts and cross linking; interference with DNA strand separation; cell cycle growth arrest and membrane associated effects. (Gewirtz, 1999; Campiglio et al., 2003)

The relationship between Her-2 receptor status and the success of anthracycline-based regimens in patients was initially assessed in the Cancer and Leukemia Group B 8541 study in 1994. (Muss et al. 1994) Numerous subsequent studies have failed to demonstrate any predictive value between Her-2 receptor status and anthracycline-based chemotherapeutics. Many of these retrospective studies have included few patients and thus have reduced statistical power. Some retrospective studies have evaluated overall response rates (ORR) and predictive value of the Her-2 receptor status of tumours to dose intensity of anthracylcines. Multi-variant analysis suggested the following: anthracyclines in Her-2 negative tumours predicated an intermediate ORR, low-dose anthracyclines in Her-2 positive tumours predicted a poor ORR while high-dose anthracycline in Her-2 positive tumours predicted high ORR. This data suggested that anthracycline dose intensity plays a role in differential responses of molecular subtypes of cancer. (Petit et al., 2001)

These retrospective clinical correlations between Her-2 receptor over-expression and doxorubicin sensitivity suggest a role of Her-2 receptor signalling in response to doxorubicin. Elucidations of responses to doxorubicin in primary breast cancer tissue as well as breast cancer cell lines with different endogenous levels of Her-2 receptors have been conducted. Although a trend towards greater doxorubicin sensitivity was seen in Her-2 over-expressing cells, it was deemed statistically insignificant. (Campiglio et al., 2003)

Campiglio *et al*. (2003) also established that SK-Br-3 cells are more sensitive to the effects of doxorubicin than MCF-7 cells and possess topoisomerase II-α amplification not seen in MCF-7 cells. While amplification of topoisomerase II-α was observed in various breast cancer cells, it did not directly correlate with doxorubicin sensitivity. This lack of correlation suggests that response to doxorubicin cannot be explained solely by topoisomerase II-α amplification. However, it was concluded that doxorubicin sensitivity was found to decrease with an associated decrease in cell proliferation rate.

Doxorubicin (0.17 µM) exposure resulted in a substantially decreased MCF-7 cell viability of 52.91% (±0.65). Concurrent trastuzumab (100 µg/ml) exposure resulted in an additional decline in viability to 41.11% (±1.55). An even greater reduction to 40.93% (±1.39) was observed in SK-Br-3 cell viability after doxorubicin exposure. Concurrent trastuzumab lead to cell viability of 31.85% (±1.53) which was significantly greater than either agent used alone (Figure 6.1; Table 6.1)

Thus, consistent with data by Campiglio, Her-2 rich SK-Br-3 cells demonstrated a greater sensitivity to doxorubicin than MCF-7 cells. Concurrent exposure in both cell lines significantly reduced viability compared to either trastuzumab or doxorubicin alone with the exception in MCF-7 cells at a trastuzumab concentration of 25 µg/ml. This data suggests that trastuzumab and doxorubicin have a co-ordinated relationship that allows both drugs to function without mechanistically interfering interactions on cell signalling pathways.

Topoisomerase II-α amplification in SK-Br-3 cells may not be the sole cause of the difference in the two cell lines; SK-Br-3 cells characteristically have a faster doubling time compared to MCF-7 cells which could provide an additional explanation for the results observed.

Doxorubicin induced activation of executioner caspases-3 and -7 was detected between 12 and 30 hours for both MCF-7 (Figure 6.3) and SK-Br-3 cells (Figure 6.4) although the time of maximum response differed between cell lines. Concurrent trastuzumab did not significantly alter the presence or onset of caspase activity. Doxorubicin appeared to play a role in apoptotic cell death during DNA synthesis possibly by influencing the ability of topoisomerase II-α to adequately cut and reanneal DNA. The detection of caspase-3 and -7 over an extended period of 18 hours could be because the cells were not synchronized and thus possibly in different stages of the cell cycle. Activation of caspase 3 in human ovarian teratocarcinoma (PA-1) has previously been observed as early as 4 and 8 hours after doxorubicin exposure (0.1 to 0.5 µM) and been found to increase with prolonged incubation time. (Wang et al., 2004)

Furthermore, the annexin-V assay detecting phosphatidylserine flips in the cell membrane showed significant differences between untreated controls versus both doxorubicin and the doxorubicin-trastuzumab combination in both cell lines. Following doxorubicin exposure at 48 hours, MCF-7 cells expressed 60.37% (±1.97) normal cells with 16.37% (±0.73) being annexin-V positive which is indicative of early apoptosis. Concurrent trastuzumab resulted in a cell distribution of 59.63% (±1.73) normal cells and 21.63% (±3.10) of cells in early apoptosis. By 72 hours the percentage of normal cells decreased to 50.63% (±2.38) with 24.47% (±1.22) being double stained and considered necrotic. Concurrent trastuzumab resulted in a similar distribution of cells to doxorubicin exposed cells (Figure 6.5; Table 6.4).

By 72 hours, SK-Br-3 cells expressed 46.63% (±1.91) normal cells with 39.90% (±1.23) of cells in necrosis while concurrent trastuzumab resulted in 48.73% (±1.87) normal cells and 39.17% (±2.24) of cells in necrosis. There were no statistically significant differences in the fluorescence detected in the caspase or annexin-V assay between doxorubicin alone and doxorubicin-trastuzumab combinations in either cell line (Table 6.5). The differences in cell viability noted earlier may have been due to trastuzumab eliciting an anti-proliferative effect with doxorubicin inducing apoptosis.

While doxorubicin is known to induce caspase activation and disrupt inner mitochondrial membrane potential (Gamen et al., 2000), the ability of doxorubicin to induce mitotic catastrophe is becoming an area of interest. Castedo *et al.* (2004) proposed that mitotic catastrophe is a type of cell death occurring during mitosis resulting from a combination of cellular-damage and deficient cell-cycle checkpoints which results in cells undergoing abnormal mitosis and aberrant chromosomal segregation.

Other researchers have observed that low concentrations of doxorubicin (sub-apoptotic concentration: 50 ng/ml) induced a senescence-like phenotype accompanied by abnormal mitosis, which was morphologically and biochemically characterized by formation of multiple nuclei and membrane integrity loss. This was distinctly different from high concentrations of doxorubicin (10 µg/ml) which induced characteristics typical of apoptosis. Processing of pro-caspase-3 in response to high dose doxorubicin was detected at 4, 8 and 12 hours post-exposure. However, substantial losses and concomitant appearance of processed subunits of the pro-form of caspase-3 was most extensive at 48 hours. (Eom et al., 2005) The concentration of doxorubicin used in our study was 0.1 µg/ml (0.17 µM) which was between the low and high doses considered by Eom *et al.* (2005) and while mechanistic features of cell death were observed, induction of a senescence-like phenotype cannot be ruled out.

In MCF-7 cells, accumulation of cells in the S phase became apparent after doxorubicin exposure from 48 hours [S_{48}: 59.98% (±2.54)] compared to the untreated control [S: 52.99% (±2.33)]. At 72 hours the increase in S phase accumulation induced by doxorubicin was statistically significant [S_{72}: 67.88% (±1.85)]. Contrastingly, exposure to the doxorubicin-trastuzumab combination yielded a statistically significant difference in the G1 phase [G1: 47.86% (±1.11)] compared to either the untreated control [G1: 23.25% (±0.86)] or to doxorubicin [$G1_{72}$: 22.13% (±3.91)] at all three time points. A high S phase was still maintained in the doxorubicin-trastuzumab combination (Figure 6.2; Table 6.2).

The sub-G1 or background aggregates and debris (B.A.D) increased significantly between successive time points, and in support of the difference in cell viability, sub-G1 was 15.71% (±3.19) for doxorubicin and double [sub-$G1_{72}$: 32.48% (±3.79]) for the doxorubicin-trastuzumab combination. Alterations in cell cycle kinetics resulted in re-distribution at 72 hours that clearly showed differences between each group; the combination mimicked neither trastuzumab nor doxorubicin. While the use of deconvolution software is considered the most accurate method to assess cell cycle distribution removing observer bias, some of the histograms were difficult to deconvolute because of the extent of cell death. This may have resulted in an over or under-estimation in certain phases.

Doxorubicin exposed SK-Br-3 cells showed a statistically significant S phase accumulation at 24 hours [S_{24}: 57.09% (±2.89)] and 48 hours [S_{48}: 50.84% (±2.35)]. However, at 72 hours the S phase accumulation was no longer significant and the sub-G1 phase significantly increased. Between 24 and 48 hours the combination reflected a similar cell cycle distribution to doxorubicin alone, with a minor increase in the G1 phase.

At 72 hours the combination showed significant G1 accumulation of 63.95% (±2.19). The dramatic re-distribution in cell cycle kinetics at 72 hour may have been due to over or under-estimation in certain phases because of the low cell number (due to the extent of cell death). The dramatic increase in sub-G1 phase of the doxorubicin-trastuzumab combination by almost 20% between 48 and 72 hours suggests an increase in cell death. Differentiating doxorubicin from the combination showed a significant increase in sub-G1 from 24.38% (±1.89) for doxorubicin compared to 33.50% (±2.21) for the combination (Table 6.3).

Bar-On *et al.* (2007) observed that doxorubicin exposure differentially altered cell cycle kinetics, which was cell type specific. Doxorubicin resulted in G1-S and G2-M checkpoint arrests in MCF-7 cells as opposed to only G2-M checkpoint arrests in MDA-MB-231 cells. (Bar-On, Shapira, & Hershko, 2007) Some have also shown differences in other cell types. For instance, doxorubicin resulted in a dramatically increased S-phase population with a concomitant decrease in G1-phase with high concentration doxorubicin, which resulted in an obvious gradual increase in the sub-G1 population in human hepatoma cells. (Eom et al., 2005) Flow cytometric analysis of the cell phase specificity of DNA damage was performed using HeLa cells exposed to doxorubicin. This analysis showed that while DNA damage was increased over time in each cell cycle phase, cells in the G2-M phase were found to be the most susceptible to doxorubicin. (Potter et al., 2002) This could explain the increase in the percentage of cells observed in the S-phase cells in both our cell lines.

Relative Her-2 receptor density assays in MCF-7 cells revealed unobservable differences between unstained, untreated, doxorubicin or combination-treated sample at any time point. In SK-Br-3 cells, no relevant decrease in Her-2 receptors was observed when comparing untreated controls [$untreated_{12}$: 99.49% (±2.52)] to cells treated with doxorubicin alone [DOX_{12}: 90.15% (±2.79)] at 12, 24 and 48 hours.

However, a statistically significant decrease in Her-2 receptors was observed between untreated controls [$untreated_{12}$: 99.49% (±2.52)] and trastuzumab [T_{12}: 64.77% (±3.60)] as well as the doxorubicin-trastuzumab combination [$DOX+T_{12}$: 62.75% (±1.76)] at 12, 24 and 48 hours (Figure 6.6; Table 6.6). These results suggest that as a single agent, doxorubicin had no influence on the density of Her-2 receptors on the cell surface. Furthermore, trastuzumab resulted in an equivalent decrease in receptors in combination with doxorubicin to when it was used alone.

Pegram *et al*. (1999) also demonstrated that Her-2 expression remained unaltered following exposure to doxorubicin and considered the possibility that cytotoxic drugs such as doxorubicin potentiate Her-2 functional activity as opposed to altering expression levels. As apoptosis assays did not distinguish differences between doxorubicin and the doxorubicin-trastuzumab combination, the consistent decrease in Her-2 receptors by trastuzumab in combination with doxorubicin may be what ultimately aids in significantly altering cell viability. The induction of apoptosis by doxorubicin and cytostatic effects of trastuzumab appear to provide an effective treatment modality *in vitro*.

Enhancing anti-tumour activity of targeted therapy would have significant clinical implications. Corroborating evidence comes from Baselaga *et al*. (1998) who observed that a modest enhancement of growth inhibition in cell lines and *in vivo* models over-expressing Her-2 receptors occurred in a concentration-dependent manner when trastuzumab was combined with doxorubicin. These results support the use of doxorubicin in trastuzumab-based therapies in terms of efficacy. However, the cardiotoxicity of anthracycline-trastuzumab combinations still casts a shadow over this apparently effective treatment modality.

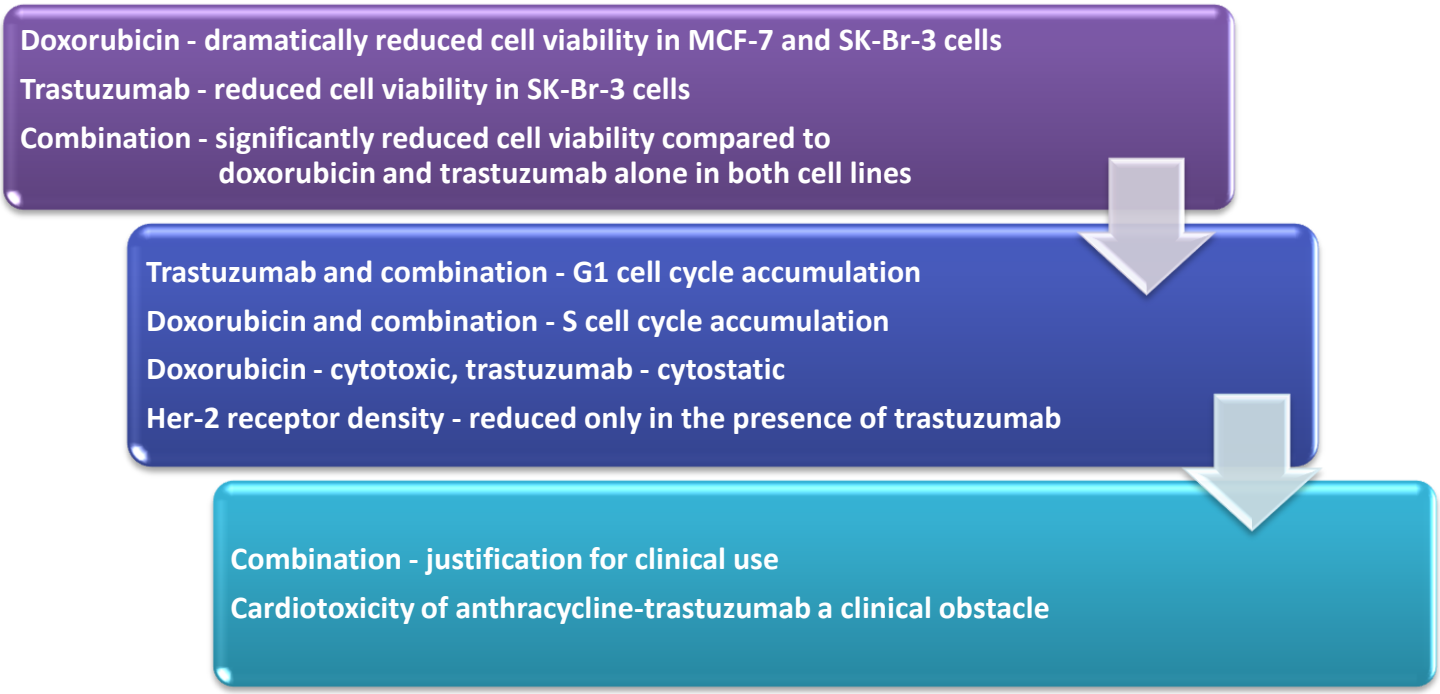

Chapter 7: Results and Discussion: EGF

7.1 Cell Viability

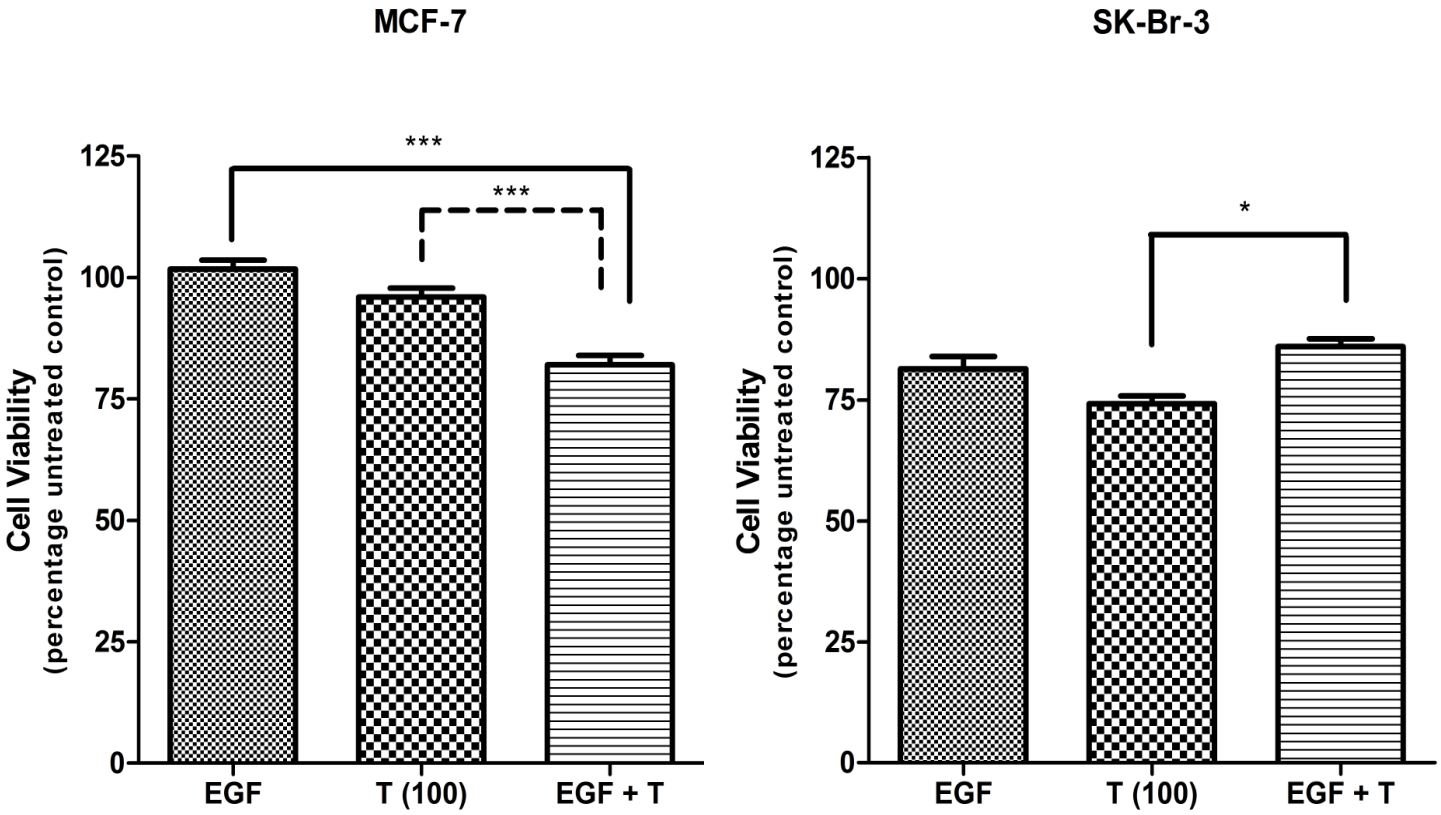

Figure 7.1: Cell viability in MCF-7 and SK-Br-3 cells expressed as a percentage of the untreated controls. Statistically significant differences were found between trastuzumab alone versus EGF alone and the EGF-trastuzumab combination. Further statistically significant differences (P < 0.001) were found when comparing the average cell viability of EGF alone between MCF-7 and SK-Br-3 cells. EGF: Epidermal growth factor (66 nM), T (100): trastuzumab 100 µg/ml. (Statistical significance followed the same trend for combinations at 25 µg/ml, 50 µg/ml, 200 µg/ml in both cell lines. Exception: no significance comparing EGF alone to EGF-trastuzumab combination at 25 µg/ml in MCF-7 cells.)

Table 7.1: Cell viability results for EGF and the EGF-trastuzumab combination

	MCF-7	SK-Br-3
	Mean ± SEM	Mean ± SEM
EGF (66 nM)	101.70 ± 1.84	81.43 ± 2.46
EGF + Trastuzumab (25 µg/ml)	100.60 ± 2.48	89.98 ± 2.07
EGF + Trastuzumab (50 µg/ml)	89.52 ± 1.95	89.40 ± 2.20
EGF + Trastuzumab (100 µg/ml)	81.97 ± 1.99	86.02 ± 1.60
EGF + Trastuzumab (200 µg/ml)	83.80 ± 2.07	87.09 ± 1.83

7.2 Cell Cycle Analysis

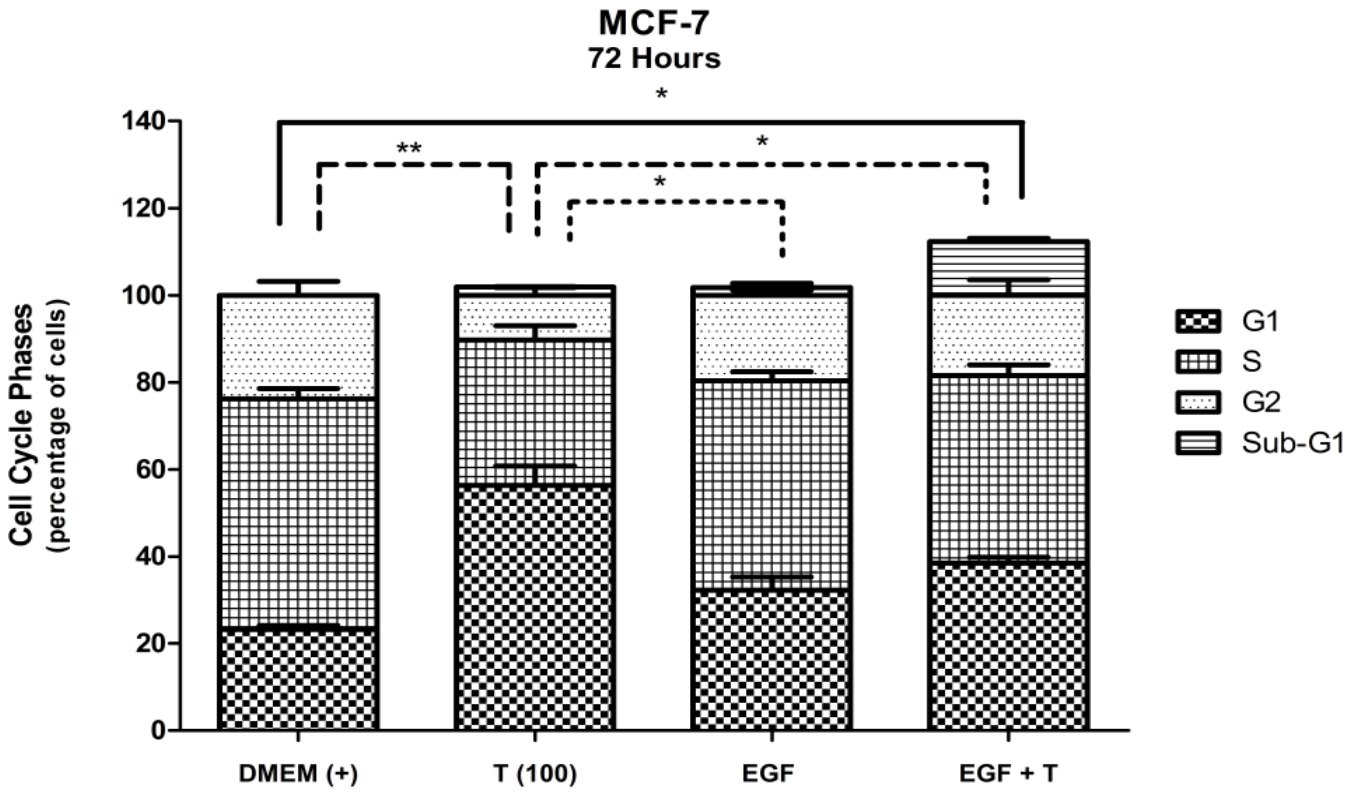

Figure 7.2: Cell cycle analysis in MCF-7 cells expressed as a percentage after deconvolution. Statistically significant differences in the G1 and S phases of the cell cycle were observed between various comparisons of untreated control (DMEM+), trastuzumab, EGF and the EGF-trastuzumab combination after 72 hours. EGF: Epidermal growth factor (66 nM), T (100): trastuzumab 100 µg/ml.

Table 7.2: Cell cycle results for EGF, trastuzumab and the EGF-trastuzumab combination in MCF-7 cells

MCF-7	Mean ± SEM				Significance			
24 Hours	**G1**	**S**	**G2**	**Sub G1**	**C**	**EGF**	**EGF + T**	**T**
Control (C)	23.25 ± 0.86	52.99 ± 2.33	23.76 ± 3.17		-		**	
EGF	23.42 ± 3.21	60.40 ± 0.28	16.18 ± 3.33	2.22 ± 1.02		-	**	
EGF + T	40.78 ± 2.95	44.13 ± 6.86	15.09 ± 5.74	6.48 ± 2.07	**	**	-	**
T	23.46 ± 1.21	53.03 ± 2.62	23.51 ± 1.63	1.87 ± 0.10			**	-
48 Hours	**G1**	**S**	**G2**	**Sub G1**	**C**	**EGF**	**EGF + T**	**T**
Control (C)	23.25 ± 0.86	52.99 ± 2.33	23.76 ± 3.17		-	**	***	
EGF	42.56 ± 2.93	41.15 ± 4.07	16.29 ± 3.35	1.45 ± 0.12	**	-		
EGF + T	44.10 ± 1.79	40.08 ± 2.14	15.93 ± 2.59	6.12 ± 0.66	***		-	*
T	32.40 ± 2.34	50.86 ± 4.87	16.74 ± 3.22	1.86 ± 0.01			*	-
72 Hours	**G1**	**S**	**G2**	**Sub G1**	**C**	**EGF**	**EGF + T**	**T**
Control (C)	23.25 ± 0.86	52.99 ± 2.33	23.76 ± 3.17		-		*	**
EGF	32.22 ± 3.08	48.14 ± 2.04	19.64 ± 1.11	1.74 ± 0.99		-		*
EGF + T	38.54 ± 1.25	43.04 ± 2.38	18.42 ± 3.53	12.30 ± 0.77	*		-	*
T	56.37 ± 4.48	3.34 ± 3.23	10.29 ± 1.72	1.89 ± 0.02	**	*	*	-

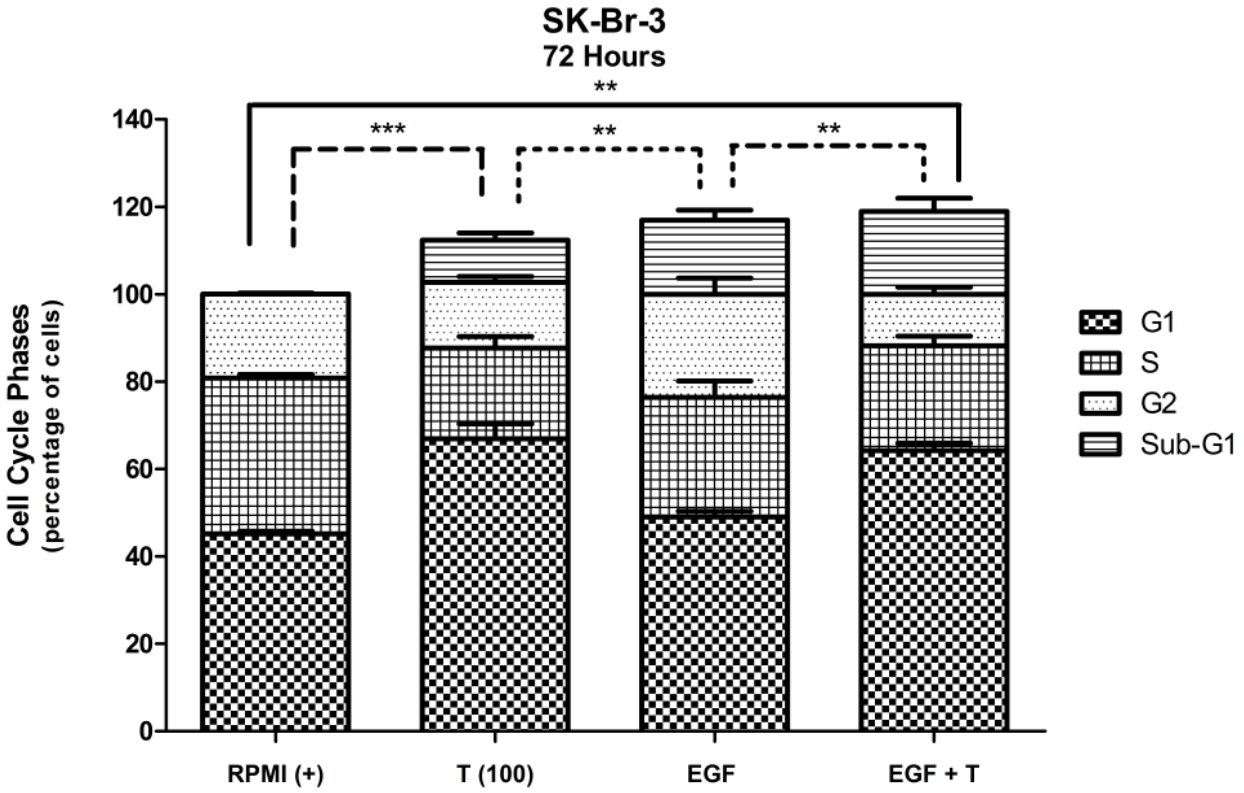

Figure 7.3: Cell cycle analysis in SK-Br-3 cells expressed as a percentage after deconvolution. Statistically significant differences in the G1 phase of the cell cycle were observed between various comparisons of untreated control (RPMI+), trastuzumab, EGF and the EGF-trastuzumab combination after 72 hours. EGF: Epidermal growth factor (66 nM), T (100): trastuzumab 100 µg/ml.

Table 7.3: Cell cycle results for EGF, trastuzumab and the EGF-trastuzumab combination in SK-Br-3 cells

SK-Br-3	Mean ± SEM				Significance			
24 Hours	**G1**	**S**	**G2**	**Sub G1**	**C**	**EGF**	**EGF + T**	**T**
Control (C)	45.19 ± 0.65	35.68 ± 0.81	19.16 ± 0.31		-			**
EGF	43.50 ± 3.65	37.74 ± 3.37	18.76 ± 2.06	7.03 ± 1.43		-		*
EGF + T	47.47 ± 3.46	38.77 ± 3.62	13.76 ± 4.28	9.01 ± 2.13			-	*
T	60.15 ± 1.81	23.72 ± 2.38	16.13 ± 2.07	7.68 ± 2.48	**	*	*	-
48 Hours	**G1**	**S**	**G2**	**Sub G1**	**C**	**EGF**	**EGF + T**	**T**
Control (C)	45.19 ± 0.65	35.68 ± 0.81	19.16 ± 0.31		-		*	**
EGF	51.47 ± 1.20	29.90 ± 1.35	18.95 ± 1.44	7.30 ± 1.96		-		***
EGF + T	52.96 ± 1.80	28.12 ± 1.59	18.92 ± 1.56	6.88 ± 0.96	*		-	**
T	64.15 ± 1.41	20.84 ± 3.55	15.02 ± 4.56	11.48 ± 1.28	**	***	**	-
72 Hours	**G1**	**S**	**G2**	**Sub G1**	**C**	**EGF**	**EGF + T**	**T**
Control (C)	45.19 ± 0.65	35.68 ± 0.81	19.16 ± 0.31		-		**	***
EGF	49.09 ± 1.28	27.30 ± 3.82	23.62 ± 3.72	17.02 ± 2.29		-	**	**
EGF + T	64.23 ± 1.74	24.01 ± 2.16	11.77 ± 1.64	18.93 ± 3.09	**	**	-	
T	66.93 ± 3.41	20.78 ± 2.60	15.02 ± 1.38	11.69 ± 2.20	***	**		-

7.3 Relative Her-2 Receptor Density

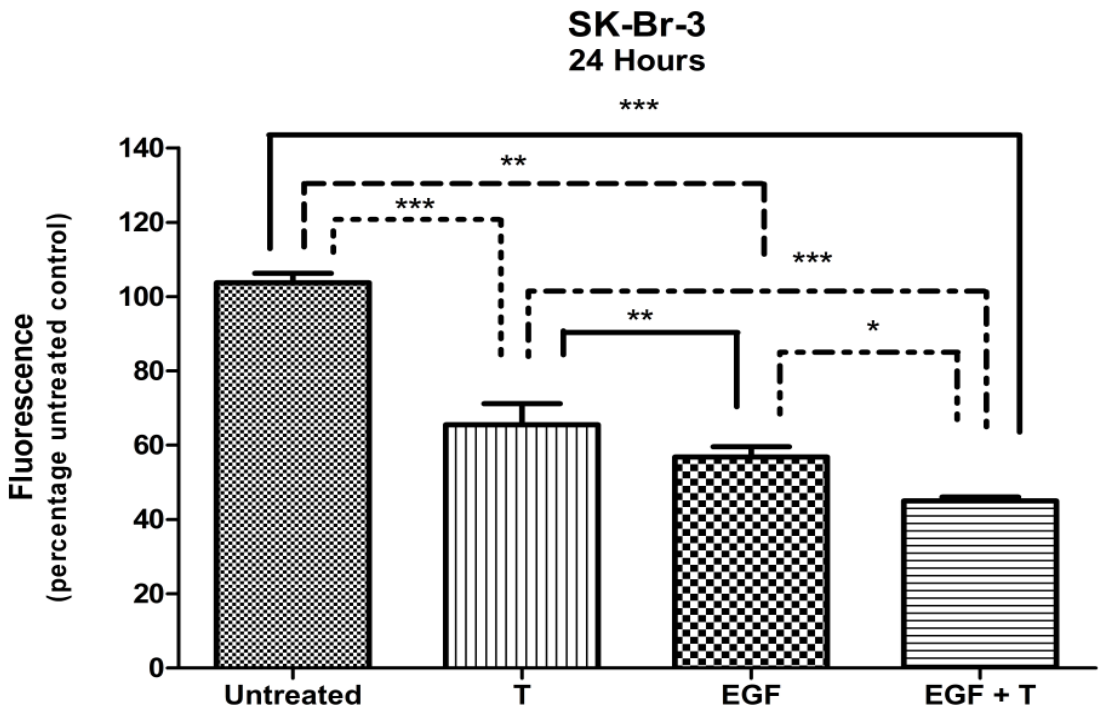

Figure 7.4: Relative Her-2 receptor density analysis at 24 hours in SK-Br-3 cells expressed as a percentage of the fluorescence of untreated controls (standardised to 100%). EGF: Epidermal growth factor (66 nM), T (100): trastuzumab 100 µg/ml. A similar trend was observed at 48 hours with the exception that EGF vs EGF-trastuzumab combination was no longer statistically significant.

Table 7.4: Fluorescent intensity (histogram x-mean) of SK-Br-3 cells exposed to EGF, trastuzumab and the EGF-trastuzumab combination

SK-Br-3	Mean ± SEM	Significance			
12 Hours		**U**	**EGF**	**EGF + T**	**T**
Untreated (U)	99.49 ± 2.52	-	***	***	***
EGF	66.49 ± 2.71	***	-		
EGF + T	61.11 ± 1.11	***		-	
T	64.77 ± 3.60	***			-
24 Hours		**U**	**EGF**	**EGF + T**	**T**
Untreated (U)	103.70 ± 2.61	-	***	***	***
EGF	56.82 ± 2.82	***	-	*	**
EGF + T	45.01 ± 1.06	***	*	-	***
T	65.47 ± 4.76	***	**	***	-
48 Hours		**U**	**EGF**	**EGF + T**	**T**
Untreated (U)	100.00 ± 1.95	-	***	***	***
EGF	41.39 ± 3.41	***	-		**
EGF + T	39.84 ± 2.27	***		-	***
T	61.83 ± 4.42	***	**	***	-

Epidermal growth factor (EGF) is a Her-1 receptor ligand. Binding of receptor-specific ligands results in the formation of strongly inter-dependent interactive dimers with other Her-family members. (Burgess et al., 2003) Cell membrane located Her-family members, found in normal epithelium, are spatially and chronologically defined and play a role in cell growth and differentiation. (Srinivasan et al., 1998) However, Her-1 receptors are over-expressed in approximately 45% of breast adenocarcinoma and are commonly correlated with oestrogen receptor (ER) and progesterone receptor (PR) negativity. (Koutras & Evans, 2008)

Single molecule imaging techniques have been implemented to study dimerization of EGF ligand-receptor complexes and receptor auto-phosphorylation. Sako *et al*. (2000) detected the location, movement and biochemical reactions of Her-1 receptors and illustrated that EGF-$(Her\text{-}1)_2$ complexes form prior to binding a second EGF molecule. Due to conformational fluctuations, Her-1 receptor dimers exist in several different states and dimeric combinations result in receptor auto-phosphorylation. Furthermore, it has been suggested that heterodimerization between Her-1 related receptors (Her-2 and Her-3) is induced by bivalency of a ligand. (Tzahar et al., 1997)

While neoplastic transformation associated with Her-1 receptors appears to be independent of those in Her-2 genes, synergistic effects within cellular transformation have been suggested. (Koutras & Evans, 2008) Gene amplification is usually present in Her-2 over-expression. However, the amount of Her-2 mRNA or Her-2 protein in primary tumours does not always directly correlate with Her-2 gene copies, suggesting that alternate mechanisms for expression are present. Likely candidates for alternate regulation include oestrogens and EGF. (Harris & Nicholon, 1988)

Furthermore, Her-2 receptors are thought to potentiate Her-1 receptor signalling by enhancing binding affinity of EGF (Karunagaran et al., 1996), predisposing the receptor to recycling (Lenferink et al., 1998) and reducing its degradation. (Worthylake, Opresko, & Wiley, 1999) All of these factors confound the co-ordinated regulation of signal transduction in this highly interactive family of receptors.

It was postulated that binding of EGF (66 nM) to the Her-1 receptor and subsequent formation of homo- or heterodimer complexes would result in auto-phosphorylation and intracellular signal propagation, promoting proliferation. However, exposing MCF-7 cells to EGF resulted in no observable response in cell viability [101.7% (±1.84)].

While assessing mechanisms for *de novo* resistance, Sahin *et al.* (2009) determined the mRNA levels of the Her-family receptors in both MCF-7 and SK-Br-3 cells. SK-Br-3 cells expressed high levels of Her-2 and intermediate levels of Her-1 mRNA. In contrast, MCF-7 cells expressed low levels of both Her-1 and Her-2 mRNA. While mRNA levels do not always directly correlate with cell surface receptor protein it provides a reasonable comparison for the effects of Her-family ligands (Figure 7.1; Table 7.1).

Because mRNA can be a deceptive framework for referencing ligand efficacy, Konecny *et al*. (2006) performed quantitative analysis of Her-2 and Her-1 receptor expression in 22 established breast cancer cell lines using ELISA. MCF-7 cells were found to express 4.7 ng/mg (±1.6) of Her-2 protein and 2.7 ng/ml (±0.6) of Her-1 protein, while SK-Br-3 cells were found to express 913 ng/ml (±114) Her-2 protein and 38 ng/ml (±7.4) Her-1 protein.

Given the above, it was therefore not surprising that MCF-7 cells that have relatively low levels of Her-1, were unresponsive to EGF stimulation. What was surprising, however, was that when EGF was combined with trastuzumab, cell viability of MCF-7 cells was significantly reduced to 81.97% (±1.99). The cell viability trend was similar for trastuzumab concentrations from 50 µg/ml to 200 µg/ml in MCF-7 cells while no statistical significance was observed between any group with 25 µg/ml trastuzumab. This significant reduction in MCF-7 cell viability at higher trastuzumab concentrations suggested that EGF possibly sensitised cells to the effects of high concentrations of trastuzumab.

Overall, it could be summarised that SK-Br-3 cells would be more responsive to EGF stimulation than MCF-7 cells. Considering the extent of Her-1 receptor expression in SK-Br-3 cells, EGF exposure resulted in a surprising decrease in cell viability (rather than an increase) to 81.43% (±2.46). Furthermore, rather than increasing this anti-proliferate effect, concurrent trastuzumab abrogated this effect, resulting in a cell viability of 86.40% (±2.20) (Figure 7.1; Table 7.1). These results pose an interesting paradigm; MCF-7 cell viability was significantly decreased with concurrent trastuzumab whereas SK-Br-3 cell viability was increased compared to either agent used alone.

Mechanisms for Her-1 receptor dependent cellular outcomes are strongly dependent on the actual level of Her-1 expression. Tikhomirov *et al.* (2005) illustrated that ligand binding to Her-1 receptors leads to proliferation when receptors are expressed at low levels, but can lead to cell death when these receptors are over-expressed.

Binding of EGF in cells with elevated levels of both Her-1 and Her-2 receptors resulted in Bax activation (Bcl-2 gene family protein promoting apoptosis) and translocation leading to loss of mitochondrial membrane potential and eventual cell death. (Tikhomirov & Carpenter, 2005)

Tikhomirov *et al.* (2005) also suggested that parental SK-Br-3 cells do not undergo extensive cell death in the presence of proliferative ligands unless transfected to express higher levels of Her-1 receptors, while biphasic cellular responses are still possible. Pro-survival pathways such as Her-1 and Her-2 over-expression which are implicated in tumour formation appear to not act synergistically beyond a certain receptor threshold and instead of promoting proliferation, may activate pathways that decrease cellular transformation.

The exceptionally low levels of Her-1 mRNA and protein in MCF-7 cells could provide insight into the inability of EGF to produce proliferation. The ability of EGF-trastuzumab combinations to significantly reduce cell viability remains obscure. The trend was maintained for the three higher concentrations of trastuzumab which suggests it is not just an experimental anomaly. The presence of receptor reservoirs that are capable of rapidly translocating to the cell surface in response to certain stimuli remains inconclusive. However, this notion of the initiation of *de novo* synthesis in response to EGF may result in increased surface Her-2 receptor expression and provide an explanation for the reduction in cell viability which was significant compared to the non-response observed for trastuzumab alone in MCF-7 cells.

The intermediate levels of Her-1 and extensive over-expression of Her-2 receptors in SK-Br-3 cells, appeared to produce a co-receptor status beyond the threshold for synergism and may therefore have functioned to decrease cellular transformation when exposed to proliferatory ligands such as EGF. When used in combination, trastuzumab may have decreased Her-2 receptors (observed in relative Her-2 receptor density assay) and in doing so, adjusted the over-expression ratio of receptors. This may have diminished the anti-proliferative effects of EGF, resulting in altered cell viability. Thus it was important to determine Her-2 receptor density at this point.

Her-2 receptor density analysis revealed that MCF-7 cells showed minimal differences in the overlay plot of unstained and untreated samples. EGF, trastuzumab or combination treated samples were indistinguishable from untreated samples at any time point.

Contrastingly, SK-Br-3 cells showed significantly decreased Her-2 receptors compared to untreated controls [untreated$_{12}$: 99.49% (±2.52)] when treated with trastuzumab [T_{12}: 64.77% (±3.60)], EGF [EGF_{12}: 66.49% (±2.71)] or the combination [EGF+T_{12}: 61.11% (±1.11)] at 12 hours. At 24 hours an apparent stepwise and statistically significant decrease was observed between all comparisons of untreated controls [untreated$_{24}$: 103.7% (±2.61], EGF [EGF_{24}: 56.82% (±2.82)], trastuzumab [T_{24}: 65.47% (±4.76)] and the combination [EGF+T_{24}: 45.01% (±1.06)]. Relative Her-2 receptor density was further decreased by 48 hours [EGF_{48}: 41.39% (±3.41)]. However, the significance between EGF and the combination was no longer evident (Figure 7.4; Table 7.4).

These results suggest that as a single agent, EGF may cause Her-2 receptor internalisation, likely in the form of Her-1:Her-2 heterodimers. The addition of concurrent trastuzumab further decreased relative Her-2 receptor density on the cell surface. EGF and trastuzumab may function independently to decrease Her-2 receptor density because the reduction did not appear to be additive.

Rapid internalization of Her-1 and its subsequent lysosomal degradation occurs after ligand binding and Her-1 is uncoupled from activation of downstream signalling. Others have noted that rapid internalization of Her-2 does not readily occur following transactivation by Her-1 receptors, concluding that when found in heterodimers, Her-1 receptor internalization is impeded, resulting in its longer presence on the cell surface and increased activation of this signalling pathway. (Tikhomirov & Carpenter, 2004)

Brockhoff *et al.* (2001) observed that EGF binding resulted in a 10% down regulation of Her-1 receptors in SK-Br-3 cells but had no effect on any of the other Her-family members, including Her-2, which could ultimately bias dimer formation. While previous researchers have noted Her-2 resistance to internalisation upon activation by EGF, in our study an almost 60% reduction of surface Her-2 receptors in SK-Br-3 cells was observed. At 24 hours the relative receptor density was further reduced by the addition of trastuzumab. However, it remains unclear how long the alterations were maintained and what the downstream implications for signalling and cell viability could be.

Antoniotti *et al.* (1994) studied the mechanisms by which EGF regulates Her-2 expression in two ER^+ breast cancer cell lines. T47D (ductal epithelial breast tumour) and ZR75.1 (human breast carcinoma) cell lines express moderate levels of Her-2 and Her-1 receptors and express a 5 to 10 fold reduction in Her-2 receptors compared to SK-Br-3 cells.

EGF exposure resulted in growth stimulation via Her-2 activation but with an accompanying down regulation in Her-2 receptor levels. Despite positive effects at the mRNA level, kinase activity and Her-2 phosphorylation resulted in decreased protein levels. Antoniotti *et al.* (1994) concluded that EGF treatment lead to activation of Her-2 receptors and that effects on Her-2 promoter activity was greater than any transcriptional effect or effect on mRNA levels. This suggests a post-transcriptional regulation by EGF or influence on distal repressors in Her-2 regulatory sequences.

The mechanisms of receptor internalisation promoting a reduction in surface Her-2 receptors may be two-fold: firstly by inhibition of Her-2 receptors by trastuzumab or secondly by EGF binding to Her-1: Her-2 heterodimers. A direct correlation with cell viability was confounded by these factors. The exact extent or lack of EGF-trastuzumab interactions would require more mechanistic studies.

No caspase-3 and -7 activation was observed along the time line assessed in either cell line when exposed to EGF, trastuzumab or the EGF-trastuzumab combination (data not shown), suggesting that executioner caspases are not involved in the reduction in cell viability and that anti-proliferative effects may be the preferred mechanism. Furthermore, the annexin-V assay showed no difference in fluorescent staining between untreated controls and experimental samples supporting the concept that the reductions in cell viability were cytostatic as opposed to cytotoxic.

Cell lines with a certain co-expression ratio of Her-1 and Her-2 receptors have resulted in ligand-dependent cell death mediated by the MAPK pathway. Tikhomirov *et al.* (2004) found that while no significant activation of caspase 3 was present in EGF induced cell death, a portion of the cells remained viable in the presence of EGF.

In MCF-7 cells statistically significant G1 phase increase became apparent at 48 hours [$G1_{48}$: 42.56% (±2.93)] when EGF was compared to the untreated control [G1: 23.25% (±0.86)]. Considering the function of EGF as a proliferative ligand, it may be possible that EGF accelerated cell cycle kinetics. However, this was not reflected by any significant increase in cell viability. By 72 hours the increased G1 phase [$G1_{72}$: 32.22% (±3.08)] had diminished and was no longer statistically significant suggesting that the effects of EGF had ceased.

When observing the combination in MCF-7 cells, G1 accumulation was statistically significant from 24 hours through to 72 hours. However, similar to EGF alone, the accumulation was the greatest at 48 hours [$G1_{48}$: 44.10 (±1.79)].

At 24 hours there was a significant difference between EGF alone [$G1_{24}$: 23.42% (±3.21)] versus the EFG-trastuzumab combination [$G1_{24}$: 40.78% (±2.95)] (Figure 7.2; Table 7.2). This raised the possibility of two processes occurring simultaneously, with EGF attempting to promote proliferation and trastuzumab inhibiting proliferation and resulting in a G1 accumulation. However, the reduction in cell viability with the EGF-trastuzumab combination may also suggest that all G1 phase inhibition was mediated solely by trastuzumab.

In SK-Br-3 cells, EGF did not alter cell cycle kinetics in a statistically significant manner at any of the three time points when compared to the untreated control [G1: 45.19% (±0.65)]. However, at 72 hours there was a statistically significant difference between trastuzumab [$G1_{72}$: 66.15% (±3.41)] or the combination [$G1_{72}$: 64.23% (±1.74)] versus EGF alone [$G1_{72}$: 49.09% (±1.74)] (Figure 7.3; Table 7.3). In SK-Br-3 cells trastuzumab may primarily have resulted in G1 accumulation, even in the presence of EGF. These results may provide an explanation for EGF having less of an anti-proliferative effect. While some increase in G1 phase was observed in SK-Br-3 cells in response to EGF at 48 and 72 hours, it was not as profound as that noted by Brockhoff *et al*. (2001) who observed that EGF resulted in prolongation of G1 phase in SK-Br-3 cells.

SK-Br-3 cells simultaneously express elevated Her-1 and Her-2 receptors, resulting in tumour cells being less susceptible to quiescence induction by trastuzumab. Diermeier *et al*. (2005) assessed EGF and trastuzumab in SK-Br-3 cells and illustrated G1-phase prolongation for EGF and trastuzumab as single agents as well as when used in combination. While G1-prolongation for EGF alone was not observed in our study, Diermeier concluded that receptor density and growth factors are of mutual importance in proliferation of cell subtypes and that over-expression of targets may not be sufficient as prognostic markers for therapeutic effect.

In conclusion, trastuzumab is only licensed for use in Her-2 positive breast cancer. Furthermore, the influence of EGF is dependent on the absolute receptor expression and cross activation which results in cell type specific interactions which is illustrated by the improved cell viability of SK-Br-3 cells in response to the EGF-trastuzumab combination. Surprisingly, the EGF-trastuzumab combination resulted in a reduction in cell viability in ER positive MCF-7 cells. Although the mechanisms for these alterations have been hypothesised, they are still to be fully elucidated.

Her-family ligand binding, in the form of EGF, appeared to result in internalisation of Her-2 receptor-containing heterodimers in SK-Br-3 cells, which was further decreased in the presence of trastuzumab. A certain threshold of surface Her-2 receptors is required to ensure clinical benefit for trastuzumab. While it is unclear whether these alterations in receptor expression will be maintained for a period long enough to be clinically relevant, the reduction could result in insufficient cancer targeting and diminish the relevance of trastuzumab as a targeted therapy.

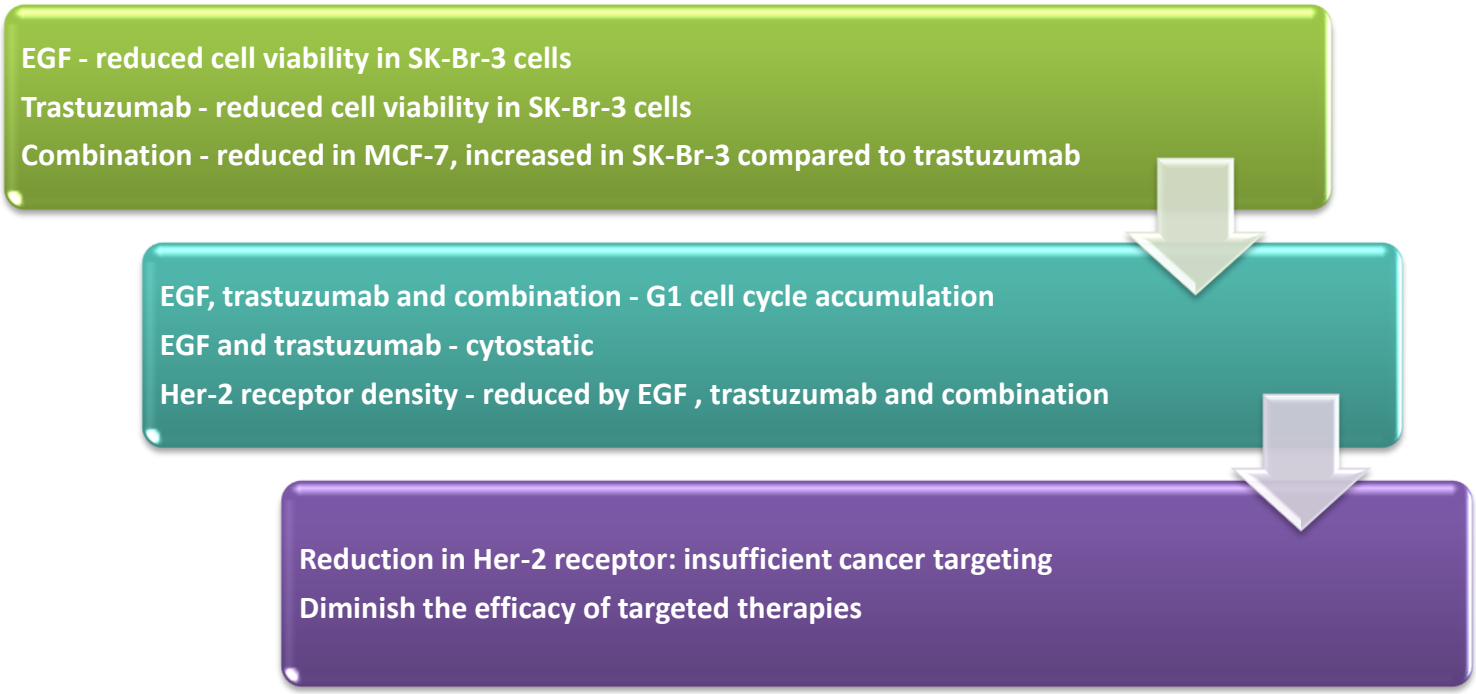

Chapter 8: Results and Discussion: Geldanamycin

8.1 Cell Viability

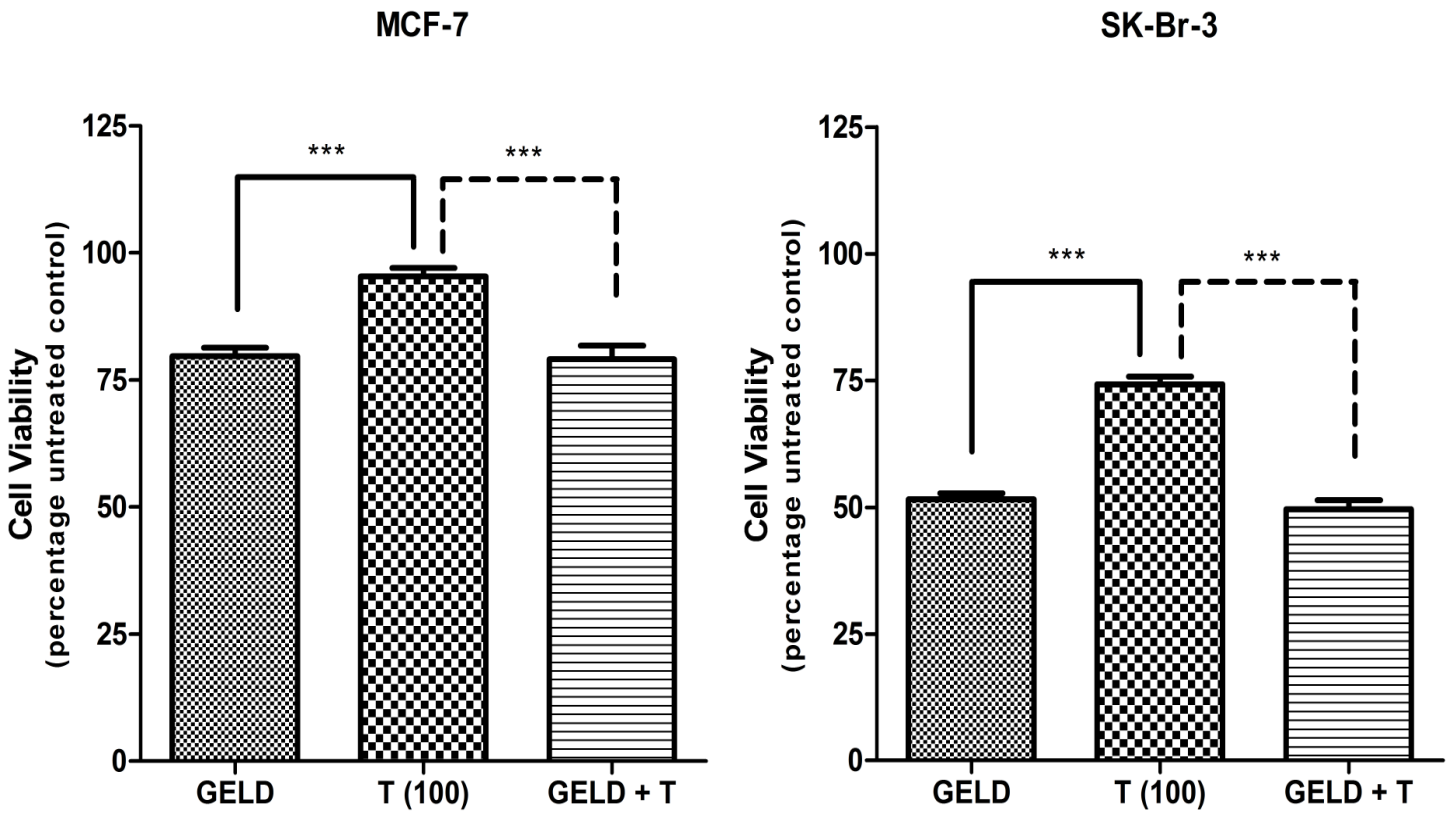

Figure 8.1: Cell viability in MCF-7 and SK-Br-3 cells expressed as a percentage of the untreated controls. Statistically significant differences were found between trastuzumab alone versus geldanamycin alone and the geldanamycin-trastuzumab combination. Further statistically significant differences (P < 0.001) were found when comparing the average cell viability of geldanamycin alone between MCF-7 and SK-Br-3 cells. GELD: geldanamycin (0.35 µM), T (100): trastuzumab 100 µg/ml. (Statistical significance followed the same trend for combinations at 25 µg/ml, 50 µg/ml, 200 µg/ml in both cell lines.)

Table 8.1: Cell viability results for geldanamycin and the geldanamycin-trastuzumab combination

	MCF-7	SK-Br-3
	Mean ± SEM	**Mean ± SEM**
Geldanamycin (GELD) (0.35 µM)	79.71 ± 1.58	51.54 ± 1.19
GELD + Trastuzumab (25 µg/ml)	80.47 ± 4.41	54.29 ± 1.26
GELD + Trastuzumab (50 µg/ml)	81.93 ± 3.81	52.40 ± 1.44
GELD + Trastuzumab (100 µg/ml)	79.13 ± 2.64	49.61 ± 1.77
GELD + Trastuzumab (200 µg/ml)	83.34 ± 3.02	48.69 ± 1.63

8.2 Cell Cycle Analysis

Table 8.2: Cell cycle results for GELD, trastuzumab and the GELD-trastuzumab combination in MCF-7 cells.

MCF-7	Mean ± SEM				Significance			
72 Hours	**G1**	**S**	**G2**	**Sub G1**	**C**	**GELD**	**GELD + T**	**T**
Control (C)	23.25 ± 0.86	52.99 ± 2.33	23.76 ± 3.17		-	***	***	**
GELD	28.60 ± 4.34	11.94 ± 1.48	57.32 ± 1.88	21.35 ± 2.02	***	-		***
GELD + T	33.25 ± 1.81	14.42 ± 3.62	52.33 ± 3.92	23.43 ± 3.05	***		-	***
T	56.37 ± 4.48	33.34 ± 3.23	10.29 ± 1.72	1.89 ± 0.02	**	***	***	-

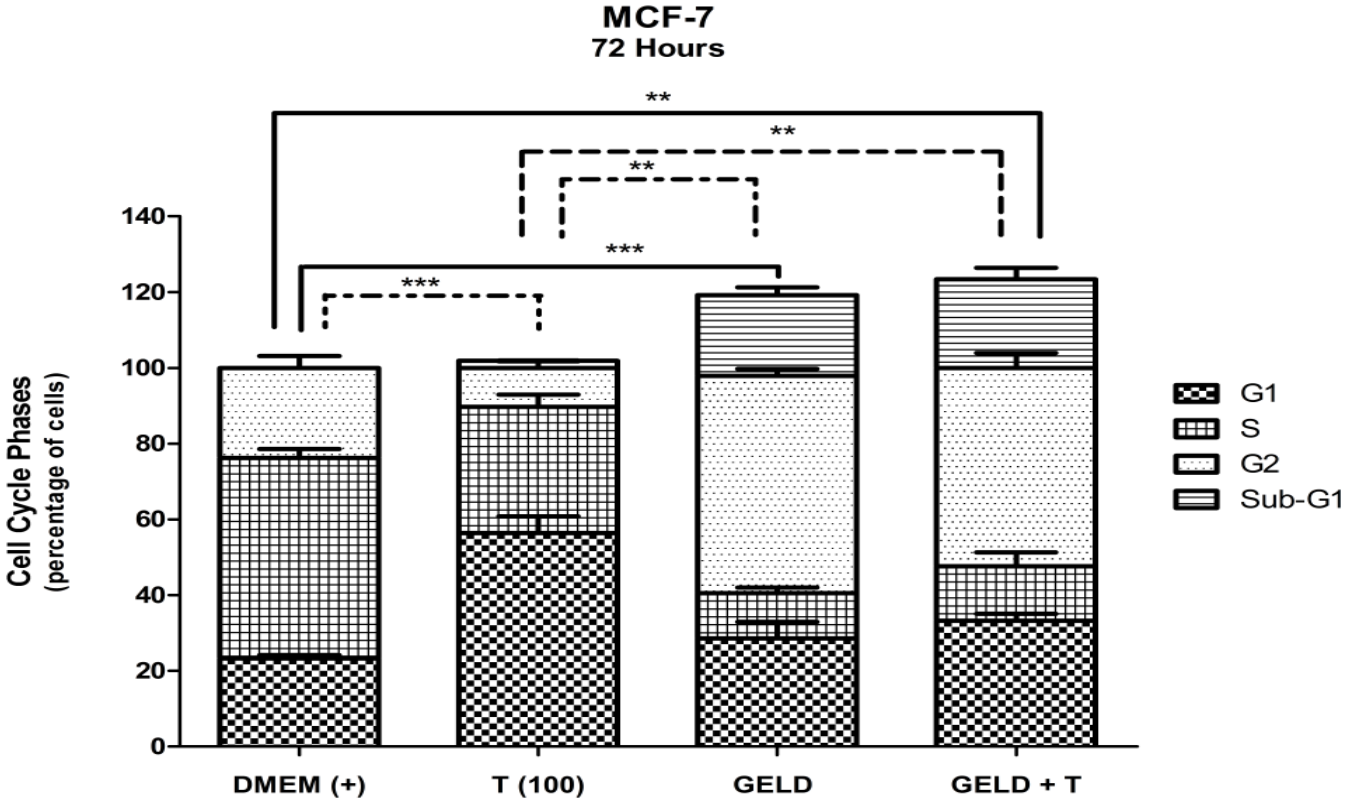

Figure 8.2: Cell cycle analysis in MCF-7 cells expressed as a percentage after deconvolution. Statistically significant differences in the G1 and G2 phase of the cell cycle were observed between various comparisons of the untreated control (DMEM+) versus trastuzumab, geldanamycin and the geldanamycin-trastuzumab combination after 72 hours. GELD: geldanamycin (0.35 µM), T (100): trastuzumab 100 µg/ml. [Significance followed similar trends for SK-Br-3 cells]

Table 8.3: Cell cycle results for GELD, trastuzumab and the GELD-trastuzumab combination in SK-Br-3 cells

SK-Br-3	Mean ± SEM				Significance			
48 Hours	**G1**	**S**	**G2**	**Sub G1**	**C**	**GELD**	**GELD + T**	**T**
Control (C)	45.19 ± 0.65	35.68 ± 0.81	19.16 ± 0.31		-	*	**	**
GELD	54.88 ± 0.67	12.86 ± 2.44	32.26 ± 1.87	10.76 ± 0.56	*	-		**
GELD + T	50.54 ± 2.12	11.49 ± 0.82	37.93 ± 1.39	10.07 ± 1.93	**		-	**
T	64.15 ± 1.41	20.84 ± 3.55	15.02 ± 4.56	11.48 ± 1.28	**	**	**	-
72 Hours	**G1**	**S**	**G2**	**Sub G1**	**C**	**GELD**	**GELD + T**	**T**
Control (C)	45.19 ± 0.65	35.68 ± 0.81	19.16 ± 0.31		-	***	**	***
GELD	43.83 ± 1.99	11.17 ± 1.41	45.00 ± 1.85	16.64 ± 2.55	***	-	**	**
GELD + T	54.30 ± 3.23	18.67 ± 3.43	27.03 ± 0.29	18.41 ± 1.83	**	**	-	**
T	66.93 ± 3.41	20.78 ± 2.60	15.02 ± 1.38	11.69 ± 2.20	***	**	**	-

8.3 Apoptosis-Necrosis

Table 8.4: Apoptosis-Necrosis in MCF-7 cells after 72 hours

Statistical significance expressed with differences in two or more phases (E: Early, L: Late)

MCF-7	Mean ± SEM				Significance			
72 Hours	Normal	E Apoptosis	L Apoptosis	Necrosis	U	GELD	GELD + T	T
Untreated (U)	95.37 ± 1.07	0.80 ± 0.49	0.20 ± 0.06	3.63 ± 0.56	-	*	**	
GELD	72.33 ± 5.45	16.87 ± 3.05	2.40 ± 0.35	8.43 ± 3.42	*	-		*
GELD + T	67.27 ± 4.57	19.07 ± 7.12	6.60 ± 3.49	7.07 ± 2.49	**		-	**
T	94.57 ± 0.54	1.03 ± 0.18	0.47 ± 0.03	3.97 ± 0.42		*	**	-

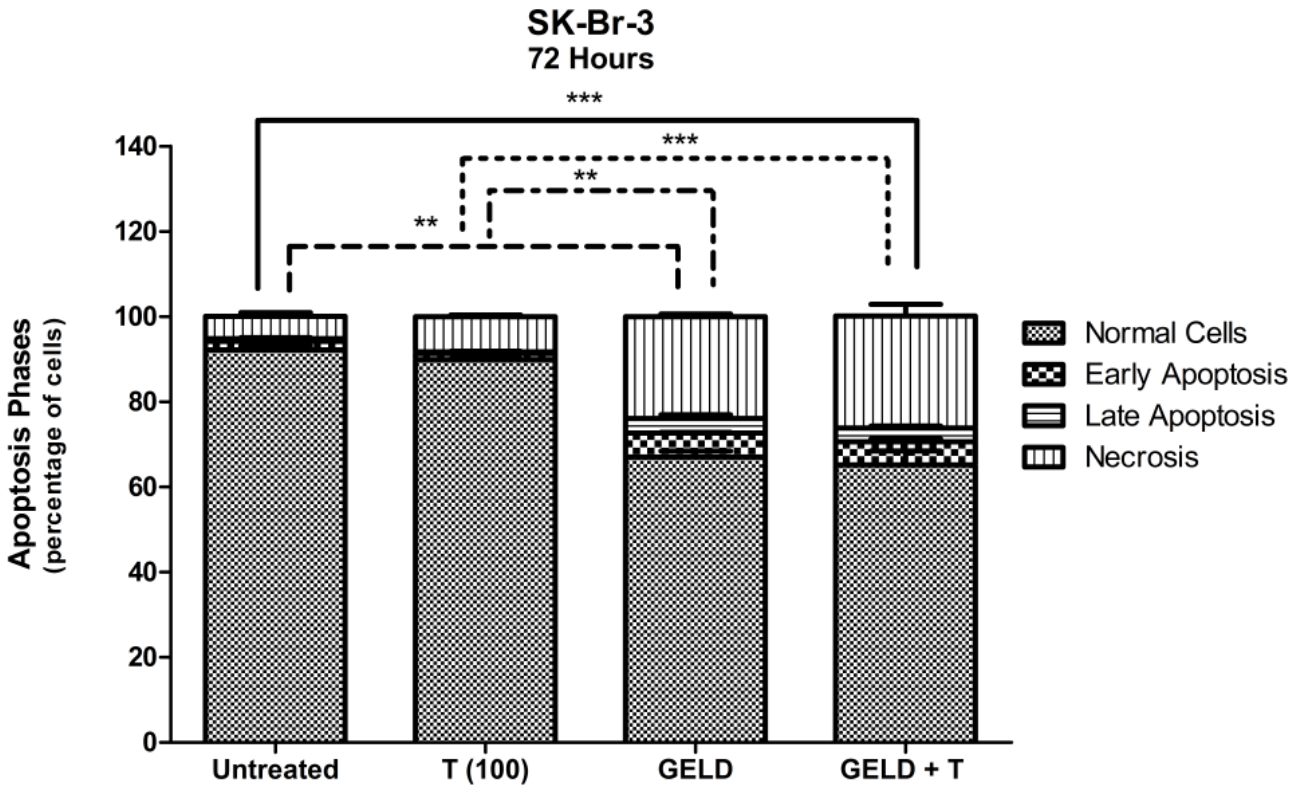

Figure 8.3: Annexin-V assay in SK-Br-3 cells expressed as a percentage of normal cells, early apoptosis, late apoptosis and necrosis. Statistically significant differences between untreated control or trastuzumab versus geldanamycin or the geldanamycin-trastuzumab combination after 72 hours. GELD: geldanamycin (0.35 µM), T (100): trastuzumab 100 µg/ml. [Significance followed similar trends for MCF-7 cells]

Table 8.5: Apoptosis-Necrosis in SK-Br-3 cells after 72 hours

Statistical significance expressed with differences in two or more phases (E: Early, L: Late)

SK-Br-3								
72 Hours	Normal	E Apoptosis	L Apoptosis	Necrosis	U	GELD	GELD + T	T
Untreated (U)	91.25 ± 1.13	1.80 ± 0.47	0.50 ± 0.23	6.48 ± 1.36	-	**	***	
GELD	67.00 ± 1.40	5.60 ± 0.20	3.46 ± 0.83	23.90 ± 0.57	**	-		***
GELD + T	65.17 ± 3.23	5.36 ± 0.66	3.23 ± 0.52	26.37 ± 2.75	**		-	**
T	89.90 ± 0.15	1.40 ± 0.31	0.37 ± 0.12	8.33 ± 0.37		***	**	-

8.4 Relative Her-2 Receptor Density

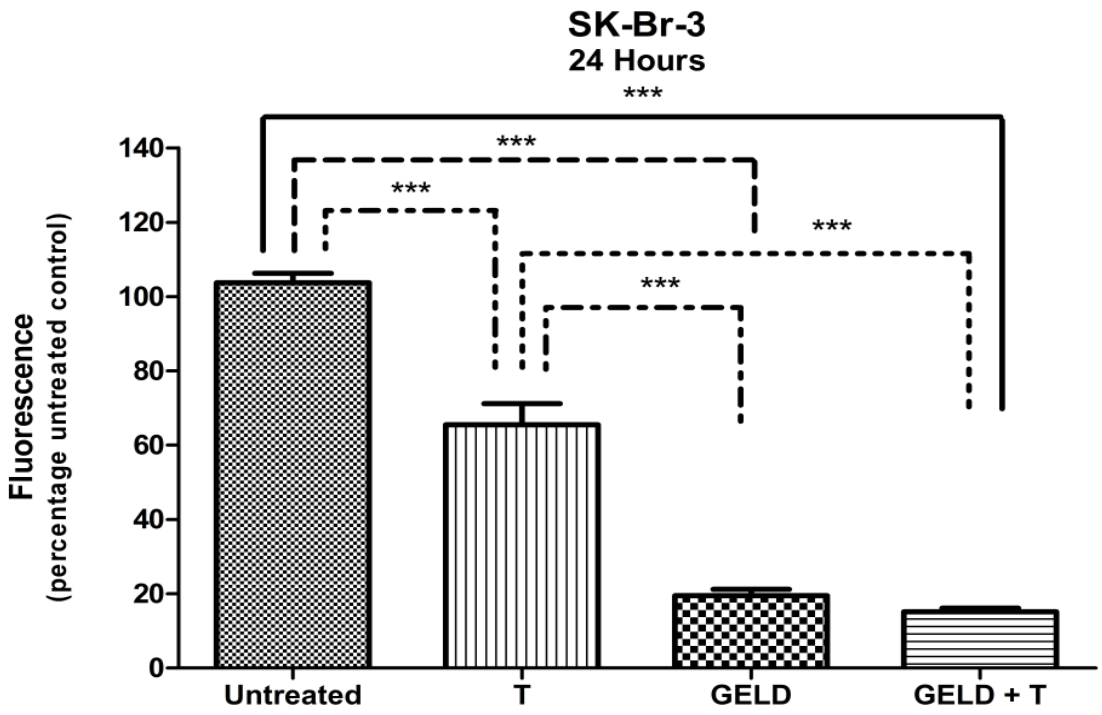

Figure 8.4: Relative Her-2 receptor density at 12 hours in SK-Br-3 cell expressed as a percentage of the fluorescence of untreated controls (standardised to 100%). Statistical significance followed the same trend at 24 and 48 hours. GELD: geldanamycin (0.35 µM), T (100): trastuzumab 100 µg/ml.

Table 8.6: Fluorescent intensity (histogram x-mean) of SK-Br-3 cells exposed to geldanamycin, trastuzumab and the geldanamycin-trastuzumab combination

SK-Br-3	Mean ± SEM	Significance			
12 Hours		**U**	**GELD**	**GELD + T**	**T**
Untreated (U)	99.49 ± 2.52	-	***	***	***
GELD	13.89 ± 1.53	***	-		***
GELD + T	10.87 ± 1.33	***		-	
T	64.77 ± 3.60	***	***	***	-
24 Hours		**U**	**GELD**	**GELD + T**	**T**
Untreated (U)	103.70 ± 2.61	-	***	***	***
GELD	19.47 ± 1.80	***	-		***
GELD + T	15.23 ± 0.89	***		-	
T	65.47 ± 4.76	***	***	***	-
48 Hours		**U**	**GELD**	**GELD + T**	**T**
Untreated (U)	100.00 ± 1.95	-	***	***	***
GELD	14.15 ± 1.21	***	-		***
GELD + T	14.48 ± 1.45	***		-	
T	61.83 ± 4.42	***	***	***	-

Heat shock protein 90 (hsp90), is an abundant transient 90kDa cellular protein which functions as a crucial "house-keeping" chaperone for numerous cell signalling proteins. Under normal circumstances, hsp90 has a wide variety of clients which include a diverse group of transcription factors as well as various protein kinases. However, hsp90 as well as other chaperone proteins are known to become up-regulated in stressed cells. (Toft, 1998; Neckers et al., 1999) Moreover, ubiquitous hsp90 protein is constitutively expressed at higher levels in tumour cells compared to normal cell counterparts. This suggests that hsp90 may be a preferential target for treatment in neoplastic tissue. (Bisht et al., 2003)

Geldanamycin, a hsp90 inhibitor, was the first benzoquinone ansamycin antibiotic identified from spore of the bacterium species *Streptomyces hygrocopicus* in 1970. (Deboer & Peterson, 1970) Geldanamycin is capable of binding to a conserved pocket of the hsp90 protein and inhibiting maturation and refolding of signalling proteins. Antagonizing multi-molecular hsp90 chaperone complexes results in client protein destabilization and degradation. (Toft, 1998; Neckers et al., 1999; Münster, Marchion, Basso, Mu, & Rosen, 2002)

Chaperone proteins are merely mediators in the assembly of polypeptides and are ultimately not integrated into the assembled structure. Hsp90 has two isoforms, hsp90α and hsp90β, which exist mainly as homo-dimers (hsp90α-hsp90α) but occasionally as heterodimers. Although usually found in the cytosol, under stress conditions, hsp90 accumulates in the nucleus. The hsp90 N-terminal contains a non-conventional binding site for ATP or ADP which is also the binding site for geldanamycin. (Toft, 1998; Neckers et al., 1999)

Hsp90 association is required for tumour suppressor protein p53, Src family kinases, Wee1 kinase, transmembrane tyrosine kinases including the Her-family, Raf-1 kinase-protein, casein kinase II and Cdk4/cyclin-D complexes. (Neckers et al., 1999) Thus, hsp90 chaperones are key intracellular mediators in the maintenance of critical biological functions including conformation, stability and signal transduction, amongst others. These factors ultimately affect proliferation, cell cycle and apoptosis. (Bisht et al., 2003) Geldanamycin and other hsp90-specific inhibitors have been used in clinical trials to assess their efficacy in advanced solid tumours, lymphomas, relapsed hematologic cancer, ovarian epithelial, breast cancer and peritoneal cavity cancers amongst others. (Fukuyo, Hunt, & Horikoshi, 2010)

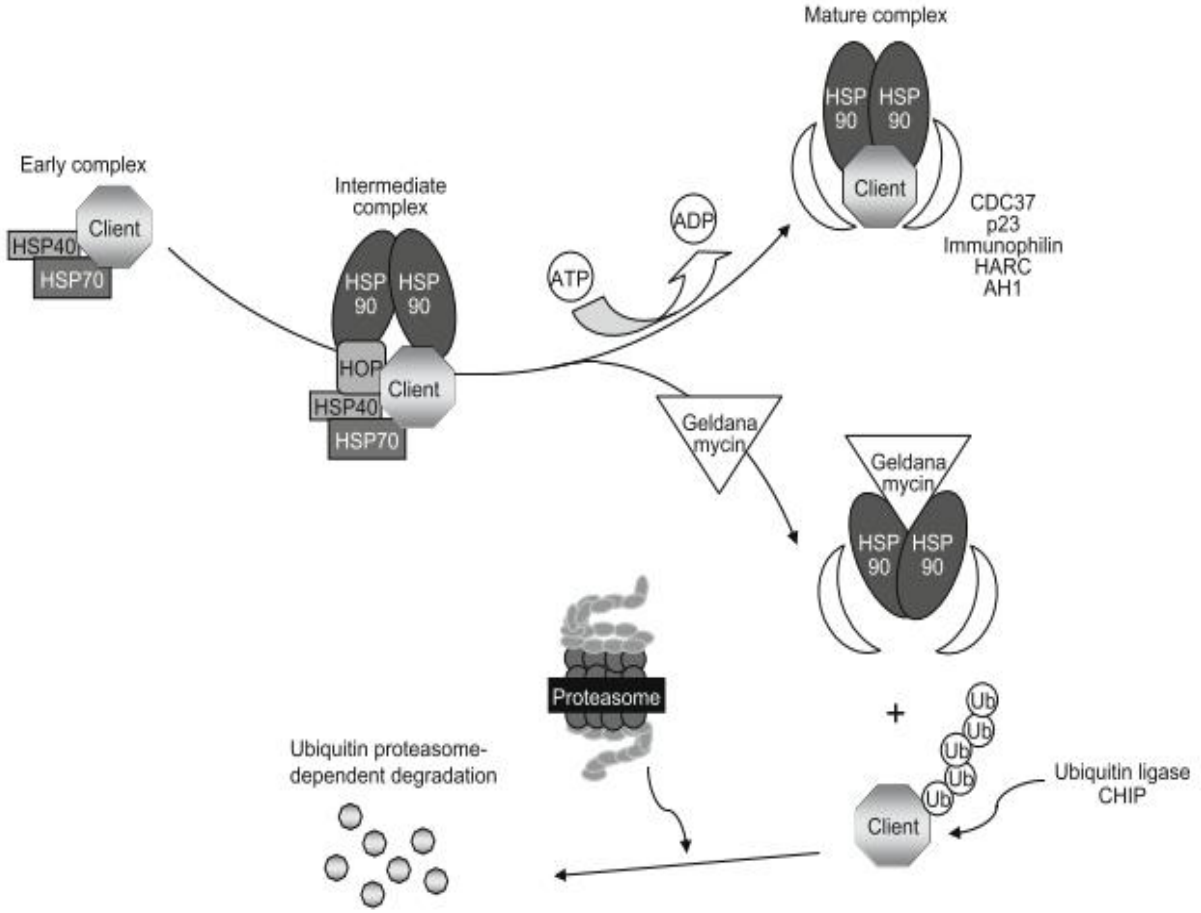

Figure 8.5: HSP90 chaperone–client protein cycle. Initially, the client protein is bound to the early complex (HSP40/HSP70) that then interacts with the HSP90 homo-dimer through HOP. ATP hydrolysis releases HSP40/HSP70 and HOP from the intermediate complex. In addition, the mature protein complex is formed by association between HSP90 and co-chaperones (CDC37, p23, Immunophilin, HARC, AH1) or client proteins. Geldanamycin blocks the formation of mature complex by binding to the ATP-binding site of HSP90, leading to ubiquitin proteasome-dependent degradation of the client proteins which are targeted by the CHIP E3 ligase. [HOP: HSP90/HSP70 organizing protein; CHIP: carboxy-terminus of HSP70-interacting protein.] (Fukuyo et al., 2010)

The anti-neoplastic potential of geldanamycin was supported by our results, where geldanamycin (0.35 µM) exposure resulted in a decreased cell viability of 79.71% (±1.57) in MCF-7 cells. Concurrent trastuzumab (100 µg/ml) exposure resulted in an almost identical cell viability of 79.13% (±2.64). While significantly lower, the trend for SK-Br-3 cell viability was similar with 51.54% (±1.19) for geldanamycin and 49.69% (±1.63) for geldanamycin-trastuzumab exposure (Figure 8.1; Table 8.1). Even in Her-2 receptor over-expressing cells, geldanamycin appeared to influence cell viability independently of trastuzumab.

As mentioned, geldanamycin disrupts hsp90 association with client proteins and affects chaperone complexes via interactions with the catalytic sub-domain. Geldanamycin has also been shown to decrease pro-survival factors which include Akt1, Her-2, cAMP-dependent protein kinases, Raf-1 and extracellular signal-regulated kinase (ERK) in cervical tumour cell lines. (Bisht et al., 2003) Depletion of c-Raf-1, an integral part of a protein kinase cascade of the MAPK signalling pathways, by hsp90 is strongly implicated in reductions in cell proliferation. (Hostein, Robertson, Distefano, Workman, & Clarke, 2001) Several proteins assessed by Bisht *et al*. (2003) do not appear to require hsp90 for stabilization, illustrating extensive indirect effects via alterations in upstream clients on multiple non-client proteins.

Other ansamycin antibiotics such as 17-allylamino-17-demethoxy-geldanamycin (17-AAG), a less toxic derivative of geldanamycin, also inhibit hsp90. Signalling proteins that require hsp90 exhibit different levels of sensitivity to chaperone inhibition; Her-kinases demonstrate particularly high susceptibility. Münster *et al.* (2002) exposed a panel of cells to 17-AAG and observed that cells with elevated Her-2 expression were more sensitive to the anti-proliferative effects of the hsp90 inhibitor. Furthermore, it was noted that Her-3 plays a crucial role in the anti-proliferative effects of geldanamycin, suggesting that Her-2:Her-3 heterodimerization and PI3K signalling pathways are of importance.

The cell viability results obtained in our study supported this concept as SK-Br-3 cells were found to be more sensitive to the hsp90 inhibitor than MCF-7 cells. However, there was little evidence in support of using geldanamycin-trastuzumab combinations in either cell line as the combination failed to result in additional reductions in cell viability. The combination of cytotoxic drug and cytostatic antibody may be rendered ineffective because theoretically, geldanamycin influences Her-2 receptor expression and thus reduces the target for trastuzumab binding.

No caspase-3 and -7 activation was observed in either cell line when exposed to geldanamycin or the geldanamycin-trastuzumab combinations over the time period of 4 to 30 hours (data not shown). This suggests that either apoptosis is not the mechanism for the reduction in cell viability, or that caspases are only detectable after 30 hours; it is possible that geldanamycin initially caused alterations in cell cycle kinetics prior to executioner caspases being present.

Testing geldanamycin by Kim *et al*. (2003) in SH-S5Y5 neuroblastoma cells resulted in activation of the caspase pathway and mitochondrial release of cytochrome C. Activation of initiator and executioner caspases 9 and 3 respectively were significantly increased after 48 hour. Western blot analysis substantiated these finding with a time-dependent induction of caspase 3 activation present at 48 hours which was not detected at 24 hours. Furthermore, reduction of Raf-2 and Akt which play important roles in Raf/MEK and PI3K/Akt dependent proliferation was observed. The detection of caspase-3 activation at 48 hours suggests that the time points in our study should have been extended to accurately quantify executioner caspase activity.

The annexin-V assay demonstrated evidence of apoptotic cell death at 48 and 72 hours in both cell lines, with significant differences between untreated controls or trastuzumab alone (no effect) versus geldanamycin and the geldanamycin-trastuzumab combination. Geldanamycin exposure to MCF-7 cells at 48 hours resulted in 75.30% (±1.22) normal cells (annexin-V and PI negative) with 22.30% (±1.57) in the early stages of apoptosis (annexin-V positive). Concurrent trastuzumab resulted in a similar percentage: 78.87% (±2.48) normal cells with 18.63% (±2.81) in early apoptosis. After 72 hours MCF-7 cells illustrated a similar percentage of normal cells. However, an increase to 8.43% (±3.42) in necrotic cells was noted which was also reflected in the geldanamycin-trastuzumab combination (Table 8.4).

Geldanamycin exposure for 48 hours in SK-Br-3 cells resulted in 73.57% (±2.56) normal cells with 5.13% (±0.84) in early stages of apoptosis and a large percentage, 17.23% (±1.66), of necrotic cells. Concurrent trastuzumab resulted in a similar percentage: 72.20% (±1.79) normal cells with 4.16% (±0.63) in early apoptosis and 17.83% (±1.24) in necrosis. After 72 hours SK-Br-3 cells showed a further decrease in the percentage of normal cells to 67.00% (±1.40) and 65.17% (±3.23) for geldanamycin alone and the geldanamycin-trastuzumab combination respectively. This decrease in living cells was accompanied by an increase in necrotic cells (Figure 8.3; Table 8.5).

In MCF-7 cells, early apoptosis was the dominant feature at 48 hours, while a greater percentage of cells were found in late apoptosis and necrosis by 72 hours. Contrastingly, in SK-Br-3 cells significant necrosis was evident from 48 hours. The difference in the doubling time and the degree of sensitivity to geldanamycin could explain why the trend through early apoptosis to necrosis was not observed as predictably in the SK-Br-3 cells. This data provided evidence for apoptosis despite executioner caspases not being detected.

Apoptosis has previously been observed in response to 17-AAG in cell lines sensitive or more resistant to geldanamycin using the TUNEL assay (DNA fragmentation), poly(ADP-ribose) polymerase (PARP) cleavage and proteolytic activation of caspase 3. (Shimamura, Lowell, Engelman, & Shapiro, 2005) Despite the potential complexities, the kinetics of molecular responses to 17-AAG induced differential cytostatic and apoptotic responses dependent on particular cell subtype. (Hostein et al., 2001)

Supporting the theory that cell cycle kinetics are altered prior to geldanamycin-induced cell death, apoptosis was observed using double staining of annexin-V/ PI and further by the cleavage of both caspases 9, 3 and PARP for up to 72 hours in mantle cell lymphoma (MCL) cell lines. The mechanisms were found to be down-regulation of cylcin-D1 and cdk4 with an accompanying up-regulation in p27, a cdk inhibitor. (Georgakis, Li, & Younes, 2006)

A statistically significant G2 phase accumulation became apparent in geldanamycin exposed MCF-7 cells at 24 hours [$G2_{24}$: 47.16% (±1.94)] compared to the untreated control [G2: 23.76% (±3.17)]. Significant G2 phase accumulation continued through to 72 hours [$G2_{72}$: 57.32% (±1.88)]. However, there was no statistically significant difference between time points. The geldanamycin-trastuzumab combination resulted in a similar statistically significant G2 accumulation evident from 24 hours [$G2_{24}$: 47.48% (±3.11)] through to 72 hours [$G2_{72}$: 52.33% (±3.92)]. G2 phase accumulation was the most prominent alteration in cell cycle kinetics induced by geldanamycin. However, a significant increase in G1 phase was evident at all three time points [$G1_{48}$: 30.97% (±4.47)] compared to the control [G1: 23.25% (±0.86)] (Table 8.2).

The greatest G1 accumulation was observed at 24 hours, yet there was no noticeable differences between geldanamycin alone [$G1_{24}$: 39.67% (±2.40)] and the geldanamycin-trastuzumab combination [$G1_{24}$: 36.96% (±2.46)]. Even with two potential points of cell cycle alteration for geldanamycin, there was no potentiation in effects in the presence of trastuzumab. This suggests that geldanamycin activity, even when used in combination, is independent of trastuzumab.

Similarly, geldanamycin promoted G2 phase accumulation in SK-Br-3 cells, which was statistically significant at 24 hours [$G2_{24}$: 29.86% (±0.30)] through to 72 hours [$G2_{72}$: 45.00% (±1.85)] compared to untreated controls [G2: 19.16% (±0.31)]. Furthermore, G1 accumulation was evident when compared to the control [G1: 45.16% (±0.65)], with the greatest significance observed at 24 hours for geldanamycin [$G1_{24}$: 59.62% (±2.61)] and the combination [$G1_{24}$: 67.84% (±2.06)] (Figure 8.2; Table 8.3).

In this case the G1 accumulation was significantly different between geldanamycin alone and the geldanamycin-trastuzumab combination, suggesting a potential influence of trastuzumab on cell cycle kinetics. However, the alteration was not translated into differential responses in apoptosis or cell viability, which suggests that the difference was perhaps merely an experimental anomaly or a transient, non-translatable effect of the combination. At 48 hours G1 accumulation was insignificant, after which it reappeared at 72 hours. The percentage of cells in sub-G1 increased significantly over this period of time which may have skewed the cell cycle distribution. Although differences in G1 accumulation at 24 hours in SK-Br-3 cells may pose some questions, geldanamycin still appeared to primarily influence cells even in the presence of trastuzumab.

Others have shown that geldanamycin decreased cell viability after exposure for 48 to 72 hours and that this occurred secondary to cell cycle arrest at both G1-S and G2-M boundaries. (Shimamura et al., 2005) Hostein *et al.* (2001) observed G2-M phase accumulation at 24 and 48 hours in human colon adenocarcinoma cells, which was no longer evident at 72 hours. Other observed that geldanamycin also perpetuated G2-M phase accumulation in three follicular thyroid cancer (FTC) cell lines which was followed by associated increases in apoptosis determined by annexin-V/PI staining. The mechanisms for these effects in FTC cells were shown to include down-regulation of both c-Raf-1 and mutant p53 protein. (Park, 2003)

Wee1 kinase, a nuclear tyrosine kinase, is an integral player in controlling the duration of the G2 phase of the cell cycle via cdk2 phosphorylation. A positive feedback loop regulates cdk2 whereby cdk2 itself negatively regulates Wee1 phosphorylation and reduces cdk2. Alinque *et al.* (1994) elucidated the activity of Wee1 nuclear kinases and observed that formation of this kinase is dependent on interactions with Swo1, a hsp90 homolog. If geldanamycin is capable of interrupting the chaperone capabilities of hsp90 homologs and disrupting Wee1 kinase activity, the sequential cell cycle phases may be disrupted resulting in a G2 phase block.

D-type cyclins facilitate G1 progression in part by binding inactive monomeric cdks as a part of cdk4-cyclin-D complexes. Cdk4 can exist in complex with hsp90 where hsp90 sequesters cdk4 in a primed, inactive conformation which is dissociated upon cyclin-D binding. Destabilized cdk4, in the absence of hsp90 function, results in post-translational destabilization suggesting a role for chaperones in kinase stabilization. (Stepanova, Leng, Parker, & Harper, 1996) Geldanamycin may induce G1 inhibition by limiting access to stabilized cdk4. Thus it is possible for geldanamycin to promote cell cycle blocks in two phases of the cell cycle which was evident in both MCF-7 and SK-Br-3 cells.

Alterations in G1-S and G2-M transitions observed in our study were strongly supported by researchers including Shimamura *et al*. (2005) who observed the same trends.

Assessing Her-2 receptor density revealed that MCF-7 cells showed differences in the overlay plot of unstained and untreated samples that were impossible to differentiate. Cells exposed to geldanamycin, trastuzumab and combination were indistinguishable from untreated samples at any time point. Contrastingly, trastuzumab-exposed SK-Br-3 cells [T_{12}: 64.77% (±3.60)] illustrated a statistically significant decrease in Her-2 receptors compared to untreated controls [untreated$_{12}$: 99.49% (±2.52)] at 12 hours. An even greater decrease in Her-2 receptors was observed for geldanamycin alone [GLD_{12}: 13.89% (±1.53)] and the geldanamycin-trastuzumab combination [GLD+T_{12}: 10.87% (±1.33)] at 12 hours (Figure 8.4; Table 8.6). This trend was sustained for 24 and 48 hours. These results suggest that as a single agent, geldanamycin may be the sole influence on surface Her-2 receptors density in SK-Br-3 cells.

Geldanamycin and other benzoquinone antibiotics are suspected inhibitors of normal maturation of tyrosine kinase receptors which include Her-1, IGF receptor, platelet-derived growth factor receptor, and Her-2 receptors. (Chavany et al., 1996; Helmbrecht, Zeise, & Rensing, 2000) Geldanamycin and various analogues have been reported to deplete Her-2 gene products in SK-Br-3 cells. Schnur *et al*. (1995) did not find alterations in gene products but noted that inhibition of Her-2 oncogene function was possible and required the oxidized form of the quinine moiety for inhibition.

Sepp-Lorenzino *et al.* (1995) assessed the effects of herbimycin A on degradation of tyrosine kinase receptors and observed dose and time-dependent decreases in steady-state levels of tyrosine kinase receptors such as IGF-IR in breast cancer cells. Herbimycin A resulted in rapid reductions in cellular content from 4 hours which was complete by 24 hours. This receptor degradation appeared to be strongly dependent on the 20S proteasome and the ubiquitin-conjugation system as opposed to direct interaction with kinase functionality.

Many researchers have examined the effects of related benzoquinone ansamycins in cells over-expressing Her-2 gene products and have noted rapid depletion of tyrosine phosphorylation followed by delayed depletion of the Her-2 protein. (Miller, Diorio, Moyer, Schnur, & Moyer, 1994; Mimnaugh et al., 1996) Decreased tyrosine phosphorylation or reduction in Her-2 protein varies between cell types. However, mRNA levels remain the same, suggesting that ansamycins increase the rate of receptor degradation instead of influencing protein synthesis. (Miller et al., 1994)

Geldanamycin reportedly mediates depletion of Her-2 receptors via binding to glucose-related protein (GRP94), an endoplasmic member of the hsp90 family of stress proteins, and dissociating hetero-complexes which lead to Her-2 receptor degradation. Further studies observed that complexes between Her-2 and GRP94 are disrupted within an hour after exposure and that polyubiquitination precedes the decline in Her-2 levels in geldanamycin exposed SK-Br-3 cells. (Mimnaugh et al., 1996; Chavany et al., 1996)

Geldanamycin is an attractive chemotherapeutic agent considering its ability to antagonise hsp90 functions which are crucial for cellular "house-keeping" duties. Differential responses of cell types to hsp90 inhibition may be due to preferential proliferative signalling pathways and the necessity of hsp90 in regulating these functions. The notion that Her-2 receptor expression plays a role in the susceptibility to geldanamycin was observed in our study. However, the ability of geldanamycin to rapidly and dramatically reduce relative surface Her-2 receptor density demonstrates that this combinatorial regimen would not have any clinical benefit. Removal of Her-2 as a target for trastuzumab would result in negligible effects of this targeted therapy in tumour reduction.

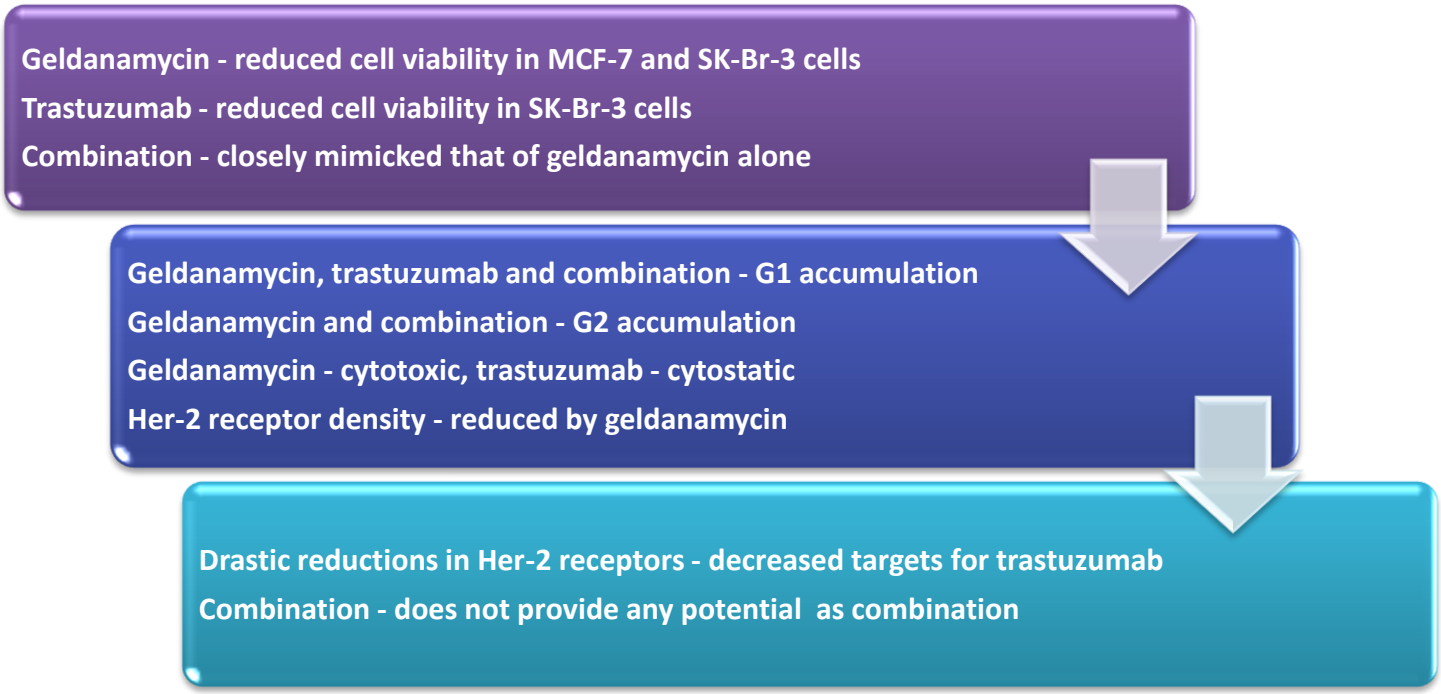

Chapter 9: Results and Discussion: Heregulin-β1

9.1 Cell Viability

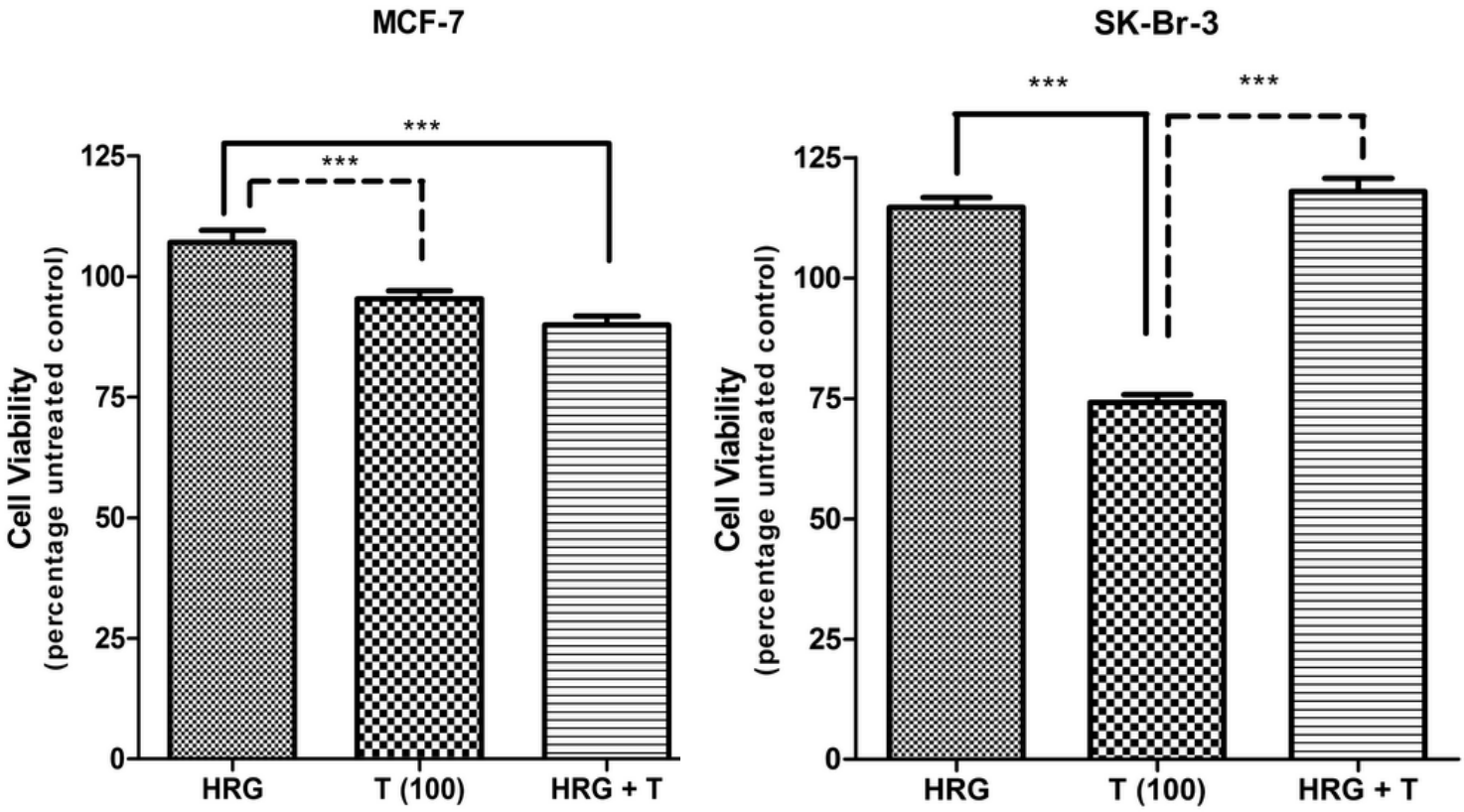

Figure 9.1: Cell viability in MCF-7 and SK-Br-3 cells expressed as a percentage of the untreated controls. Statistically significant differences were found between trastuzumab alone versus heregulin alone and the heregulin-trastuzumab combination in SK-Br-3 cells. Further statistically significant differences (P < 0.001) were found when comparing the average cell viability of heregulin alone between MCF-7 and SK-Br-3 cells. HRG: heregulin (28 nM), T (100): trastuzumab 100 µg/ml. (Statistical significance followed the same trend for combinations at 25 µg/ml, 50 µg/ml, 200 µg/ml in both cell lines. Exception no significance for HRG alone compared to HRG-trastuzumab combination at 25 µg/ml in MCF-7 cells.)

Table 9.1: Cell viability results for heregulin and the heregulin-trastuzumab combination

	MCF-7	SK-Br-3
	Mean ± SEM	**Mean ± SEM**
Heregulin-β1 (HRG) (28 nM)	107.01 ± 2.42	115.40 ± 2.08
HRG + Trastuzumab (25 µg/ml)	93.66 ± 2.53	112.90 ± 1.76
HRG + Trastuzumab (50 µg/ml)	93.76 ± 2.52	114.50 ± 1.98
HRG + Trastuzumab (100 µg/ml)	89.90 ± 1.95	118.10 ± 2.71
HRG + Trastuzumab (200 µg/ml)	95.32 ± 1.79	118.00 ± 2.14

9.2 Cell Cycle Analysis

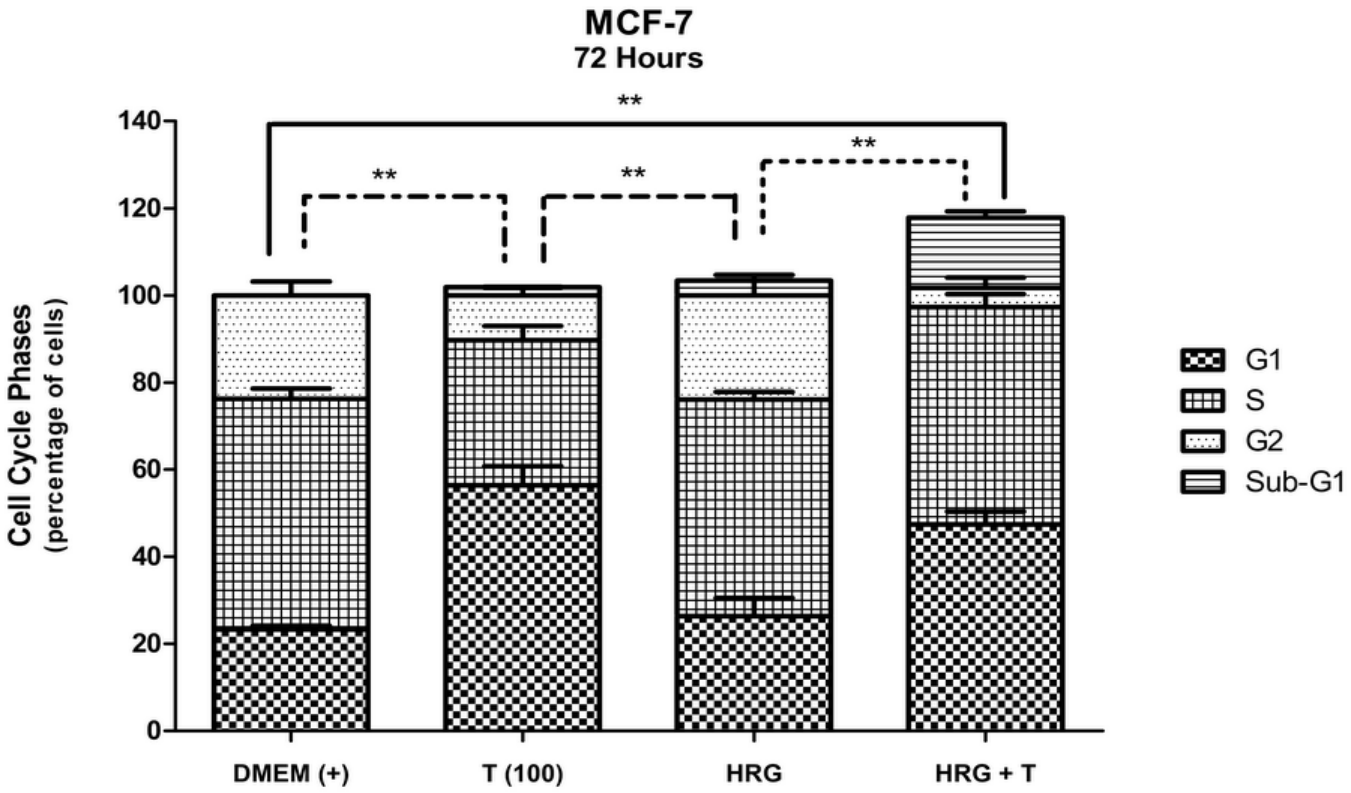

Figure 9.2: Cell cycle analysis in MCF-7 cells expressed as a percentage after deconvolution. Statistically significant differences in the G1 phase of the cell cycle were observed between various comparisons of untreated control (DMEM+), trastuzumab, heregulin and the heregulin-trastuzumab combination after 72 hours. HRG: heregulin (28 nM), T (100): trastuzumab 100 µg/ml.

Table 9.2: Cell cycle results for HRG, trastuzumab and the HRG-trastuzumab combination in MCF-7 cells

MCF-7	Mean ± SEM				Significance			
24 Hrs	**G1**	**S**	**G2**	**Sub G1**	**C**	**HRG**	**HRG + T**	**T**
Control (C)	23.25 ± 0.86	52.99 ± 2.33	23.76 ± 3.17		-	**		
HRG	12.92 ± 0.71	53.84 ± 3.24	33.24 ± 2.72	4.48 ± 0.24	**	-	***	**
HRG + T	28.35 ± 2.01	40.86 ± 2.46	30.79 ± 0.49	2.10 ± 0.73		***	-	
T	23.46 ± 1.21	53.03 ± 2.62	23.51 ± 1.63	1.87 ± 0.10		**		-
48 Hrs	**G1**	**S**	**G2**	**Sub G1**	**C**	**HRG**	**HRG + T**	**T**
Control (C)	23.25 ± 0.86	52.99 ± 2.33	23.76 ± 3.17		-		***	
HRG	24.91 ± 0.14	53.41 ± 1.83	21.68 ± 1.84	2.11 ± 0.75		-	**	*
HRG + T	37.01 ± 1.03	44.37 ± 4.42	17.22 ± 3.46	5.67 ± 0.80	***	**	-	
T	32.40 ± 2.34	50.86 ± 4.87	16.74 ± 3.22	1.86 ± 0.01		*		-
72 Hrs	**G1**	**S**	**G2**	**Sub G1**	**C**	**HRG**	**HRG + T**	**T**
Control (C)	23.25 ± 0.86	52.99 ± 2.33	23.76 ± 3.17		-		**	**
HRG	26.39 ± 4.11	49.71 ± 1.71	23.87 ± 4.73	3.39 ± 0.15		-	**	**
HRG + T	47.46 ± 2.92	49.82 ± 2.97	4.48 ± 2.37	16.03 ± 1.52	**	**	-	*
T	56.37 ± 4.48	33.34 ± 3.23	10.29 ± 1.72	1.89 ± 0.02	**	**	*	-

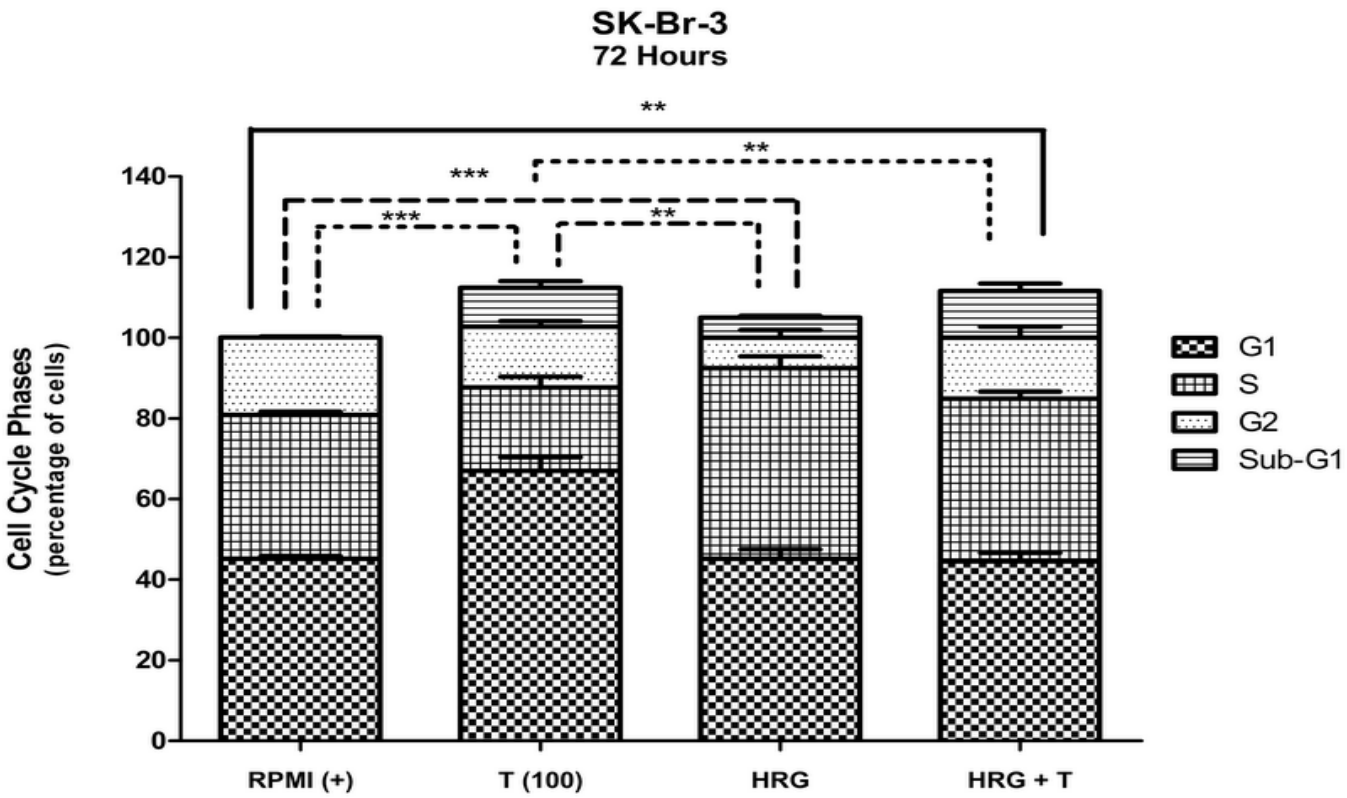

Figure 9.3: Cell cycle analysis in SK-Br-3 cells expressed as a percentage after deconvolution. Statistically significant differences in the G1 phase of the cell cycle were observed between various comparisons of untreated control (RPMI+), trastuzumab, heregulin and the heregulin-trastuzumab combination after 72 hours. HRG: heregulin (28 nM), T (100): trastuzumab 100 µg/ml.

Table 9.3: Cell cycle results for HRG, trastuzumab and the HRG-trastuzumab combination in SK-Br-3 cells

SK-Br-3	Mean ± SEM				Significance			
24 Hrs	**G1**	**S**	**G2**	**Sub G1**	**C**	**HRG**	**HRG + T**	**T**
Control (C)	45.19 ± 0.65	35.68 ± 0.81	19.16 ± 0.31		-	*	*	**
HRG	35.25 ± 2.18	49.73 ± 1.63	15.02 ± 3.66	9.03 ± 2.18	*	-		***
HRG + T	35.61 ± 2.26	50.11 ± 2.00	14.28 ± 1.68	10.54 ± 2.46	*		-	***
T	60.15 ± 1.81	23.72 ± 2.38	16.13 ± 2.07	7.68 ± 2.48	**	***	***	-
48 Hrs	**G1**	**S**	**G2**	**Sub G1**	**C**	**HRG**	**HRG + T**	**T**
Control (C)	45.19 ± 0.65	35.68 ± 0.81	19.16 ± 0.31		-			**
HRG	41.55 ± 2.80	39.49 ± 2.18	18.96 ± 1.14	7.73 ± 1.77		-		**
HRG + T	39.08 ± 0.89	40.78 ± 5.20	20.18 ± 4.85	7.528 ± 0.32			-	**
T	64.15 ± 1.41	20.84 ± 3.55	15.02 ± 4.56	11.48 ± 1.28	**	**	**	-
72 Hrs	**G1**	**S**	**G2**	**Sub G1**	**C**	**HRG**	**HRG + T**	**T**
Control (C)	45.19 ± 0.65	35.68 ± 0.81	19.16 ± 0.31		-	*		***
HRG	45.19 ± 2.29	47.23 ± 2.97	7.58 ± 1.96	14.98 ± 0.49	*	-		**
HRG + T	44.54 ± 2.08	40.31 ± 1.81	15.14 ± 2.76	11.61 ± 1.80			-	**
T	66.93 ± 3.41	20.78 ± 2.60	15.02 ± 1.38	11.69 ± 2.20	***	**	**	-

9.3 Relative Her-2 Receptor Density

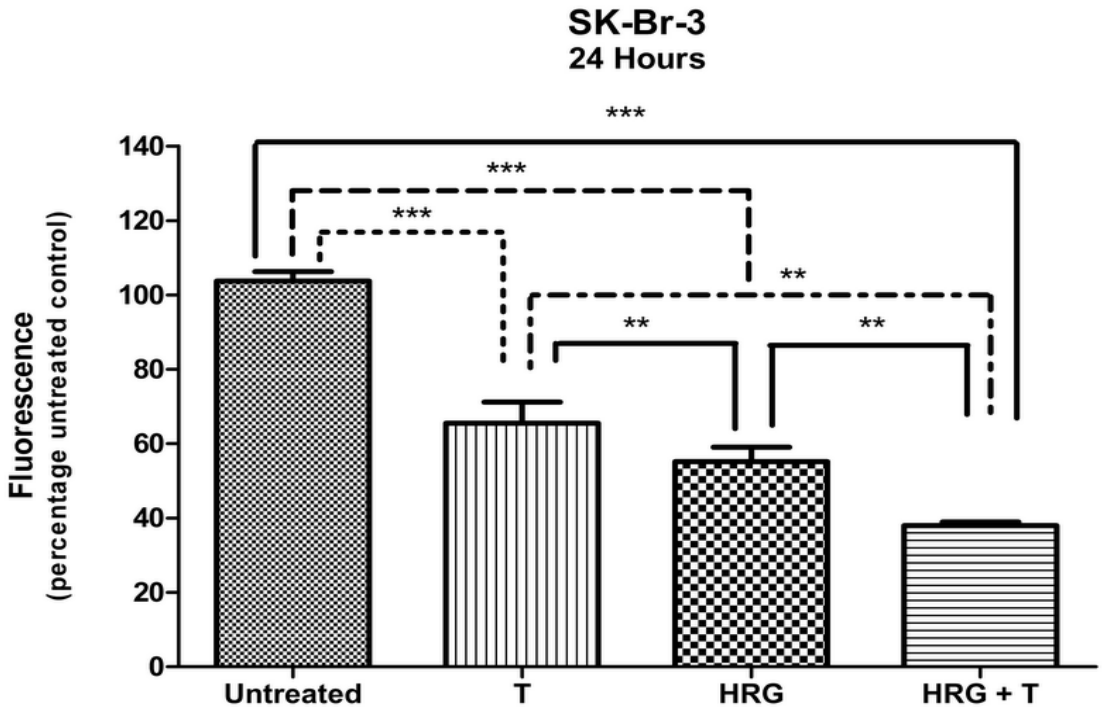

Figure 9.4: Relative Her-2 receptor density analysis at 24 hours in SK-Br-3 cells expressed as a percentage of the fluorescence of untreated controls (standardised to 100%). HRG: heregulin (28 nM), T (100): trastuzumab 100 µg/ml. A similar trend was observed at 48 hours.

Table 9.4: Fluorescent intensity (histogram x-mean) of SK-Br-3 cells exposed to HRG, trastuzumab and the HRG-trastuzumab combination

SK-Br-3	Mean ± SEM	Significance			
12 Hours		**U**	**HRG**	**HRG + T**	**T**
Untreated (U)	99.49 ± 2.52	-	***	***	***
HRG	68.94 ± 2.32	***	-	*	
HRG + T	56.38 ± 1.14	***	*	-	
T	64.77 ± 3.60	***			-
24 Hours		**U**	**HRG**	**HRG + T**	**T**
Untreated (U)	103.70 ± 2.61	-	***	***	***
HRG	55.18 ± 3.89	***	-	***	**
HRG + T	37.99 ± 0.96	***	***	-	**
T	65.47 ± 4.76	***	**	**	-
48 Hours		**U**	**HRG**	**HRG + T**	**T**
Untreated (U)	100.00 ± 1.95	-	***	***	***
HRG	40.59 ± 1.94	***	-	*	***
HRG + T	27.19 ± 2.10	***	*	-	***
T	61.83 ± 4.42	***	***	***	-

Heregulin (neuregulin) is a homologous growth factor involved in the regulation of biological processes. Heregulin-β (HRG-β) and its major isoform, heregulin-α (HRG-α) are splice variants of a single gene product which bind to Her-3 and Her-4 receptors. (Liu, Li, & Roth, 1999; Koutras & Evans, 2008) Heregulins have tissue-specific patterns of expression that can be mitogenic for tumour cells. Wen *et al*. (1994) concluded that the expansive biological role of heregulin is achieved by combinatorial designs of the mosaic structure. There are at least 10 distinct heregulin isoforms; heregulin-β has at least three isoforms with similar binding and activation characteristics. (Koutras & Evans, 2008) Heregulin-β1, which was used in our study, is more potent than α-isoforms and the β1-isoform has a higher binding affinity for Her-3 and Her-4 receptors. (Wen et al., 1994)

Early researchers suggested that Her-2 was the target for heregulin. However, heregulin-induced phosphorylation of Her-2 receptors was not always observed in cells which express Her-2 receptors. This lead to the notion that a receptor closely related to Her-2 was required for conferring responsiveness to heregulin. Sliwkowskiso *et al.* (1994) studied whether interactions between heregulin and Her-2 could be mediated by Her-3 receptors. COS-7 fibroblast-like cells transfected with Her-2 receptors demonstrated no increase in heregulin binding. However, transfection with equal amounts of Her-2 and Her-3 resulted in an increased heregulin binding affinity.

Based on this data, a novel system of interaction was proposed whereby Her-3 receptors expressed in conjunction with Her-2 receptors provided trans-phosphorylation and recruitment of signalling molecules thus enabling tyrosine kinase activity. The potential of multiple heregulin-stimulated heterodimeric complexes could be responsible for the pleiotropic biological activity associated with heregulin. (Sliwkowskiso et al., 1994) This research was supported by others who concluded that signalling via Her-3 receptors is strongly dependent on lateral signalling due to the absence of an active kinase domain in Her-3 receptors; therefore signalling competent heterodimers are required. (Koutras & Evans, 2008)

Expression of Her-3 and Her-4 receptors is limited to certain types of epithelial cells, designated by Tzahar *et al*. (1994) as low and high affinity receptors respectively for all heregulin isoforms. Both receptors are capable of heterodimerization with homologous Her-2 receptors and result in receptor phosphorylation. Following phosphorylation, Her-3 and Her-4 receptors create binding sites for a variety of SH2 domain-containing molecules (protein domain in Src oncoprotein which enables protein recognition of tyrosine phosphorylated proteins) which includes PI3-kinase and growth factor receptor-bound protein 2 (Grb2).

Progressions of cancers in response to heregulin have been studied by many researchers who have robustly demonstrated the tumour promoting capability of heregulin: *in vivo* tumours are capable of changing from an oestrogen-dependent, anti-oestrogen sensitive phenotype to a metastatic oestrogen-independent, anti-oestrogen resistant phenotype. MCF-7/HRG transfected cells appear to grow independently of oestrogen, unlike parental MCF-7 cells, and also possess higher constitutive levels of mitogen-activated protein kinase (MAPK) phosphorylation which is a downstream effector of Her-receptors. Furthermore, heregulin may propagate additional increases in MAPK phosphorylation involving ras-signalling and increase activated matrix metalloproteinase-9 (MMP-9) a peptidase involved in metastases. (Atlas et al., 2003)

Breast carcinoma cells, 21MT-2 and 21MT-1, expressing progressively elevated levels of Her-2 receptors were used to study the mitogenic properties and activation of PI3K by heregulin. PI3K is composed of heterodimers between catalytic p110 subunits and one of five variants of regulatory p85 subunits. Heregulin was a potent inducer of p85α protein recruitment which was directly related to Her-2 expression, and constitutive association was apparent in over-expressing cells. Proliferation was prevented by an inhibitor of PI3K activity, strongly supporting the role of PI3K pathways in heregulin-growth factor induced mitogenesis. (Ram & Stephen, 1996)

Hellyer *et al*. (2001) also examined heregulin-dependent activation of the PI3-kinase target, Akt, in intact cells using wild-type Her-3 receptors and mutant receptors (Her-3-6F) devoid of the ability to associate with the p85 regulatory subunit of PI3-kinase. Relative phosphorylation levels of Her-3 receptors in both Her-3-WT and Her-3-6F indicated heregulin-dependent enhancement. However, the association of PI3-kinase with Her-3 receptor was strongly-dependent on the presence of p85 regulatory binding motifs. The multiple, complex mechanisms and interactions by which heregulin is involved in tumour progression confound the ability of targeted cancer therapies to elicit clinically beneficial responses in the presence of this endogenous ligand.

As expected, in these experiments, MCF-7 cells exposed to heregulin (28 nM) resulted in a modest proliferation to 107.01% (±2.42). Concurrent trastuzumab (100 µg/ml) exposure abrogated this proliferation, deceasing cell viability to 89.90% (±1.95). The cell viability trend was similar for trastuzumab concentrations from 50 µg/ml to 200 µg/ml in these cells. Of note is that when trastuzumab was used as a single agent it showed no effect in this cell line (Figure 9.1; Table 9.1).

While trastuzumab is only licensed for use in Her-2 positive breast cancer, the heregulin-trastuzumab combination resulted in a significant decrease in cell viability in ER positive MCF-7 cells. The reduction in MCF-7 cell viability at higher trastuzumab concentrations suggested that trastuzumab negated heregulin-induced mitogenesis or that heregulin sensitised these cells to the effects of trastuzumab.

These results are supported by Liu *et al.* (1999) who confirmed that heregulin was a rapid and potent activator of Akt activity in MCF-7 cells and that activation was dependent on stimulation of PI3-kinase pathway. Her-2 monoclonal antibodies were capable of inhibiting heregulin-induced activation of PI3-kinase and downstream targets such as Akt in a dose-dependent fashion. These results implicated heregulin-induced Her-2 containing heterodimers in PI3-kinase/Akt signalling. The inhibition of the PI3-kinase/Akt pathway seen in MCF-7 cells could be the mechanism by which trastuzumab abrogated the proliferation induced by heregulin. However, in this study, the mechanism by which it did so was not elucidated.

SK-Br-3 cells exposed to heregulin (28 nM) resulted in increased proliferation to 115.40% (±2.08). However, concurrent trastuzumab (100 µg/ml) resulted in a strikingly similar proliferation of 118.10% (±2.14) (Figure 9.1; Table 9.1). As opposed to having an anti-proliferative effect in SK-Br-3 cells, trastuzumab had a negligible effect when used in combination with heregulin. These results pose an interesting paradigm of response to heregulin, with decreased cell viability in MCF-7 cells with concurrent trastuzumab, and unaltered cell viability in SK-Br-3 cells.

Liu *et al.* (1999) found that cells over-expressing Her-2 receptors (BT-474) possessed increased basal Akt activity compared to MCF-7 cells. This increase in basal Akt activity could further be potentiated by heregulin; inhibition by Her-2 monoclonal antibodies may not be as effective when basal Akt activity is heightened and Her-2 receptors over-expressed. This heregulin-induced activation of PI3-kinase/Akt pathway and increased basal Akt activity in Her-2 over-expressing cells may possibly contribute to the ability of Her-2 transformed cells to become resistant to targeted therapy. This may provide insight into the mechanism by which heregulin-exposed SK-Br-3 cells, even in the presence of trastuzumab, proliferate more than MCF-7 cells.

Xu *et al.* (1997) determined the effects of heregulin in SK-Br-3 cells and observed increases in invasive and metastatic potential with increases in adhesion molecules (CD44 and CD54) and proteinase MMP-9. Prognosis is not solely determined by proliferation capacity but is also influenced by metastases, resistance to chemotherapy and the co-expression of related receptors. However, the ability of these heregulin-inducible factors to be reversed is still a matter of debate.

For instance, Lewis *et al*. (1996) assessed cellular responses to heregulin (HRG-β1) and cytostatic monoclonal antibodies (4D5, 2C4 and 7F3) in breast and ovarian tumour cell lines. It was concluded that Her-2 plays a crucial role in heregulin mediated responses over a diverse receptor range and resulted in cell type specific proliferation. In these experiments, heregulin binding assays quantified Her-3 and Her-4 receptors. MCF-7 cells expressing 12, 700 ± 1300 Her-3 and -4 receptors per cell and SK-Br-3 cells expressing 27, 300 ± 1500 Her-3 and -4 receptors per cell were arbitrarily characterized as intermediate and high levels of receptors respectively. The well characterized anti-Her-2 antibody, 4D5, was found to inhibit heregulin-stimulated tyrosine phosphorylation and disrupt Her-2 heterodimers. In our study we did not assess phosphorylation, however, disrupted signalling would likely be translated into altered cell viability. This phenomenon was not observed in our study where cell viability remained uninfluenced by the presence of trastuzumab in SK-Br-3 cells.

SK-Br-3 cells express high levels of Her-2 and Her-3 mRNA. (Sahin et al., 2009) While mRNA levels do not always correlate with surface receptor protein it provides a reasonable comparison for the effect of Her-family ligands. It has been suggested that Her-2:Her-3 heterodimers are the most potent mitogenic dimer pair and that co-operated signalling may result in synergistic action in cellular transformation. (Koutras & Evans, 2008) This potent dimer pair could explain why trastuzumab had a negligible anti-proliferative effect when combined with heregulin in SK-Br-3 cells.

While proliferation was noted in both cell lines in response to heregulin, no caspase-3 and -7 activation was observed when cell viability was reduced in MCF-7 cells (data not shown). This suggests that executioner caspases are not involved in the reduction in cell viability and that anti-proliferative effects may be the preferred mechanism. Furthermore, the annexin-V assay showed no difference in fluorescent staining between untreated controls and experimental samples supporting the concept that the reductions in cell viability are cytostatic as opposed to cytotoxic.

The heterogeneity of breast cancer is reflected by heregulin having both growth-stimulatory and growth-inhibitory effects in breast tumours over-expressing Her-2 receptors. Additionally, heregulin

effects are dependent on cell-specific expression patterns of the Her-family. (Daly et al., 1997) Heregulin isoforms have unpredictable actions in different tissue types with several lines of evidence to support both mitogenesis or differentiation and apoptosis. Various heregulin isoforms, tissue-specific interactions or properties and the degree of Her-3 and Her-4 expression provide a basis for the ability of novel isoforms such as HRG-β3b and HRG-β2c to induce apoptosis (Weinstein, Grimm, & Leder, 1998) which is not observed when using the HRG-β1 isoform in MCF-7 and SK-Br-3 cells.

In MCF-7 cells it was shown that heregulin exposure resulted in a cell cycle distribution that mimicked that of the untreated control. However, after 24 hours of heregulin exposure, there was a statistically significant increase in the G2 phase [$G2_{24}$: 33.24% (±2.72)] compared to the untreated control [G2: 23.76% (±3.17)] suggesting that heregulin accelerated cell cycle kinetics, accompanying the increase in proliferation. Statistically significant G1 accumulation was evident after 48 hours [$G1_{48}$: 37.01% (±0.33)] through to 72 hours [$G1_{72}$: 47.46% (±2.92)] after exposure to the heregulin-trastuzumab combination compared to untreated controls [G1: 23.25% (±0.86)]. This supported the decrease in cell viability results and illustrated that heregulin was less effective in promoting cell cycling in this context (Figure 9.2; Table 9.2).

In SK-Br-3 cells, heregulin promoted a statistically significant increase in the percentage of cells in the S phase at 24 hours [S_{24}: 49.73% (±1.63)] when compared to untreated controls [S: 35.68% (±0.81)]. However, after 24 hours the distribution of cells exposed to heregulin essentially mimicked that of the untreated control. Considering the ability of heregulin to promote cell proliferation, the alterations in the cell cycle suggested that heregulin accelerated S phase entry. When exposed to the heregulin-trastuzumab combination, a similar S phase increase [S_{24}: 50.11% (±2.00)] was observed (Figure 9.3; Table 9.3). Accelerated S phase entry was apparent in the heregulin-trastuzumab exposed cells as opposed to G1 accumulation observed for trastuzumab on its own which suggests that in the presence of heregulin, the anti-proliferative effects of trastuzumab are rendered negligible.

These results are supported by Diermeier *et al*. (2005) who assessed heregulin and trastuzumab in SK-Br-3 cells and illustrated that accelerated S-phase entry occurred when treated with heregulin as well as the heregulin-trastuzumab combination. However, trastuzumab alone resulted in prolongation of the G1 phase. Thus, as a potent stimulator, heregulin was capable of compensating for the inhibition elicited by trastuzumab.

Observing the effect of heregulin on cell cycle progression, Altiok *et al.* (1999) illustrated that a gradual progression from G1 phase was evident between 6 hours and 24 hours and that this S phase entry occurred only after BRCA1 phosphorylation was observed. Furthermore, Brockhoff *et al*. (2001) illustrated that heregulin was a strong stimulator of cell proliferation by reducing the G1-phase duration in SK-Br-3 cells and that a constitutive Her-2:Her-3 interaction was present even in the absence of ligands.

Daly *et al*. (1999) who determined the effects of heregulin on biological responses in SK-Br-3 cells suggested that heregulin induced phosphorylation of Her-2:Her-3 heterodimers and coupled PI3K promoted cell cycle progression with an increase in the S phase fraction. These results support those observed in this study where accelerated S-phase entry was observed at 24 hours and which became less prominent at the later time points assessed.

Her-2 receptor density analysis in Her-2 normal MCF-7 cells illustrated minimal differences in the overlay plot of unstained and untreated samples. Heregulin, trastuzumab and combination treated samples were indistinguishable from untreated samples. Contrastingly, SK-Br-3 cells showed a decrease in Her-2 receptors when comparing untreated controls [$untreated_{12}$: 99.49% (±2.52)] to cells treated with heregulin [HRG_{12}: 68.94% (±2.32)], trastuzumab [T_{12}: 64.77% (±3.60)] as well as to the combination [$HRG+T_{12}$: 56.38% (±1.14)] at 12 hours. Furthermore, the difference between heregulin and the heregulin-trastuzumab combination was already statistically significant at 12 hours (Figure 9.4; Table 9.4).

At 24 hours a stepwise and significant decrease was observed between all comparisons of untreated controls [$untreated_{24}$: 103.7% (±2.61)], trastuzumab [T_{24}: 65.47% (±4.76)], heregulin [HRG_{24}: 55.18% (±3.89)] and the combination [$HRG+T_{24}$: 45.01% (±1.06)]. The reduction was least prominent in trastuzumab followed by HRG alone and then the heregulin-trastuzumab combination. Relative Her-2 receptor density was further decreased at 48 hours [HRG_{48}: 40.59% (±1.94)], with the significance between heregulin and the combination remaining evident throughout. These results suggest that heregulin alone is capable of inducing significant Her-2 receptor internalisation, likely in the format of heterodimer pairs with Her-3 and Her-4 receptors. Moreover, the decrease in Her-2 density was even greater when cells were exposed to both heregulin and trastuzumab.

Decreased surface Her-2 receptors in SK-Br-3 cells could result from possible increased internalisation or degradation which could be either due to inhibition by trastuzumab or to heregulin binding to Her-2 containing heterodimers or a combination of both. The presence of trastuzumab did not negatively influence heregulin-induced increase in cell viability which suggests that heregulin promotes proliferation independently of the anti-proliferative effects of trastuzumab. Daly *et al*. (1997) also observed a decreased in Her-2 in response to exposure to heregulin after 48 hours. Direct correlations between decreased Her-2 receptors and cell viability remain confounding. The exact extent of heregulin-trastuzumab interactions would require more mechanistic studies.

A certain threshold of surface Her-2 receptors is required to ensure clinical benefit for trastuzumab. In this study it was found that endogenous ligands reduce surface Her-2 receptors and alter parameters assessed for trastuzumab. While it is unclear whether these alterations in receptor expression are maintained for a period long enough to be clinically relevant, the reduction could result in insufficient cancer targeting by the antibody and diminish the efficacy of trastuzumab.

Complicating research of heregulin isoforms is the possibility of differential responses from each isoform and also the ability of FCS, seeding density and confluence to provide differences in endpoint experiments. (Daly et al., 1997) Cell viability was not reduced in the presence of the heregulin-trastuzumab combination in SK-Br-3 cells which may require alternate Her-receptor co-expression ratios to promote significant anti-proliferative effects. The use of heregulin and trastuzumab in combination did not provide any potential treatment prospects. However, the ability of heregulin to promote proliferation in the presence of trastuzumab may provide insight into resistance to trastuzumab as a targeted therapy.

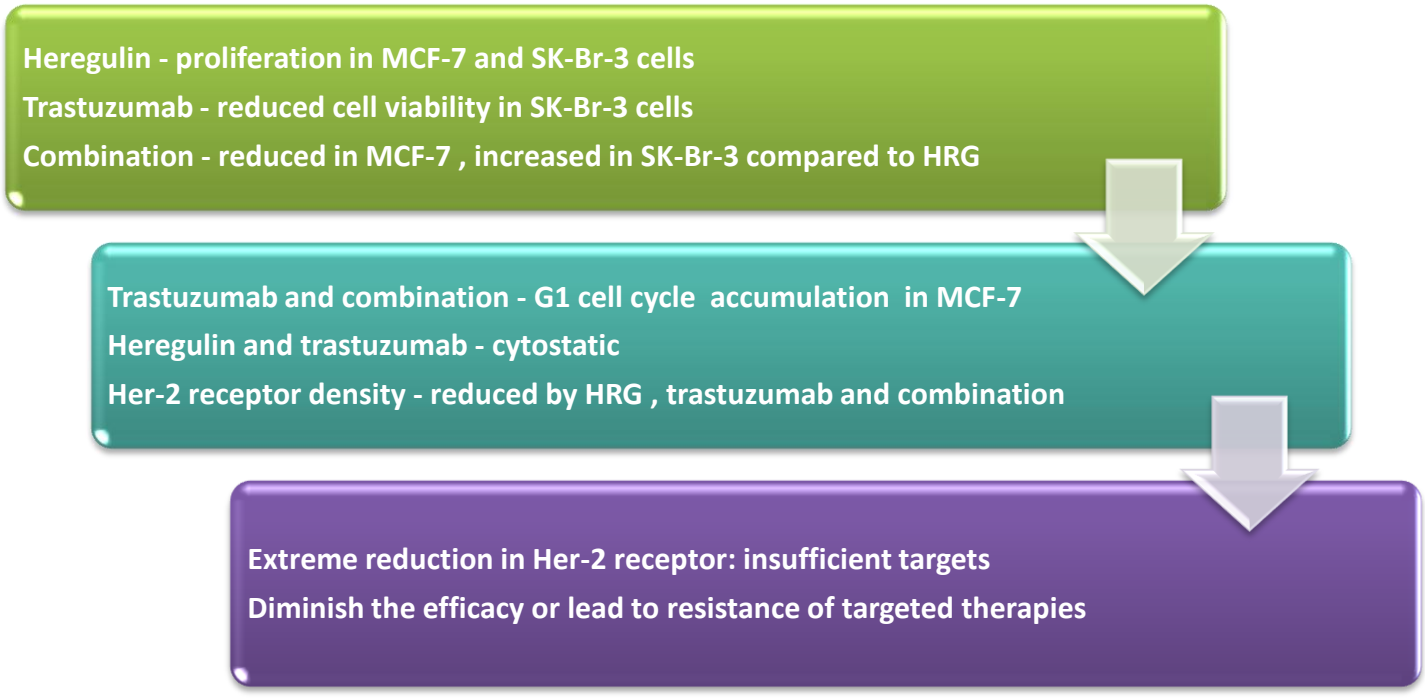

Chapter 10: Results and Discussion: β-Oestradiol

10.1 Cell Viability

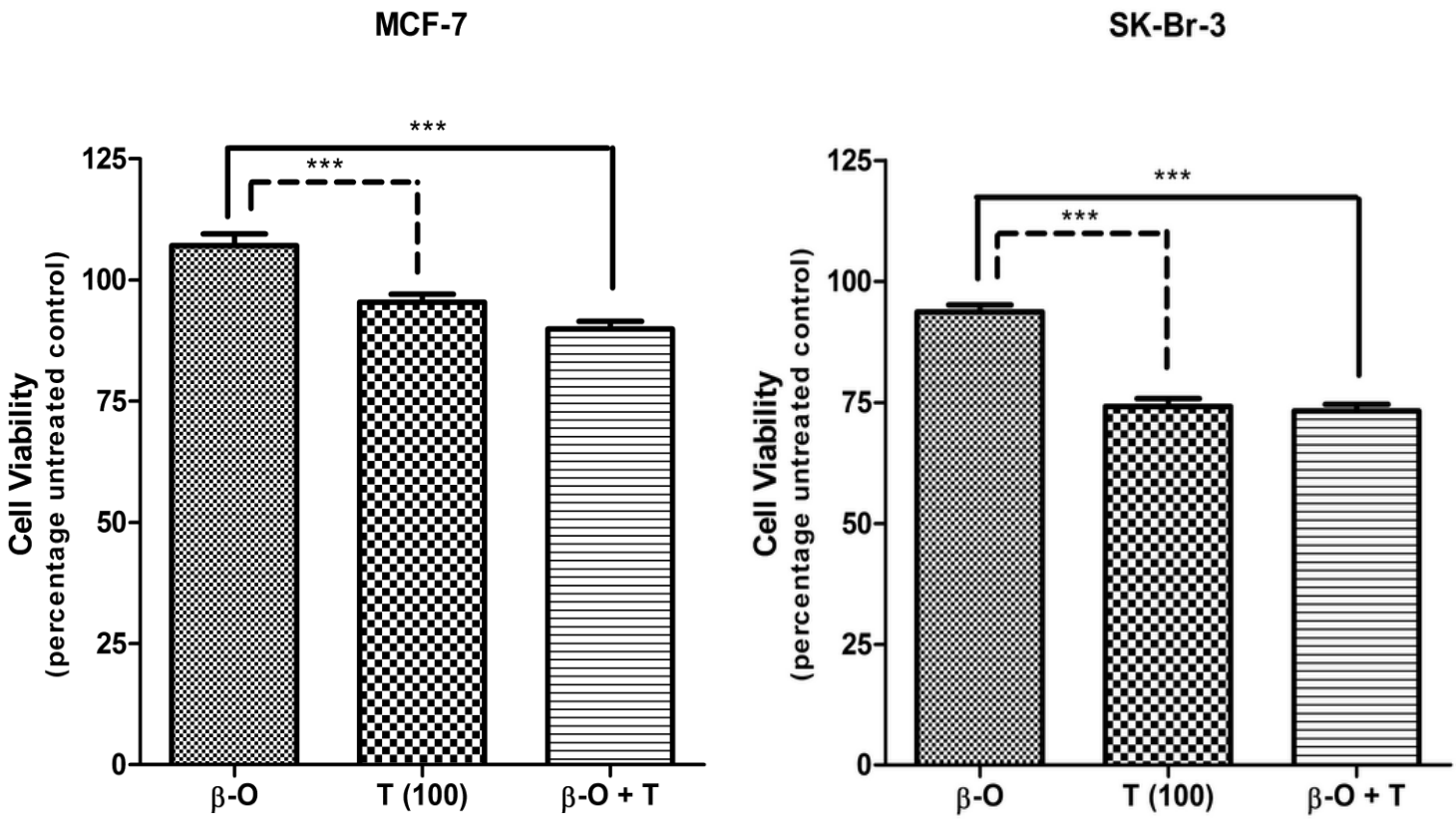

Figure 10.1: Cell viability in MCF-7 and SK-Br-3 cells expressed as a percentage of the untreated controls. Statistically significant differences were found between β-Oestradiol alone versus trastuzumab alone and the β-Oestradiol-trastuzumab combination. Further statistically significant differences (P < 0.001) were found when comparing the average cell viability of β-Oestradiol alone between MCF-7 and SK-Br-3 cells. β-O: β-Oestradiol (0.36 µM), T (100): trastuzumab 100 µg/ml. (Statistical significance followed the same trend for trastuzumab combinations at 25 µg/ml, 50 µg/ml, 200 µg/ml in both cell line. (Exception no significance comparing with β-Oestradiol alone compared to β-Oestradiol-trastuzumab combination at 25 µg/ml in MCF-7 cells.)

Table 10.1: Cell viability results for β-oestradiol and the β-oestradiol-trastuzumab combination

	MCF-7	SK-Br-3
	Mean ± SEM	Mean ± SEM
β-Oestradiol (β-O) (0.36 µM)	107.10 ± 2.38	93.70 ± 1.49
β-O + Trastuzumab (25 µg/ml)	101.00 ± 1.94	77.52 ± 1.83
β-O + Trastuzumab (50 µg/ml)	98.57 ± 1.87	75.77 ± 2.18
β-O + Trastuzumab (100 µg/ml)	89.88 ± 1.63	73.24 ± 1.28
β-O + Trastuzumab (200 µg/ml)	94.59 ± 2.60	75.35 ± 1.63

10.2 Cell Cycle Analysis

Table 10.2: Cell cycle results for β-oestradiol, trastuzumab and the combination in MCF-7 cells

MCF-7	Mean ± SEM				Significance			
72 Hours	G1	S	G2	Sub G1	C	β-O	β-O + T	T
Control (C)	23.25 ± 0.86	52.99 ± 2.33	23.76 ± 3.17		-	*	***	**
β-O	39.36 ± 1.88	45.76 ± 2.42	14.88 ± 2.13	4.96 ± 1.31	*	-	**	
β-O + T	60.45 ± 3.30	25.27 ± 1.01	14.28 ± 4.30	13.24 ± 1.25	***	**	-	
T	56.37 ± 4.48	33.34 ± 3.23	10.29 ± 1.72	1.89 ± 0.02	**			-

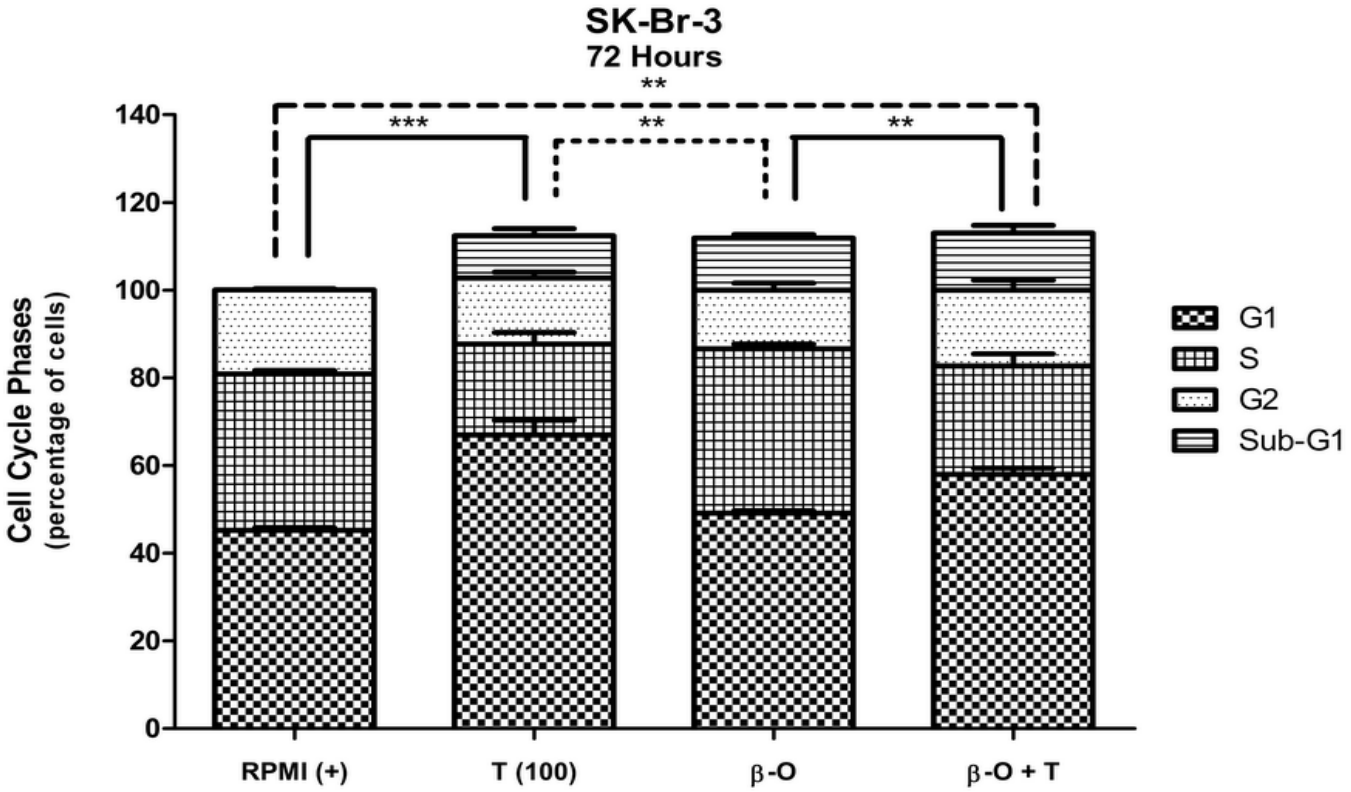

Figure 10.2: Cell cycle analysis in SK-Br-3 cells expressed as a percentage after deconvolution. Statistically significant differences in the G1 phase of the cell cycle were observed between untreated control (RPMI+) versus trastuzumab and the β-Oestradiol-trastuzumab combination after 72 hours. β-O: β-Oestradiol (0.36 µM), T (100): trastuzumab 100 µg/ml.

Table 10.3: Cell cycle results for β-oestradiol, trastuzumab and the combination in SK-Br-3 cells

SK-Br-3	Mean ± SEM				Significance			
72 Hours	G1	S	G2	Sub G1	C	β-O	β-O + T	T
Control (C)	45.19 ± 0.65	35.68 ± 0.81	19.16 ± 0.31		-		**	***
β-O	49.16 ± 0.55	37.45 ± 1.07	13.39 ± 1.62	11.89 ± 0.78		-	**	**
β-O + T	57.98 ± 1.40	24.75 ± 2.72	17.28 ± 2.28	12.98 ± 1.80	**	**	-	
T	66.93 ± 3.41	20.78 ± 2.60	15.02 ± 1.38	11.69 ± 2.20	***	**		-

10.3 Relative Her-2 Receptor Density

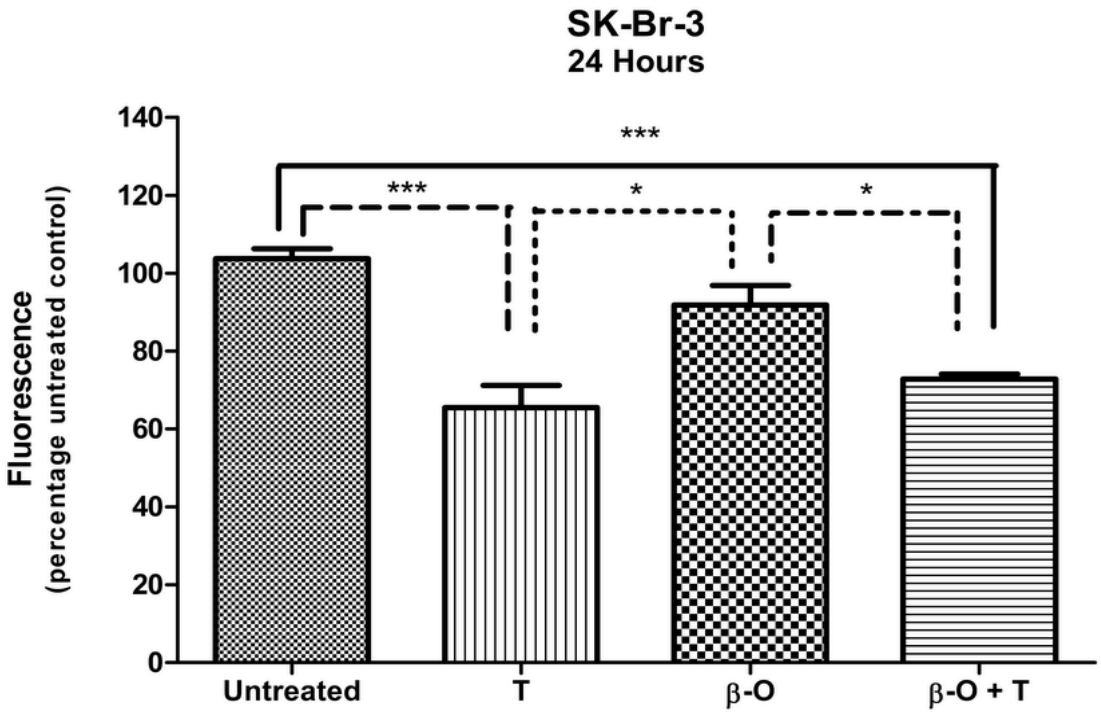

Figure 10.3: Relative Her-2 receptor density analysis at 24 hours in SK-Br-3 cell expressed as a percentage of the fluorescence of untreated controls (standardised to 100%). Statistical significance followed the same trend at 12, 24 and 48 hours. ß-O: ß-Oestradiol (0.36 µM), T (100): trastuzumab 100 µg/ml.

Table 10.4: Fluorescent intensity (histogram x-mean) of SK-Br-3 cells exposed to β-oestradiol, trastuzumab and the β-oestradiol-trastuzumab combination

SK-Br-3	Mean ± SEM	Significance			
12 Hours		**U**	**β-O**	**β-O + T**	**T**
Untreated (U)	99.49 ± 2.52	-		***	***
β-O	101.10 ± 6.76		-	***	***
β-O + T	67.11 ± 3.69	***	***	-	
T	64.77 ± 3.60	***	***		-
24 Hours		**U**	**β-O**	**β-O + T**	**T**
Untreated (U)	103.70 ± 2.61	-		**	***
β-O	89.32 ± 4.54		-	*	*
β-O + T	72.85 ± 1.22	**	*	-	
T	65.47 ± 4.76	***	*		-
48 Hours		**U**	**β-O**	**β-O + T**	**T**
Untreated (U)	100.00 ± 1.95	-		***	***
β-O	92.29 ± 5.47		-	**	***
β-O + T	66.63 ± 5.09	***	**	-	
T	61.83 ± 4.42	***	***		-

Oestrogen receptor (ER) positive human breast cancer tumours (comprising luminal A and B) are dependent on oestrogen for proliferation responses. (Perou et al., 2000) ERs are found in 60-70% of breast tumour tissue and mediate the biological effects of oestrogens via structurally and functionally distinct binding to the nuclear super-family of oestrogen receptors (ERα and ERβ) which possess distinct expression patterns. (Norderu et al. 1994; Adachi et al. 1995; Picard et al. 1997)

Oestrogen receptor status has been identified as a prognostic indicator for less aggressive breast cancer phenotypes. However, progression to a hormone insensitive phenotype following initial responses to endocrine treatment has been documented and crosstalk between alternate growth factor pathways has been implicated in this progression. (Norderu et al. 1994; Adachi et al. 1995; Picard et al. 1997) Molecular mechanisms of oestrogen signalling, broadly consists of four pathways which include: 1) classical ligand-dependent; 2) ligand-independent [polypeptide growth factors activate ER and increase the expression of ER target genes]; 3) DNA binding-independent genomic actions and 4) cell-surface (non-genomic) signalling linked to intracellular signal transduction proteins. (Hall, Couse, & Korach, 2001)

Despite the multiple mechanisms of oestrogen signalling, effects of oestrogen are primarily mediated via binding to ERα receptors which exist as monomers bound to multi-protein inhibitory heat shock proteins. Oestradiol is capable of passive diffusion through the cell membrane and upon binding, promotes heat shock protein dissociation, serine-or-threonine residue phosphorylation and receptor activation. Once activated, ER homo-dimerize and form complexes with a multiplicity of co-regulatory (co-activators) molecules. Complexes then bind with oestrogen response elements (ERE) in promoter regions of target genes resulting in nuclear-initiated steroid signalling or genomic actions. (Osborne et al. 2001; Stoica et al., 2003; Pancholi et al., 2008)

The availability and relative accessibility of co-regulatory molecules influence the type of transcriptional activity initiated. Furthermore, the diversity of factors involved in oestrogen regulation provide numerous interactions in governing transcriptional activity. (Osborne et al. 2001) Interplay between proliferation mechanisms support the potential to generate resistant phenotypes, and characterization of these mechanisms is critical in the design of therapeutic strategies. (Pancholi et al., 2008)

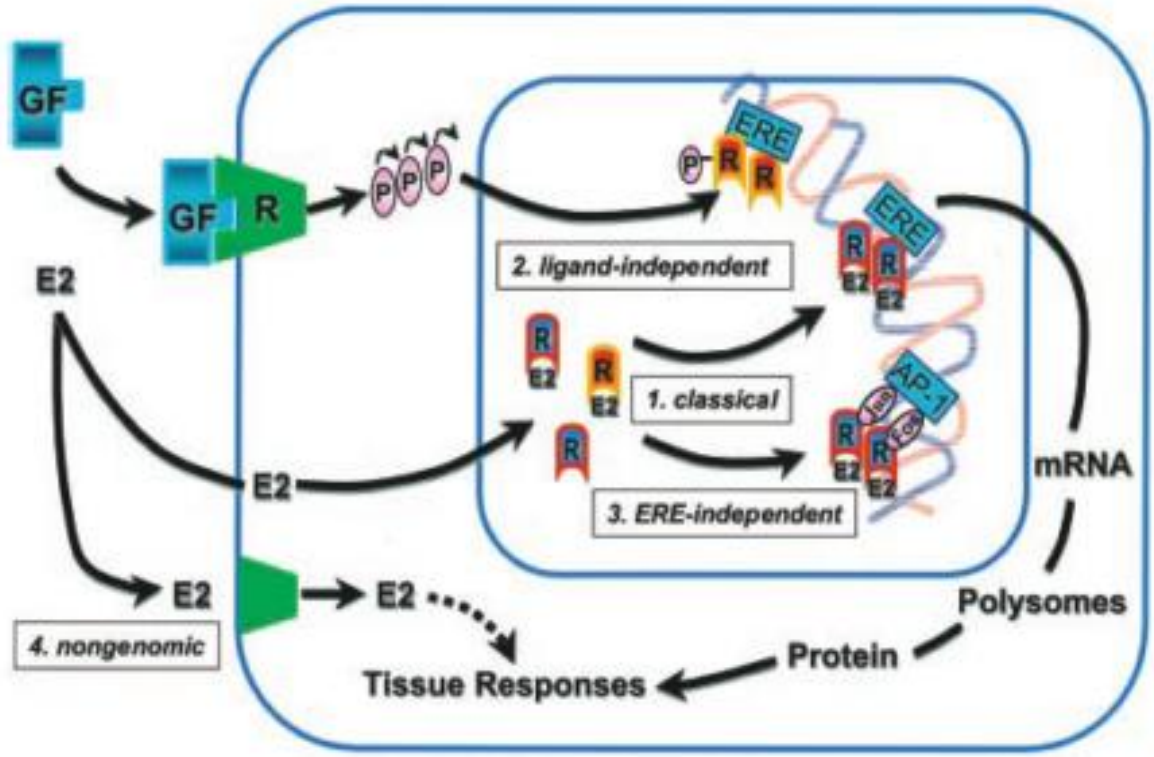

Figure 10.4: The biological effects of oestradiol are mediated through at least four ER pathways. 1) Classical ligand-dependent, E2-ER complexes bind to ERE's in target promoters leading to an up- or down- regulation of gene transcription and subsequent tissue responses. 2) Ligand- independent. Growth factors (GF) or cyclic adenosine monophosphate (not shown) activate intracellular kinase pathways, leading to phosphorylation (P) and activation of ER at ERE-containing promoters in a ligand-independent manner. 3) ERE-independent. E_2-ER complexes alter transcription of genes containing alternative response elements such as AP-1 through association with other DNA-bound transcription factors (Fos/Jun), which tether the activated ER to DNA, resulting in an up-regulation of gene expression. 4) Cell-surface (non-genomic) signalling, E2 activates a putative membrane- associated binding site, possibly a form of ER linked to intracellular signal transduction pathways that generate rapid tissue responses. (Hall et al., 2001)

Inverse relationships between ER and Her-receptors have been noted in breast cancer cell lines and primary tumour biopsies. (Davidson et al., 1987; Hall et al., 1990; Koenders et al., 1991) Alternate regulatory mechanisms for expression and signalling pathways are probably present in breast tumours. Likely candidates for alternate regulation include oestrogens and EGF since these ligand receptors are inversely correlated in breast cancer: ER positive (ER^+) tumours have superior differentiation, while Her-2 over-expressing tumours are more invasive. (Harris & Nicholon, 1988)

DeFazio *et al*. (1997) assessed total RNA from cancer cell lines and normal breast epithelium and demonstrated a close functional inverse relationship between ER and Her-1:ER inhibition of Her-1 receptors was noted. Several possible mechanisms could account for the ability of ER to suppress Her-1 expression which includes interaction of ER with elements of the Her-1 promoter. Alternatively, ER may regulate Her-1 transcription via controlling mRNA stability or post-transcriptional regulation.

Furthermore, van Agthoven *et al.* (1992) determined that transfection of oestrogen-dependent breast cancers with Her-1 cDNA resulted in progression into a hormone independent phenotype which used EGF-mediated growth to circumvent effects of anti-oestrogens. Dual immunohistochemical analysis found ER and Her-1 to be mutually exclusive *in vivo* which is further suggestive of inverse regulation.

Stoica *et al.* (2000) determined that EGF decreased oestrogen receptors in oestrogen dependent MCF-7 cells. This was accompanied by a sustained decrease in the mRNA concentration and ER gene transcription, although the affinity of oestradiol for ER was not altered. Thus, significant, complex, cross-talk between ER and Her-1 signalling pathways have been demonstrated; research in this area strongly supports the possibility of interactions between polypeptide growth factor signalling and steroid receptor pathways which introduces an additional dimension to the modelled autocrine loop. (Ignar-Trowbridge et al., 1992)

Development of resistance to anti-oestrogen therapy is a prominent clinical issue; there is increasing evidence that activation of growth signalling cascades can promote proliferation and survival signalling irrespective of treatment. Evidence of changes in the Her-family of receptors has been reported in non-clinical studies of anti-oestrogen resistance. In fact, treatment with Her-family ligands is capable of rescuing cells from the effects of fulvestrant (oestrogen receptor antagonist), which confirms the ability of anti-oestrogen sensitive and resistant MCF-7 cells to switch between ER and Her-signalling. (Sonne-Hansen et al., 2010) The nature of crosstalk between ER and growth factor mediated pathways is still vastly unexplored. However, there is evidence for strong bi-directional connections in altering molecular subtypes which enhance growth and survival of breast cancer. (Massarweh & Schiff, 2006) Further elucidation of molecular crosstalk between oestrogen and other growth factor signalling pathways which become integrated to alter carcinogenic phenotypes, is integral in determining therapeutic strategies that will be effective while conferring minimal resistance. (Osborne et al. 2001)

β-oestradiol (0.36 µM), promoted proliferation of MCF-7 cells resulting in a cell viability of 107.10% (±2.38). Concurrent trastuzumab (100 µg/ml) abrogated this proliferative effect and decreased cell viability to 89.88% (±1.63). This trend was observed for all concentrations of trastuzumab in MCF-7 cells, while at 25 µg/ml no statistical significance was observed between any pair assessed. Trastuzumab appeared to negate the proliferation induced by oestrogen. However, the reduction was not greater than when trastuzumab was used alone (Figure 10.1; Table 10.1).

Exposure to β-oestradiol (0.36 µM), resulted in a slight decrease in SK-Br-3 cell viability to 93.70% (±1.49). Concurrent trastuzumab exposure resulted in a cell viability of 73.24% (±1.28) which closely mimicked viability of cells exposed to trastuzumab alone (Figure 10.1; Table 10.1). Considering that Her-2 over-expressing tumours cells are generally ER negative, this could account for the inconsequential effects of β-oestradiol in SK-Br-3 cells.

The mitogenic properties of β-oestradiol were evident in MCF-7 cells. However the β-oestradiol-trastuzumab combination appeared to mimic trastuzumab alone, suggesting that the anti-proliferative effects of trastuzumab hindered the ability of β-oestradiol to induce proliferation in these ER-positive cells. The same result for the combination was found in the SK-Br-3 cells, which implies that β-oestradiol would not interfere with trastuzumab in the treatment of Her-2 positive breast cancer.

Non-genomic interactions of ER at the plasma membrane result in activation of MAP-kinase activity and promote proliferation. (Migliaccio et al.1996) Pancholi *et al*. (2008) illustrated that Her-2/ER membrane-associated complexes resulted in non-genomic activation of Akt and that proliferation could be independently driven via Her-2 or ER signalling pathways. Tamoxifen resistant MCF-7 cells expressed elevated levels of Her-2 which was accompanied by decreased ER-mediated transcription. Furthermore, while genomic activity of ER was down-regulated, these receptors remained functional. Inhibition of Akt resulted in a significant decrease in proliferation of tamoxifen resistant cells which suggested a pivotal role for kinase signalling due to the lack of ER trans-activation.

Oestrogen is capable of translocating ER to the nucleus of parental MCF-7 cells while promotion of ER translocation and co-localization with Her-2 on the cell membrane has been observed in MCF-7/Her-2 cells. Her-2 over-expressing cells are known to possess elevated levels of activated extracellular-signal-regulated kinases (ERK1/2; MAP kinases) which increase above the elevated baseline in response to oestrogen stimulation. (Yang, Barnes, & Kumar, 2004) This supports a noteworthy relationship between ERK1/2 (also known as MAPK) hyper-stimulation and Her-2 over-expression. Of note is that trastuzumab has been shown to restore primary localization of nuclear ER from the cell membrane in MCF-7/Her-2 cells while reducing the levels of activated ERK1/2. (Yang et al., 2004)

Her-2/PI3K/Akt and MAPK/ERK signalling is important in promoting proliferation, and inhibition of Her-2 by trastuzumab may result in a decrease in the non-genomic actions of ER. The ability of trastuzumab to reduce the level of activated ERK1/2 provides a basis for the reduction in cell viability seen in SK-Br-3 cells. Furthermore, trastuzumab may disrupt oestrogen activated ERK1/2 and abrogate signal transduction resulting in the decreased viability observed in MCF-7 cells. No caspase-3 and -7 activation was observed in either cell line when cell viability was reduced (data not shown). This suggests that executioner caspases may only be detectable at a time point beyond 30 hours or that the effects were anti-proliferative. Furthermore, the annexin-V assay showed no difference in fluorescent staining between untreated controls and β-oestradiol alone or with concurrent trastuzumab.

MCF-7 cells exposed to β-oestradiol resulted in a gradual G1 phase increase from 24 hours, which became statistically significant at 48 and 72 hours [$G1_{72}$: 39.36% (±1.88)] compared to untreated controls [G1: 23.25% (±0.86)]. A similar trend was observed for the β-oestradiol-trastuzumab combination where G1 accumulation was the greatest at 72 hours [$G1_{72}$: 60.45% (±3.30)]. This increase was statistically significantly greater than β-oestradiol alone and more closely resembled that of trastuzumab at 72 hours [$G1_{72}$: 56.37% (±4.48)] (Table 10.2).

Oestradiol is capable of activating MAPK and Akt signalling pathways in breast cancer cells. Stimulation of Akt increases cyclin D1 transcription and progression through the G1 phase of the cell cycle. Stoica *et al.* (2003) hypothesised that oestradiol binding to membrane bound ER interacts with Her-2 containing dimers and hence induces activation of PI3K-signalling which then proceeds to activate Akt pathways and phosphorylate ER. The observations lead to conclude that Her-2/PI3K/Akt mediated signalling plays a role in signalling of hormone-dependent tumours, probably by influencing non-genomic effects that complement genomic functions. Furthermore, Her-2/Akt/steroid receptor cross-talk may be a general mechanism for hormone-dependent cell growth.

β-oestradiol causes proliferation in MCF-7 cells. Consequently it is possible that β-oestradiol accelerated cell cycle kinetics and increased the number of cells entering the G1 phase for cell division. Trastuzumab is a known G1 phase inhibitor, while β-oestradiol accelerates G1 entry. Therefore this combination could potentiate elevated G1 accumulation. Considering the ability of trastuzumab to inhibit proliferation in MCF-7 cells, steroid receptor activity may be minimised via Her-2/Akt/steroid receptor cross-talk.

In SK-Br-3 cells, β-oestradiol did not result in any alterations of cell cycle distribution at any of the three time points compared to untreated controls. However, when using the combination, statistically significant G1 accumulation was apparent from 24 hours [G1: 56.22% (±3.67)] through to 72 hours [G1: 57.98% (±1.40)] (Figure 10.2; Table 10.3). This G1 accumulation in the β-oestradiol-trastuzumab combination resulted in statistically significant differences versus β-oestradiol alone, but no differences were found when compared to trastuzumab alone. The distribution through the phases for the combination closely mimicked that of trastuzumab alone, illustrating that β-oestradiol provided negligible effects in SK-Br-3 cells.

In terms of Her-2 receptor density, MCF-7 cells showed minimal differences in the overlay plot of unstained and untreated samples. β-oestradiol, trastuzumab or combination treated samples were indistinguishable from untreated samples. Tumours highly expressing ER are generally well differentiated and less invasive than tumours expressing high levels of Her-2 receptors. Researchers have observed that 17β-oestradiol, a mitogenic inducer binding to ER receptors, inhibits Her-2 expression at the mRNA and protein level in ER positive cell lines which express approximately 10-fold fewer Her-2 receptors than SK-Br-3 cells. (Hynes et al., 1989; Antoniotti et al., 1994) While mRNA reduction was evident, it may not be translated into a detectable change on the cell surface.
Her-2 rich SK-Br-3 cells illustrated maintenance of Her-2 receptors when comparing β-oestradiol [$\beta\text{-}O_{12}$: 101.1% (±6.76)] to untreated controls [$untreated_{12}$: 99.49% (±2.52)] at 12 hours while a non-significant decrease was observed at 24 and 48 hours. In contrast, a statistically significant decrease in Her-2 receptors was observed when comparing untreated controls [$untreated_{12}$: 99.49% (±2.52)] to cells treated with the combination [$\beta\text{-}O+T_{12}$: 67.11% (±3.69)] or trastuzumab [T_{12}: 64.77% (±3.60)] alone at 12, 24 and 48 hours in SK-Br-3 cells (Figure 10.3; Table 10.4). These results suggest that as a single agent, β-oestradiol had minor effects on surface Her-2 receptor density in SK-Br-3 cells, while in combination, trastuzumab functioned to decrease Her-2 receptors in a similar or identical fashion to when it was used alone.

Inhibition of Her-2 receptors at the mRNA level by oestrogens could potentially explain the decreased receptor expression at 24 and 48 hours that was not observed at 12 hours in SK-Br-3 cells. If transcriptional repression occurs, the level of Her-2 receptors may be reduced by both β-oestradiol and trastuzumab. However, there appeared to be no direct augmentation in effects when comparing β-oestradiol and trastuzumab-induced reduction in receptors in these cells. Yet co-ordination between ER and Her-receptor signalling pathways cannot be disputed and intracellular interactions are thought to strongly influence types of signal transduction.

While β-oestradiol has been found to result in transcriptional repression and reduce Her-2 protein, the ability of ER to influence surface Her-2 receptor density has not been widely researched. In addition, the resulting cell viability when exposed to the β-oestradiol-trastuzumab combinations in both MCF-7 and SK-Br-3 cells would suggest that trastuzumab is able to influence cell viability regardless of the suspected repression in transcription.

It is important to summarise that trastuzumab abrogated the proliferation induced by β-oestradiol in MCF-7 cells resulting in a cell viability that was directly comparable to that of trastuzumab in these Her-2 receptor deficient cells. Furthermore, trastuzumab reduced SK-Br-3 cell viability and the β-oestradiol-trastuzumab combination resulted in a similar reduction. The use of β-oestradiol and trastuzumab in combination did not appear to provide any potential prospects for Her-2 positive breast cancer. However, the ability of trastuzumab to influence Her-2/Akt/steroid receptor cross-talk may provide aid during anti-oestrogen therapies in an attempt to circumvent the prevalence of resistance to treatment.

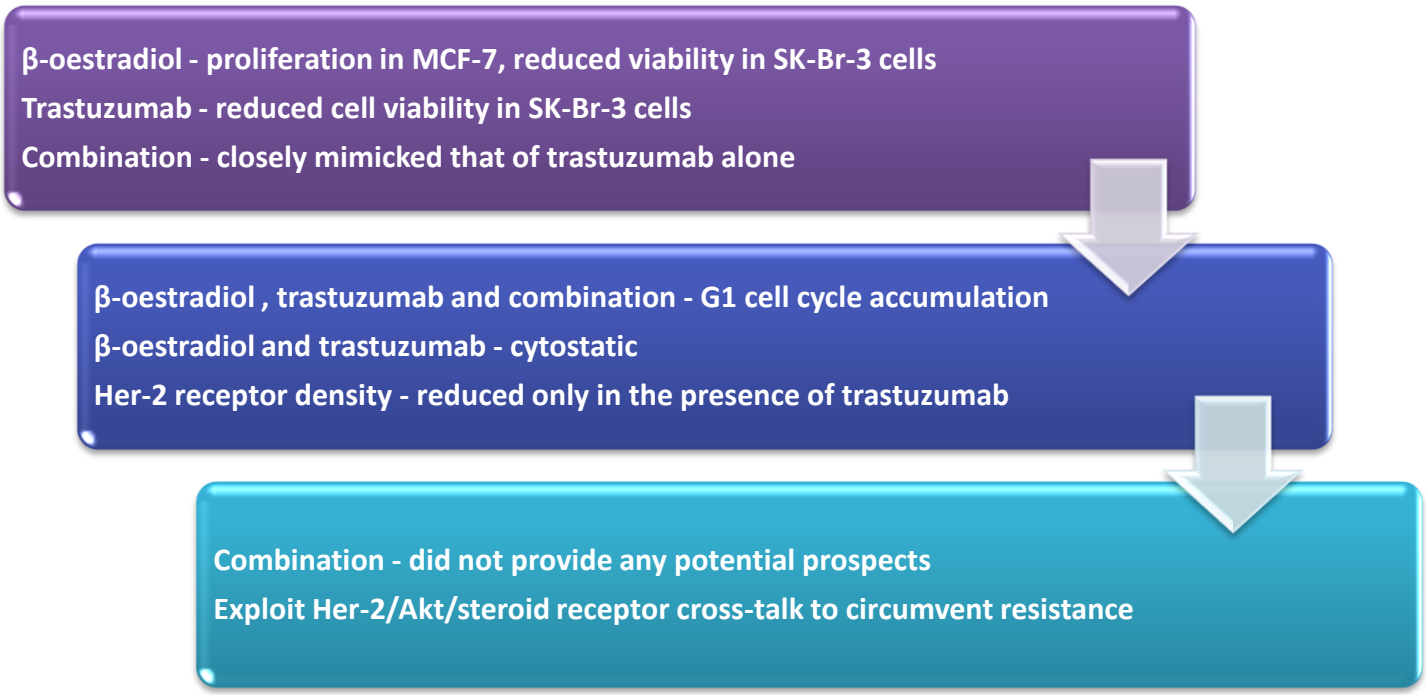

Chapter 11: Conclusion

Her-2 positive breast cancer is aggressive and resistance to targeted therapies frequently occurs. The aim of these experiments was to investigate whether there was potential to enhance or alter trastuzumab's efficacy *in vitro.* SK-Br-3 cells were used as a model for Her-2 positive breast cancer while MCF-7 cells were used as a Her-2 normal-expressing control. As expected, differential cell responses were observed, reflecting cellular receptor expression, preferential proliferative pathways and their ability to compensate by employing alternative proliferative mechanisms.

Doxorubicin was the only agent tested to show harmonious and beneficial effects when combined with trastuzumab. The cytotoxic effects of doxorubicin complemented trastuzumab's cytostatic effects without interfering with Her-2 receptor targets. However, cardiotoxicity associated with the concurrent administration of these drugs, continues to over-shadow the efficacy of this particular combination. Aspirin (high concentration) and geldanamycin demonstrated substantial reductions in SK-Br-3 cell viability. Nevertheless, when used in combination with trastuzumab, these reductions did not complement those of the antibody, suggesting interference with trastuzumab action. There was no *in-vitro* evidence for their potential use in combination, although sequential treatment with these agents and trastuzumab might be promising.

Calcipotriol and β-oestradiol had negligible effects in SK-Br-3 cells, either when used alone, or in combination with trastuzumab. Reassuringly, both of these drugs demonstrated no interference with trastuzumab action. Many women with Her-2 positive breast cancer are concerned about taking oestrogen or vitamin D (for other indications) while receiving trastuzumab treatment. The endogenous Her-receptor ligands, EGF and heregulin, differentially altered the viability parameters assessed for trastuzumab. In some cases, the presence of these proliferative ligands negated the effects of trastuzumab. This data supports the concept that receptor density and growth ligands are of mutual importance in proliferation of cell subtypes.

The data accumulated in this study provide potential insights into effective treatment combinations for trastuzumab as a targeted therapy. This would hypothetically include the use of a cytotoxic agent capable of inducing apoptosis and cell cycle arrest at either the S or G2 phase as opposed to G1. This may allow any cells capable of overcoming the G1 cell arrest imposed by trastuzumab to undergo further arrest. The use of cytotoxic-conjugated-antibodies appears to be under extensive study. However, the efficacy of these agents would be highly dependent on the maintenance of a continuous and consistent receptor threshold.

11.1 Study Limitations

The use of a third cell line, one which expresses an intermediate level of Her-2 receptors such as MDA-MB-231 cells, may have provided a more complete picture of the efficacy of the combinations. Furthermore, a second Her-2 over-expressing cell line such as BT-474 cells would have enabled more definitive conclusions. To support the cell viability results, a comparative assay would have added strength to our conclusions. The requirement of MTT conversion may result in under-estimating cell viability if mitochondria are compromised. Assessing viability by a different mechanism such as sulforhodamine-B (SRB) which measures cellular protein content would have been ideal.

Caspase substrates are dependent on the peptide sequence, and preferred substrate sequences are primarily found to differ between caspases. The catalytic efficiency of enzyme catalysed reactions determines the substrate specificity. These substrate specificities have been found to significantly overlap between executioner caspases. This suggests that because substrate specificity is not absolute, multiple executioner caspases will be detected. Homogenous caspase assay are effective in determining apoptosis, but, in order to minimise the overlap in substrate specificity of caspases, an assay which uses a coating solution to bind a specific caspase to a micro-titre plate (to ensure substrate cleavage by a single caspase) could have been conducted.

Relative Her-2 receptor density was determined with the use of a flow cytometric method and fluorescent imaging molecule. The anti-Her-2 affibody molecule illustrated significant differences following exposure to some of the agents. However, absolute receptors quantification was not done. The use of calibration beads that are coated with defined quantities of monoclonal antibody molecules allows the generation of a calibration curve for accurate quantification of receptors. While a calibrated reduction would provide more exact data, the use of the affibody molecule was more cost effective and observable differences were obtained and statistical significance achieved.

SK-Br-3 cells were extremely sensitive to changes in FCS concentration resulting in attachment problems occurring when cells required synchronisation. SK-Br-3 cells could not be synchronised for longer than 24 hours otherwise the absence of FCS would result in the inability of cells to reattach. The inability of adherent cells to attach to culture surfaces can result in a type of cell death known as anoikis. Therefore, in some cases, the sensitivity of these cell lines to attachment require the use of Corning CellBIND flasks which are treated with a derivatized core polymer chain with an increased amount of oxygen containing functional groups and aid attachment. Despite these limitations, the results obtained in these experiments were reproducible, thought-provoking and provided numerous avenues for future research.

11.2 Future Work

Data concerning the ability of trastuzumab to influence Her-2 receptor density remains to a large degree conflicting and inconclusive. In this study a significant decrease in surface Her-2 receptors was observed in response to trastuzumab, Her-receptor ligands and cytotoxic agents which may potentiate or augment the efficacy of trastuzumab.

Many researchers have sought to quantify Her-2 receptor density. However, non-standardised methodologies hinder direct comparisons between agents, cellular subtypes and research facilities. Enzyme-linked immunosorbent assay (ELISA) remains one of the most popular techniques for receptor quantification, but the use of cell extracted proteins (independent of phosphorylation state) results in the detection of both surface and cytoplasmic receptors. The rate of lysosomal degradation, receptor recycling to the cell surface, receptor reservoirs and de novo synthesis still confound receptor analyses. Future research would involve quantifying cell surface receptors comparatively with cell lysates to determine if significant differences are present. Extended time periods could be assessed where agents known to decrease Her-2 receptors (including trastuzumab) are used, after which the agents are removed to determine whether reductions in Her-2 receptor density are maintained or if the absence of agents enables receptors to re-accumulate on the cell surface.

Receptor density, growth-promoting ligands and the presence of cytostatic or cytotoxic agents appear to be of mutual importance in proliferation of cell subtypes. Combining current research with previous conclusions brings to light that the ability of trastuzumab to induce immunological response may over-shadow mechanistic features uncovered *in vitro*. Therefore potentiating the effects of trastuzumab by using drug combinations may only be fully understood within an immunologically functioning system.

Animal models offer clinically translatable data within physiological systems which are capable of capturing dynamic interactions within the tumour environment. Murine models are important for studying the evolution of breast cancer. However, species dependent pharmacological differences are evident between mice and humans. For instance, two mouse mammary tumour models available from Jackson Laboratory (USA) which closely mimic Her-2 positive breast cancer in humans have been a very successful model for studying this subtype of breast cancer. Her-2 receptor quantification and assessment of tumour burden may provide insight into the absolute efficacy of these combinations or help provide potential explanations for the emergence of clinical resistance.

References

Aggarwal BB. (2004) Nuclear factor-κB : The enemy within. *Cancer Cell* 6: 203–208.

Aligue R, Akhavan-Niak H, Russell P. (1994) A role for Hsp90 in cell cycle control: Wee1 tyrosine kinase activity requires interaction with Hsp90. *The EMBO Journal* 13(24): 6099–6106.

Altiok S, Batt D, Altiok N, Papautsky A, Downward J, Roberts TM, Avraham H. (1999) Heregulin induces phosphorylation of BRCA1 through phosphatidylinositol 3-Kinase/AKT in breast cancer cells. *The Journal of Biological Chemistry* 274(45): 32274–32278.

Antoniotti S, Taverna D, Maggiora P, Sapei ML, Hynes NE, De Bortolil M. (1994) Oestrogen and epidermal growth factor down-regulate erbB-2 oncogene protein expression in breast cancer cells by different mechanisms. *British Journal of Cancer 70*: 1095–1101.

Arola OJ, Saraste A, Pulkki K, Kallajoki M, Parvinen M, Voipio-Pulkki L. (2000) Acute doxorubicin cardiotoxicity involves cardiomyocyte apoptosis. *Cancer Research* 60: 1789–1792.

Asanuma H, Torigoe T, Kamiguchi K, Hirohashi Y, Ohmura T, Hirata K, Sato M, Sato N. (2005) Survivin expression is regulated by coexpression of human epidermal growth factor receptor 2 and epidermal growth factor receptor via phosphatidylinositol 3-kinase/AKT signaling pathway in breast cancer cells. *Cancer Research* 65(23): 11018–11025.

ATCC: Catalog Search MCF-7. (n.d.) Retrieved January 1, 2012, from http://www.atcc.org/ATCCAdvancedCatalogSearch/ProductDetails/tabid/452/Default.aspx?ATCCNum=HTB-22&Template=cellBiology

ATCC: Catalog Search SK-Br-3. (n.d.) Retrieved January 3, 2012, from http://www.atcc.org/ATCCAdvancedCatalogSearch/ProductDetails/tabid/452/Default.aspx?ATCCNum=HTB-30&Template=cellBiology

Atlas E, Cardillo M, Mehmi I, Zahedkargaran H, Tang C, Lupu R. (2003) Heregulin is sufficient for the promotion of tumorigenicity and metastasis of breast cancer cells in vivo. *Molecular Cancer Research* 1: 165–175.

Barbacci EG, Guarino BJ, Stroh JG, Singleton DH, Rosnack KJ, Moyer JD, Andrews G. (1995) The Structural Basis for Specificity of Epidermal Growth Factor and Heregulin Binding. *The Journal of Biological Chemistry* 270(16), 9585–9589.

Bar-On O, Shapira M, Hershko DD. (2007) Differential effects of doxorubicin treatment on cell cycle arrest and Skp2 expression in breast cancer cells. *Anti-Cancer Drugs* 18(10), 1113–1121.

Baselga J, Norton L, Albanell J, Kim Y, Mendelsohn J. (1998) Recombinant humanized anti-HER2 antibody (Herceptin™) enhances the antitumor activity of paclitaxel and doxorubicin against HER2/neu overexpressing human breast cancer xenografts. *Cancer Research* 58: 2825–2831.

Bisht KS, Bradbury CM, Mattson D, Kaushal A, Sowers A, Markovina S, Ortiz KL *et al*. (2003) Geldanamycin and 17-Allylamino-17-demethoxygeldanamycin potentiate the in vitro and in vivo radiation response of cervical tumor cells via the heat shock protein 90-mediated intracellular signaling and cytotoxicity. *Cancer Research* 63: 8984–8995.

Borowsky A. (2007) Special considerations in mouse models of breast cancer. *Breast disease* 28: 29–38.

Bouillon R, Okamura WH, Norman AW. (1995). Structure-function relationships in the vitamin D endocrine system. *Endocrine Reviews* 16(2): 200–257.

Bray F, McCarron P, Parkin DM. (2004) The changing global patterns of female breast cancer incidence and mortality. *Breast Cancer Research* 6(6): 229–239.

Brockhoff G, Heiß P, Schlegel J, Hofstaedter F, Knuechel R. (2001) Epidermal growth factor receptor, c-erbB2 and c-erbB3 receptor interaction, and related cell cycle kinetics of SK-BR-3 and BT474 breast carcinoma cells. *Cytometry* 44(348): 338–348.

Buras RR, Schumaker LM, Davoodi F, Brenner RV, Shabahang M, Nauta RJ, Evans SRT. (1994) Vitamin D receptors in breast cancer cells. *Breast Cancer Research and Treatment* 31: 191–202.

Burgess AW, Cho H, Eigenbrot C, Ferguson KM, Garrett TPJ, Leahy DJ, Lemmon MA *et al*. (2003) An open-and-shut case? Recent insights into the activation of EGF/ErbB receptors. *Molecular Cell* 12: 541–552.

Burstein HJ. (2005) The distinctive nature of HER2-positive breast cancers. *The New England Journal of Medicine* 353(16): 1652–1654.

Callahan R, Hurvitz S. (2011) Human epidermal growth factor receptor-2-positive breast cancer: current management of early, advanced, and recurrent disease. *Current Opinion in Obstetrics and Gynecology* 23: 37–43.

Campiglio M, Somenzi G, Olgiati C, Beretta G, Balsari A, Zaffaroni N, Valagussa P, Menard S. (2003) Role of proliferation in HER2 status predicted response to doxorubicin. *International Journal of Cancer* 105: 568–573.

CANSA - The Cancer Association of South Africa. (n.d.) Retrieved March 3, 2012, from http://www.cansa.org.za/cgi-bin/giga.cgi?cmd=cause_dir_news&cat=822&cause_id=1056&limit=a

Castedo M, Perfettini JL, Roumier T, Andreau K, Medema R, Kroemer G. (2004) Cell death by mitotic catastrophe: a molecular definition. *Oncogene* 23(16): 2825–2837.

Cell Cycle Image. (n.d.) *The Encyclopedia of Science*. Retrieved October 23, 2012, from http://www.daviddarling.info/encyclopedia/C/cell_cycle.html

Chavany C, Mimnaugh E, Miller P, Bitton R, Nguyen P, Trepel J, Whitesell L *et al*. (1996) p185erbB-2 binds to GRP94 in vivo. *The Journal of Biological Chemistry* 271(9): 4974–4977.

Citri A, Yarden Y. (2006) EGF-ERBB signalling: towards the systems level. *Nature Reviews. Molecular Cell Biology* 7(7): 505–516.

Daly JM, Olayioye MA, Wong AML, Neve R, Lane HA, Maurer FG, Hynes NE. (1999) NDF/heregulin-induced cell cycle changes and apoptosis in breast tumour cells: role of PI3 kinase and p38 MAP kinase pathways. *Oncogene* 18(23): 3440–3451.

Daly JM, Jannot CB, Beerli RR, Graus-Porta D, Maurer FG, Hynes NE. (1997) Neu differentiation factor Induces ErbB2 down-regulation and apoptosis of ErbB2-overexpressing breast tumor cells. *Cancer Research* 57*:* 3804–3811.

Dang C, Fornier M, Sugarman S, Troso-Sandoval T, Lake D, D'Andrea G, Seidman A *et al*. (2008) The safety of dose-dense doxorubicin and cyclophosphamide followed by paclitaxel with trastuzumab in HER-2/neu overexpressed/amplified breast cancer. *Journal of Clinical Oncology* 26(8): 1216–1222.

Darzynkiewicz Z, Crissman H, Jacobberger JW. (2004) Cytometry of the cell cycle: cycling through history. *Cytometry. Part A: Journal of the International Society for Analytical Cytology 58*(1): 21–32.

DeBoer C, Meilman PA, Wnuk RJ, Peterson DH. (1970) Geldanamycin, A New Antibiotic. *The Journal of Antibiotics* 23(9): 442–447.

deFazio A, Chiew Y, McEvoy M, Watts CKW, Sutherland RL. (1997) Antisense estrogen receptor RNA expression increases epidermal growth factor receptor gene expression in breast cancer cells. *Cell Growth & Differentiation* 8: 903–911.

Dejardin E, Deregowski V, Chapelier M, Jacobs N, Gielen J, Merville M, Bours V. (1999) Regulation of NF-kB activity by IkB-related proteins in adenocarcinoma cells. *Oncogene* 18:2567-2577.

Diermeier S, Horváth G, Knuechel-Clarke R, Hofstaedter F, Szöllosi J, Brockhoff G. (2005) Epidermal growth factor receptor coexpression modulates susceptibility to Herceptin in HER2/neu overexpressing breast cancer cells via specific erbB-receptor interaction and activation. *Experimental Cell Research* 304(2): 604–619.

Din FVN, Dunlop MG, Stark LA. (2004) Evidence for colorectal cancer cell specificity of aspirin effects on NF kappa B signalling and apoptosis. *British Journal of Cancer* 91(2): 381–388.

Dogan I, Cumaoglu A, Aricioglu A, Ekmekci A. (2011) Inhibition of ErbB2 by Herceptin reduces viability and survival, induces apoptosis and oxidative stress in Calu-3 cell line. *Molecular and Cellular Biochemistry* 347: 41–51.

Eisman JA, Koga M, Sutherland RL, Barkla DH, Tutton PJM. (1989) 1,25-Dihydroxyvitamin D3 and the regulation of human cancer cell replication. *Proceedings Of The Society For Experimental Biology And Medicine* 191*:* 221–226.

Elder DJE, Hague A, Hicks DJ, Paraskeva C. (1996) Differential growth inhibition by the aspirin metabolite salicylate in human colorectal tumor cell lines: enhanced apoptosis in carcinoma and in vitro -transformed adenoma relative to adenoma cell lines. *Cancer Research* 56*:* 2273–2276.

Emlet DR, Schwartz R, Brown KA, Pollice AA, Smith CA, Shackney SE. (2006) HER2 expression as a potential marker for response to therapy targeted to the EGFR. *British Journal of Cancer* 94(8): 1144–1153.

Eom YW, Kim MA, Park SS, Goo MJ, Kwon HJ, Sohn S, Kim WH *et al*. (2005) Two distinct modes of cell death induced by doxorubicin: apoptosis and cell death through mitotic catastrophe accompanied by senescence-like phenotype. *Oncogene* 24(30): 4765–4777.

Ferenc P, Solár P, Mikeš J, Kovaľ J, Fedoročko P. (2010) Breast Cancer and Current Therapeutic Approaches : From Radiation to Photodynamic Therapy. *Breast Cancer – Current and Alternative Therapeutic Modalities* 63–87.

Ferlay J, Shin H, Bray F, Forman D, Mathers C, Parkin DM. (2010) Estimates of worldwide burden of cancer in 2008: GLOBOCAN 2008. *International Journal of Cancer* 127(12), 2893–2917.

Friedländer E, Barok M, Szöllosi J, Vereb G. (2008) ErbB-directed immunotherapy: antibodies in current practice and promising new agents. *Immunology Letters* 116(2): 126–140.

Fukuyo Y, Hunt CR, Horikoshi N. (2010) Geldanamycin and its anti-cancer activities. *Cancer Letters* 290(1): 24–35.

Gamen S, Anel A, Pérez-Galán P, Lasierra P, Johnson D, Piñeiro A, Naval J. (2000) Doxorubicin treatment activates a Z-VAD-sensitive caspase, which causes Δψm loss, caspase-9 activity, and apoptosis in Jurkat cells. *Experimental Cell Research* 258(1): 223–235.

Georgakis GV, Li Y, Younes A. (2006) The heat shock protein 90 inhibitor 17-AAG induces cell cycle arrest and apoptosis in mantle cell lymphoma cell lines by depleting cyclin D1, Akt, Bid and activating caspase 9. *British Journal of Haematology* 135(1): 68–71.

Gewirtz DA. (1999) A Critical Evaluation of the Mechanisms of Action Proposed for the Antitumor Effects of the Anthracycline Antibiotics Adriamycin and Daunorubicin. *Science* 57(98): 727–741.

Goel A, Chang DK, Ricciardiello L, Gasche C, Boland CR. (2003) A novel mechanism for aspirin-mediated growth inhibition of human colon cancer cells. *Clinical Cancer Research* 9: 383–390.

Gong Y, Booser DJ, Sneige N. (2005) Comparison of HER-2 status determined by fluorescence in situ hybridization in primary and metastatic breast carcinoma. *Cancer* 103(9): 1763–1769.

Guarneri V, Barbieri E, Dieci MV, Piacentini F, Conte P. (2010) Anti-HER2 neoadjuvant and adjuvant therapies in HER2 positive breast cancer. *Cancer Treatment Reviews* 36 Suppl 3: S62–66.

Half E, Tang XM, Gwyn K, Sahin A, Wathen K, Sinicrope FA. (2002) Cyclooxygenase-2 expression in human breast cancers and adjacent ductal carcinoma in Situ. *Cancer Research* 62: 1676–1681.

Hall JM, Couse JF, Korach KS. (2001) The multifaceted mechanisms of estradiol and estrogen receptor signaling. *The Journal of Biological Chemistry* 276(40): 36869–36872.

Hanahan D, Weinberg RA. (2000). The Hallmarks of Cancer. *Cell* 100*:* 57–70.

Hanif R, Pittas A, Feng Y, Koutsos MI, Qiao L, Staiano-Coico L, Shiff SI, Rigas B. (1996) Effects of nonsteroidal anti-inflammatory drugs on proliferation and on induction of apoptosis in colon cancer cells by a prostaglandin-independent pathway. *Biochemical Pharmacology* 52(2): 237–245.

Harant H, Andrew PJ, Reddy GS, Foglar E, Lindley IVD. (1997) 1α,25-Dihydroxyvitamin D3 and a variety of its natural metabolites transcriptionally repress nuclear factor-κB-mediated interleukin-8 gene expression. *European Journal of Biochemistry* 250(1): 63–71.

Harris AL, Nicholon S. (1988) Epidermal growth factor receptors in human breast cancer. *Cancer Research* 40*:* 93–118.

Hellyer NJ, Kim MS, Koland JG. (2001) Heregulin-dependent activation of phosphoinositide 3-kinase and Akt via the ErbB2/ErbB3 co-receptor. *The Journal of Biological Chemistry* 276(45): 42153–42161.

Helmbrecht K, Zeise E, Rensing L. (2000) Chaperones in cell cycle regulation and mitogenic signal transduction: a review. *Cell Proliferation 33*(6): 341–365.

Hendriks BS, Wiley HS, Lauffenburger D. (2003) HER2-mediated effects on EGFR endosomal sorting: analysis of biophysical mechanisms. *Biophysical Journal* 85(4): 2732–2745.

Hostein I, Robertson D, Distefano F, Workman P, Clarke PA. (2001) Inhibition of signal transduction by the Hsp90 inhibitor 17-Allylamino-17-demethoxygeldanamycin results in cytostasis and apoptosis. *Cancer Research* 61*:* 4003–4009.

Hudis CA. (2007) Trastuzumab--mechanism of action and use in clinical practice. *The New England Journal of Medicine* 357(1): 39–51.

Hudziak RM, Lewis GD, Winget M, Fendly BM, Shepard HM, Ullrich A. (1989) p185HER2 monoclonal antibody has antiproliferative effects in vitro and sensitizes human breast tumor cells to tumor necrosis factor. *Molecular and Cellular Biology 9*(3): 1165–1172.

Hutchinson JN, Muller WJ. (2000) Transgenic mouse models of human breast cancer. *Oncogene* 19(53): 6130–6137.

Ignar-Trowbridge DM, Nelson KG, Bidwell MC, Curtis SW, Washburn TF, McLachlan JA, Korach KS. (1992) Coupling of dual signaling pathways: Epidermal growth factor action involves the estrogen receptor. *Proceedings of the National Academy of Science* 89*:* 4658–4662.

Issa LL, Leong GM, Eisman JA. (1998) Review: Molecular mechanism of vitamin D receptor action. *Inflammation Research* 47: 451–475.

Karunagaran D, Tzahar E, Beerli RR, Chen X, Graus-Porta D, Ratzkin BJ, Seger R *et al.* (1996) ErbB-2 is a common auxiliary subunit of NDF and EGF receptors: implications for breast cancer. *The EMBO Journal* 15(2): 254–264.

Kim S, Kang J, Hu W, Evers BM, Chung DH. (2003) Geldanamycin decreases Raf-1 and Akt levels and induces apoptosis in neuroblastomas. *International Journal of Cancer* 103(3): 352–359.

Koga M, Eisman JA, Sutherland RL. (1988) Regulation of epidermal growth factor receptor levels by 1,25-dihydroxyvitamin D3 in human breast cancer cells. *Cancer Research* 48(10): 2734–2739.

Konecny GE, Pegram MD, Venkatesan N, Finn R, Yang G, Rahmeh M, Untch M *et al.* (2006) Activity of the dual kinase inhibitor lapatinib (GW572016) against HER-2-overexpressing and trastuzumab-treated breast cancer cells. *Cancer Research* 66(3): 1630–1639.

Koutras AK, Evans TRJ. (2008) The epidermal growth factor receptor family in breast cancer. *OncoTargets and Therapy* 1*:* 5–19.

Kruser TJ, Wheeler DL. (2010) Mechanisms of resistance to HER family targeting antibodies. *Experimental Cell Research* 316(7): 1083–1100.

Lane HA, Motoyama AB, Beuvink I, Hynes NE. (2001) Symposium article: Modulation of p27/Cdk2 complex formation through 4D5-mediated inhibition of HER2 receptor signaling. *Annals of Oncology* 12 (Suppl. 1)*:* S21–22.

Lane HA, Beuvink I, Motoyama AB, Daly JM, Neve RM, Hynes NE. (2000) ErbB2 potentiates breast tumor proliferation through modulation of p27 Kip-Cdk2 complex formation: receptor overexpression does not determine growth dependency. *Molecular and Cellular Biology* 20(9): 3210–3223.

Lee E, Jeon SH, Yi JY, Jin YJ, Son YS. (2001) Calcipotriol inhibits autocrine phosphorylation of EGF receptor in a calcium-dependent manner, a possible mechanism for its inhibition of cell proliferation and stimulation of cell differentiation. *Biochemical and Biophysical Research Communications* 284(2): 419–425.

Lenferink AE, Pinkas-Kramarski R, Van de Poll MLM, van Vugt MJ, Klapper LN, Tzahar E, Waterman H *et al.* (1998) Differential endocytic routing of homo- and hetero-dimeric ErbB tyrosine kinases confers signaling superiority to receptor heterodimers. *The EMBO Journal* 17(12): 3385–3397.

Lewis GD, Lofgren JA, McMurtrey AE, Nuijens A, Fendly BM, Bauer KD, Sliwkowski MX. (1996) Growth regulation of human breast and ovarian tumor cells by heregulin: evidence for the requirement of ErbB2 as a critical component in mediating heregulin responsiveness. *Cancer Research* 56: 1457–1465.

Lichtenstein AV. (2008) Cancer: Shift of the paradigm. *Medical Hypotheses* 71(6): 839–850.

Liu W, Li J, Roth RA. (1999) Heregulin regulation of Akt/protein kinase B in breast cancer cells. *Biochemical and Biophysical Research Communications* 261(3): 897–903.

Liu X, Rose DP. (1996) Differential expression and regulation of cyclooxygenase-1 and -2 in two human breast cancer cell lines. *Cancer Research* 56(22): 5125–5127.

Lower EE, Glass E, Blau R, Harman S. (2009) HER-2/neu expression in primary and metastatic breast cancer. *Breast Cancer Research and Treatment* 113(2): 301–306.

Lu M, Strohecker A, Chen F, Kwan T, Bosman J, Jordan VC, Cryns VL. (2008) Aspirin sensitizes cancer cells to TRAIL-induced apoptosis by reducing survivin levels. *Clinical Cancer Research* 14(10): 3168–3176.

Massarweh S, Schiff R. (2006) Resistance to endocrine therapy in breast cancer: exploiting estrogen receptor/growth factor signaling crosstalk. *Endocrine Related Cancer* 13: S15–24.

Miller P, DiOrio C, Moyer M, Schnur CR, Bruskin A, Cullen W, Moyer JD. (1994) Depletion of the erbB-2 gene product p185 by benzoquinoid ansamycins. *Cancer Research* 54: 2724–2730.

Mimnaugh EG, Chavany C, Neckers L. (1996) Polyubiquitination and proteasomal degradation of the $p185^{c\text{-}erbB\text{-}2}$ receptor protein-tyrosine kinase induced by geldanamycin. *The Journal of Biological Chemistry* 271(37): 22796–22801.

Mohsin SK, Weiss HL, Gutierrez MC, Chamness GC, Schiff R, DiGiovanna MP, Wang C *et al.* (2005) Neoadjuvant trastuzumab induces apoptosis in primary breast cancers. *Journal of Clinical Oncology* 23(11): 2460–2468.

Morrow PKH, Zambrana F, Esteva FJ. (2009) Recent advances in systemic therapy: Advances in systemic therapy for HER2-positive metastatic breast cancer. *Breast Cancer Research* 11(4): 207-217.

Mountzios G, Sanoudou D, Syrigos KN. (2010) Clinical pharmacogenetics in oncology: the paradigm of molecular targeted therapies. *Current Pharmaceutical Design* 16(20): 2184–2193.

Münster PN, Marchion DC, Basso AD, Rosen N. (2002) Degradation of HER2 by ansamycins induces growth arrest and apoptosis in cells with HER2 overexpression via a HER3, phosphatidylinositol 3'-kinase-AKT-dependent pathway. *Cancer Research* 62: 3132–3137.

Murphy CG, Modi S. (2009) HER2 breast cancer therapies: a review. *Biologics:Targets & Therapy* 3: 289–301.

Muss HB, Thor AD, Berry DA, Kute T, Liu ET, Koerner F *et al*. (1994) c-erbB-2 expression and response to adjuvant therapy in women with node-positive early breast cancer. *The New England Journal of Medicine* 330(18): 1260–1266.

Nagpal S, Lu J, Boehm MF. (2001) Vitamin D analogs: mechanism of action and therapeutic applications. *Current Medicinal Chemistry* 8(13): 1661–1679.

Nagy P, Claus J, Jovin TM, Arndt-Jovin DJ. (2010) Distribution of resting and ligand-bound ErbB1 and ErbB2 receptor tyrosine kinases in living cells using number and brightness analysis. *Proceedings of the National Academy of Sciences of the United States of America* 107(38): 16524–16539.

Nagy P, Jenei A, Kirsch AK, Szöllosi J, Damjanovich S, Jovin TM. (1999) Activation-dependent clustering of the erbB2 receptor tyrosine kinase detected by scanning near-field optical microscopy. *Journal of Cell Science* 112*:* 1733–1741.

Nam E, Lee SN, Im S, Kim D, Lee KE, Sung SH. (2005) Expression of cyclooxygenase-2 in human breast cancer: relationship with HER-2/neu and other clinicopathological prognostic factors. *Cancer Research and Treatment* 37(3): 165–170.

Neckers L, Schulte TW, Mimnaugh E. (1999) Geldanamycin as a potential anti-cancer agent: its molecular target and biochemical activity. *Investigational New Drugs* 17(4): 361–373.

Pahl HL. (1999) Activators and target genes of Rel/NF-kB transcription factors. *Oncogene* 18*:* 6853–6866.

Pancholi S, Lykkesfeldt AE, Hilmi C, Banerjee S, Leary A, Drury S, Johnston S *et al*. (2008) ERBB2 influences the subcellular localization of the estrogen receptor in tamoxifen-resistant MCF-7 cells leading to the activation of AKT and RPS6KA2. *Endocrine-Related Cancer* 15: 985–1002.

Park JW, Yeh MW, Wong MG, Lobo M, Hyun WC, Duh Q, Clark OH. (2003) The heat shock protein 90-binding geldanamycin inhibits cancer cell proliferation, down-regulates oncoproteins, and inhibits epidermal growth factor-induced invasion in thyroid cancer cell lines. *Journal of Clinical Endocrinology & Metabolism* 88(7): 3346–3353.

Pedersen NM, Breen K, Rødland MS, Haslekås C, Stang E, Madshus IH. (2009) Expression of epidermal growth factor receptor or ErbB3 facilitates geldanamycin-induced down-regulation of ErbB2. *Molecular Cancer Research* 7(2): 275–284.

Pegram MD, Konecny GE, O'Callaghan C, Beryt M, Pietras R, Slamon DJ. (2004) Rational combinations of trastuzumab with chemotherapeutic drugs used in the treatment of breast cancer. *Journal of the National Cancer Institute*, 96(10): 739–749.

Pegram MD, Hsu S, Lewis G, Pietras R, Beryt M, Sliwkowski M *et al*. (1999) Inhibitory effects of combinations of HER-2/neu antibody and chemotherapeutic agents used for treatment of human breast cancers. *Oncogene* 18: 2241-2251.

Perez EA, Suman VJ, Davidson NE, Sledge GW, Kaufman PA, Hudis CA *et al.* (2008) Cardiac safety analysis of doxorubicin and cyclophosphamide followed by paclitaxel with or without trastuzumab in the North Central Cancer Treatment Group N9831 adjuvant breast cancer trial. *Journal of Clinical Oncology* 26(8): 1231–1238.

Pero SC, Shukla GS, Cookson MM, Flemer S, Krag DN. (2007) Combination treatment with Grb7 peptide and doxorubicin or trastuzumab (Herceptin) results in cooperative cell growth inhibition in breast cancer cells. *British Journal of Ccancer* 96(10): 1520–1525.

Perou CM, Sørlie T, Eisen MB, van de Rijn M, Jeffrey SS, Rees CA, Pollack JR *et al*. (2000) Molecular portraits of human breast tumours. *Nature* 406(August): 747–752.

Petit T, Borel C, Ghnassia JP, Rodier J, Escande A, Mors R, Haegelé P. (2001) Chemotherapy respose of breast cancer depends on Her-2 status and anthracycline dose intensity in the neoadjuvant setting. *Clinical Cancer Research* 7(6): 1577–1581.

Pohlmann PR, Mayer IA, Mernaugh R. (2009) Resistance to trastuzumab in breast cancer. *Clinical Cancer Research* 15(24): 7479–7491.

Potter AJ, Gollahon KA, Palanca BJA, Harbert MJ, Choi YM, Moskovitz AH *et al.* (2002) Flow cytometric analysis of the cell cycle phase specificity of DNA damage induced by radiation, hydrogen peroxide and doxorubicin. *Carcinogenesis* 23(3): 389–401.

Ram TG, Stephen EP. (1996) Phosphatidylinositol 3-kinase recruitment by p185erbB-2 and erbB-3 is potently induced by neu differentiation factor/heregulin during mitogenesis and is constitutively elevated in growth factor-independent breast carcinoma cells with c-erbB-2 gene amplification. *Cell Growth & Differentiation* 7(May): 551–561.

Rayet B, Gelinas C. (1999) Aberrant rel/nfkb genes and activity in human cancer. *Oncogene* 18: 6938–6947.

Ray A, Perfontaine KE, Ray P. (1994) Down-modulation of interleukin-6 gene expression by 17B-estradiol in the absence of high affinity DNA binding by the estrogen receptor. *The Journal of Biological Chemistry* 269(17), 12940–12946.

Rayson D, Richel D, Chia S, Jackisch C, van der Vegt S, Suter T. (2008) Anthracycline-trastuzumab regimens for HER2/neu-overexpressing breast cancer: current experience and future strategies. *Annals of Oncology: Official Journal of the European Society for Medical Oncology* 19(9): 1530–1539.

Rhodes A, Jasani B, Couturier J, McKinley MJ, Morgan JM, Dodson AR *et al*. (2002) A formalin-fixed, paraffin-processed cell line standard for quality control of immunohistochemical assay of HER-2/neu expression in breast cancer. *American Journal of Clinical Pathology 117*(1): 81–89.

Ross JS, Slodkowska E, Symmans WF, Pusztai L, Ravdin PM, Hortobagyi GN. (2009) The HER-2 receptor and breast cancer: ten years of targeted anti-HER-2 therapy and personalized medicine. *The Oncologist* 14(4): 320–368.

Sahin Ö, Fröhlich H, Löbke C, Korf U, Burmester S, Majety M, Mattern J *et al.* (2009) Modeling ERBB receptor-regulated G1/S transition to find novel targets for de novo trastuzumab resistance. *BioMedical Central Systems Biology* 3(1): 1–20.

Sako Y, Minoguchi S, Yanagida T. (2000) Single-molecule imaging of EGFR signalling on the surface of living cells. *Nature Cell Biology* 2(March): 168- 172.

Savage RC, Inagami T, Cohens S. (1972) The Primary Structure of Epidermal Growth Factor. *The Journal of Biological Chemistry* 247(23): 7612–7621.

Schechter AL, Stern DF, Vaidyanathan L, Decker SJ, Drebin JA, Greene MI. (1984) The neu oncogene: an erb-B-related gene encoding a 185,000-Mr tumour antigen. *Nature 312:* 513–516.

Schnur RC, Corman ML, Gallaschun RJ, Cooper BA, Dee MF, Doty JL *et al*. (1995) erbB-2 oncogene inhibition by geldanamycin derivatives: synthesis, mechanism of action, and structure-activity relationships. *Journal of Medicinal Chemistry* 38(19): 3813–3820.

Sepp-Lorenzino L, Ma Z, Lebwohl DE, Vinitsky A, Rosen N. (1995) Herbimycin A induces the 20 S proteasome-and ubiquitin-dependent degradation of receptor tyrosine kinases. *The Journal of Biological Chemistry* 270(28): 16580–16587.

Shimamura T, Lowell AM, Engelman J, Shapiro GI. (2005) Epidermal growth factor receptors harboring kinase domain mutations associate with the heat shock protein 90 chaperone and are destabilized following exposure to geldanamycins. *Cancer Research* 65(14): 6401–6408.

Sigma Product Information. (n.d.-a) *Cell Growth Determination KIt, MTT Based*. Retrieved from http://www.sigmaaldrich.com/catalog/product/sigma/m2003?lang=en&region=ZA

Sigma Product Information. (n.d.-b) *Caspase 3 Assay Kit, Fluorimetric*. Retrieved from http://www.sigmaaldrich.com/catalog/product/sigma/casp3f?lang=en&region=ZA

Sigma Product Information. (n.d.-c) *Annexin V-FITC Apoptosis Detection Kit*. Retrieved from http://www.sigmaaldrich.com/catalog/product/sigma/apoaf?lang=en&region=ZA

Sliwkowskiso MX, Schaefers G, Akita RW, Lofgrens JA, Fitzpatricks VD, Nuijenss A M *et al.* (1994) Co-expression of of erbB2 and erbB3 proteins reconstitutes a high affinity receptor for heregulin. *The Journal of Biological Chemistry* 269(20): 14661–14665.

Sonne-Hansen K, Norrie IC, Emdal KB, Benjaminsen RV, Frogne T, Christiansen IJ *et al*. (2010) Breast cancer cells can switch between estrogen receptor alpha and ErbB signaling and combined treatment against both signaling pathways postpones development of resistance. *Breast Cancer Research and Treatment* 121(3): 601–613.

Srinivasan R, Poulsom R, Hurst HC, Gullick WJ (1998) Expression of the c-erbB-4/HER4 protein and mRNA in normal human fetal and adult tissues and in a survey of nine solid tumour types. *The Journal of Pathology* 185(3): 236–245.

Stark LA, Reid K, Sansom OJ, Din FV, Guichard S, Maye I *et al.* (2007) Aspirin activates the NF-kappaB signalling pathway and induces apoptosis in intestinal neoplasia in two in vivo models of human colorectal cancer. *Carcinogenesis* 28(5): 968–976.

Stepanova L, Leng X, Parker SB, Harper JW. (1996) Mammalian p50^{Cdc37} is a protein kinase-targeting subunit of Hsp90 that binds and stabilizes Cdk4. *Genes & Development* 10(12): 1491–1502.

Stoica A, Saceda M, Doraiswamy VL, Coleman C, Martin MB. (2000) Regulation of estrogen receptor-gene expression by epidermal growth factor. *Journal of Endocrinology* 165: 371–378.

Stoica GE, Franke TF, Moroni M, Mueller S, Morgan E, Iann MC *et al.* (2003) Effect of estradiol on estrogen receptor-α gene expression and activity can be modulated by the ErbB2/PI3-K/Akt pathway. *Oncogene* 22(39): 7998–8011.

Tai W, Mahato R, Cheng K. (2010) The role of HER2 in cancer therapy and targeted drug delivery. *Journal of Controlled Release* 146(3): 264–275.

Telli ML, Hunt SA, Carlson RW, Guardino AE. (2007) Trastuzumab-related cardiotoxicity: calling into question the concept of reversibility. *Journal of Clinical Oncology* 25(23): 3525–3533.

Tikhomirov O, Carpenter G. (2004) Ligand-induced, p38-dependent apoptosis in cells expressing high levels of epidermal growth factor receptor and ErbB-2. *The Journal of Biological Chemistry* 279(13): 12988–12996.

Tikhomirov O, Carpenter G. (2005). Bax activation and translocation to mitochondria mediate EGF-induced programmed cell death. *Journal of Cell Science* 118(24): 5681–5690.

Toft DO. (1998) Recent advances in the study of hsp90 structure and mechanism of action. *Trends in Endocrinology and Metabolism* 9(6): 238–243.

Tzahar E, Levkowitz G, Karunagaran D, Yi L, Peles E, Lavi S *et al*. (1994) ErbB-3 and ErbB-4 function as the respective low and high affinity receptors of all neu differentiation factor/heregulin isoforms. *The Journal of Biological Chemistry* 269(40): 25226–25233.

Tzahar E, Pinkas-Kramarski R, Moyer JD, Klapper LN, Alroy I, Levkowitz G *et al.* (1997) Bivalence of EGF-like ligands drives the ErbB signaling network. *The EMBO Journal* 16(16): 4938–4950.

van Agthoven T, van Agthoven TLA, Portengen H, Foekens JA, Dorssers LCJ. (1992) Ectopic expression of epidermal growth factor receptors induces hormone independence in ZR-75-1 human breast cancer cells. *Cancer Research* 52: 5082–5088.

Wang S, Konorev EA, Kotamraju S, Joseph J, Kalivendi S, Kalyanaraman B. (2004) Doxorubicin induces apoptosis in normal and tumor cells via distinctly different mechanisms. *The Journal of Biological Chemistry* 279(24): 25535–25543.

Weigelt B, Geyer FC, Reis-Filho JS (2010) Histological types of breast cancer: how special are they? *Molecular Oncology* 4(3): 192–208.

Weinstein EJ, Grimm S, Leder P. (1998) The oncogene heregulin induces apoptosis in breast epithelial cells and tumors. *Oncogene* 17: 2107–2113.

Weinstein IB. (1988) The origins of human cancer: molecular mechanisms of carcinogenesis and their implications for cancer prevention and treatment –– Twenty-seventh G . H . A . Clowes Memorial Award Lecture. *Cancer Research* 48*:* 4135–4143.

Wen D, Suggs SV, Karunagaran D, Liu N, Cupples RL, Luo Y A *et al*. (1994) Structural and functional aspects of the multiplicity of neu differentiation factors. *Molecular and Cellular Biology* 14(3): 1909–1919.

Wietrzyk J, Chodyński M, Fitak H, Wojdat E, Kutner A, Opolski A. (2007) Antitumor properties of diastereomeric and geometric analogs of vitamin D3. *Anti-Cancer Drugs* 18(4): 447–457.

Worthylake R, Opresko LK, Wiley HS. (1999) ErbB-2 amplification inhibits down-regulation and induces constitutive activation of both ErbB-2 and epidermal growth factor receptors. *The Journal of Biological Chemistry* 274(13): 8865–8874.

Xu FJ, Stack S, Boyer C, O'Briant K, Whitaker R, Mills GB *et al.* (1997). Heregulin and agonistic anti-$p185^{c\text{-}erbB2}$ antibodies inhibit proliferation but increase invasiveness of breast cancer cells that overexpress $p185^{c\text{-}erbB2}$: increased invasiveness may contribute to poor prognosis. *Clinical Cancer Research 3*(9): 1629–1634.

Yamamoto K, Arakawa T, Ueda N, Yamamoto S. (1995) Transcriptional roles of nuclear factor κB and nuclear factor-interleukin-6 in the tumor necrosis factor α-dependent induction of cyclooxygenase-2 in MC3T3-E1 cells. *The Journal of Biological Chemistry* 270(52): 31315–31320.

Yang Z, Barnes CJ, Kumar R. (2004) Human epidermal growth factor receptor 2 status modulates subcellular localization of and interaction with estrogen receptor α in breast cancer cells. *Clinical Cancer Research* 10(11): 3621–3628.

Yarden Y, Sliwkowski MX. (2001) Untangling the ErbB signalling network. *Nature reviews. Molecular cell Biology* 2(2): 127–137.

Zhang DY, Li Y, Rizvi SMA, Qu C, Kearsley J, Allen BJ. (2005) Cytotoxicity of breast cancer cells overexpressing HER2 by ^{213}Bi-Herceptin radioimmunoconjugate. *Cancer Letters* 218(2): 181–90.

Zhu H, Zhang G, Wang Y, Xu N, He S, Zhang W *et al*. (2010) Inhibition of ErbB2 by Herceptin reduces survivin expression via the ErbB2-beta-catenin/TCF4-survivin pathway in ErbB2-overexpressed breast cancer cells. *Cancer Science* 101(5): 1156–1162.

Zhuang SH, Schwartz GG, Cameron D, Burnstein KL. (1997) Vitamin D receptor content and transcriptional activity do not fully predict antiproliferative effects of vitamin D in human prostate cancer cell lines. *Molecular and Cellular Endocrinology* 126(1): 83–90.

Zinser GM, Welsh J. (2004) Vitamin D receptor status alters mammary gland morphology and tumorigenesis in MMTV-neu mice. *Carcinogenesis* 25(12): 2361–2372.